

**Report Title**

*“Integrated Geologic-Engineering Model for Reef and Carbonate Shoal Reservoirs Associated with Paleohighs: Upper Jurassic Smackover Formation, Northeastern Gulf of Mexico”*

**Type of Report**

Technical Progress Report for Year 2

**Reporting Period Start Date**

September 1, 2001

**Reporting Period End Date**

August 31, 2002

**Principal Author**

Ernest A. Mancini (205/348-4319)  
Department of Geological Sciences  
Box 870338  
202 Bevill Building  
University of Alabama  
Tuscaloosa, AL 35487-0338

**Date Report was Issued**

September 25, 2002

**DOE Award Number**

DE-FC26-00BC15303

**Name and Address of Participants**

Ernest A. Mancini Dept. of Geological Sciences Box 870338 Tuscaloosa, AL 35487-0338	Bruce S. Hart Earth & Planetary Sciences McGill University 3450 University St. Montreal, Quebec H3A 2A7 CANADA	Thomas Blasingame Dept. of Petroleum Engineering Texas A&M University College Station, TX 77843-3116
Robert D. Schneeflock, Jr. Paramount Petroleum Co., Inc. 230 Christopher Cove Ridgeland, MS 39157	Richard K. Strahan Strago Petroleum Corporation 811 Dallas St., Suite 1407 Houston, TX 77002	Roger M. Chapman Longleaf Energy Group, Inc. 319 Belleville Ave. Brewton, AL 36427

**Disclaimer**

This report was prepared as an account of work sponsored by an agency of the United States Government. Neither the United States Government nor any agency thereof, nor any of their employees, makes any warranty, express or implied, or assumes any legal liability or responsibility for the accuracy, completeness, or usefulness of any information, apparatus, product, or process disclosed, or represents that its use would not infringe privately owned rights. Reference herein to any specific commercial product, process, or service by trade name, trademark, manufacturer, or otherwise does not necessarily constitute or imply its endorsement, recommendation, or favoring by the United States Government or any agency thereof. The views and opinions of authors expressed herein do not necessarily state or reflect those of the United States Government or any agency thereof.

## **ABSTRACT**

The University of Alabama in cooperation with Texas A&M University, McGill University, Longleaf Energy Group, Strago Petroleum Corporation, and Paramount Petroleum Company are undertaking an integrated, interdisciplinary geoscientific and engineering research project. The project is designed to characterize and model reservoir architecture, pore systems and rock-fluid interactions at the pore to field scale in Upper Jurassic Smackover reef and carbonate shoal reservoirs associated with varying degrees of relief on pre-Mesozoic basement paleohighs in the northeastern Gulf of Mexico. The project effort includes the prediction of fluid flow in carbonate reservoirs through reservoir simulation modeling which utilizes geologic reservoir characterization and modeling and the prediction of carbonate reservoir architecture, heterogeneity and quality through seismic imaging.

The primary objective of the project is to increase the profitability, producibility and efficiency of recovery of oil from existing and undiscovered Upper Jurassic fields characterized by reef and carbonate shoals associated with pre-Mesozoic basement paleohighs.

The principal research effort for Year 2 of the project has been reservoir characterization, 3-D modeling and technology transfer. This effort has included six tasks: 1) the study of rock-fluid interactions, 2) petrophysical and engineering characterization, 3) data integration, 4) 3-D geologic modeling, 5) 3-D reservoir simulation and 6) technology transfer. This work was scheduled for completion in Year 2.

Overall, the project work is on schedule. Geoscientific reservoir characterization is essentially completed. The architecture, porosity types and heterogeneity of the reef and shoal reservoirs at Appleton and Vocation Fields have been characterized using geological and geophysical data. The study of rock-fluid interactions is near completion. Observations regarding

the diagenetic processes influencing pore system development and heterogeneity in these reef and shoal reservoirs have been made. Petrophysical and engineering property characterization has been essentially completed. Porosity and permeability data at Appleton and Vocation Fields have been analyzed, and well performance analysis has been conducted. Data integration is up to date, in that, the geological, geophysical, petrophysical and engineering data collected to date for Appleton and Vocation Fields have been compiled into a fieldwide digital database. 3-D geologic modeling of the structures and reservoirs at Appleton and Vocation Fields has been completed. The model represents an integration of geological, petrophysical and seismic data. 3-D reservoir simulation of the reservoirs at Appleton and Vocation Fields has been completed. The 3-D geologic model served as the framework for the simulations. A technology workshop on reservoir characterization and modeling at Appleton and Vocation Fields was conducted to transfer the results of the project to the petroleum industry.

## Table of Contents

	Page
Title Page .....	i
Disclaimer .....	i
Abstract .....	ii
Table of Contents .....	iv
Introduction .....	1
Executive Summary .....	9
Experimental .....	12
Work Accomplished in Year 2 .....	12
Work Planned for Year 3 .....	183
Results and Discussion .....	203
Geoscientific Reservoir Characterization.....	203
Rock-Fluid Interactions .....	210
Petrophysical and Engineering Property Characterization.....	218
3-D Geologic Modeling .....	219
3-D Reservoir Simulation Model .....	222
Data Integration .....	223
Conclusions .....	223
References .....	226

## **INTRODUCTION**

The University of Alabama in cooperation with Texas A&M University, McGill University, Longleaf Energy Group, Strago Petroleum Corporation, and Paramount Petroleum Company is undertaking an integrated, interdisciplinary geoscientific and engineering research project. The project is designed to characterize and model reservoir architecture, pore systems and rock-fluid interactions at the pore to field scale in Upper Jurassic Smackover reef and carbonate shoal reservoirs associated with varying degrees of relief on pre-Mesozoic basement paleohighs in the northeastern Gulf of Mexico. The project effort includes the prediction of fluid flow in carbonate reservoirs through reservoir simulation modeling that utilizes geologic reservoir characterization and modeling and the prediction of carbonate reservoir architecture, heterogeneity and quality through seismic imaging.

The Upper Jurassic Smackover Formation (Figure 1) is one of the most productive hydrocarbon reservoirs in the northeastern Gulf of Mexico. Production from Smackover carbonates totals 1 billion barrels of oil and 4 trillion cubic feet of natural gas. The production is from three plays: 1) basement ridge play, 2) regional peripheral fault play, and 3) salt anticline play (Figure 2). Unfortunately, much of the oil in the Smackover fields in these plays remains unrecovered because of a poor understanding of the rock and fluid characteristics that affects our understanding of reservoir architecture, heterogeneity, quality, fluid flow and producibility. This scenario is compounded because of inadequate techniques for reservoir detection and the characterization of rock-fluid interactions, as well as imperfect models for fluid flow prediction. This poor understanding is particularly illustrated for the case with Smackover fields in the basement ridge play (Figure 3) where independent producers dominate the development and management of these fields. These producers do not have the financial resources and/or staff

<i>System</i>	<i>Series</i>	<i>Stage</i>	<i>Formation (Member)</i>
Jurassic	Upper Jurassic	Kimmeridgian	Haynesville Formation
			Buckner Anhydrite Member
	Middle Jurassic	Oxfordian	Smackover Formation
		Callovian	Norphlet Formation
Paleozoic			" Basement "

Figure 1. Jurassic stratigraphy in the study area.

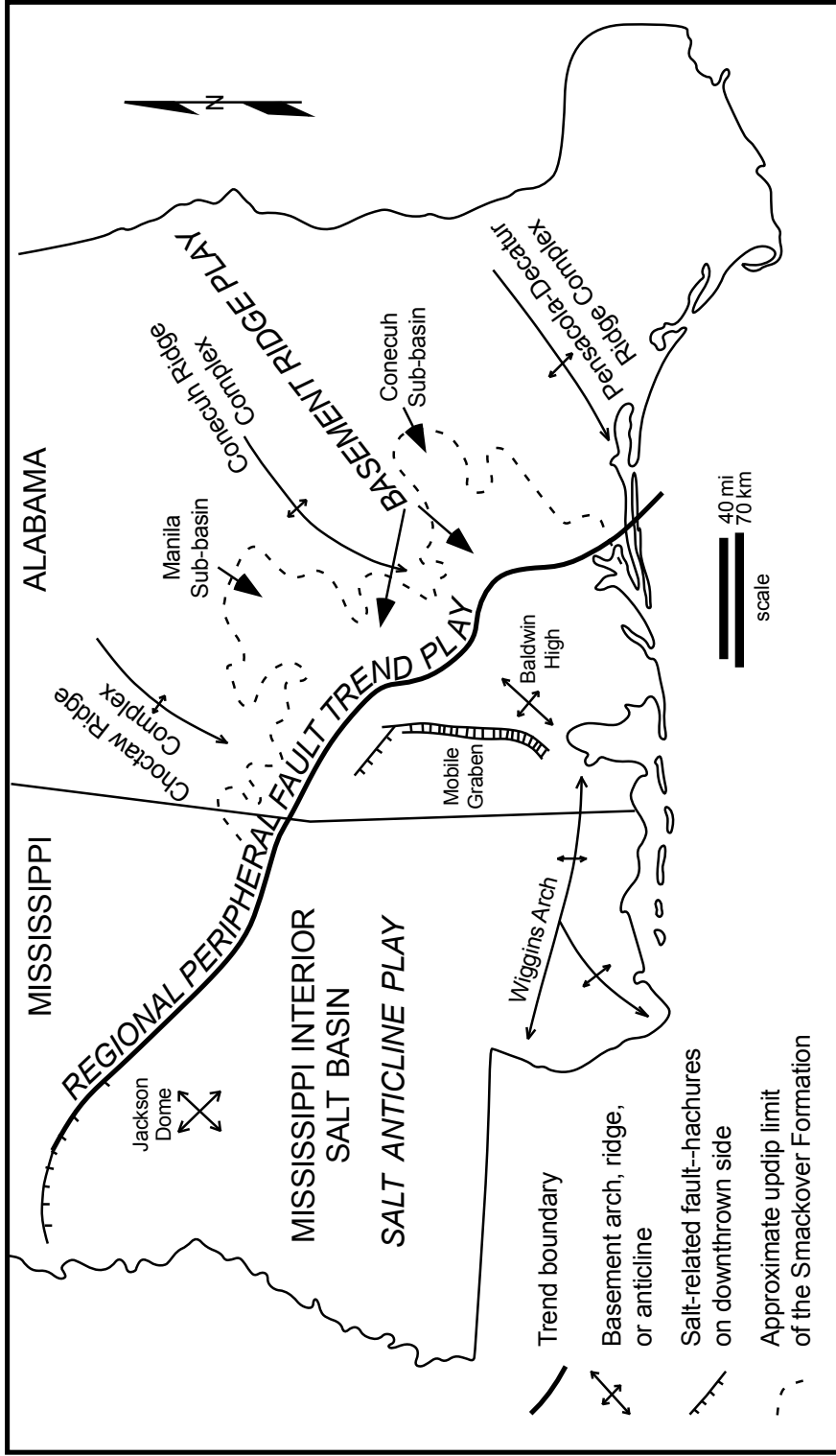


Figure 2. Major petroleum trends in study area.

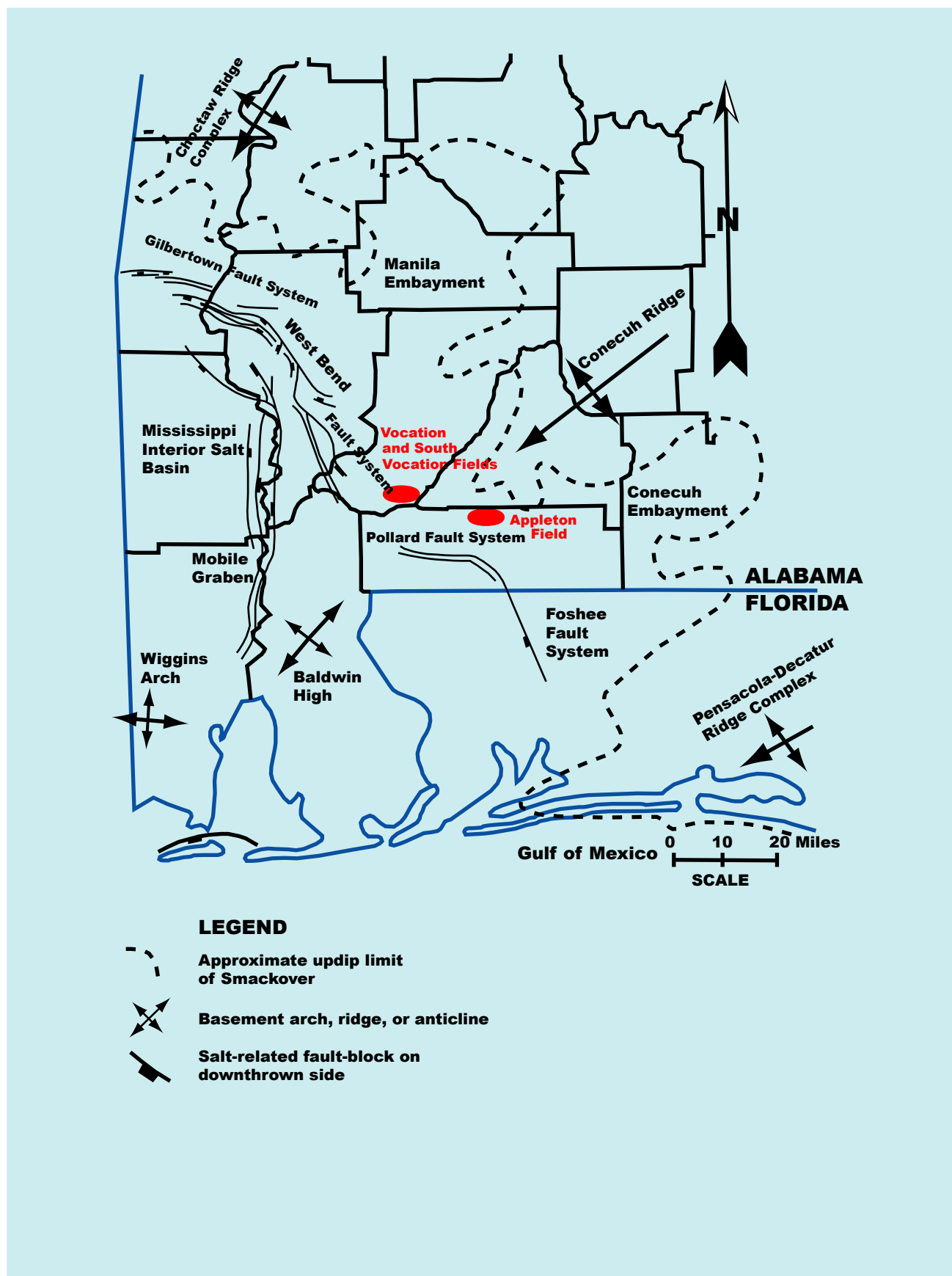


Figure 3. Location of Appleton and Vocation / South Vocation Fields.



expertise to substantially improve the understanding of the geoscientific and engineering factors affecting the producibility of Smackover carbonate reservoirs, which makes research and application of new technologies for reef-shoal reservoirs all that more important and urgent. The research results from studying the fields identified for this project will be of direct benefit to these producers.

This interdisciplinary project is a 3-year effort to characterize, model and simulate fluid flow in carbonate reservoirs and consists of 3 phases and 11 tasks. Phase 1 (1 year) of the project involves geoscientific reservoir characterization, rock-fluid interactions, petrophysical and engineering property characterization, and data integration. Phase 2 (1.5 years) includes geologic modeling and reservoir simulation. Phase 3 (0.5 year) involves building the geologic-engineering model, testing the geologic-engineering model, and applying the geologic-engineering model.

The principal goal of this project is to assist independent producers in increasing oil producibility from reef and shoal reservoirs associated with pre-Mesozoic paleotopographic features through an interdisciplinary geoscientific and engineering characterization and modeling of carbonate reservoir architecture, heterogeneity, quality and fluid flow from the pore to field scale.

The objectives of the project are as follows:

1. Evaluate the geological, geophysical, petrophysical and engineering properties of reef-shoal reservoirs and their associated fluids, in particular, the Appleton (Figure 4) and Vocation (Figure 5) Fields.
2. Construct a digital database of integrated geoscience and engineering data taken from reef-shoal carbonate reservoirs associated with basement paleohighs.

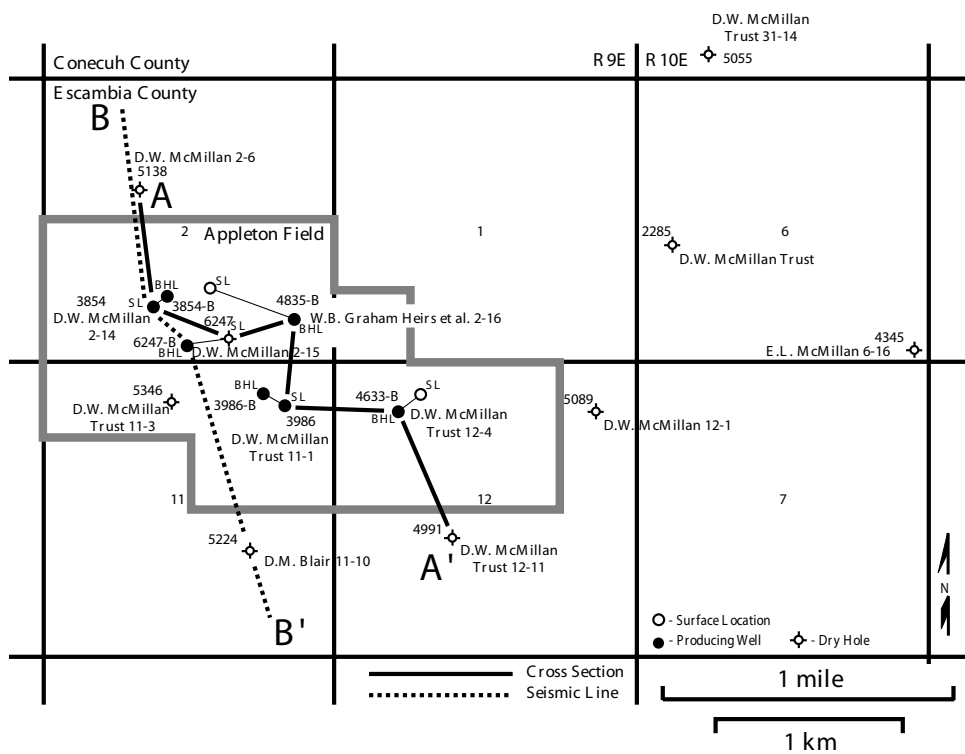


Figure 4. Appleton Field Unit area.

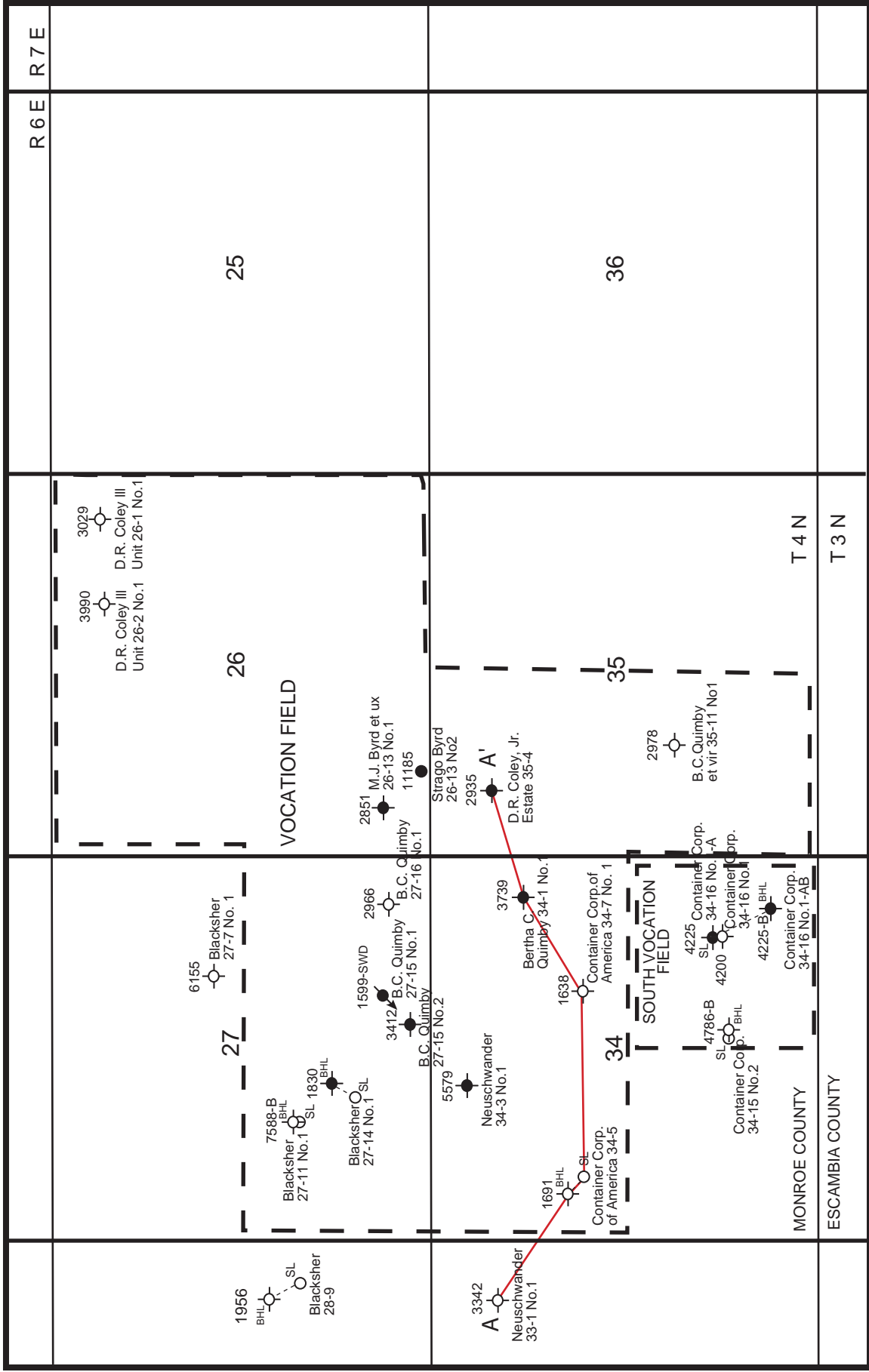


Figure 5. Vocation Field area.

3. Develop a geologic-engineering model(s) for improving reservoir detection, reservoir characterization, flow-space imaging, flow simulation, and performance prediction for reef-shoal carbonate reservoirs based on a systematic study of Appleton and Vocation Fields.
4. Validate and apply the geologic-engineering model(s) on a prospective Smackover reservoir through an iterative interdisciplinary approach, where adjustments of properties and concepts will be made to improve the model(s).

This project has direct and significant economic benefits because the Smackover is a prolific hydrocarbon reservoir in the northeastern Gulf of Mexico. Smackover reefs represent an underdeveloped reservoir, and the basement ridge play in which these reefs are associated represents an underexplored play. Initial estimations indicate the original oil resource target available in this play from the 40 fields that have been discovered and developed approximates at least 160 million barrels. Any newly discovered fields are expected to have an average of 4 million barrels of oil. The combined estimated reserves of the Smackover fields (Appleton and Vocation Fields) proposed for study in this project total 9 million barrels of oil. Successful completion of the project should lead to increased oil producibility from Appleton and Vocation Fields and from Smackover reservoirs in general. Production of these domestic resources will serve to reduce U.S. dependence on foreign oil supplies.

Completion of the project will contribute significantly to the understanding of: the geologic factors controlling reef and shoal development on paleohighs, carbonate reservoir architecture and heterogeneity at the pore to field scale, generalized rock-fluid interactions and alterations in carbonate reservoirs, the geological and geophysical attributes important to geologic modeling of reef-shoal carbonate reservoirs, the critical factors affecting fluid flow in carbonate reservoirs, particularly with regard to reservoir simulation and the analysis of well performance, the

elements important to the development of a carbonate geologic-engineering model, and the geological, geophysical, and/or petrophysical properties important to improved carbonate reservoir detection, characterization, imaging and flow prediction.

## **EXECUTIVE SUMMARY**

The University of Alabama in cooperation with Texas A&M University, McGill University, Longleaf Energy Group, Strago Petroleum Corporation, and Paramount Petroleum Company are undertaking an integrated, interdisciplinary geoscientific and engineering research project. The project is designed to characterize and model reservoir architecture, pore systems and rock-fluid interactions at the pore to field scale in Upper Jurassic Smackover reef and carbonate shoal reservoirs associated with varying degrees of relief on pre-Mesozoic basement paleohighs in the northeastern Gulf of Mexico. The project effort includes the prediction of fluid flow in carbonate reservoirs through reservoir simulation modeling which utilizes geologic reservoir characterization and modeling and the prediction of carbonate reservoir architecture, heterogeneity and quality through seismic imaging.

The primary objective of the project is to increase the profitability, producibility and efficiency of recovery of oil from existing and undiscovered Upper Jurassic fields characterized by reef and carbonate shoals associated with pre-Mesozoic basement paleohighs.

The principal research effort for Year 2 of the project has been reservoir description and characterization. This effort has included four tasks: 1) geoscientific reservoir characterization, 2) the study of rock-fluid interactions, 3) petrophysical and engineering characterization and 4) data integration.

Geoscientific reservoir characterization is essentially completed. The architecture, porosity types and heterogeneity of the reef and shoal reservoirs at Appleton and Vocation Fields have

been characterized using geological and geophysical data. All available whole cores have been described and thin sections from these cores have been studied. Depositional facies were determined from the core descriptions and well logs. The thin sections studied represent the depositional facies identified. The core data and well log signatures have been integrated and calibrated on graphic logs. The well log and seismic data have been tied through the generation of synthetic seismograms. The well log, core, and seismic data have been entered into a digital database. Structural maps on top of the basement, reef, and Smackover/Buckner have been constructed. An isopach map of the Smackover interval has been prepared, and thickness maps of the Smackover facies have been prepared. Cross sections have been constructed to illustrate facies changes across these fields. Maps have been prepared using the 3-D seismic data that Longleaf and Strago contributed to the project to illustrate the structural configuration of the basement surface, the reef surface, and Buckner/Smackover surface. Seismic forward modeling and attribute-based characterization has been completed for Appleton Field. Petrographic analysis has been completed and a paragenetic sequence for the Smackover in these fields has been prepared.

The study of rock-fluid interactions is near completion. Thin sections (379) have been studied from 11 cores from Appleton Field to determine the impact of cementation, compaction, dolomitization, dissolution and neomorphism has had on the reef and shoal reservoirs in this field. Thin sections (237) have been studied from 11 cores from Vocation Field to determine the paragenetic sequence for the reservoir lithologies in this field. An additional 73 thin sections have been prepared for the shoal and reef lithofacies in Vocation Field to identify the diagenetic processes that played a significant role in the development of the pore systems in the reservoirs at Vocation Field. The petrographic analysis and pore system studies essentially have been

completed. A paragenetic sequence for the Smackover carbonates at Appleton and Vocation Fields has been prepared. Pore systems studies continue.

Petrophysical and engineering property characterization is essentially completed. Petrophysical and engineering property data have been gathered and tabulated for Appleton and Vocation Fields. These data include oil, gas and water production, fluid property (PVT) analyses and porosity and permeability information. Porosity and permeability characteristics of Smackover facies have been analyzed for each well using porosity histograms, permeability histograms and porosity versus depth plots. Log porosity versus core porosity and porosity versus permeability cross plots for wells in the fields have been prepared.

Well performance studies through type curve and decline curve analyses have been completed for the wells in Appleton and Vocation Fields, and the original oil in place and recoverable oil remaining for the fields has been calculated.

3-D geologic modeling of the structure and reservoirs at Appleton and Vocation Fields has been completed. The model represents an integration of geological, petrophysical and seismic data.

3-D reservoir simulations of the reservoirs at Appleton and Vocation Fields have been completed. The 3-D geologic model served as the framework for these simulations. The acquisition of additional pressure data would improve the simulation models.

Data integration is up to date, in that, geological, geophysical, petrophysical and engineering data collected to date for Appleton and Vocation Fields have been compiled into a fieldwide digital database for development of the geologic-engineering model for the reef and carbonate shoal reservoirs for each of these fields.

A technology workshop on reservoir characterization and modeling at Appleton and Vocation Fields was conducted to transfer the results of the project to the petroleum industry.

## EXPERIMENTAL

The principal research effort for Year 2 of the project has been reservoir characterization, including the study of rock-fluid interactions, petrophysical and engineering characterization and data integration; 3-D modeling, including 3-D geologic modeling and 3-D reservoir simulation; and technology transfer (Table 1).

**Table 1. Milestone Chart.**

Tasks	Project Year/Quarter											
	2000		2001				2002				2003	
	3	4	1	2	3	4	1	2	3	4	1	2
<b>Reservoir Characterization (Phase 1)</b>												
Task 1—Geoscientific Reservoir Characterization	xxxxxx	xxx										
Task 2—Rock-Fluid Interactions	xxxxxx	xxx										
Task 3—Petrophysical Engineering Characterization	xxxxxx	xxx										
Task 4—Data Integration				xxx								
<b>3-D Modeling (Phase 2)</b>												
Task 5—3-D Geologic Model					xxxxxx							
Task 6—3-D Reservoir Simulation Model								xxxxxx				
Task 7—Geologic-Engineering Model									xxxxxx			
<b>Testing and Applying Model (Phase 3)</b>												
Task 8—Testing Geologic-Engineering Model												xxxxxx
Task 9—Applying Geologic-Engineering Model												xxxxxx
<b>Technological Transfer</b>												
Task 10—Workshops								xx				xx
<b>Technical Reports</b>												
Task 11—Quarterly, Topical and Annual Reports			x	x	x	x	x	x	x	x	x	x

xxxxx Work Planned

## Work Accomplished in Year 2

### *Reservoir Description and Characterization (Phase 1)*

**Task 1—Geoscientific Reservoir Characterization.**--This task will characterize reservoir architecture, pore systems and heterogeneity based on geological and geophysical properties. This work will be done for all well logs, cores, seismic data and other data for Vocation Field and will be done for Appleton Field by integrating the new data obtained from drilling the



sidetrack well in Appleton Field and the data available from five additional cores and 3-D seismic in the field area. The first phase of the task includes core descriptions, including lithologies, sedimentary structures, lithofacies, depositional environments, systems tracts, and depositional sequences. Graphic logs constructed from the core studies will depict the information described above. Core samples will be selected for petrographic, XRD, SEM, and microprobe analyses. The graphic logs will be compared to available core analysis and well log data. The core features and core analyses will be calibrated to the well log patterns. A numerical code system will be established so that these data can be entered into the digital database for comparison with the core analysis data and well log measurements and used in the reservoir modeling. The next phase is the link between core and well log analysis and reservoir modeling. It involves the preparation of stratigraphic and structural cross sections to illustrate structural growth, lithofacies and reservoir geometry, and depositional systems tract distribution. Maps will be prepared to illustrate lithofacies distribution, stratigraphic and reservoir interval thickness (isolith and isopach maps), and stratal structural configurations. These cross sections and maps, in association with the core descriptions, will be utilized to make sequence stratigraphic, environment of deposition, and structural interpretations. Standard industry software, such as StratWorks and Z-Map, will be used in the preparation of the cross sections and subsurface maps. The third phase will encompass the interpreting of seismic data and performing stratigraphic and structural analyses. Seismic interpretations will be guided by the generation of synthetic seismograms resulting from the tying of well log and seismic data and by the comparison of seismic transects with geologic cross sections. Seismic forward modeling and attribute-based characterization will be performed. Structure and isopach maps constructed from well logs will be refined utilizing the seismic data. The seismic imaging of the structure and

stratigraphy, forward modeling and attribute characterization will be accomplished utilizing standard industry software, such as 2d/3d PAK, Earthwave and SeisWorks. The next phase includes identification and quantification of carbonate mineralogy and textures (grain, matrix and cement types), pore topology and geometry, and percent of porosity and is performed to support and enhance the visual core descriptions. These petrographic, XRD, SEM and microprobe analyses will confirm and quantify the observations made in the core descriptions. This analysis provides the opportunity to study reservoir architecture and heterogeneity at the microscopic scale. The fifth phase involves study of pore systems in the reservoir, including pore types and throats through SEM analysis. This phase will examine pore shape and geometry and the nature and distribution of pore throats to determine the features of the pore systems that are affecting reservoir producibility.

**Appleton Field.** All available whole cores (11) from Appleton Field have been described and thin sections (379) from these cores have been studied. Graphic logs were constructed describing each of the cores (Figures 6 through 16). Depositional facies were determined from the core descriptions. From the study of thin sections, the petrographic characteristics of these lithofacies have been described, and the pore systems inherent to these facies have been identified (Table 2). The core data and well log signatures have been integrated and calibrated on these graphic logs.

For Appleton Field (Figure 4), the well log and core data have been entered into a digital database and structural maps on top of the basement (Figure 17), reef (Figure 18), and Smackover/Buckner (Figure 19) have been constructed. An isopach map of the Smackover interval has been prepared (Figure 20), and thickness maps of the sabkha facies (Figure 21), tidal flat facies (Figure 22), shoal complex (Figure 23), tidal flat/shoal complex (Figure 24) and reef

# MADDEN 9-15 #1 PERMIT # 10084B KB: 263.2'

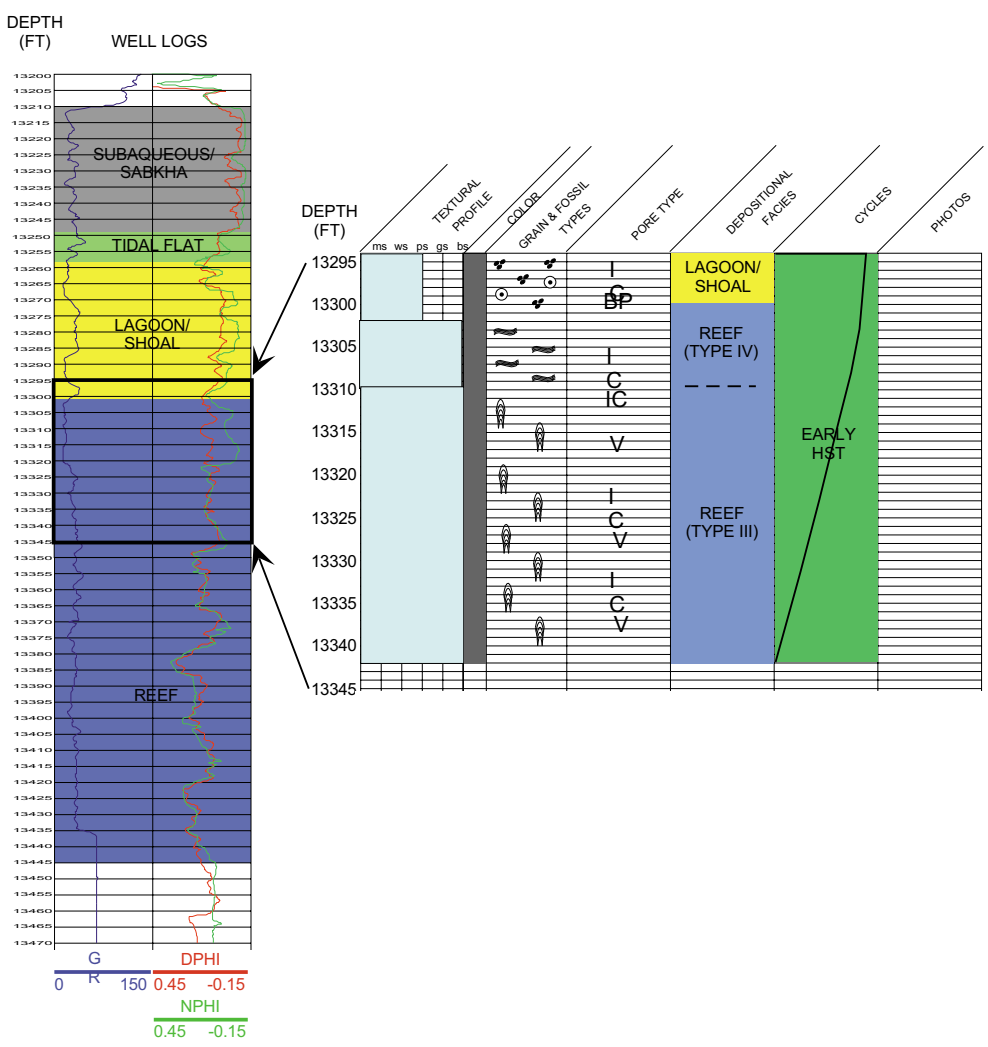


Figure 6. Graphic log for well Permit # 10084B by W.C. Parcell

# MCMILLAN 3-9 #1 PERMIT # 11030-B KB: 237'

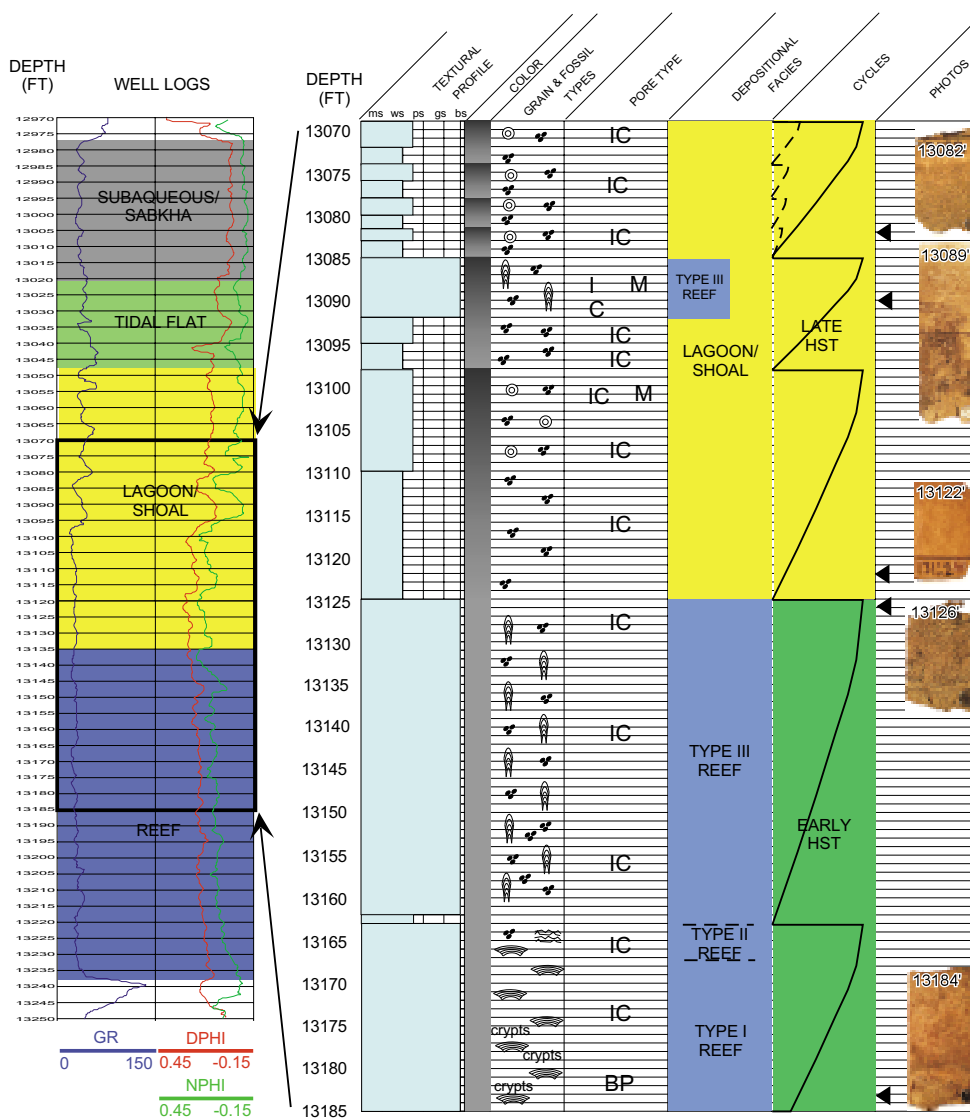


Figure 7. Graphic log for well Permit # 11030B  
by W.C Parcell

# HOOPER MATHEWS UNIT 4-8 #1 PERMIT # 2377 KB: 202.9'

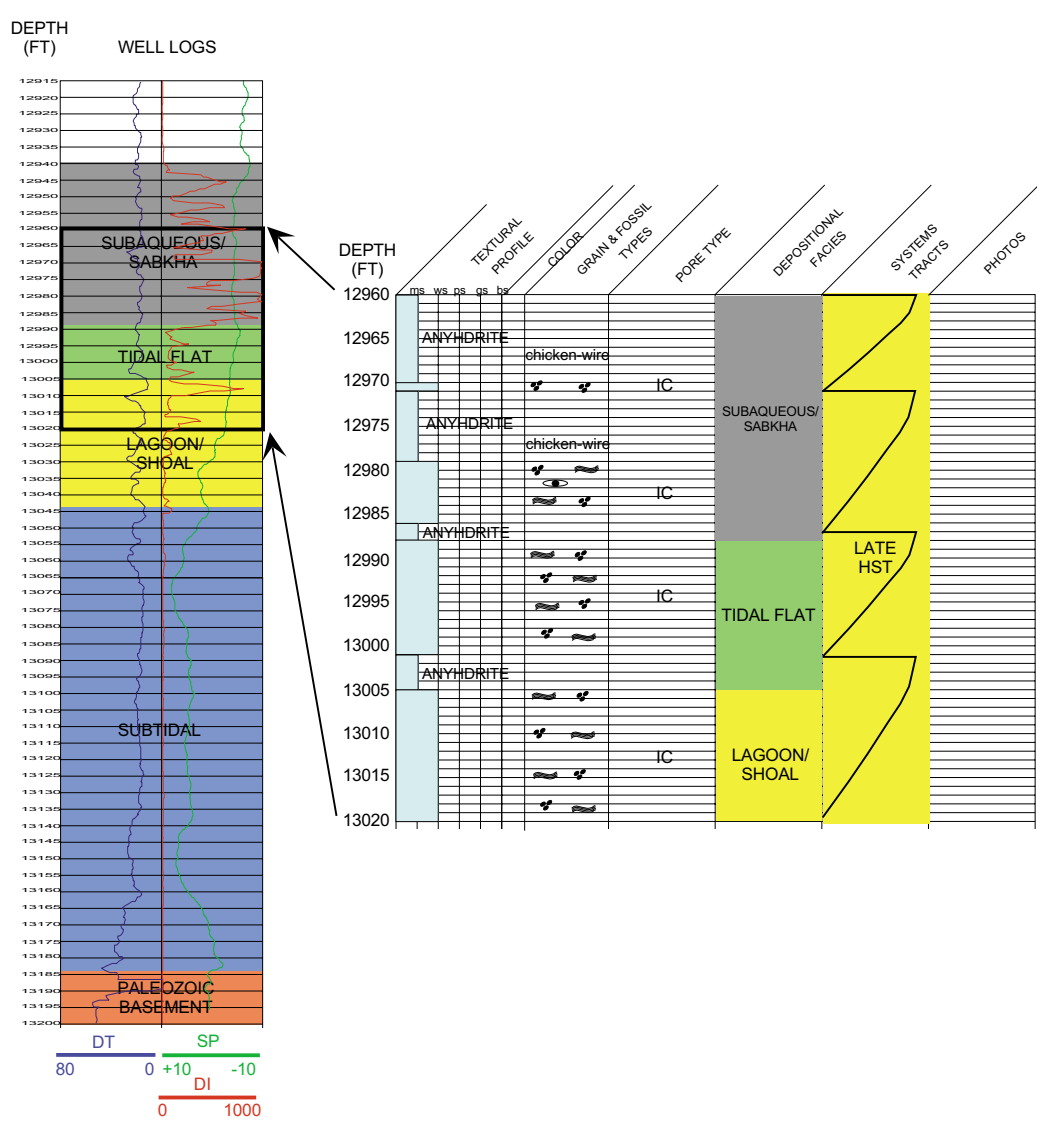


Figure 8. Graphic log for well Permit # 2377 by W.C. Parcell

# #4 D.W. McMILLAN 2-14

## Permit # 3854

### KB: 242 ft

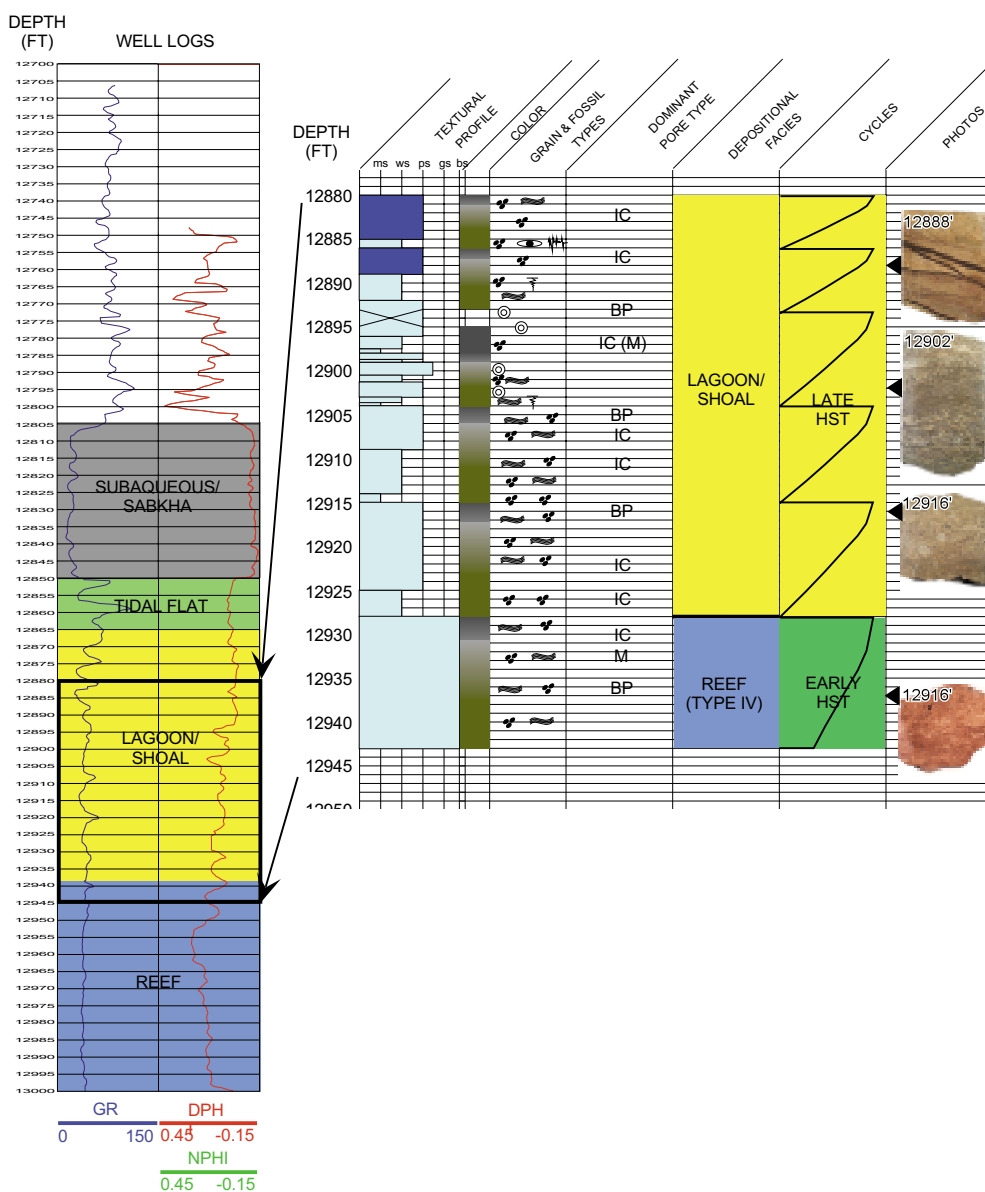


Figure 9. Graphic log for well Permit # 3854 by W.C. Parcell

# #2 D.W. McMILLAN 1-1

## Permit # 3986

### KB: 254'

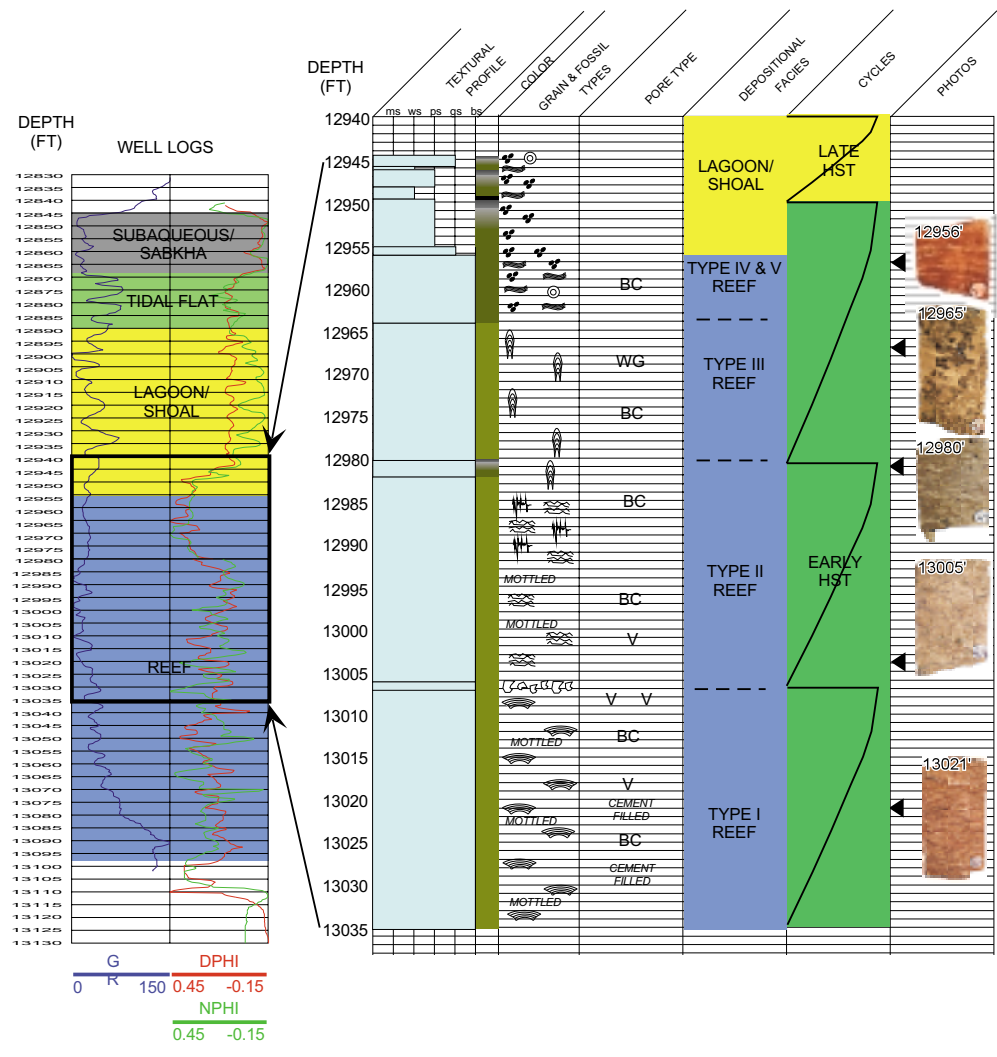


Figure 10. Graphic log for well Permit # 3986 by W.C. Parcell

# D.W. McMILLAN 12-4 Permit # 4633-B KB: 268'

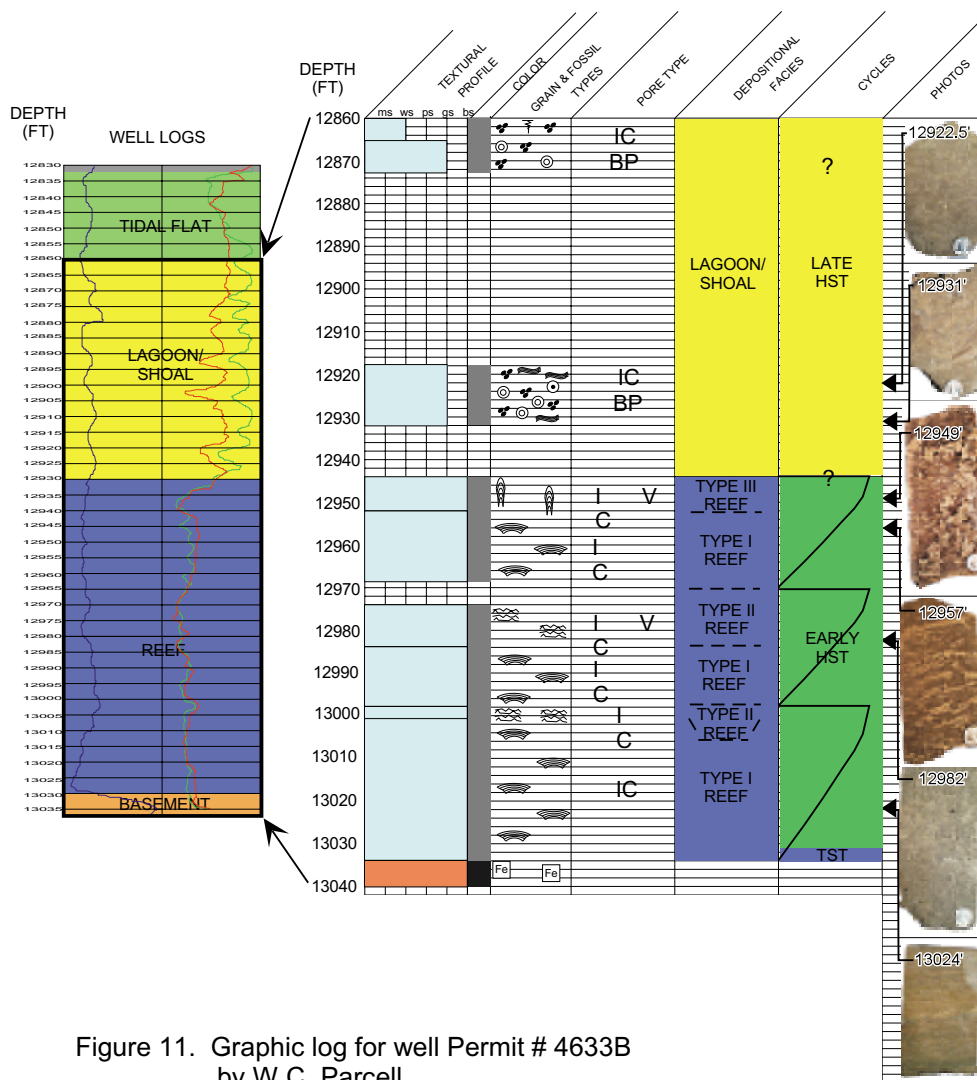


Figure 11. Graphic log for well Permit # 4633B by W.C. Parcell



# #1 W.B. GRAHAM HEIRS 2-16 PERMIT # 4835-B KB: 244'

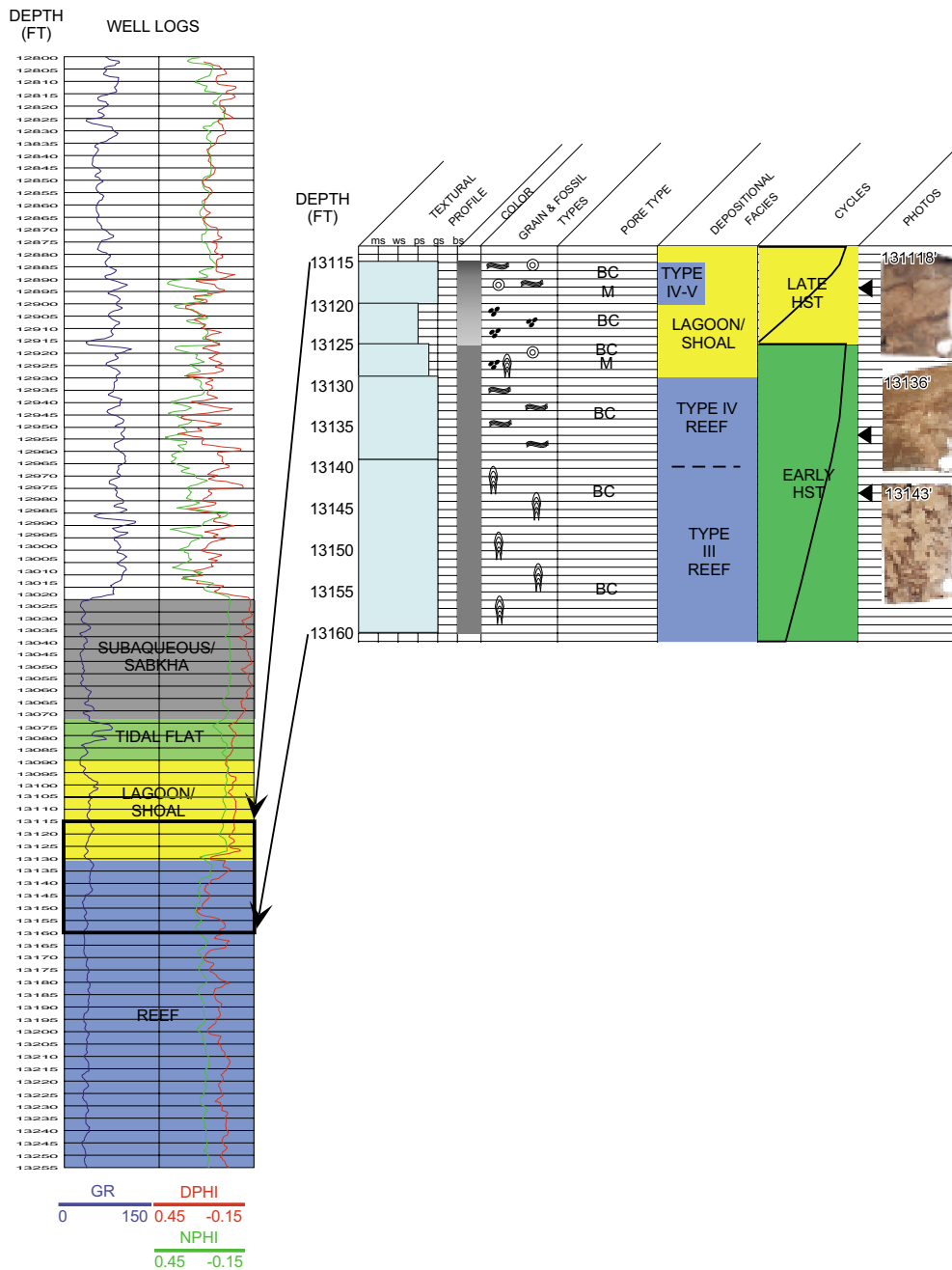


Figure 12. Graphic log for well Permit # 4835B  
by W.C. Parcell

# #4 D.W. McMILLAN 12-11 PERMIT # 4991 KB: 247'

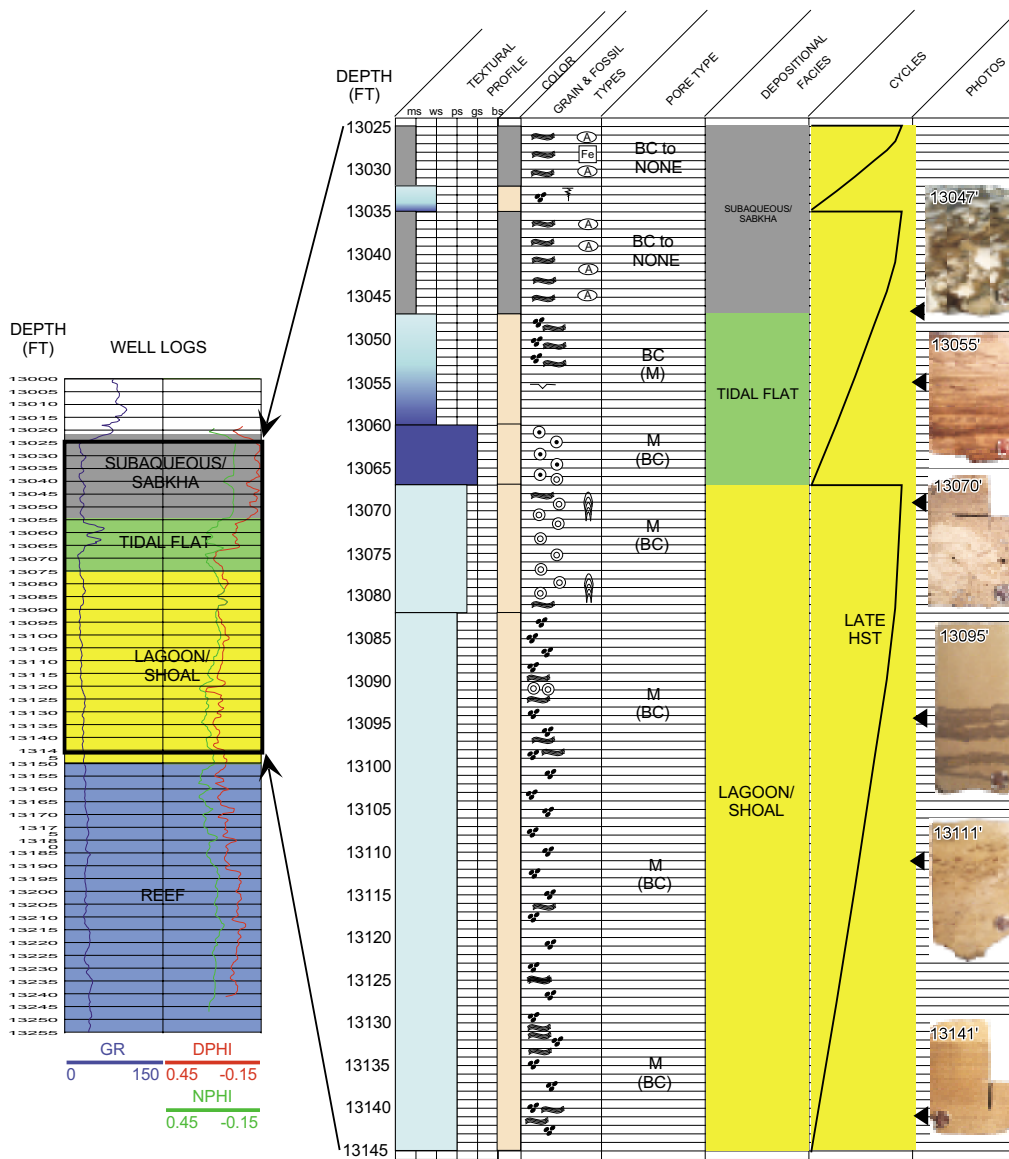


Figure 13. Graphic log for well Permit # 4991 by W.C. Parcell

# D.W. McMILLAN 12-1 PERMIT # 5089 KB: 256'

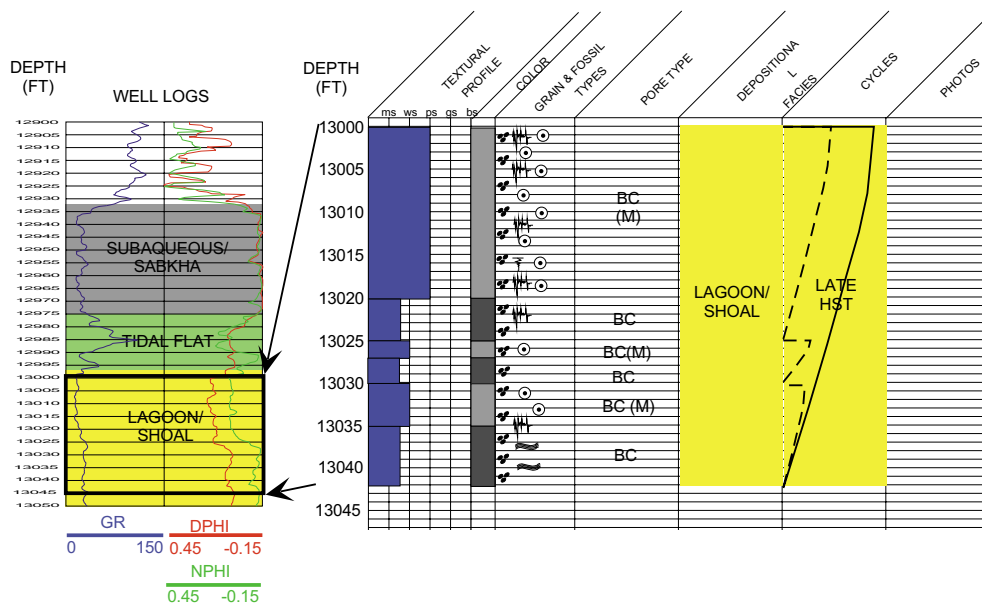


Figure 14. Graphic log for well Permit # 5089 by W.C. Parcel

# D.W. McMILLAN 2-6 #1 Permit # 5138 KB: 245'

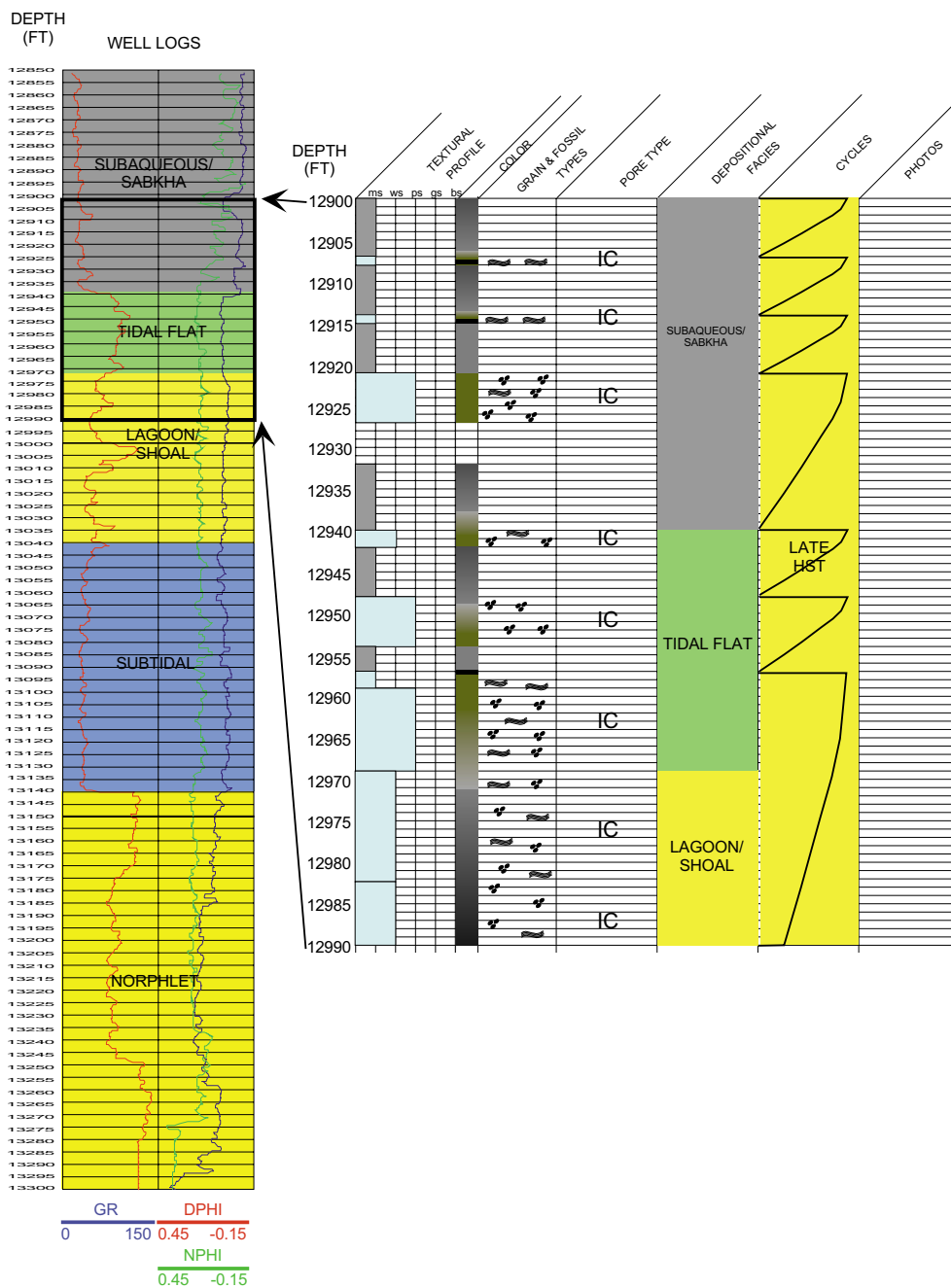


Figure 15. Graphic log for well Permit # 5138 by W.C. Parcell

# LUVETA GRAMBLING 9-13 #1 PERMIT # 6663B KB: 300'

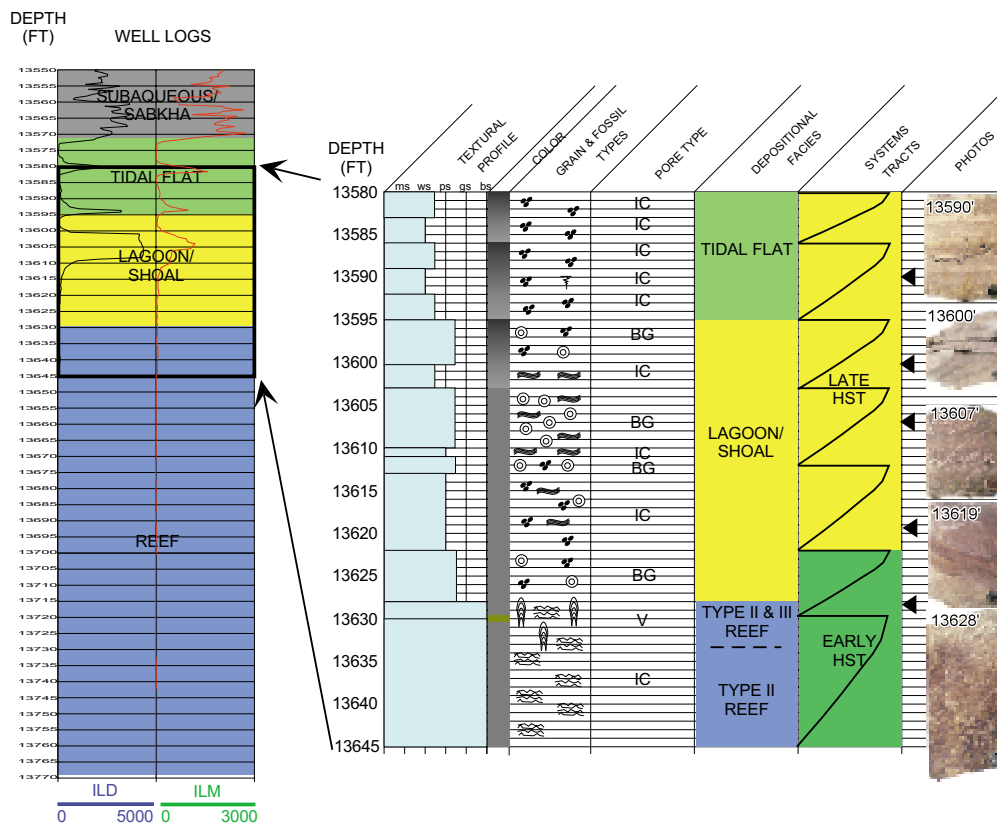


Figure 16. Graphic log for well Permit # 6663B by W.C. Parcell

Table 2. Characteristics of Smackover Lithofacies in the Appleton Field Area.

Lithofacies	Lithology	Allochems	Pore Types	Porosity	Permeability
Carbonate mudstone	Dolostone and anhydritic dolostone	None	Intercrystalline	Low (1.2 to 2.5%)	Low ( 0.01 md)
Peloidal wackestone	Dolostone to calcareous dolostone	Peloids, ooids, intraclasts	Intercrystalline, moldic	Low to moderate (2.6 to 12.4%)	Low ( 0.01 to 0.11 md)
Peloidal packstone	Dolomitic limestone	Peloids, ooids, oncoids, intraclasts	Interparticulate, moldic, intercrystalline	Low to moderate (1.1 to 12.4%)	Low to moderate ( 0.01 to 0.51 md)
Peloidal/oncoidal packstone	Dolostone to calcareous dolostone	Peloids, oncoids, intraclasts	Interparticulate	Low (1.2 to 6.1%)	Low ( 0.01 md)
Peloidal/oolitic packstone	Dolostone	Peloids, ooids, skeletal grains, intraclasts	Moldic, intercrystalline, interparticulate	Low (1.3 to 4.5%)	Low ( 0.01 md)
Peloidal grainstone	Calcareous dolostone	Peloids, oncoids, algal grains, intraclasts	Interparticulate, fenestral, moldic, interparticulate, vuggy	Low to high (1.0 to 19.9%)	Low to high ( 0.01 to 722 md)
Oncoidal grainstone	Calcareous dolostone to dolostone	Oncoids, peloids, intraclasts	Interparticulate, intraparticulate, fenestral	Low to moderate (1.4 to 11.9%)	Low to high ( 0.01 to 8.27 md)
Oolitic grainstone	Dolostone to limestone	Ooids, peloids, oncoids, intraclasts	Interparticulate, moldic, intercrystalline	Moderate to high (8.3 to 20.7%)	Moderate to high (3.09 to 406 md)
Oncoidal/peloidal/oolitic grainstone	Dolostone to calcareous dolostone	Oncoids, peloids, ooids, algal grains	Interparticulate, moldic, vuggy	Low to high (1.9 to 19%)	Low to high ( 0.01 to 219 md)
Algal grainstone	Dolomitic limestone to calcareous dolostone	Algal grains, oncoids, peloids, ooids	Interparticulate, moldic, vuggy, fenestral, intercrystalline	Low to high (1.7 to 23.1%)	Low to high ( 0.01 to 63 md)
Microbial boundstone (bafflestone)	Dolostone	Algae, intraclasts, oncoids, peloids	Shelter, vuggy, interparticulate, intercrystalline	High (11.0 to 29.0%)	High (8.13 to 4106 md)
Microbial bindstone	Dolostone	Algae, peloids, ooids	Shelter, vuggy, fenestral, moldic, interparticulate	High (11.9 to 20.7%)	High (11 to 1545 md)
Algal laminite	Dolostone to dolomitic limestone	Algae, peloids, oncoids, intraclasts	Interparticulate, intercrystalline	Low (1.1 to 7.0%)	Low ( 0.01 md)
Anhydrite	Anhydrite	None	None	Low ( 1.0%)	Low ( 0.01 md)

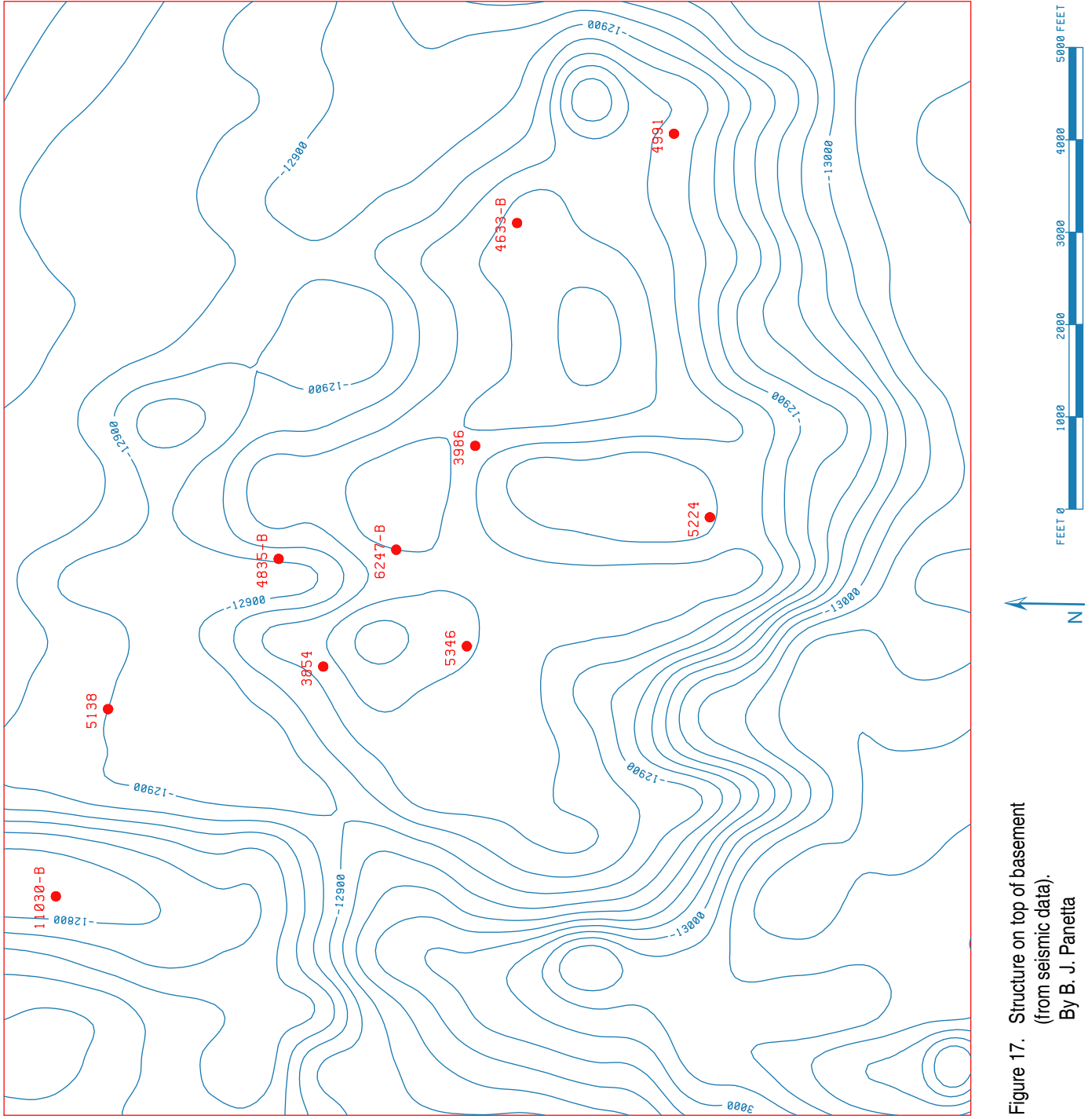


Figure 17. Structure on top of basement  
(from seismic data).  
By B. J. Panetta

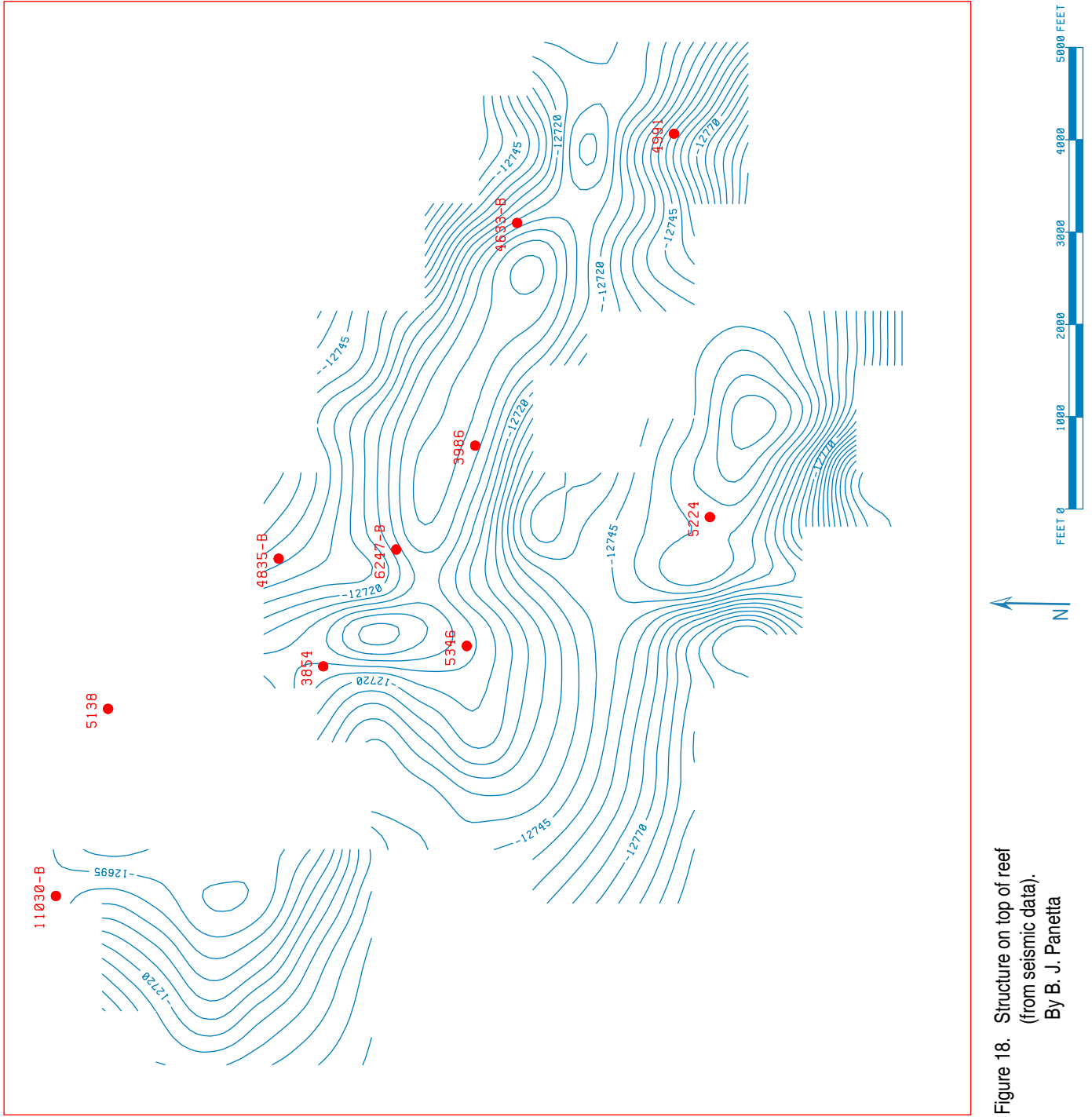


Figure 18. Structure on top of reef  
(from seismic data).  
By B. J. Panetta



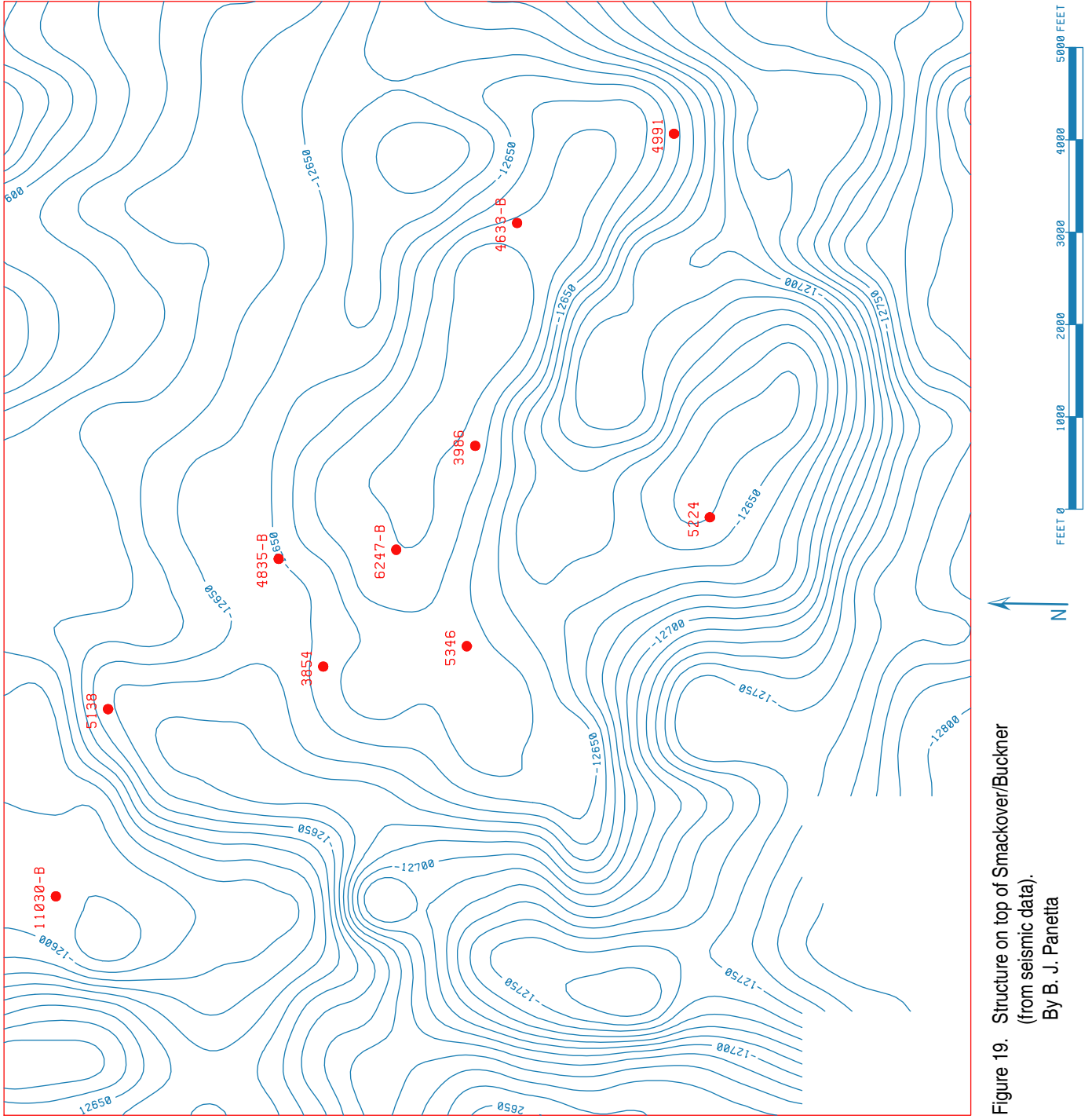


Figure 19. Structure on top of Smackover/Buckner (from seismic data).  
By B. J. Panetta

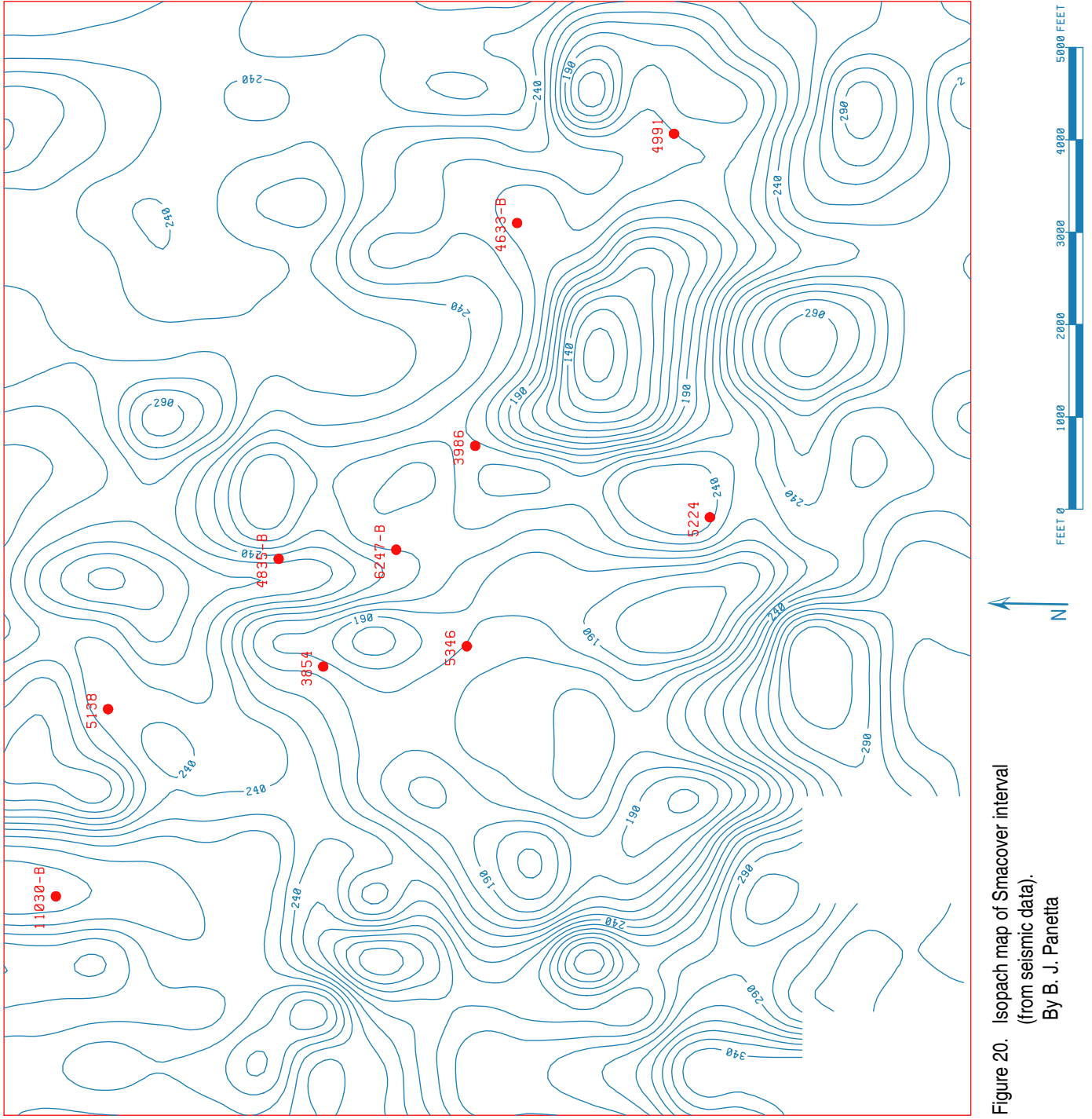


Figure 20. Isopach map of Smacover interval (from seismic data).  
By B. J. Panetta

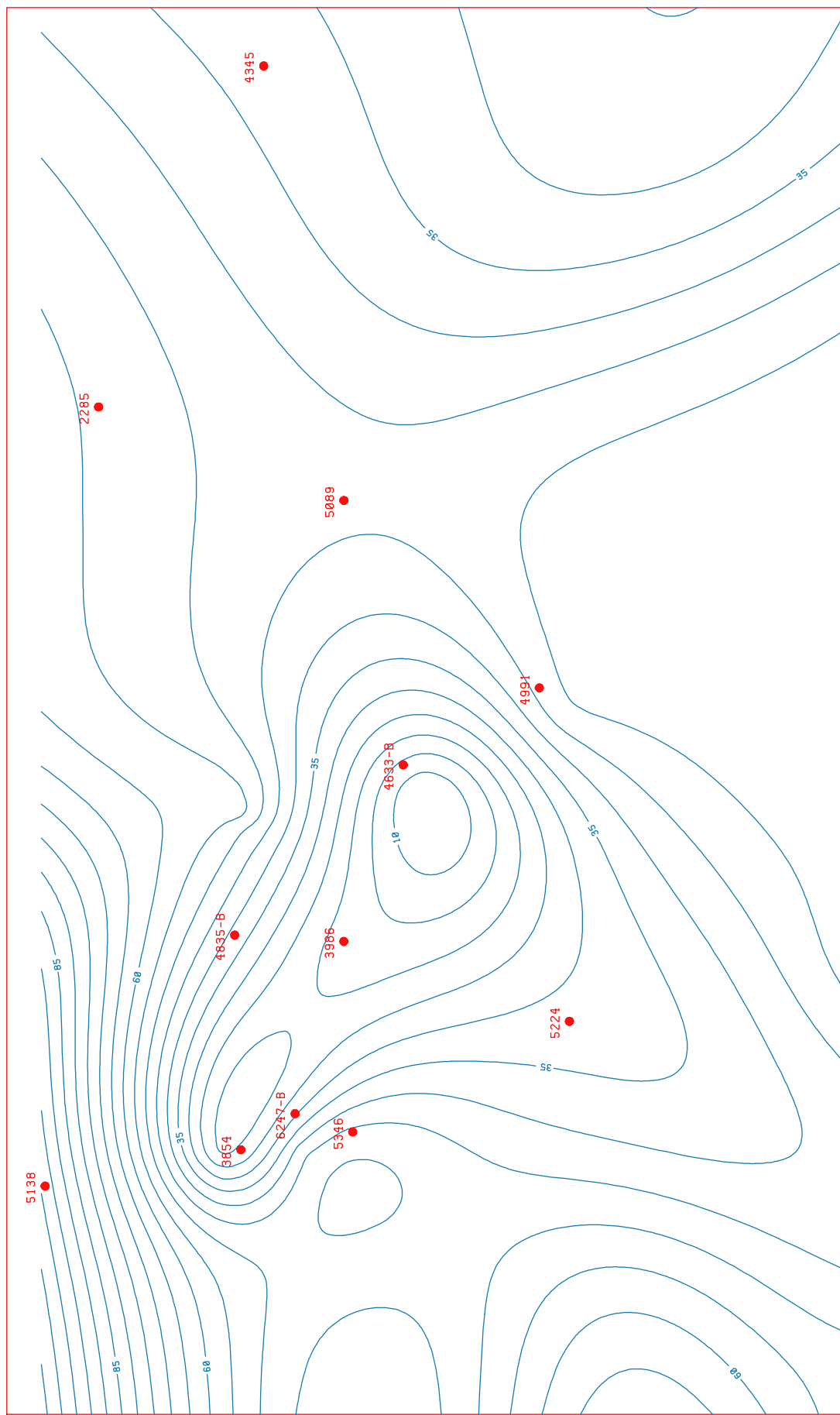


Figure 21. Thickness map of sabkha facies  
(from log data).  
By B. J. Panetta

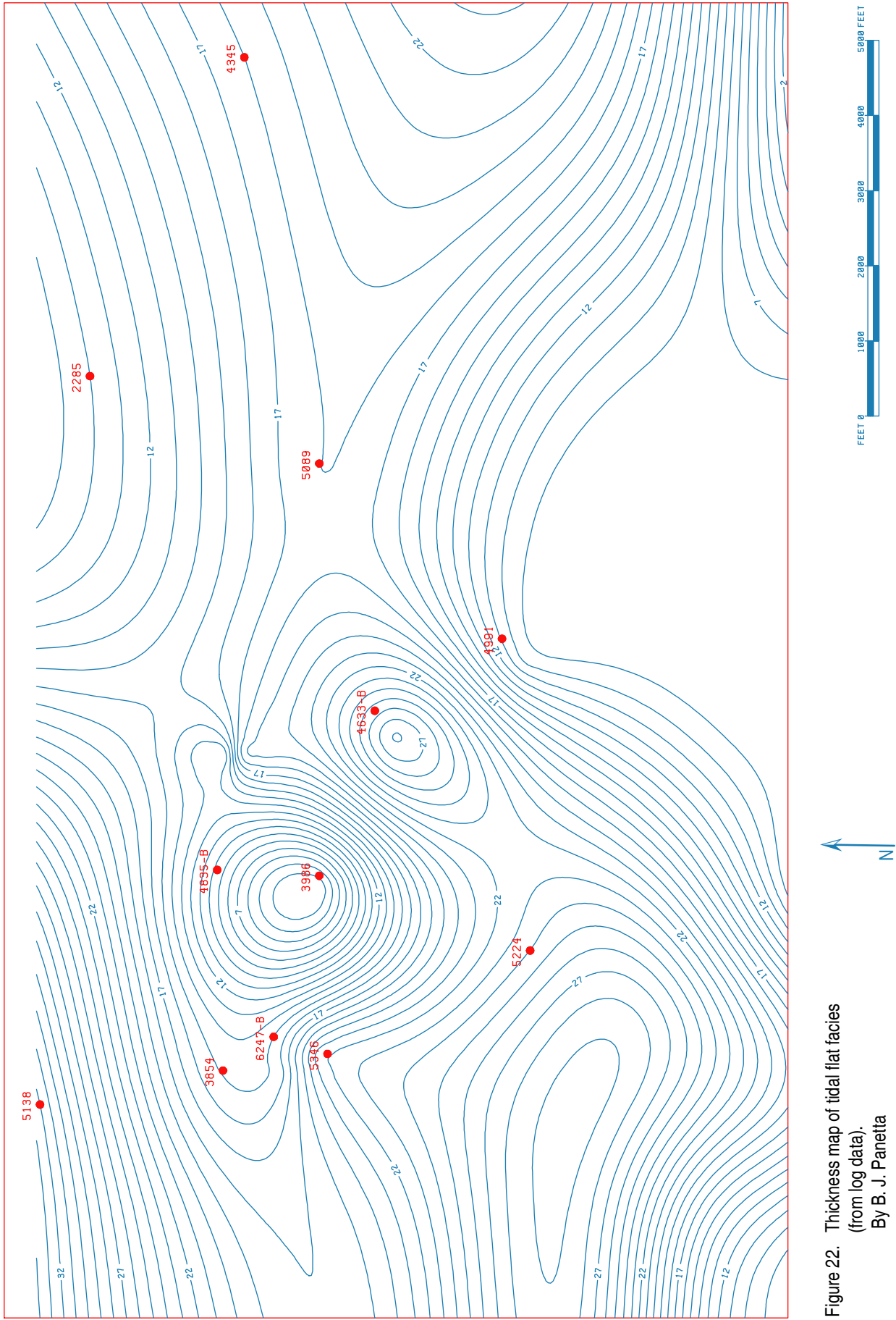


Figure 22. Thickness map of tidal flat facies  
(from log data).  
By B. J. Panetta

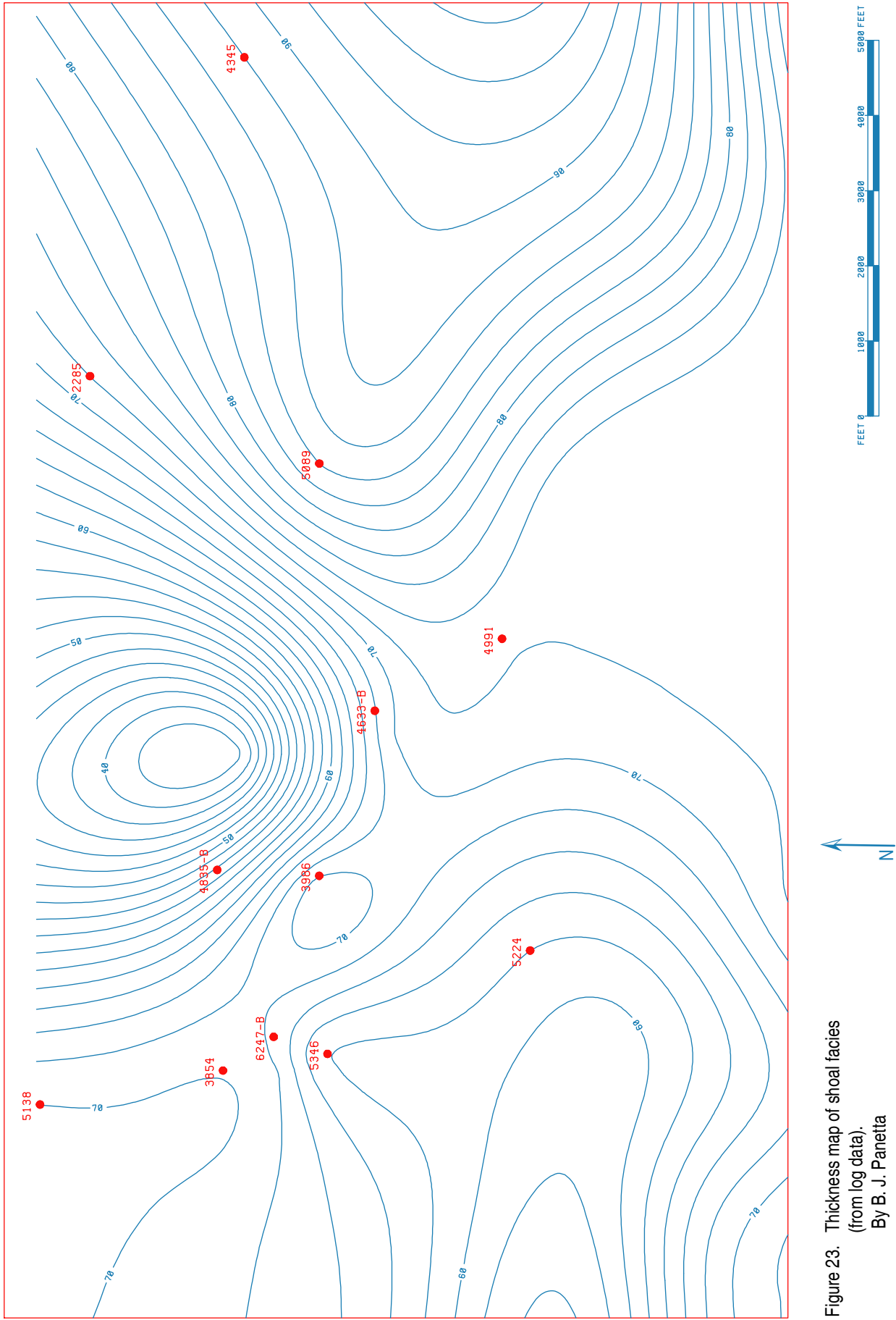


Figure 23. Thickness map of shoal facies (from log data).  
By B. J. Panetta

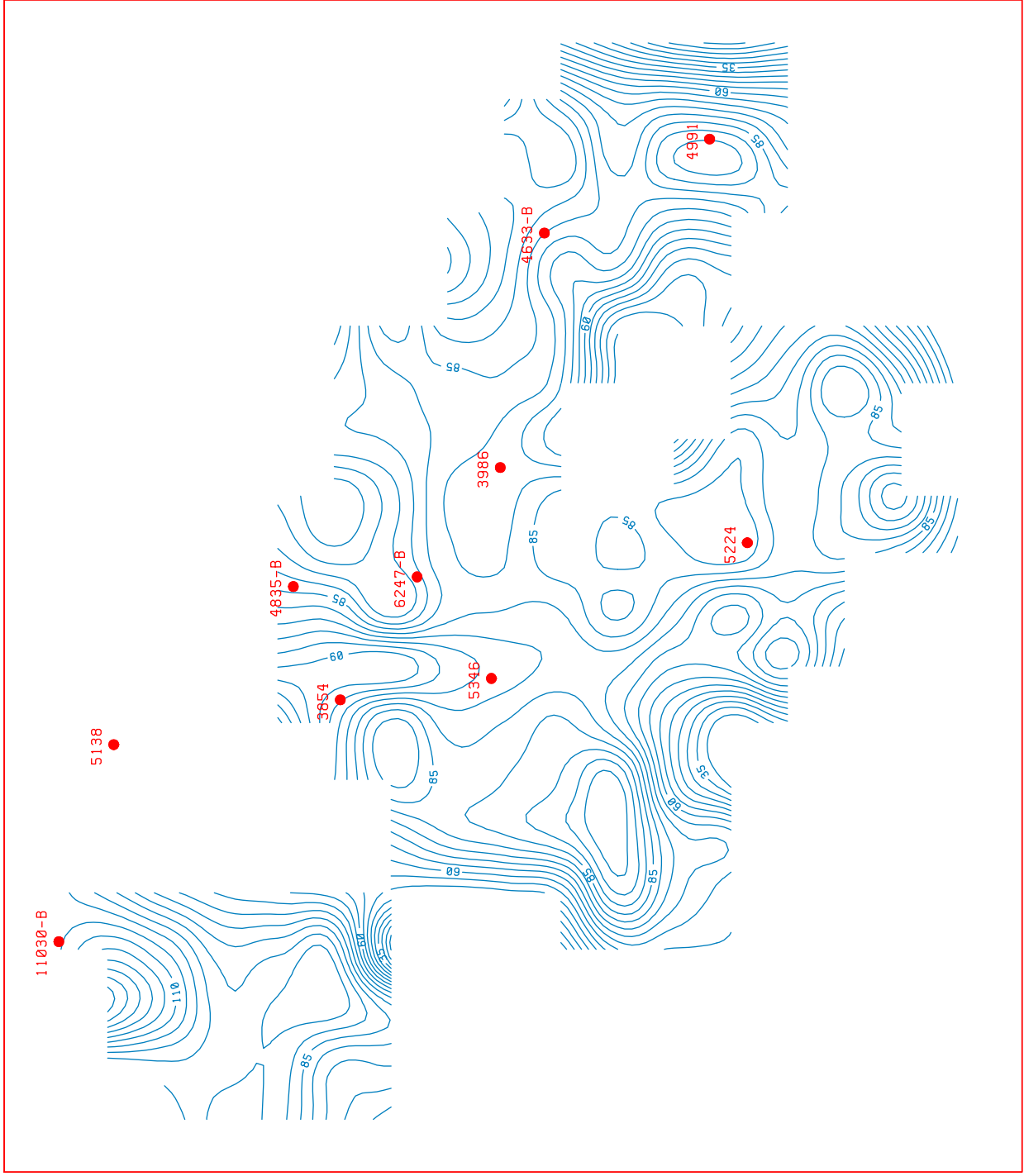


Figure 24. Thickness map of tidal flat and shoal facies (from seismic data).  
By B. J. Panetta

complex (Figure 25) facies have been constructed. A cross section (Figure 26) illustrating the thickness and facies changes across Appleton Field has been prepared.

The core and well log data have been integrated with the 3-D seismic data for Appleton Field that Longleaf contributed to the project. A typical seismic profile for the field illustrating the reef reservoir is shown in Figure 27. Figure 28 is an example of a synthetic seismogram for the field used to tie well log and seismic data. Tables 3 and 4 and Figures 29 through 33 summarize the results of the volume-base, multi-attribute seismic study.

**Vocation Field.** All available whole cores (11) from Vocation Field have been described and thin sections (237) from the cores have been studied. Graphic logs were constructed describing each of the cores (Figures 34 through 44). Depositional facies were determined from the core descriptions. From this work, an additional 73 thin sections are being prepared to provide accurate representation of the lithofacies identified. From the study of thin sections, the petrographic characteristics of these lithofacies have been described, and the pore systems inherent to these facies have been identified (Table 5). The core data and well log signatures have been integrated and calibrated on the graphic logs.

For Vocation Field (Figure 5), the well log and core data have been entered into a digital database and structural maps on top of the basement (Figure 45), reef (Figure 46), and Smackover/Buckner (Figure 47) have been constructed. An isopach of the Smackover interval has been prepared (Figure 48) and a thickness map of the reef complex facies (Figure 49) illustrating the thickness and facies changes across Vocation Field has been prepared. A cross section (Figure 50) illustrating the thickness and facies changes across the field has been constructed.

The core and well log data have been integrated with 3-D seismic data for Vocation Field

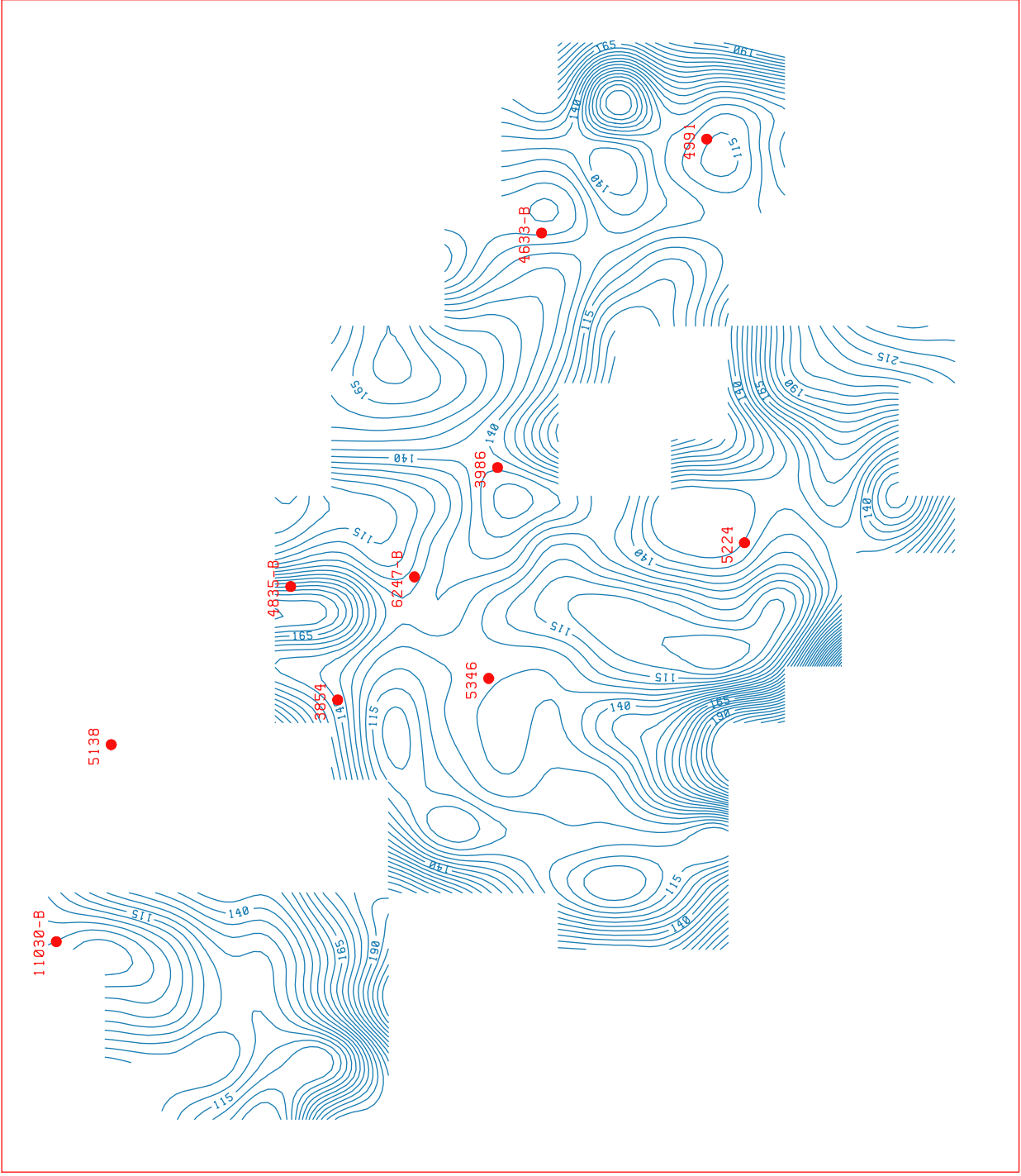


Figure 25. Thickness map of reef facies (from seismic data).  
By B. J. Panetta



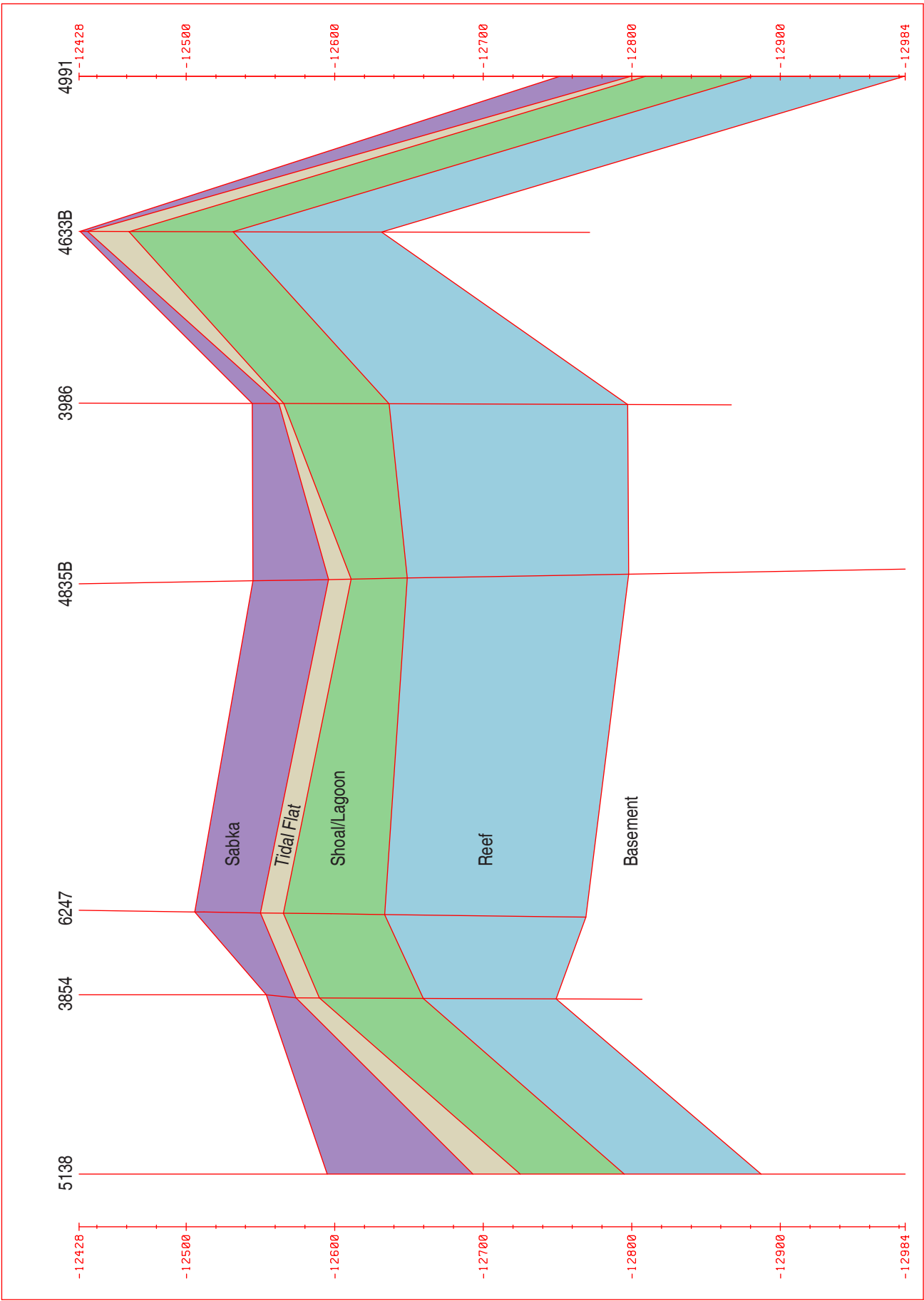


Figure 26. Cross section A - A'.  
By B. J. Panetta.

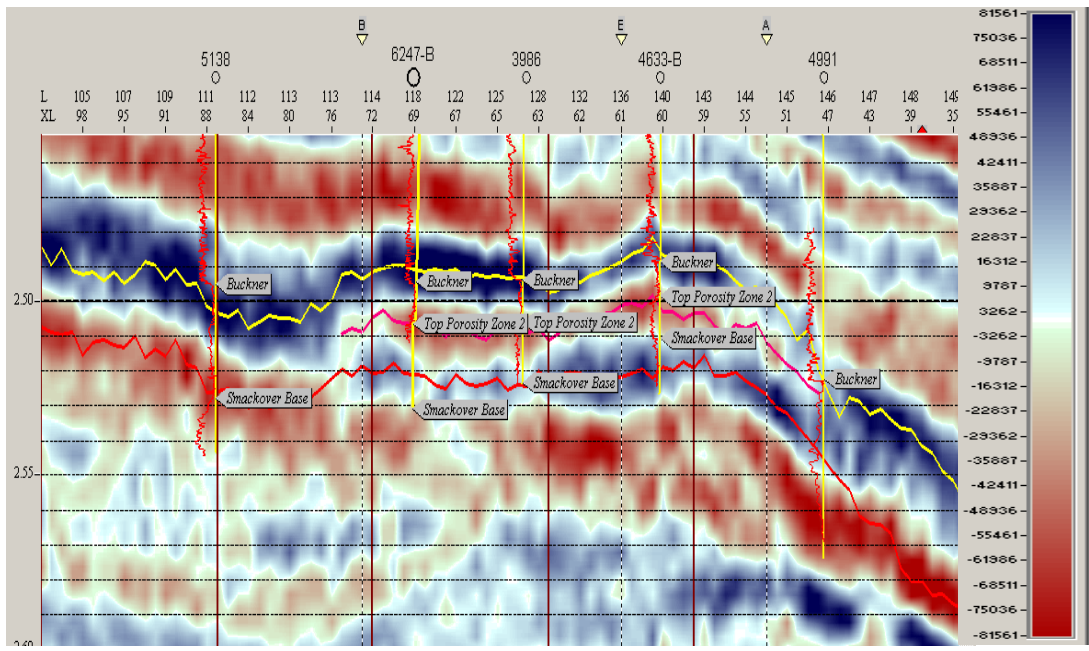


Figure 27. Sample seismic transect showing seismic character of horizons used in the multiattribute study.

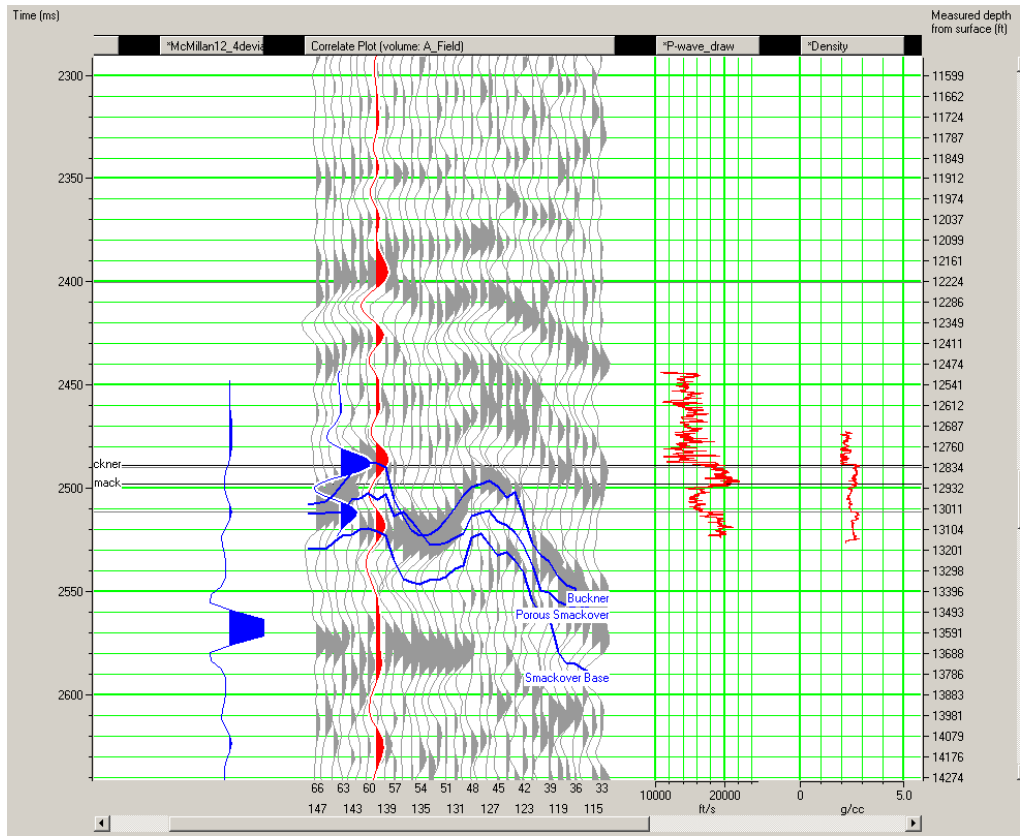


Figure 28. Example of Synthetic Seismogram used for well-seismic tie. Blue curve = synthetic, red = seismic trace extracted along wellbore at well location (McMillan 12-4#1). Wavelet uses to generate the synthetic shown in blue at left of image.

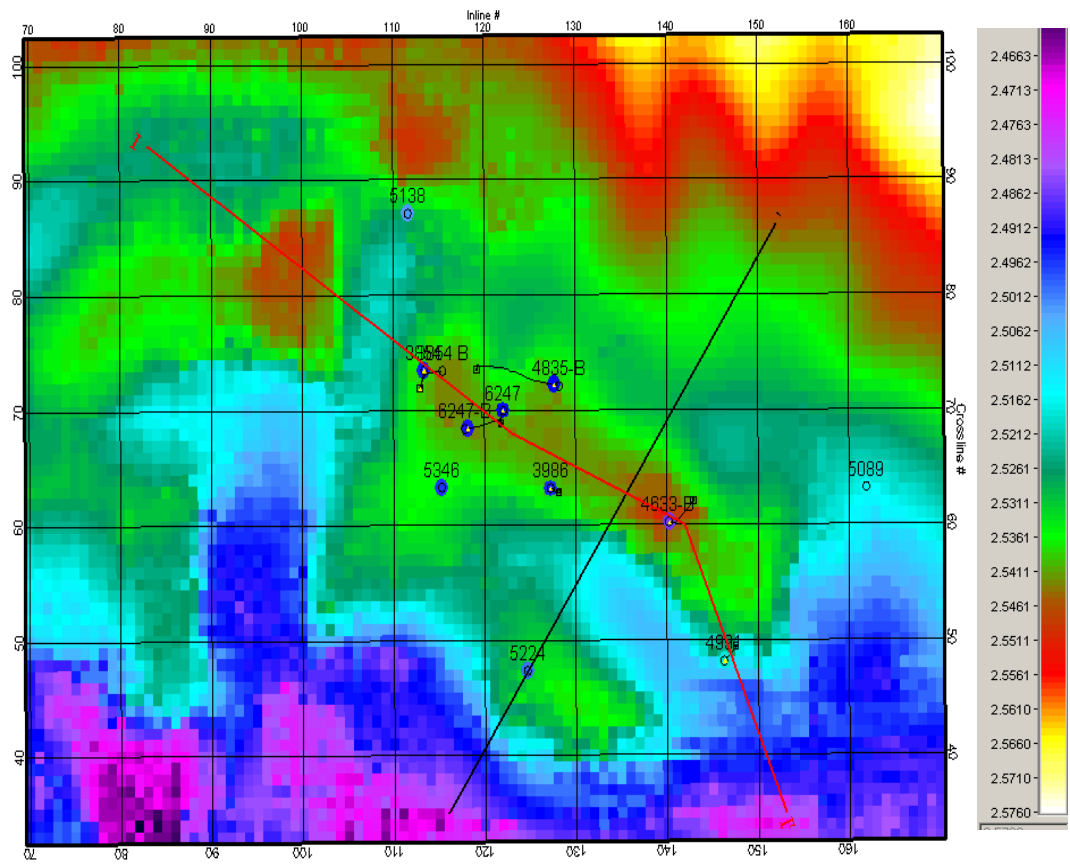


Figure 29. Time-structure map of the Buckner/Smackover seismic horizon showing principal structural features in the area of the 3-D multiattribute study. Lines show location of Figure 7a (black) and Figure 7b (red).

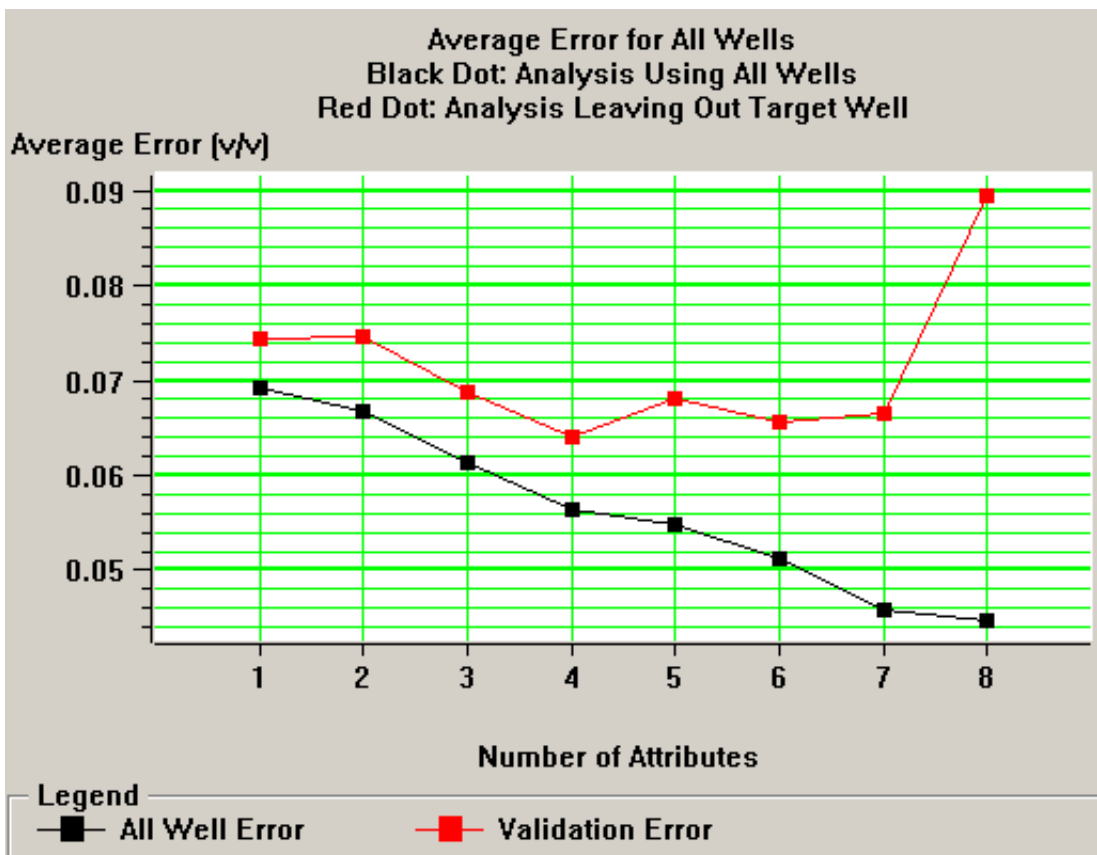


Figure 30. Cross-validation plot showing continuous decrease in average error when all wells are used (black line). The validation error (red) shows the change in average error when wells are systematically withheld from the correlation exercise. A minimum error is reached when four attributes are used, indicating that to be the optimum number of attributes. See Hampson et al. (2001) for a fuller discussion of cross-validation.

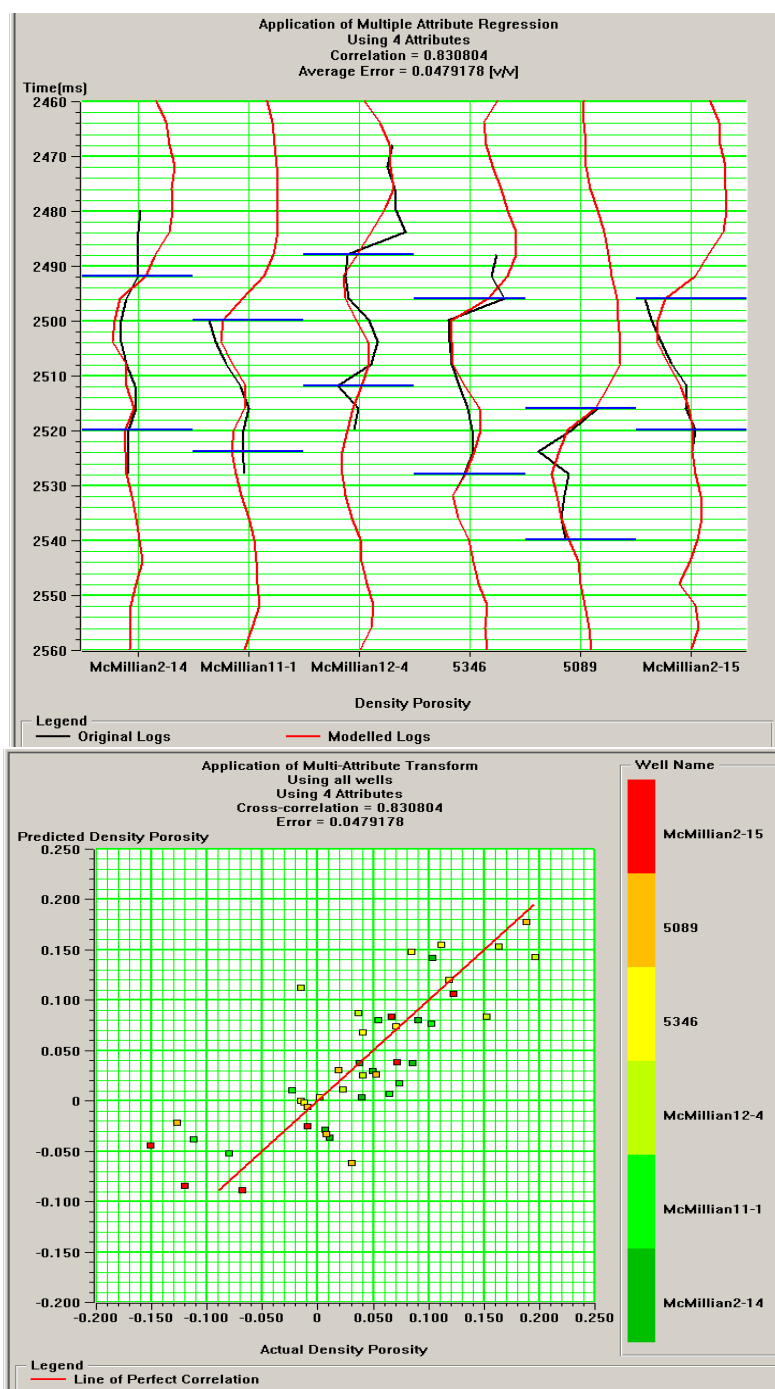


Figure 31. a) Top. Comparison of input density logs (black) and logs predicted using linear regression expression (red). Although the software converts the entire trace, the porosity values are strictly only valid for the stratigraphic interval being analyzed (between the two horizontal lines in each well. B) Bottom. Cross-plot of predicted versus measured density porosity using linear regression expression.

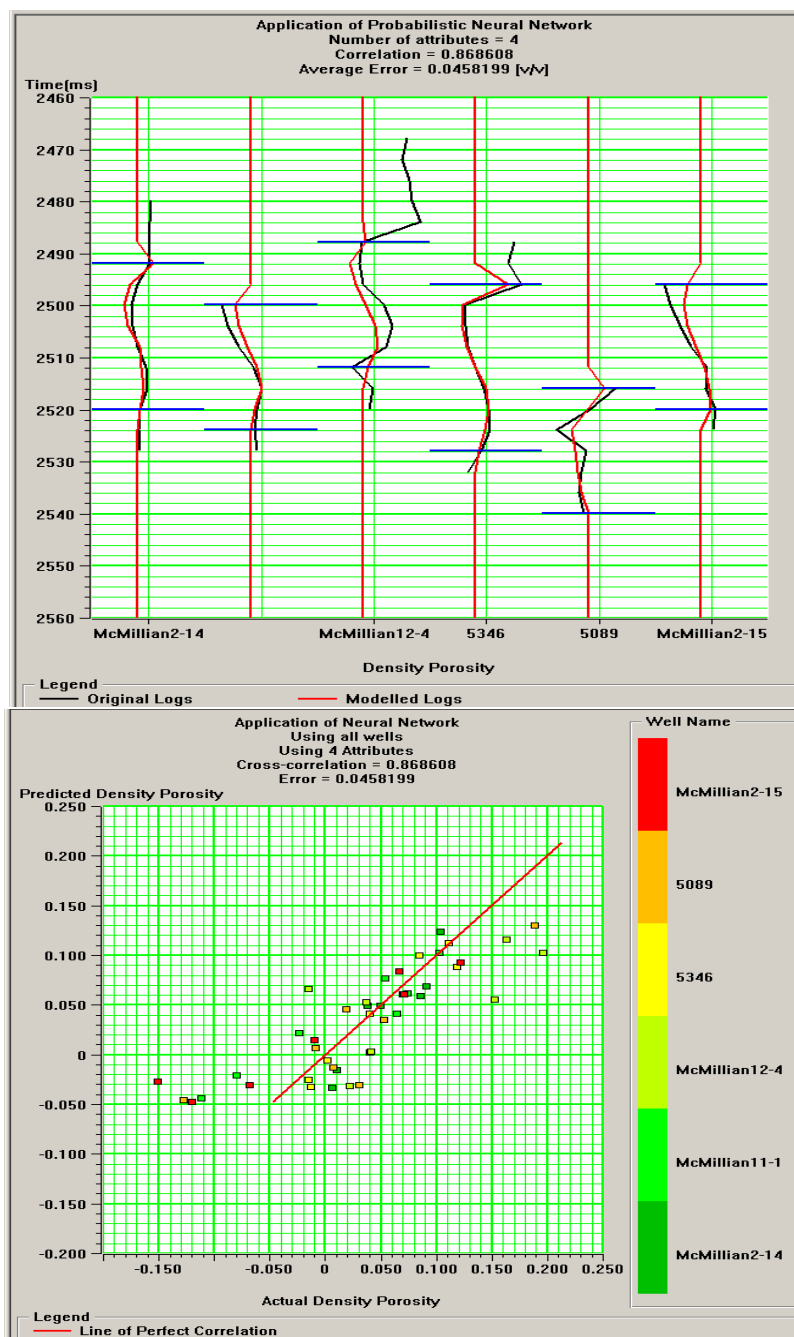


Figure 32. a) Top. Comparison of input density logs (black) and logs predicted using PNN (red). Although the software converts the entire trace, the porosity values are strictly only valid for the stratigraphic interval being analyzed (between the two horizontal lines in each well). B) Bottom. Cross-plot of predicted versus measured density porosity using PNN.

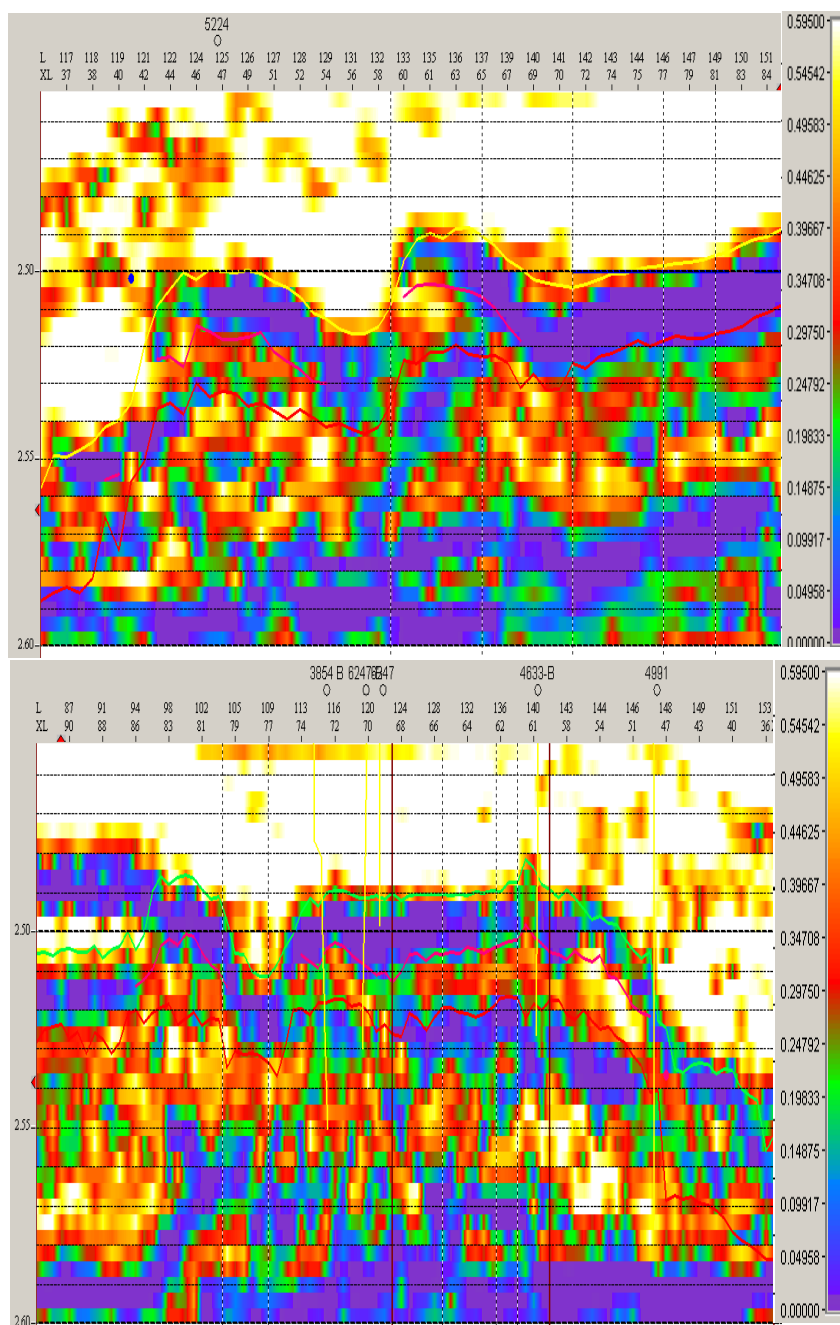


Figure 33. a) Top. NE-SW transect through porosity volume showing internal variations within the Smackover. B) Bottom. NW-SE transect through porosity volume. In both cases, porosity prediction is only valid for interval studied, between the top and base of the Smackover. See Figure 1 for location of transects.



Well Permit No. 11185  
STRAGO-BYRD 26-13 #2


MD	ms	ws	ps	gs	bs	TS	Structures & Grain Type	Porosity	Dep. Env.	Remarks
8									Haynesville Formation	
13950								iP Fr		Carbonaceous elongated clasts, up to 0.5cm Irregular distribution of porosity due to patchy cementation Vugs are completely cemented
2						X				
4										
6										
8										
13960										
2										
4										
6										
8										
13970										
2										
4										
6										
8										
13980										
2										
4										
6										
8										
13990										
2										
4										
6										
8										
14000										
2										
4										
6										
8										
14010										
2										
4										

Figure 34.  
Core description for well permit # 11185.  
By Juan Carlos Llinas.

MD	ms	ws	ps	gs	bs	TS	Structures & Grain Type	Porosity	Dep. Env.	Remarks
2										
4										
6										
8										
13980'						X	ζ ○ ●			
2						X		M/V/iC	Tidal Flat	
4										
6						X		M/V/iP		Oil impregnated Fractures filled with anhydrite
8										
13990'										
2						X	Py	Fr	Microbial Buildup	There is a white rim around the vugs that reduces their size
4							M/V			Microbial facies Type II. The vuggy porosity decreases upwards
6						X	○ ●	Fr		Interval with very high porosity (13996-14003')
8								M/V		
14000'										
2								Fr	Microbial reef, Type I facies	
4						X		V		
6										
8										
14010'										
2										All pores and fractures are cemented by anhydrite/calcite
4										
6										
8						X	○ ●	M/V iP		Microbial buildup, Type I Big anhydrite nodules
14020'										
2									Shallow Lagoon	No noticeable porosity
4										
6										
8										Type IV microbial facies
14030'										
2										Small fractures filled with An/Ca No noticeable porosity Some floating clasts of the same material Pores are cemented
4										
6						X	○ ●	M V/iP		
8										
14040'										
2										Fractures filled with calcite
4										
6										Stromatolite and thrombolite fabric. Cavities filled with anhydrite. No porosity
8										
14050'										
2										
4										
6										Some fractures filled with calcite. Very good porosity
8						X	●	M/V	Microbial Reef Complex	Microbial reef Type I fabric. Some fractures and vugs filled with calcite
14060'						X	○ ●	Fr		Fractures filled with anhydrite
2										Microbial buildup Type IV
4										
6										Low porosity
8										
14070'										
2										
4										
6										
8										
14080'										
2										Interbedding of some thin levels with thrombolite fabric No porosity due to high cementation
4										Some fractures filled with anhydrite
6										
8						X	○ ●	M/V		Reef facies with thrombolite fabric, Type I; sucrosic matrix Moderate to good porosity
14090'										

Figure 35.  
Core Description for well permit # 1599.  
By Juan Carlos Llinas.

Well Permit No. 1599 (cont.)  
B.C. QUIMBY 27-15 #1

MD	ms	ws	ps	gs	bs	TS	Structures & Grain Type	Porosity	Dep. Env.	Remarks	
2						X	⊙	M/V	Microbial Reef Complex	Reef facies with thrombolite fabric, Type I Good porosity	
4							⊙				
6											
8											
14100'											
2											
4											no core
6											
8											
14130'						X	⊙	M/V/iP			Calcite filling cavernous porosity High porosity interval (14131-14142') Anhydrite filling cavities and fractures Reef facies with Type I fabric Sucrosic matrix
2							⊙				
4							⊙				
6							⊙				
8							⊙				
14140'								M/V		Microbial facies Type II Very high to moderate porosity	
2						X	⊙				
4							⊙				
6							⊙				
8							⊙				
14150'						X	⊙	Fr		Abundant elongated vugs (fractures?)	
2							⊙				
4							⊙				
6							⊙				
8							⊙				
14160'						X	⊙	M/V		Large elongated clasts of reef fabric in a sandy matrix Anhydrite filling some fractures and voids. Good porosity	
2						X		Fr V iP		Microbial facies Type II Very low porosity	
4								V/iP		High porosity	
6								M/V/iP		Microbial facies Type II	
8											
14170'								V/iP		Some patches with low porosity, but good porosity in general	
2								M/V			
4											
6						X	⊙			Sucrosic texture	
8							⊙				
14180'						X	⊙	Fr V/iP		Moderate to low porosity due to high cementation Bioturbation?	
2							⊙				
4							⊙				
6							⊙				
8							⊙				
14190'											

Figure 35 (continued).  
Core description for well permit # 1599.  
By Juan Carlos Llinas.

MD	ms	ws	ps	gs	bs	TS	Structures & Grain Type	Porosity	Dep. Env.	Remarks
4-6										
6-8										
14110										
2-4									Sabkha	
4-6										Thin layers of nodular and layered anhydrite
6-8										
14120										
2-4									Sabkha	
4-6										No porosity
6-8										
14130										
2-4									Tidal Flat	
4-6										Layered and coalesced nodular anhydrite
6-8										
14140										
2-4									Tidal Flat	
4-6										No porosity
6-8										
14150										
2-4									Shoal Complex	
4-6										Pyrite concentrated in the stylolites
6-8										
14160										
2-4									Shoal Complex	
4-6										Very low porosity
6-8										
14170										
2-4									Shallow Lagoon	
4-6										Good porosity
6-8										
14180										
2-4									Shallow Lagoon	
4-6										Anhydrite filling bigger pores
6-8										
14190										
2-4									Shallow Lagoon	
4-6										Moderate to good porosity
6-8										
14200										
2-4									Shoal complex (?)	
4-6										Very low porosity
6-8										
14210										
2-4									Shoal complex (?)	
4-6										Oil?
6-8										
14220										
2-4									Shoal complex (?)	
4-6										Good porosity
6-8										
14230										
2-4									Shoal complex (?)	
4-6										Microbial texture?
6-8										
14240										
2-4									Shoal complex (?)	
4-6										Very low porosity
6-8										
14250										
2-4									Shoal complex (?)	
4-6										Patchy texture
6-8										
14260										
2-4									Shoal complex (?)	
4-6										Low to moderate porosity
6-8										
14270										
2-4									Shoal complex (?)	
4-6										Subtle plane parallel lamination
6-8										
14280										
2-4									Shoal complex (?)	
4-6										Moderate to good porosity
6-8										

Figure 36.  
Core description for well permit # 1691.  
By Juan Carlos Llinas.

Well Permit No. 1691(cont.)  
CONTAINER CORP. OF AMERICA 34-5 #1

MD	ms	ws	ps	gs	bs	TS	Structures & Grain Type	Porosity	Dep. Env.	Remarks
4						X	● ● ⋈	M/iP	Shoal complex (?)	Moderate porosity
6						X	● ● ⋈			
8						X	● ● ⋈			
14290'							● ● ● ● ⋈	mM/iP		High porosity
2							⋈			
4							⋈			
6						X	● ● ● ● ⋈			Patchy texture High porosity
8						X	● ● ● ● ⋈	mM/iP		Open fractures
14300'							○	Fr		
2							⋈			
4							⋈			
6							● ● ● ● ○			
8						X	⋈			
14310'							⋈			
2							⋈	mM/iP		
4							⋈			
6							⋈			
8										
14320'										
2										

Figure 36 (continued).  
Core description for well permit # 1691.  
By Juan Carlos Llinas.

Well Permit No. 2851  
M.J. BYRD ET UX 26-13 #1

MD	ms	ws	ps	gs	bs	TS	Structures & Grain Type	Porosity	Dep. Env.	Remarks
4										
6										
8						X		iP/V	Tidal Flat	
14030								iP/V		Pervasive anhydrite cement occludes porosity
2								iP/V		Moderate porosity
4						X		iP/V		
6								iP		
8						X		M/iP/V		
14040								Fr		Thin levels of oncoid cortices
2								M/V		High interparticle and moldic porosity but sometimes cemented by anhydrite. Some thin intervals < 7 cm have the oncolites leached increasing the vuggy porosity
4						X		Fr		Fractures partially occluded by anhydrite cement
6						X		M/V		Stylolites with pyrite
8						X		M/iP/V		
14050								Fr		Porosity almost completely obliterated by calcite cement
2						X		Fr		Fractures cemented by anhydrite
4						X		V		
6						X		Fr		
8								Fr		High porosity in the grainstones, moderate in the packstones
14060						X		M/iP/V	Shoal Complex	Bivalve debris
2						X		M/iP		Intraclasts horizontally aligned
4						X		M/iP/V		High porosity
6								M/iP/V		Anhydrite chicken wires
8								M/iP		Moderate to low porosity
14070						X		M/iP		Some isolated elongated pores. Low porosity
2						X		iP/V/M		Thick carbonaceous laminae and anhydrite nodules
4						X		Fr		Very porous level
6						X		Fr		Fractures filled with anhydrite
8						X		M/V/iP		Patchy areas with good porosity
14080						X		Fr		Microbial buildup Type I and Type IV-V
2						X		Fr		High porosity despite partial cementation specially along the fractures
4						X		Fr		
6						X		Fr		
8						X		Fr		
14090									Microbial Buildup	

Figure 37.  
Core description for well permit # 2851.  
By Juan Carlos Llinas.

MD	ms	ws	ps	gs	bs	TS	Structures & Grain Type	Porosity	Dep. Env.	Remarks
14020'										
2										
4								iP		
6								iP/M		Very low porosity
8						X				
14030'										
2										Good porosity
4								iP		Very low porosity
6										
8						X	Qz			
14040'										
2										
4										
6										no core
8										
14050'										
2										
4										
6										
8						X		iP Fr		Good porosity Fractures filled with anhydrite
14060'										
2								M/V/iP Fr		Big anhydrite nodules Fractures also filled with anhydrite
4						X				
6										
8						X		M/iP		
14070'										
2								Fr		
4						X				
6						X		iP		
8						X				
14080'										
2										
4										
6								M/V/iP		Low to moderate porosity
8						X				
14090'										
2										
4						X				
6										
8						X		iP		Very low porosity
14080'										
2										
4										
6										
8						X				
14090'										
2										
4						X				
6										
8						X		Fr		Moderate to good porosity
14100'										
2										
4										
6						X		iP Fr		Moderate to good porosity
8										
14110'										
2										
4										
6						X		Fr		
8										
14120'										
2										
4										
6						X				
8										
14130'										
2										
4										
6						X		M/V/iP Fr		Reef, Type II facies Very high porosity Anhydrite filling fractures Brecciated interval (14128-14144')
8										

Shoal Complex

Microbial Reef Complex

Figure 38.  
Core description for well permit # 2935.  
By Juan Carlos Llinas.

Well Permit No. 2935 (cont.)  
 D.R. COLEY, JR. ESTATE #35-4

MD	ms	ws	ps	gs	bs	TS	Structures & Grain Type	Porosity	Dep. Env.	Remarks
14140'							Ⓐ	V/iP Fr	Microbial Reef Complex	Very high porosity
2										Reef, Type II facies
4										
6										
8										
14150'							Ⓐ	V/iP Fr		Anhydrite filling fractures
2										
4										
6										
8										

Figure 38 (continued).  
 Core description for well permit # 2935.  
 By Juan Carlos Llinas.



MD	ms	lws	ps	gs	bs	TS	Structures & Grain Type	Porosity	Dep. Env.	Remarks
2							HAYNESVILLE FORMATION			
4										
6							anhydrite		Sabkha	Very low porosity
8										Anhydrite in layers and coalesced nodules
14130'							anhydrite			
2						X	Py Qz	M		
4										
6						X		iP		Very low porosity
8										
14140'									Tidal Flat	
2						X		M		
4								M		
6						X		Fr		
8								M/V		Improvement in porosity, though bigger pores are filled with anhydrite cement
14150'										Carbonaceous intraclasts
2						X		M/V		Low to moderate porosity
4								M		
6								M/V		All the big pores are filled with anhydrite while the small ones are not.
8						X				
14160'						X		M/V/iP		Carbonaceous intraclasts
2										High porosity
4										
6						X		M/V/iP		Very high porosity. Big anhydrite nodules
8										
14170'									Shoal Complex	
2						X				Small vugs filled with anhydrite
4						X	Qz	M/V/iP		Low porosity
6										
8										
14180'										
2								M/iP		Low porosity
4										
6						X				
8										
14190'										Concentration of pyrite in the stylolites
2										
4								M/iP		Moderate to low porosity
6						X				
8										
14200'										Interval with patchy texture (14196-14231'), microbial influx?
2								M/iP		Good porosity
4										Patches with high porosity
6						X				Elongated pores < 1cm
8										
14210'						X				
2							Qz	M/V/iP		Low to moderate porosity
4								M/V/iP		Patchy texture
6						X		M/V/iP		High porosity, vugs up to 1 cm in diameter
8										
14220'										High fractured interval (14220-14225)
2						X		Fr		Microbial buildup (Type II). May vugs filled with anhydrite
4						X				Big vugs upto 2cm in diameter and sometimes elongated. Some are filled partially or totally by anhydrite
6						X		M/V/iP		Moderate porosity
8										Some elongated vugs (fractures) up to 3 cm long. Patches of very high porosity
14230'										
2						X		Fr		Microbial buildup Type II
4										
6							Qz	M/V/iP		Leached intraclasts
8										Fossil remains like spicules replaced by calcite/anhydrite
14240'										

Figure 39.  
Core description for well permit # 2966.  
By Juan Carlos Llinas.

Well Permit No. 2966 (cont.)  
B.C. QUIMBY 27-16 #1

MD	ms	ws	ps	gs	bs	TS	Structures & Grain Type	Porosity	Dep. Env.	Remarks
2										
4						X		M/iP		Fossil debris resembling spicules replaced by anhydrite Leached intraclasts Moderate to good porosity Spicules
6						X				
8										
14250'										
2						X				
4								M/iP		Very low porosity
6								Fr		Oncolites disposed in thin levels
8										
14260'										
2						X		iP/V		
4								V/iP		Very low porosity
6										
8								M/V/iP		
14270'										
2								M/iP		
4								V		
6						X		M/V/iP		Low porosity
8										
14280'										
2								V		Interval with patchy texture and high vuggy porosity (14276-14288'). Microbial influence?
4								M/V/iP		Moderate to high porosity Some vugs are filled with anhydrite/calcite
6						X				
8										
14290'										
2								V		Interval with patchy texture (14290-14295'). Microbial influence?
4										
6										
8						X		M/iP		Very low porosity
14300'										
2										
4						X				
6										
8										
14310'										

Shallow Sub-wave Base Level

Figure 39 (continued).  
Core description for well permit # 2966.  
By Juan Carlos Llinas.

Well Permit No. 3412  
B.C. QUIMBY 27-15 #2

MD	ms	ws	ps	gs	bs	TS	Structures & Grain Type	Porosity	Dep. Env.	Remarks	
14010'							HAYNESVILLE FORMATION				
2									Sabkha		
4											
6											
8											
14020'							anhydrite			Layered and nodular anhydrite interbedded with the mudstone No porosity	
2											
4											
6											
8							anhydrite			Layered and nodular anhydrite	
14030'									Tidal Flat	High fenestral porosity completely filled with calcite as well as some fractures Type IV and V	
2						X		Fe			
4						X		Fr			
6						X		Ip		Type IV and V	
8						X		Fr		No porosity	
14040'									Tidal Flat		
2						X		iP/V			Very low porosity level
4						X		Py			
6						X					
8						X		M/V/iP		Highly porous grainstones Low to moderate porosity	
14050'									Shoal Complex		
2						X		M/V/iP			Very high porosity
4						X					Oncolites > 1cm Moderate to high porosity
6						X				Porosity obliterated by An/Ca	
8						X				Good porosity Bivalve fragments	
14060'									Shoal Complex		
2						X		M/V/iP			Porosity obliterated by anhydrite/calcite
4						X					
6						X					
8						X				Very low porosity	
14070'									Shallow Lagoon		
2						X					Big anhydrite nodules, approx. 5cm diam
4						X					Abundant clayey laminae. Very low porosity
6						X				Stylolites with pyrite Very thin mudstone levels interbedded Type IV/V microbial facies	
8						X					
14080'									Shallow Lagoon		
2						X		M/V/iP Fe			Moderate porosity Fenestral porosity obliterated by An/Ca
4						X		Fr			Very low porosity
6						X					
8						X		M/V/iP Fr		Oncolites up to 3mm in diam. and stromatolites Pores occluded by anhydrite	
14090'									Shallow Lagoon		
2						X		M/V			Moderate to low porosity
4						X					
6						X					
8						X					
14100'											

Figure 40.  
Core description for well permit # 3412.  
By Juan Carlos Llinas.

Well Permit No. 3739  
BERTHA C. QUIMBY 34-1 #1

MD	ms	ws	ps	gs	bs	TS	Structures & Grain Type	Porosity	Dep. Env.	Remarks
4									Tidal Flat	
6								V		
8						X				
4020'						X				
2						X	Py			14015-14025: interval with very low porosity
4						X		iP/V		
6						X				
8						X				Good porosity
4030'						X				Anhydrite cement
2						X				
4						X				
6						X		M/V		Moderate to good porosity from 14028 to 14044 Intervals with vuggy/moldic porosity, sometimes occluded with anhydrite or calcite cement Some thin wackestone layers interbedded.
8						X				
14040'						X				Oncoidal cortex
2						X		M/V/lp		Enhancement in porosity due to ooids/peloids dissolution Good porosity
4						X				
6						X				
8						X				
14050'										
2										
4										
6										
8										
14060'										
2										
4										
6						X				Interval with very low porosity (14064-14070)
8						X	Qz Py			Microbial buildup Type IV and V Elongated muddy intraclasts < 1cm long
14070'						X		iP		Pores partially obliterated by calcite cement
2						X		M/V		High porosity interval (14071-14075)
4						X		Fr		Fractures partially infilled with anhydrite/calcite cement
6						X				Pyrite
8						X				Low porosity
14080'						X				
2						X		iP		Porosity almost completely cemented
4						X	Qz			
6						X				
8						X		iP		
14090'						X		Fe		
2						X				
4						X		iP		
6						X	Qz			No porosity
8						X				
14100'						X		Fr		
2						X		iP		
4						X	Py			
6						X	Qz			
8						X		M/V		Abundant siliceous grains
14110'						X		M/V		The microbial buildup is mainly Type I and in minor degree Type IV and V.
2						X		Fe		High porosity, though in thin intervals it is completely occluded by calcite cement
4						X		Fr		
6						X				
8						X				
14110'						X			Microbial Reef Comp.	

Figure 41.  
Core description for well permit # 3739.  
By Juan Carlos Llinas.

Well Permit No. 3990  
D.R. COLEY, III UNIT 26-2 #1

MD	ms	ws	ps	gs	bs	TS	Structures & Grain Type	Porosity	Dep. Env.	Remarks
2							⊕		Tidal Flat	Very low porosity
4						X	⊕	M/iP		Carbonaceous intraclasts
6							⊕			10-15cm thick layers
8							⊕			
14270'							⊕		Tidal Flat	Carbonaceous intraclasts
2						X	⊕	Fe		Very low porosity
4							⊕	Fr	Fenestral porosity filled with cement	
6							⊕	M/iP	Thin fractures cemented by anhydrite	
8							⊕		Very low porosity	
14280'							⊕		Shoal Complex	Alternation of 40-60cm thick ws/ps beds and 8-15cms ps/gS layers
2							⊕			
4							⊕	Fr		Thin fractures cemented by anhydrite
6						X	⊕	M/iP		Moderate to good porosity
8							⊕			Alternation of 40-60cm thick ws/ps beds and 8-15cms ps/gS layers
14290'							⊕		Shoal Complex	
2						X	⊕	M/iP		Interval with moderate to good porosity (14288-14300')
4							⊕			
6							⊕	M/iP		
8							⊕			
14300'							⊕		Shallow Sub Wave Level	Wackestone rich in carbonaceous material
2							⊕			Low porosity
4						X	⊕			Glauconite
6							⊕			
8							⊕			
14310'							⊕		Shallow Sub Wave Level	Discontinuous lamination
2							⊕			No visible porosity
4							⊕			
6							⊕			
8							⊕			
14320'							⊕			

Figure 42.  
Core description for well permit # 3990.  
By Juan Carlos Llinas.

Well Permit No. 5779  
NEUSCHWANDER 34-3 #1

MD	ms	ws	ps	gs	bs	TS	Structures & Grain Type	Porosity	Dep. Env.	Remarks
13920'									Tidal Flat	
2						X	⊙ ⊙ ⊙			No porosity Abundant anhydrite nodules
4						X	⊙ ⊙ ⊙	iP/V		Cross stratification
6						X	⊙ ⊙ ⊙			
8						X	⊙ ⊙ ⊙			
13930'						X	⊙ ⊙ ⊙	iP		Grainstone with leached ooids Very high porosity
2						X	⊙ ⊙ ⊙			
4						X	⊙ ⊙ ⊙	V/M/iP		Very thin more cemented layers within the grainstone
6						X	⊙ ⊙ ⊙			
8						X	⊙ ⊙ ⊙			Very high porosity
13940'						X	⊙ ⊙ ⊙	M/iP		Big calcite nodules. Low porosity
2						X	⊙ ⊙ ⊙			
4						X	⊙ ⊙ ⊙			Moderate to good porosity
6						X	⊙ ⊙ ⊙			Very low porosity
8						X	⊙ ⊙ ⊙			
13950'						X	⊙ ⊙ ⊙	iP		
2						X	⊙ ⊙ ⊙			
4						X	⊙ ⊙ ⊙	Fr		Fractures cemented by anhydrite No porosity
6						X	⊙ ⊙ ⊙			
8						X	⊙ ⊙ ⊙			
13960'						X	⊙ ⊙ ⊙	Fr iP		Interbedding of layers of wackestone and very thin darker layers of mudstone
2						X	⊙ ⊙ ⊙			
4						X	⊙ ⊙ ⊙	Fr		No porosity Fractures cemented by anhydrite
6						X	⊙ ⊙ ⊙			
8						X	⊙ ⊙ ⊙			
13970'						X	⊙ ⊙ ⊙	iP		Very low porosity Lithoclasts No porosity Big anhydrite nodules
2						X	⊙ ⊙ ⊙			
4						X	⊙ ⊙ ⊙			
6						X	⊙ ⊙ ⊙			
8						X	⊙ ⊙ ⊙			
13980'						X	⊙ ⊙ ⊙	iP		Wavy discontinuous lamination No porosity
2						X	⊙ ⊙ ⊙			
4						X	⊙ ⊙ ⊙			
6						X	⊙ ⊙ ⊙			
8						X	⊙ ⊙ ⊙			
13990'						X	⊙ ⊙ ⊙	iP		Presence of very thin beds of black matrix with lithoclasts floating in it. No porosity
2						X	⊙ ⊙ ⊙			
4						X	⊙ ⊙ ⊙			Abundant lithoclasts
6						X	⊙ ⊙ ⊙			
8						X	⊙ ⊙ ⊙			
14000'						X	⊙ ⊙ ⊙			No porosity Angular to subangular feldspar grains up to 4cms, with an average of 1cm. Bad sorting
2						X	⊙ ⊙ ⊙			
4						X	⊙ ⊙ ⊙			
6						X	⊙ ⊙ ⊙			
8						X	⊙ ⊙ ⊙			
14010'						X	⊙ ⊙ ⊙			Chloritized granite
2						X	⊙ ⊙ ⊙			
4						X	⊙ ⊙ ⊙			
6						X	⊙ ⊙ ⊙			

Figure 43.  
Core description for well permit # 5779.  
By Juan Carlos Llinas.

Well Permit No. 7588B  
BLACKSHER 27-11 #1

MD	ms	ws	ps	gs	bs	TS	Structures & Grain Type	Porosity	Dep. Env.	Remarks
13980'								V/iP	Tidal Flat	
2								V/iP		Very low porosity
4										
6										
8										Some thin (3-4cm) intervals with M/mV
13990'						X		M/V/iP	Shoal Complex	High porosity due to oolite dissolution
2										Some pores filled in with anhydrite
4						X				
6										
8										
14000'						X		iP/V		Moderate to good porosity
2										
4										
6										
8										
14010'						X		V/iP/Fr		Moderate porosity. Fractures are partially filled with anhydrite
2										
4										
6						X		Fr		Highly fractured interval. Anhydrite cements the joints partially
8										
14020'						X		M/V	Shallow Lagoon	Oncoid cortices. Good porosity due to allochems dissolution
2								Fr		Abundant anhydrite veins
4										Thin microbial buildup layers interbedded with the wackestones
6						X				Low porosity. Some vuggy (fenestral?) porosity occluded by anhydrite cement. Pyrite disseminated
8									Fractured interval, diagenetic breccia. Nodular/layered anhydrite	
14030'						X		M/V		Abundant elongated vugs
2										Microbial buildup, Type I mainly. Vertical burrows
4										Anhydrite nodules.
6								Fr		High vuggy porosity. White crust lining the vugs.
8										Vertical burrows and fractures
										Oncolite levels interbedded with wackestone layers with abundant stylolites

Figure 44.  
Core description for well permit # 7588B.  
By Juan Carlos Llinas.

Table 5. Characterization of Smackover Lithofacies in the Vocation Field Area.

<b>Lithofacies</b>	<b>Lithology</b>	<b>Allochems</b>	<b>Pore Types</b>	<b>Porosity (percent)</b>	<b>Permeability (md)</b>
oid-dominated, grain-supported (grainstone/packstone)	dolostone, limestone	oids, oncoids, peloids	moldic, interparticulate, intercrystalline	high (1.5-28.3)	high (0-2,230)
oid-dominated, matrix-supported (wackestone)	dolostone	oids, oncoids, peloids	moldic	moderate (1.2-14.0)	moderate (0-8)
oncoid-dominated grain-supported (grainstone/packstone)	dolostone	oncoids, peloids, ooids, intraclasts	interparticulate, moldic, vuggy	high (1.6-20.1)	high (0-1,635)
oncoid-dominated matrix-supported (wackestone)	dolostone	oncoids, peloids	vuggy, moldic	low (2.5-8.3)	low (0-0.39)
peloid-dominated grain-supported (grainstone/packstone)	dolostone, limestone	peloids, oncoids, ooids	interparticulate, intercrystalline, vuggy	high (0.8-25.6)	high (0-587)
peloid-dominated matrix-supported (wackestone)	dolostone, anhydritic dolostone	peloids, oncoids	intercrystalline	moderate (1.0-18.2)	moderate (0-39)
mudstone	dolostone, limestone	none	fracture	low (1.2 to 8.8)	low (<0.01)
algal stromatolite (boundstone)	dolostone	algae, peloids, oncoids	fracture, vuggy, fenestral	low (1.1-8.8)	moderate (0-16)
algal boundstone	dolostone	algae, peloids, oncoids	vuggy, fracture, breccia, moldic	high (3.0-33.6)	high (0-2,998)



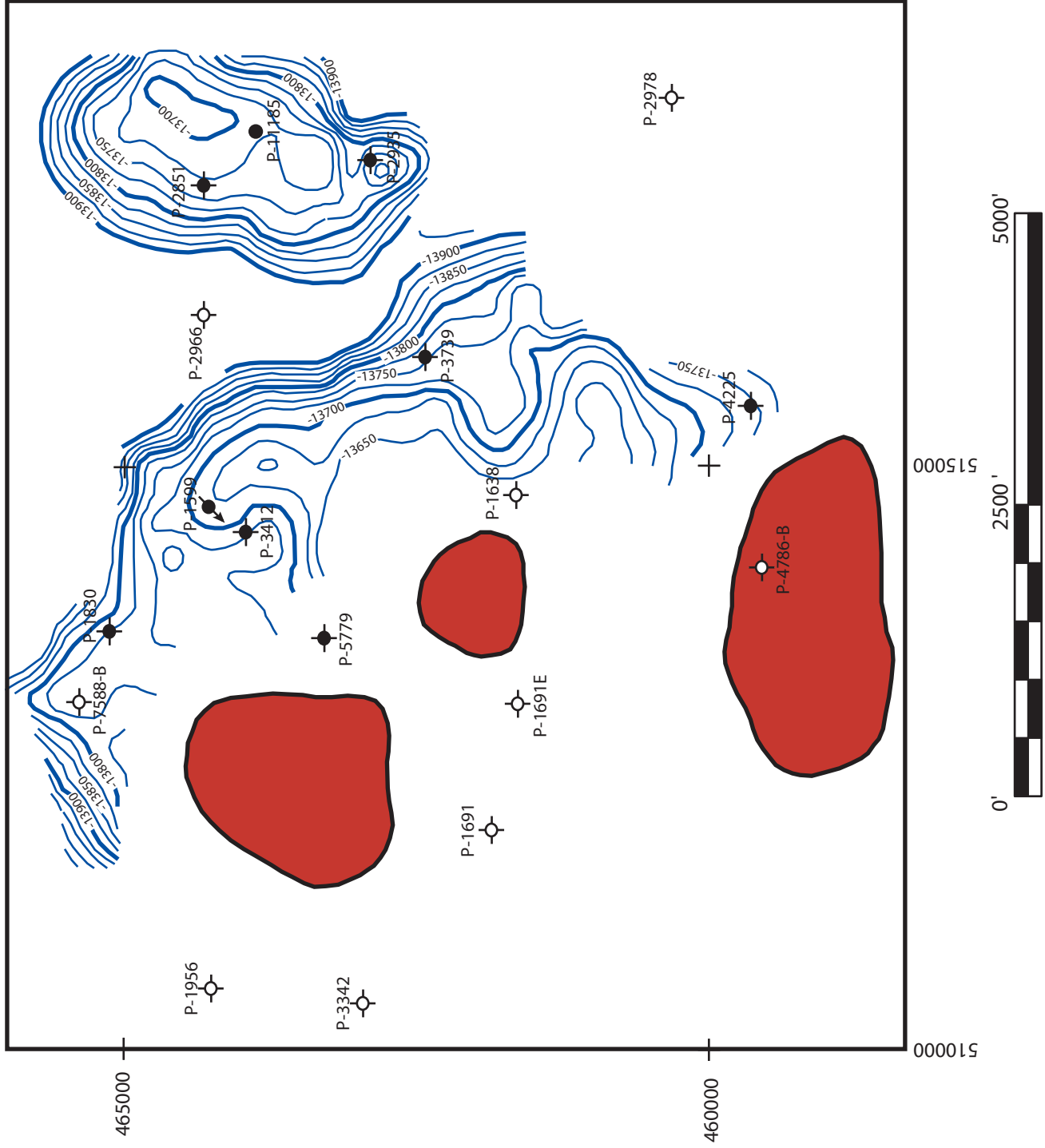


Figure 46. Contour map of the top of the microbial reef complex.

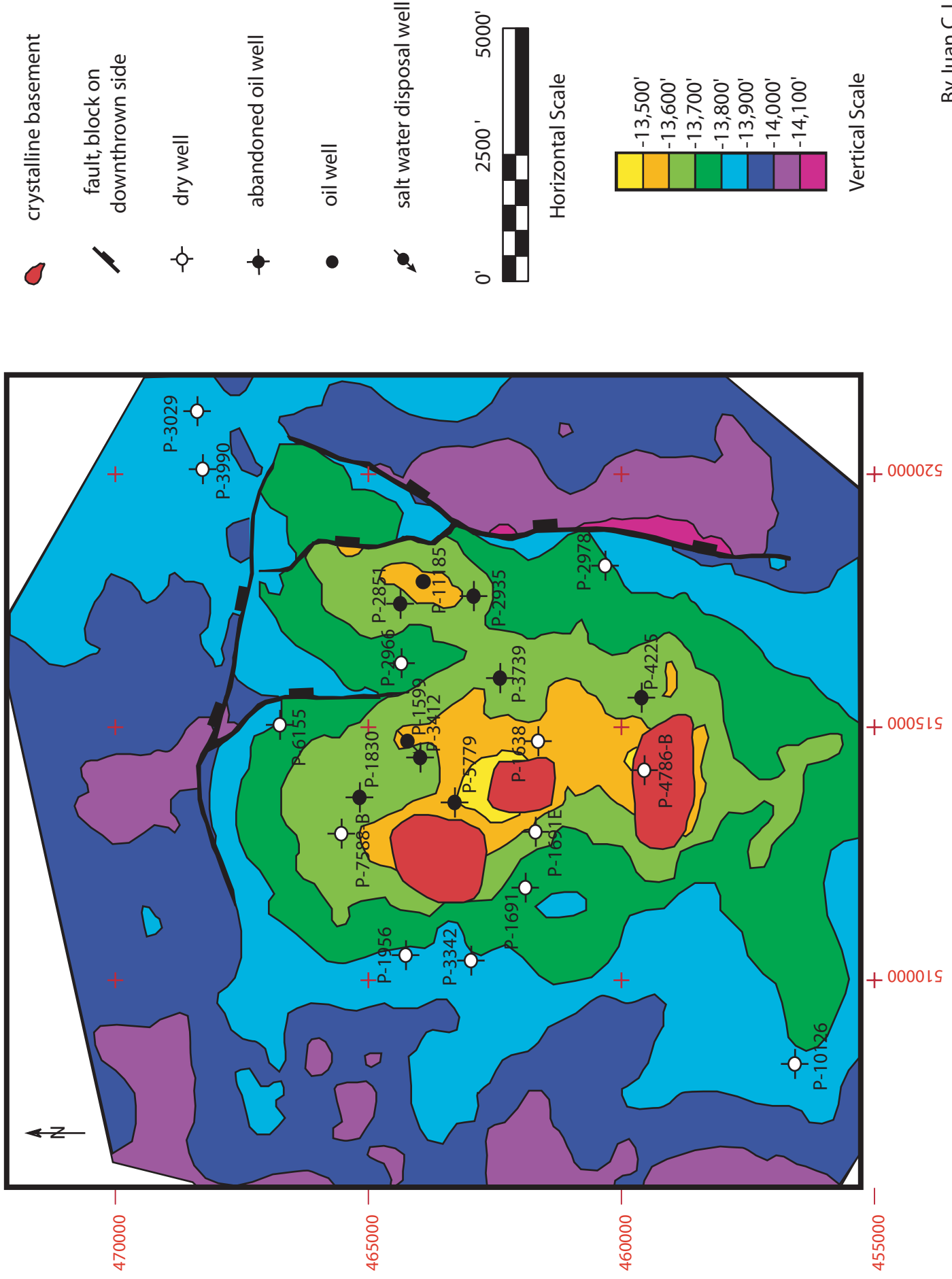
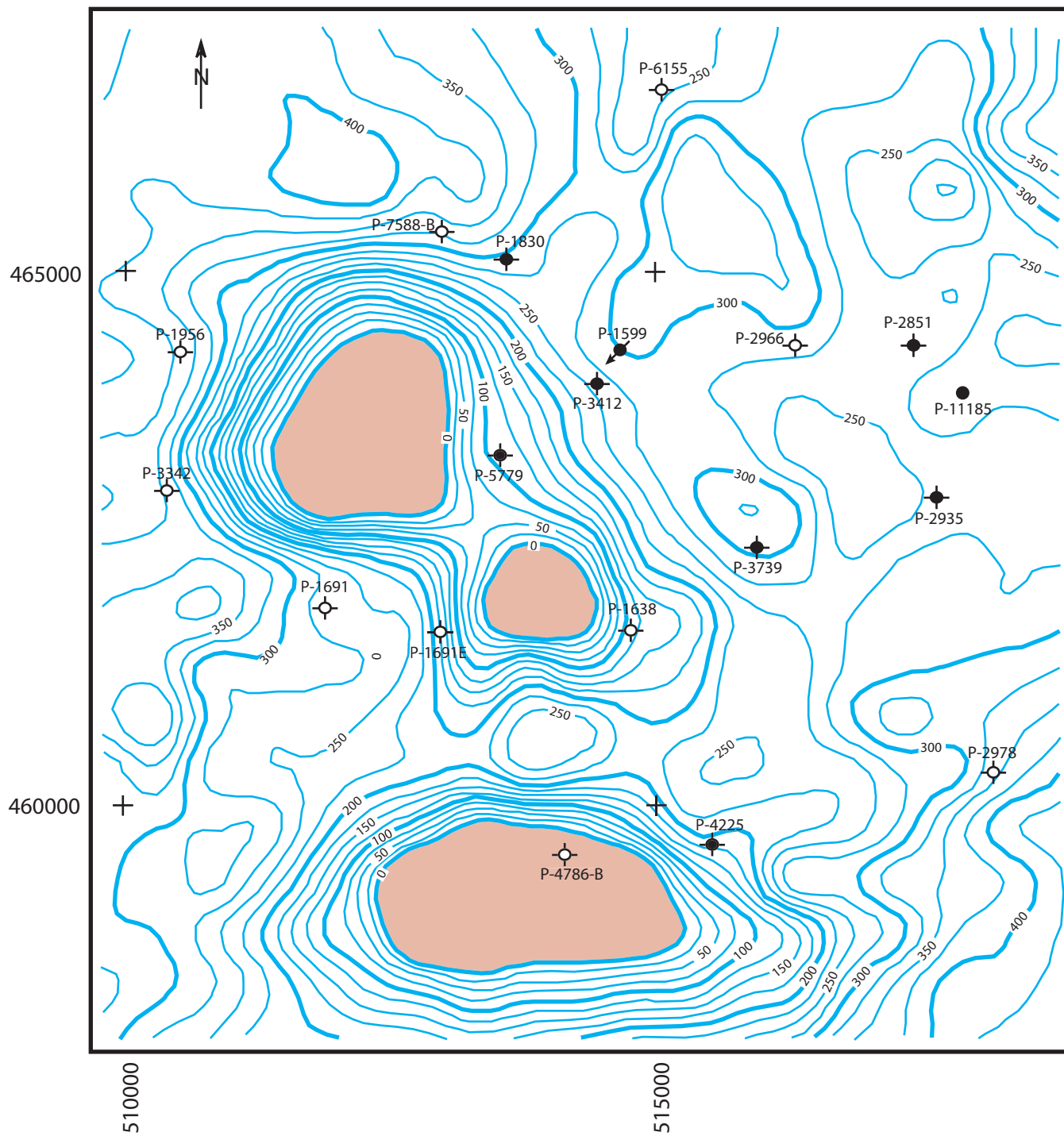







Figure 47. Structure contour map of the top of the Smackover Formation.



-  dry well
-  abandoned oil well
-  oil well
-  salt water disposal well
-  basement

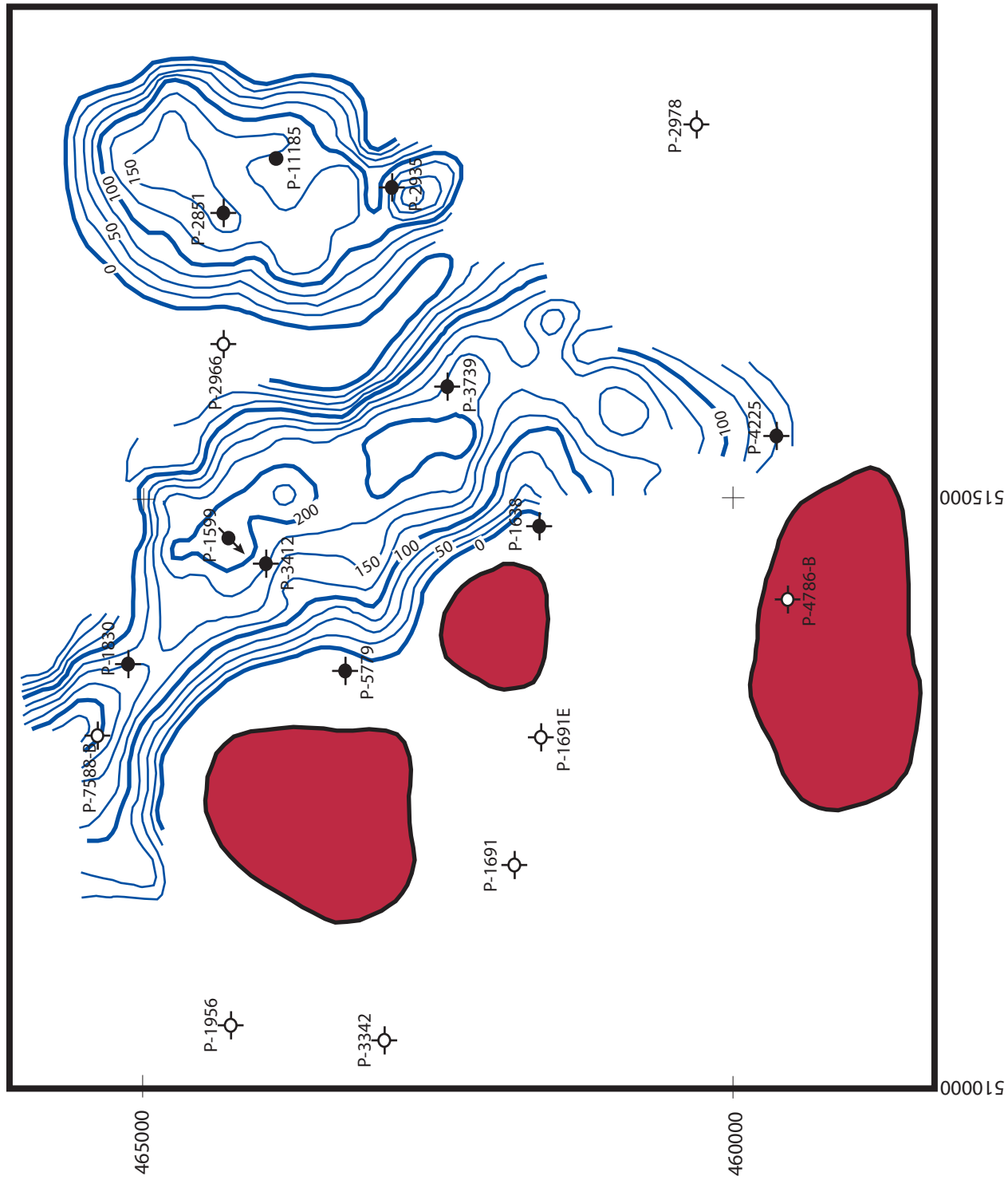







Horizontal Scale

Contour Interval = 25 feet

By Juan C. Llinas

Figure 48. Isopach map of the Smackover Formation.



-  dry well
-  abandoned oil well
-  oil well
-  salt water disposal well
-  basement

Contour Interval = 25 feet



Figure 49. Isopach map of the microbial reef complex.

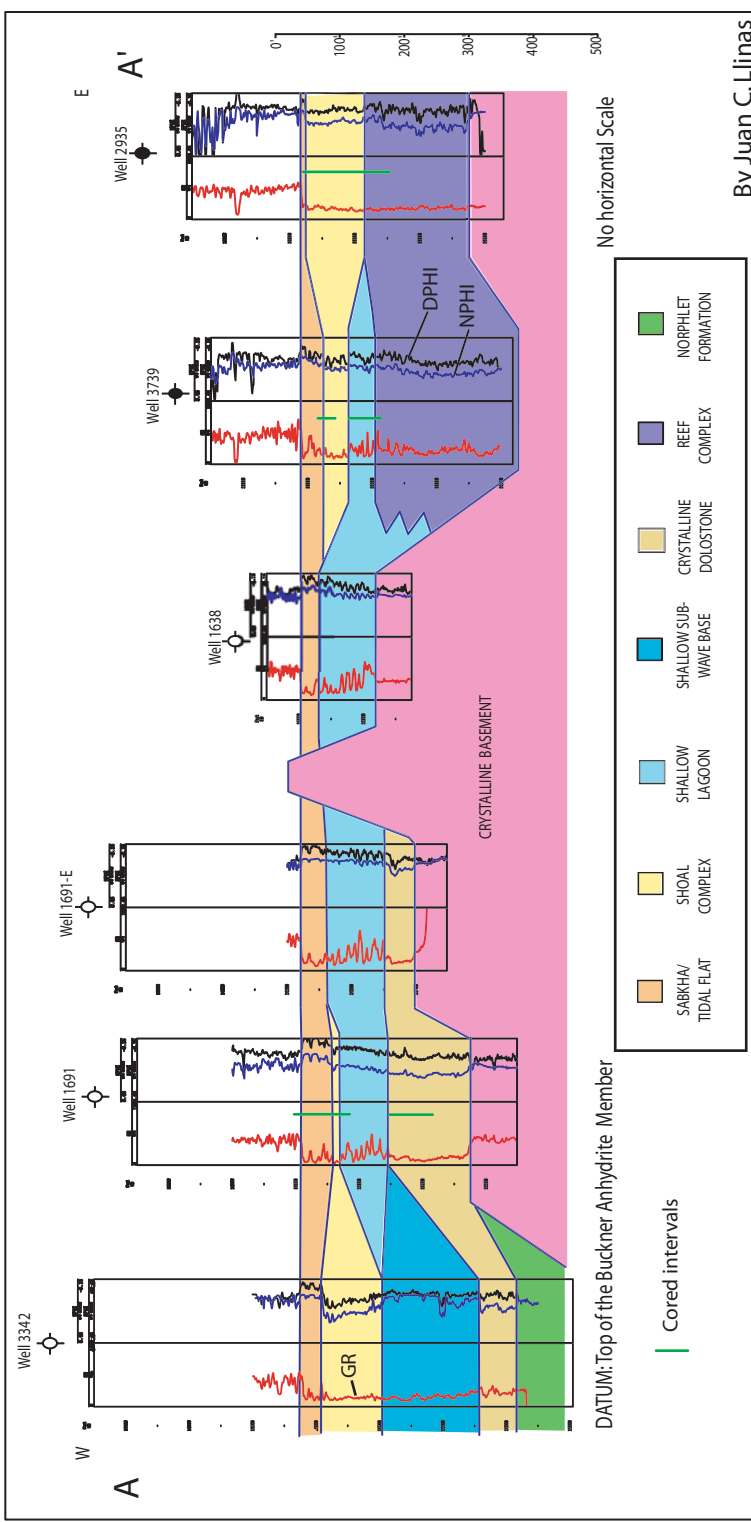


Figure 50. Cross section across Vocation Field.

that Strago contributed to the project. Typical seismic profiles for the field illustrating the reef reservoir are shown in (Figure 51). The multi-attribute seismic study of the field continues.

**Task 2—Rock-Fluid Interactions.**--This task is a continuation of the study of reservoir architecture and heterogeneity at the microscopic scale. While macroscopic and mesoscopic heterogeneities are largely a result of structural and depositional processes, microscopic heterogeneities are often a product of diagenetic modification of the pore system. Macroscopic and mesoscopic heterogeneities influence producibility by compartmentalizing the reservoir and providing barriers to large-scale fluid flow. Microscopic heterogeneities, on the other hand, influence producibility by controlling the overall rate of fluid flow through the reservoir. This task will involve an expansion of previous general studies of diagenesis within the Smackover and will identify those diagenetic processes that have influenced reef and shoal carbonates in paleohigh reservoirs using Appleton and Vocation Fields as models. This work will document the impact of cementation, compaction, dolomitization, dissolution and neomorphism on reef and shoal reservoirs. A detailed paragenetic sequence will be constructed for reservoir lithologies in each field to document the diagenetic history of these lithologies and to determine the timing of each individual diagenetic event. Attention will be focused on spatial variation in diagenesis within each field and also in variations in diagenesis between fields. The influence of paleohigh relief on diagenesis will be identified. This work will incorporate petrographic, XRD, SEM, and microprobe analyses to characterize, on a microscopic scale, the nature of the pore system in the Appleton and Vocation reservoirs. This task will focus on the evolution of the pore systems through time and on the identification of those diagenetic processes that played a significant role in the development of the existing pore systems. The ultimate goal of the task is to provide a basis for characterization of porosity and permeability with the reef and shoal reservoirs.

W

E

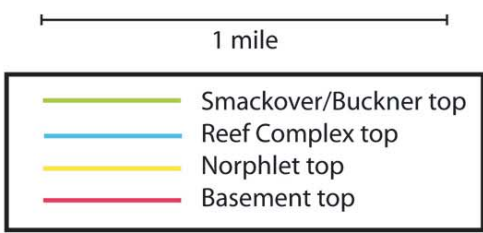
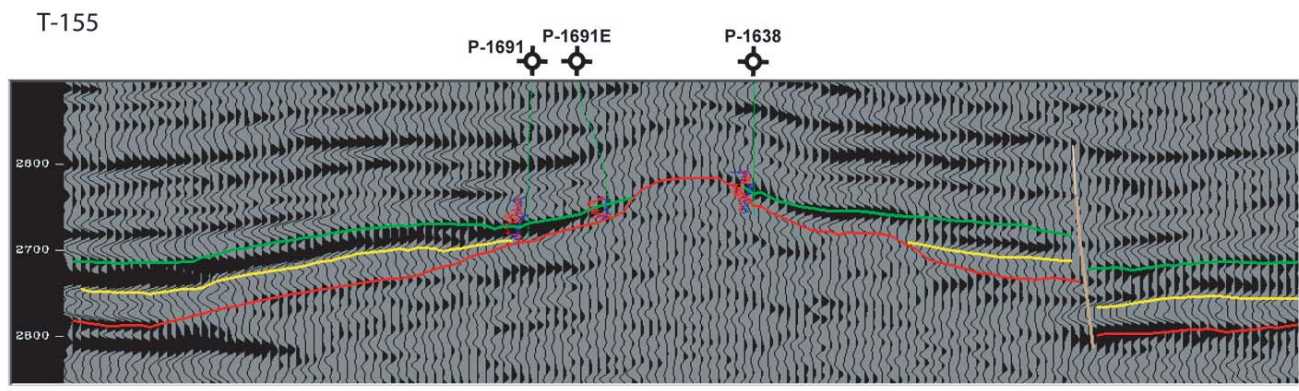
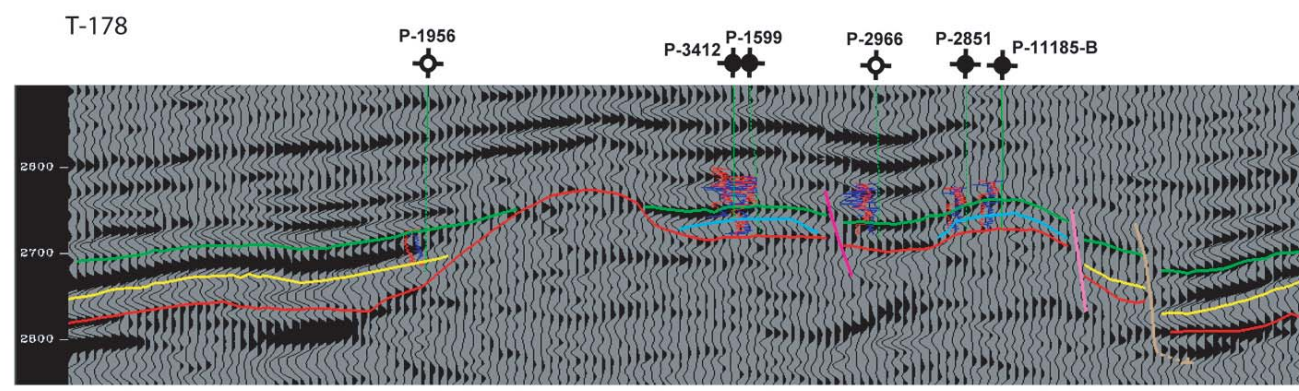
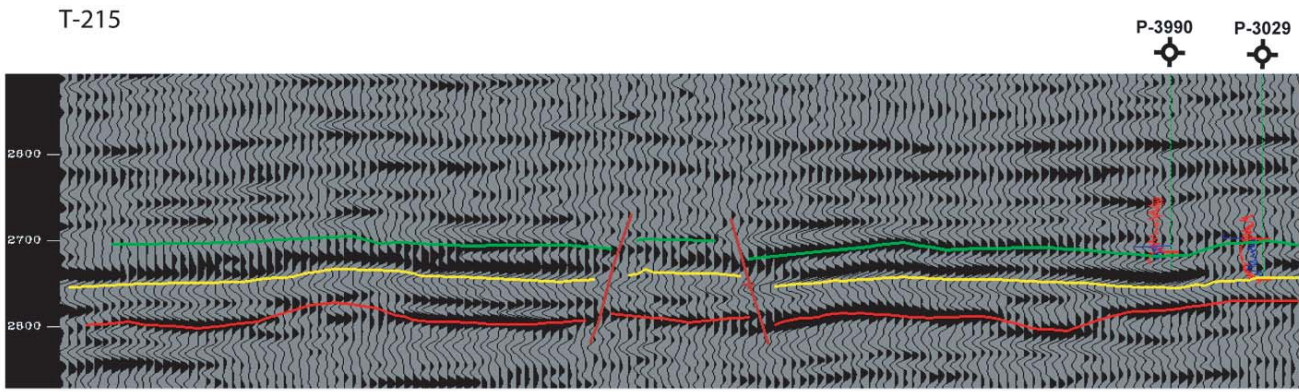


Figure 51. Interpreted seismic lines in Vocation Field.

Thin sections (379) have been studied from 11 cores from Appleton Field to determine the impact of cementation, compaction, dolomitization, dissolution and neomorphism has had on the reef and shoal reservoirs in this field. Thin sections (237) have been studied from 11 cores from Vocation Field to determine the paragenetic sequence for the reservoir lithologies in this field. An additional 73 thin sections have been studied for the shoal and reef lithofacies in Vocation Field to identify the diagenetic processes that played a significant role in the development of the pore systems in the reservoirs at Vocation Field.

The petrographic analysis and pore system studies essentially have been completed. Table 2 summarizes the petrographic characteristics for the Smackover lithofacies in Appleton Field, and Table 5 summarizes these characteristics for the Smackover in Vocation Field. Figure 52 presents a paragenetic sequence for the Smackover at Vocation Field. Pore system studies continue.

**Task 3—Petrophysical and Engineering Property Characterization.**--This task will focus on the characterization of the reservoir rock, fluid, and volumetric properties of the reservoirs at Appleton and Vocation Fields. These properties can be obtained from petrophysical and engineering data. This task will assess the character of the reservoir fluids, as well as quantify the petrophysical properties of the reservoir rock. In addition, considerable effort will be devoted to the rock-fluid behavior (i.e., capillary pressure and relative permeability). The production rate and pressure histories will be cataloged and analyzed for the purpose of estimating reservoir properties such as permeability, well completion efficiency (skin factor), average reservoir pressure, as well as in-place and movable fluid volumes. A major goal is to assess current reservoir pressure conditions and develop a simplified reservoir model. New pressure and tracer survey data will be obtained to assess communication within the reservoir at



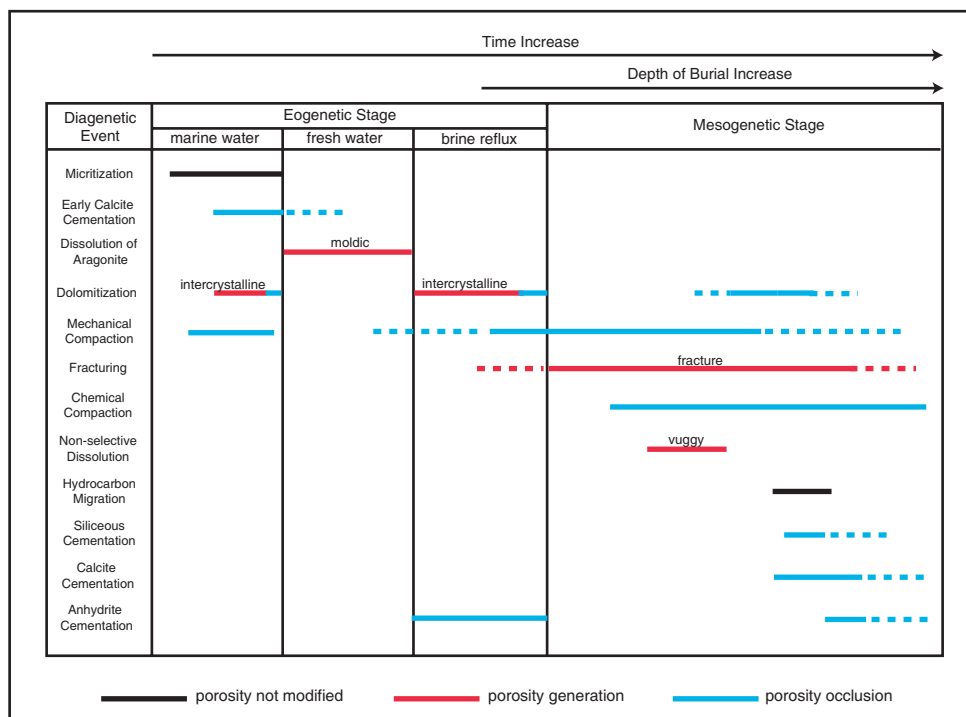


Figure 52. Diagenetic sequence of the Smackover Formation at Vocation Field.

Appleton and Vocation Fields, including among and within the various pay zones in the Smackover. This work will serve as a guide for the reservoir simulation modeling. Petrophysical and engineering data are fundamental to reservoir characterization. Petrophysical data are often considered static (non-time dependent) measurements, while engineering data are considered dynamic (time-dependent). Reservoir characterization is the coupling or integration of these two classes of data. The data are analyzed to identify fluid flow units (reservoir-scale flow sequences), barriers to flow, and reservoir compartments. Petrophysical data are essential for defining the quality of the reservoir, and engineering data (performance data) are crucial for assessing the producibility of the reservoir. Coupling these concepts, via reservoir simulation or via simplified analytical models, allows for the interpretation and prediction of reservoir performance under a variety of conditions. The first phase of the task involves the review, cataloging, and analysis of available core measurements and well log data. This information will be used to classify porosity, permeability, oil and water saturations, grain density, hydrocarbon show, and rock type for each foot of core. Core data will be correlated to the well log responses, and porosity-permeability relationships will be established for each lithofacies evident in the available data. The next phase involves the measurement of basic relative permeability and capillary pressure relations for the reservoir from existing cores. These data will be compiled and analyzed and then used for reservoir simulation and waterflood/enhanced oil recovery calculations. The third phase focuses on the collection and cataloging of fluid property (PVT) data. In particular, basic (black oil) fluid property data are available, where these analyses include standard measurements of gas-oil-ratio (GOR), oil gravity, viscosity, and fluid composition. The objective of the fluid property characterization work is to develop relations for the analysis of well performance data and for reservoir simulation. The final phase will be to

develop a performance-based reservoir characterization of Appleton and Vocation Fields. This phase will focus exclusively on the analysis and interpretation of well performance data as a mechanism to predict recoverable fluids and reservoir properties. This analysis will focus on the production data, but any other well performance data will also be considered, in particular, pressure transient test data and well completion/stimulation data will also be analyzed and integrated into the reservoir description. Historical pressure data will be compared to new pressure and tracer survey data for wells obtained as part of this work. The material balance decline type curve analysis will be emphasized for the analysis of the data.

Petrophysical and engineering property characterization is essentially completed.

**Appleton Field.** Petrophysical and engineering property data have been gathered and tabulated for Appleton Field. These data include oil, gas and water production, fluid property (PVT) analyses and porosity and permeability information (Tables 6 and 7). Porosity and permeability characteristics of Smackover facies have been analyzed for each well using porosity histograms (Figures 53-57), permeability histograms (Figures 58-62) and porosity versus depth plots (Figures 63-67). Log porosity versus core porosity and porosity versus permeability plots for wells in the field have been prepared (Figures 68-72). Porosity versus permeability cross plots for Smackover facies have been prepared (Figures 73-77). Well performance studies through type curve (Table 8 and Figures 78-82) and decline curve analyses (Figures 83-87) have been completed for the wells in the field. The original oil in place and recoverable oil remaining for the field have been calculated (Table 9 and Figures 88-95).

**Vocation Field.** Petrophysical and engineering property data have been gathered and tabulated for Vocation Field. These data include oil, gas and water production, fluid property (PVT) analyses and porosity and permeability information (Tables 10-14). Porosity and

Table 6 — Porosity and permeability characteristics in the Smackover.

Well	Minimum Porosity, (percent)	Maximum Porosity, (percent)	Average Porosity, (percent)	Minimum Permeability, (md)	Maximum Permeability, (md)	Geometric Average Permeability, (md)
3854B	3.2	24.4	13.6	0.54	618.1	21.8
3986	9.7	29.0	15.7	6.1	2200	108.3
4633B	9.2	24.1	17.0	0.37	1349	103.9
4835B	4.0	24.4	15.0	0.46	3345	191.4
6247B	1.0	6.7	2.7	0.055	0.1	0.07

Table 7 — Porosity and permeability characteristics in the Reef.

Well	Minimum Porosity, (percent)	Maximum Porosity, (percent)	Average Porosity, (percent)	Minimum Permeability, (md)	Maximum Permeability, (md)	Geometric Average Permeability, (md)
3854B	N/A	N/A	N/A	N/A	N/A	N/A
3986	10.7	22.1	14.5	8.9	1545	115.6
4633B	10.5	25.0	18.4	13.4	1748	274.0
4835B	16.0	20.8	17.9	225.8	563.8	345.9
6247B	1.0	14.3	5.6	0.025	18.8	1.79

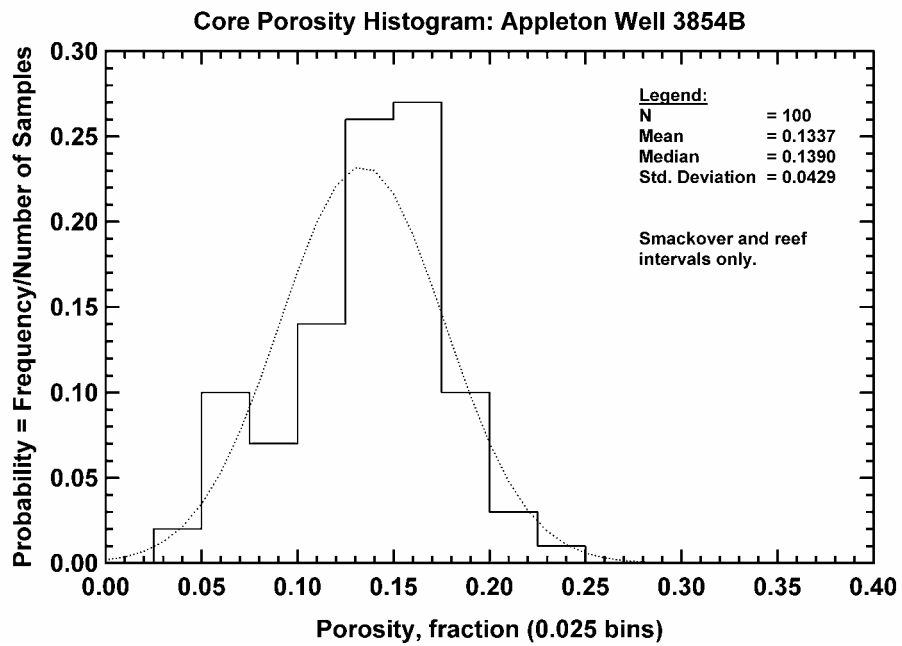


Fig. 53 — Core Porosity Histogram, Appleton Well 3854B

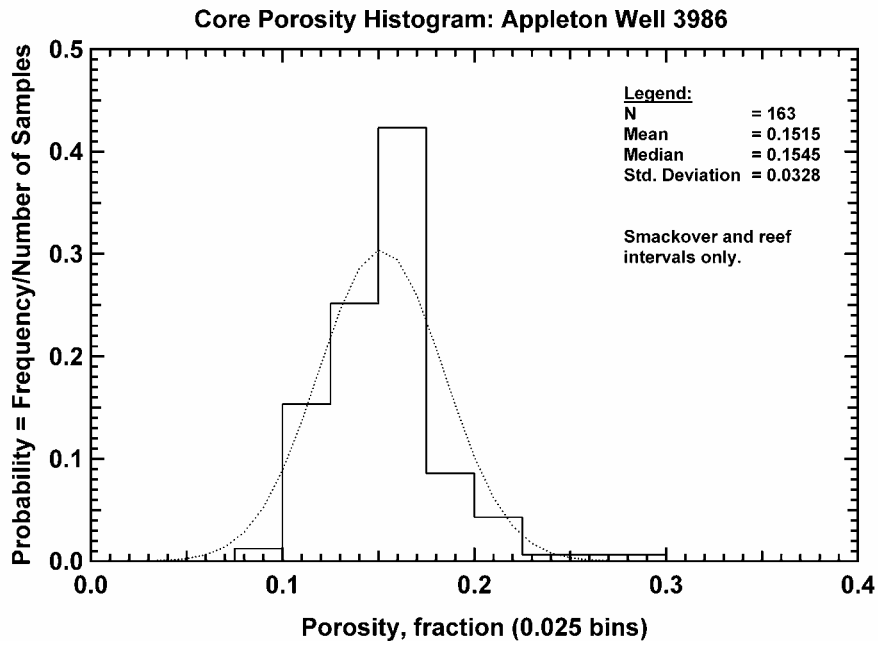


Fig. 54 — Core Porosity Histogram, Appleton Well 3986

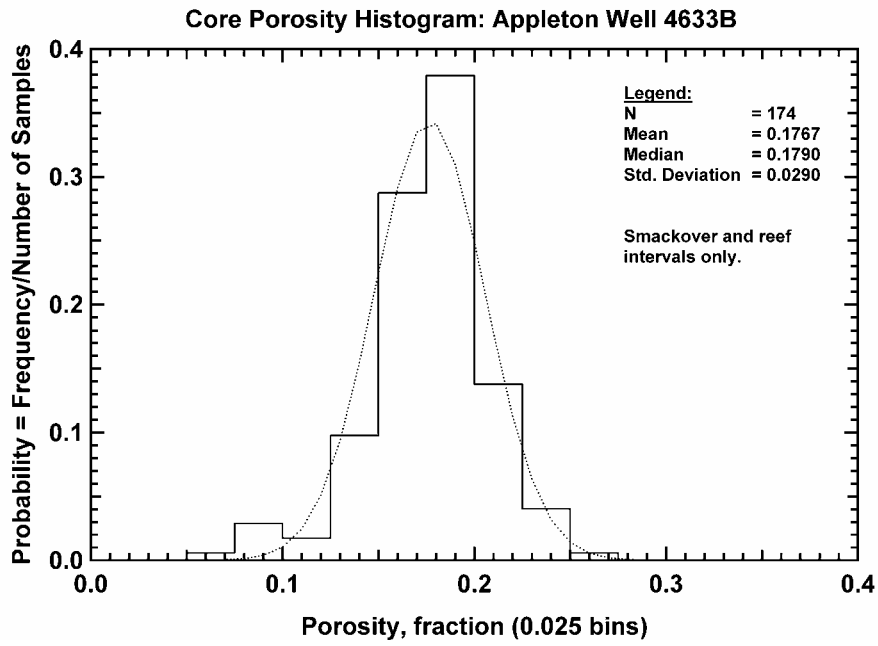


Fig. 55 — Core Porosity Histogram, Appleton Well 4633B

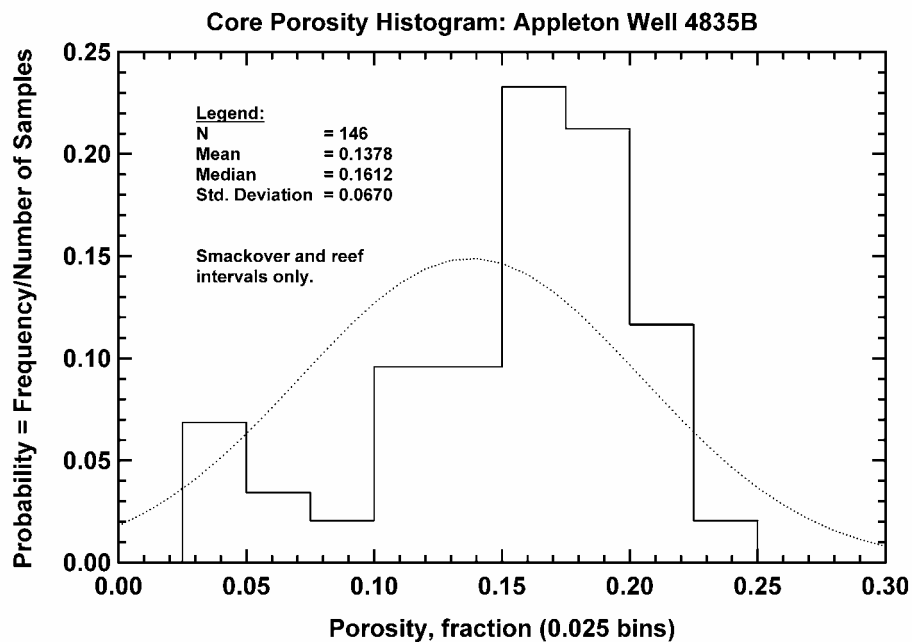


Fig. 56 — Core Porosity Histogram, Appleton Well 4835B

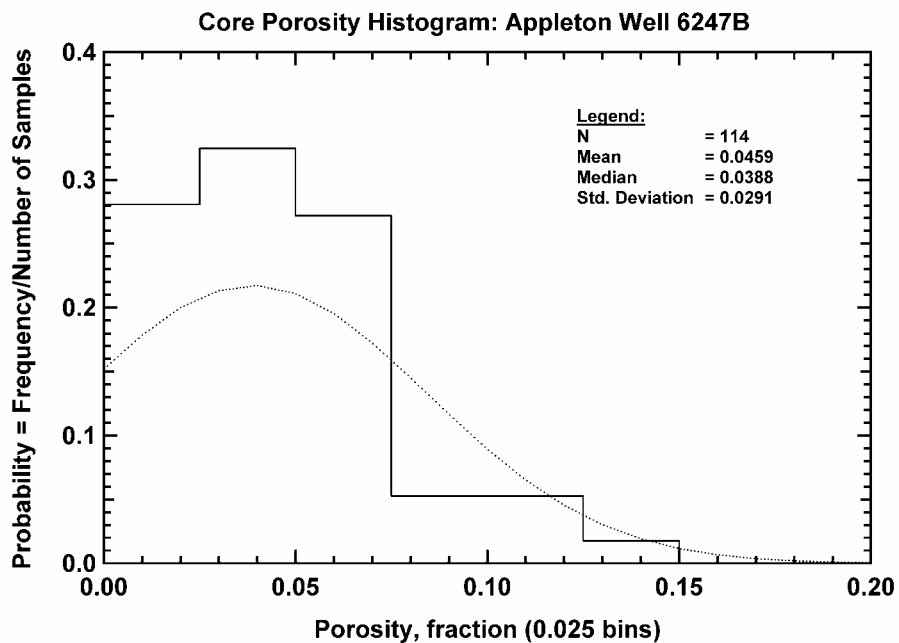


Fig. 57 — Core Porosity Histogram, Appleton Well 6247B

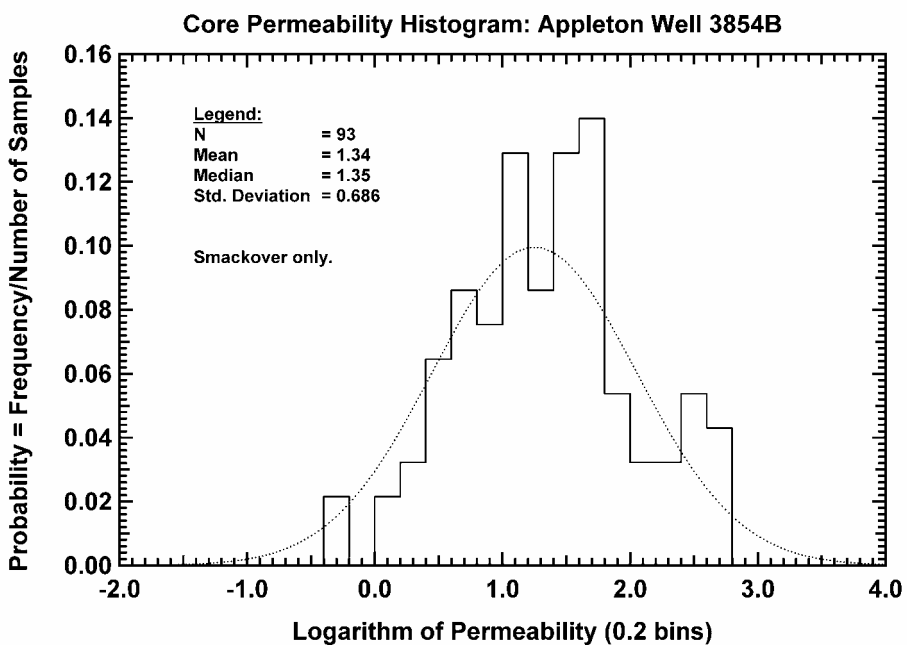


Fig. 58 — Core Permeability Histogram, Appleton Well 3854B

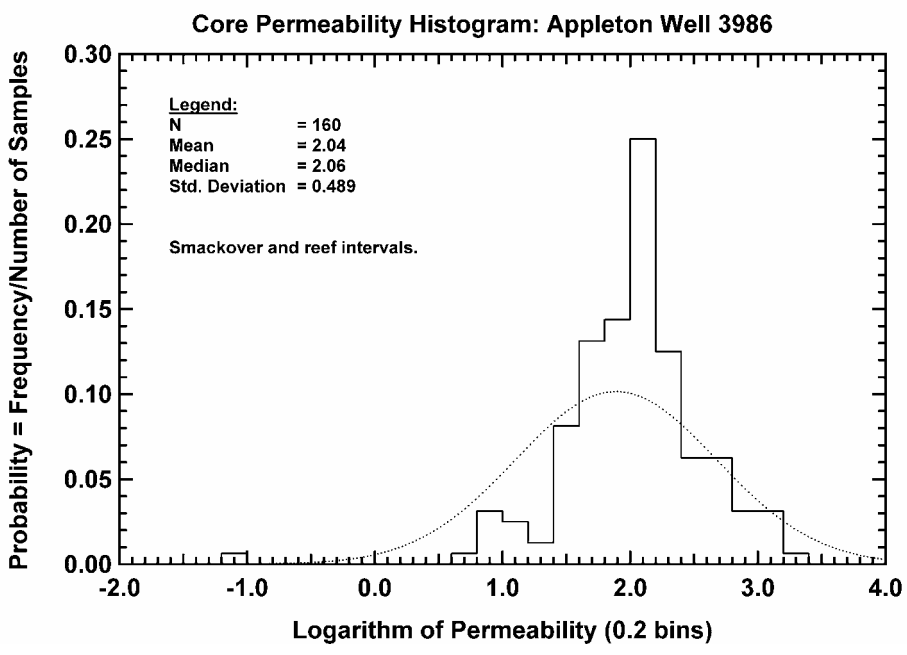


Fig. 59 — Core Permeability Histogram, Appleton Well 3986



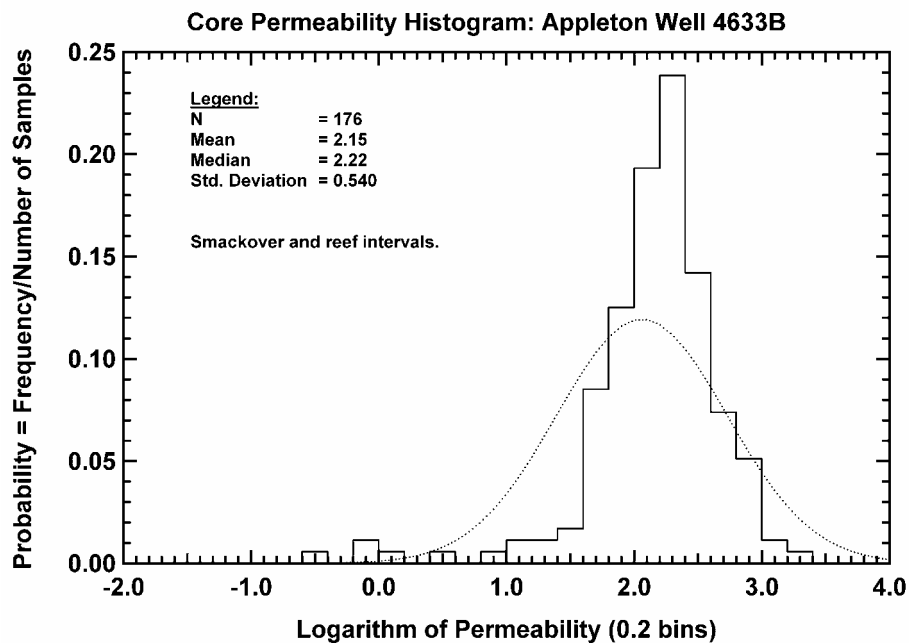


Fig. 60 — Core Permeability Histogram, Appleton Well 4633B

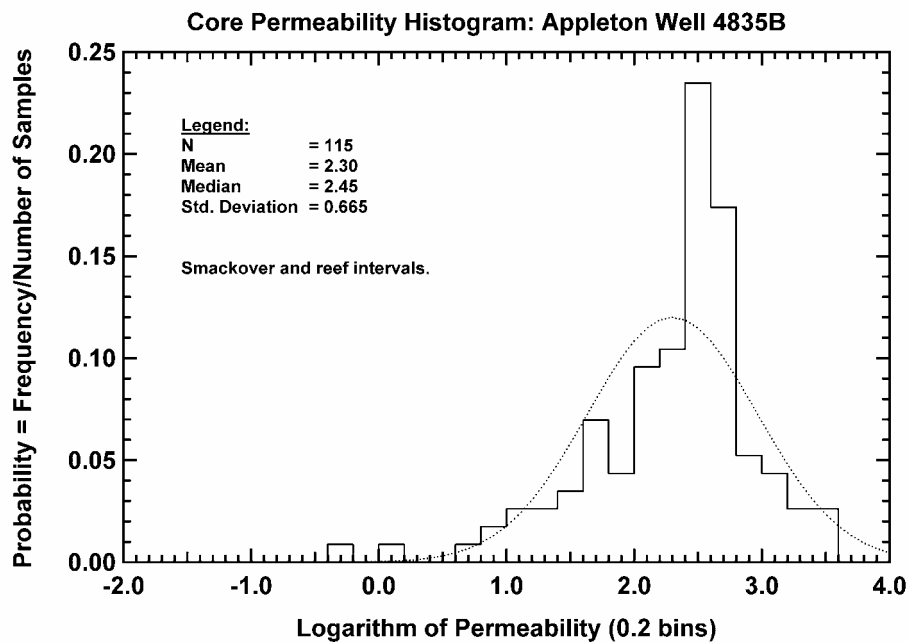


Fig. 61 — Core Permeability Histogram, Appleton Well 4835B

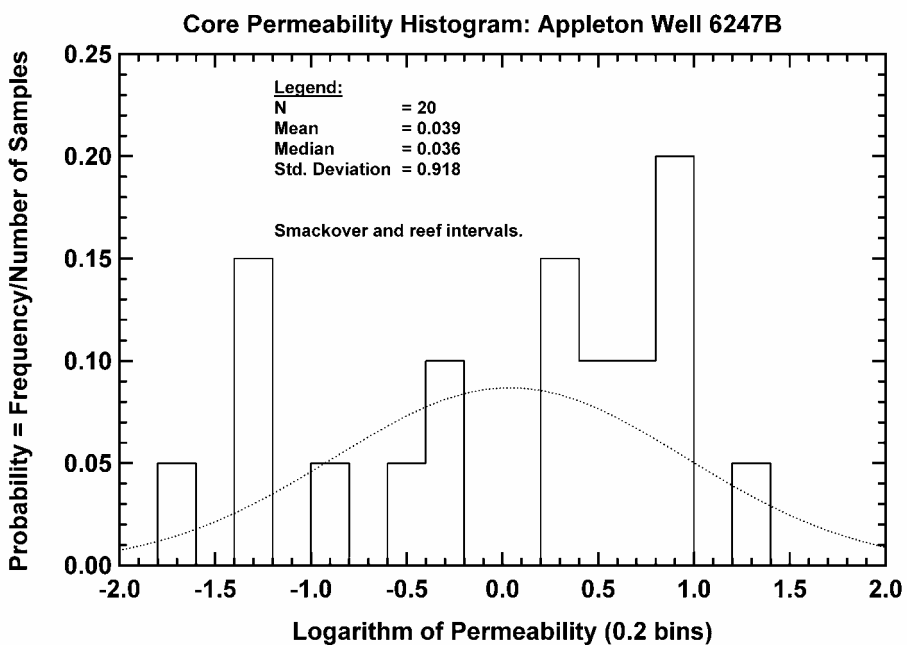


Fig. 62 — Core Permeability Histogram, Appleton Well 6247B

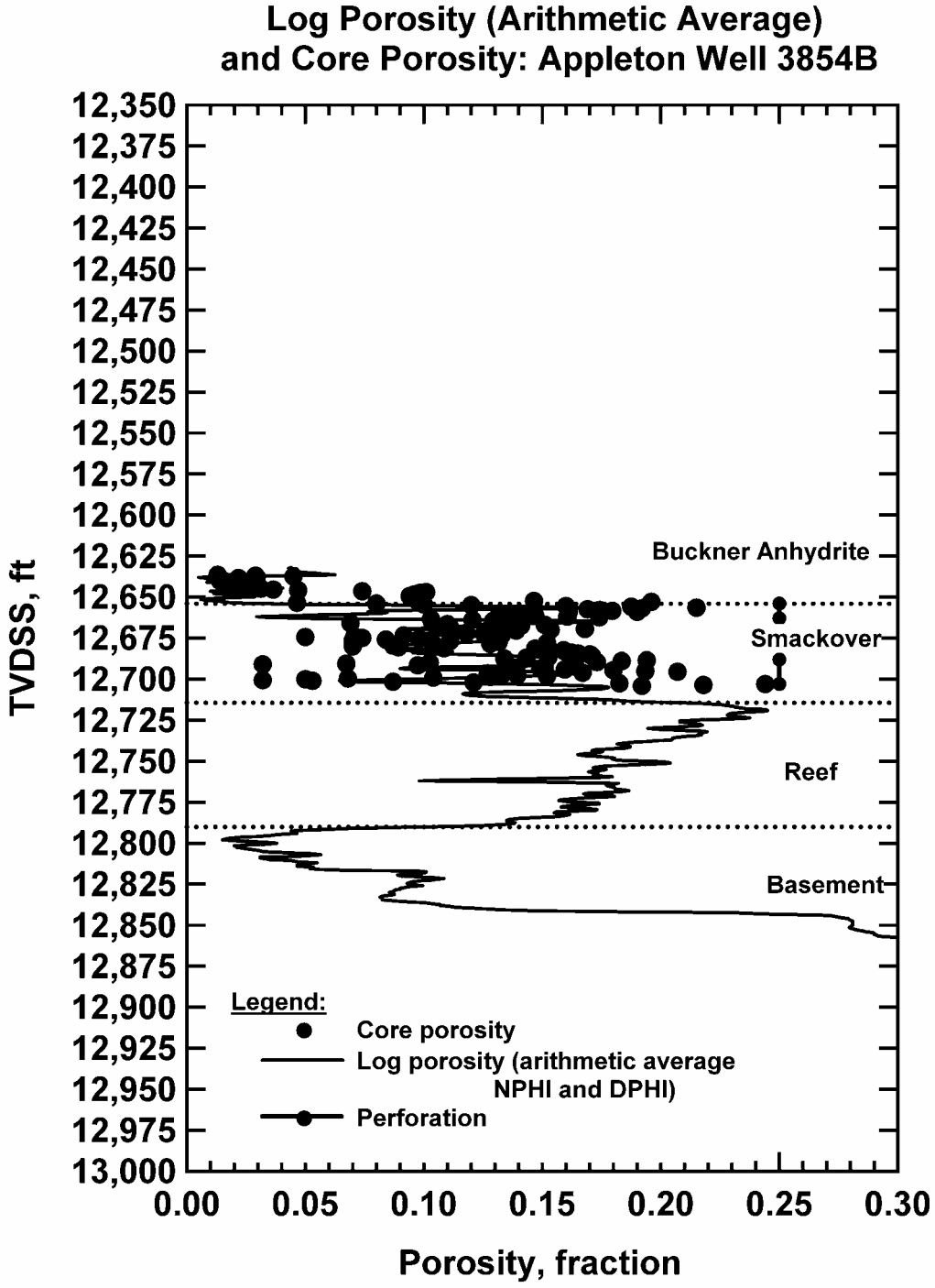


Fig. 63 — Porosity Variation with Depth, Appleton Well 3854B

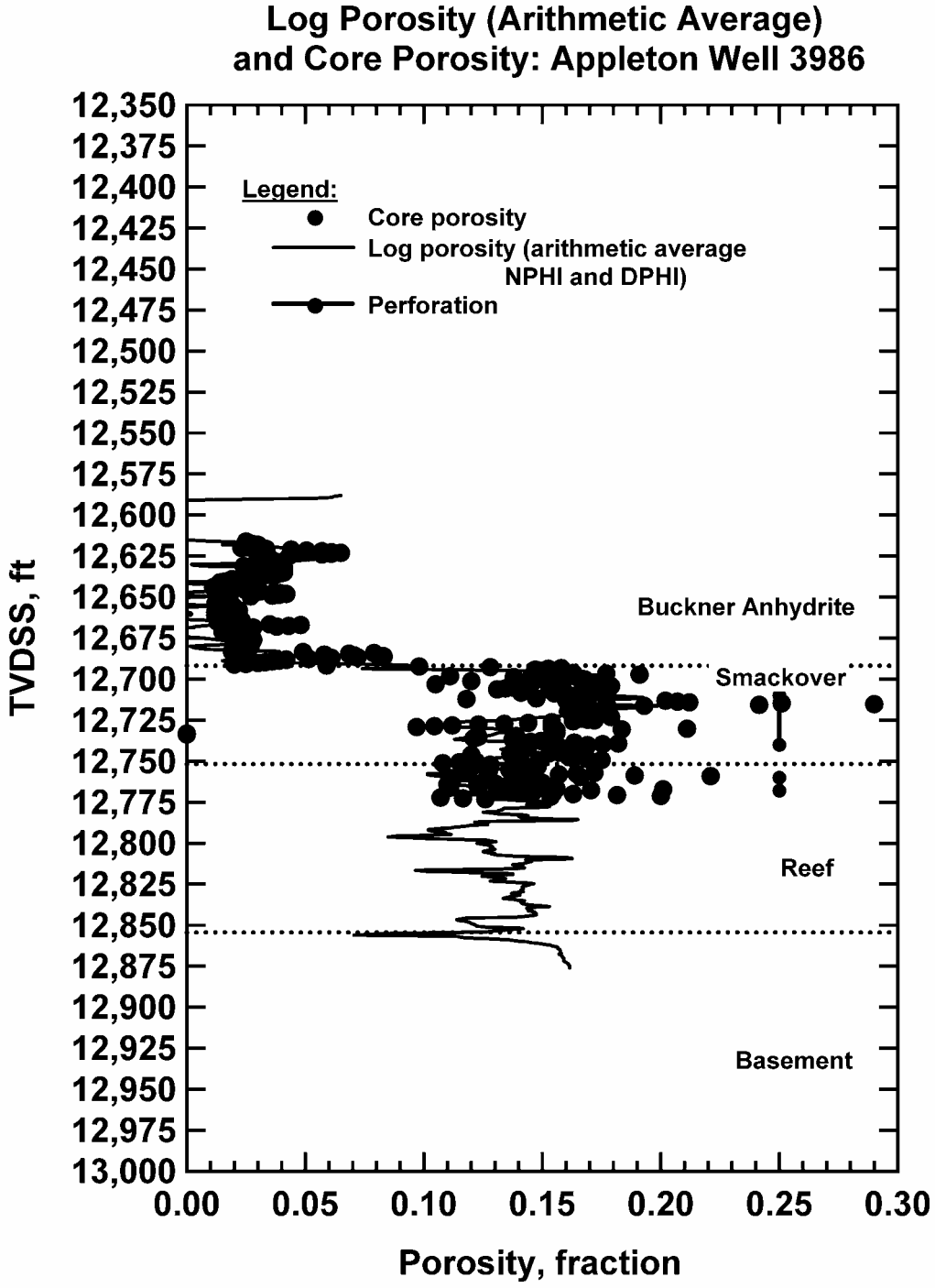


Fig. 64 — Porosity Variation with Depth, Appleton Well 3986

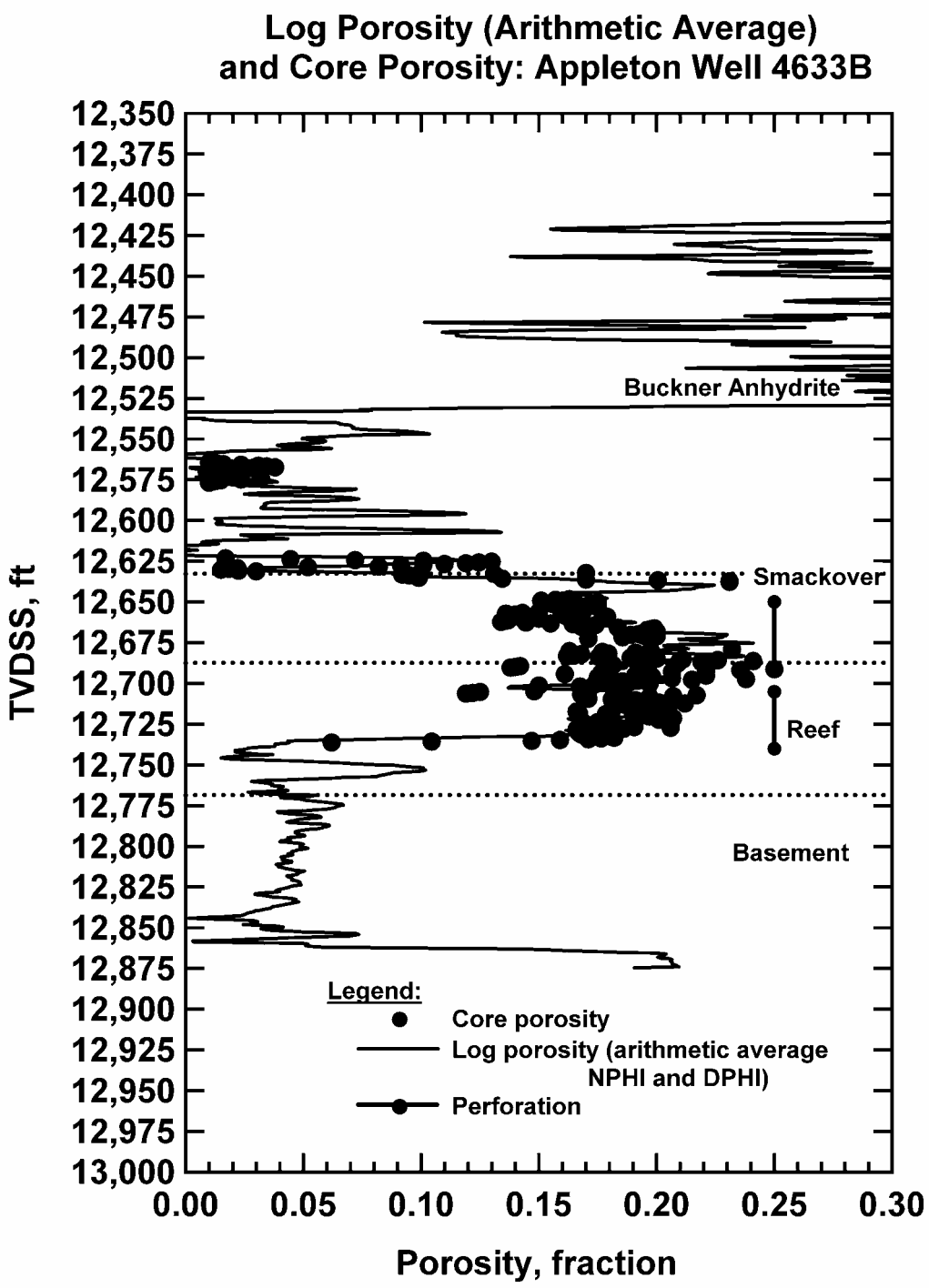


Fig. 65 — Porosity Variation with Depth, Appleton Well 4633B

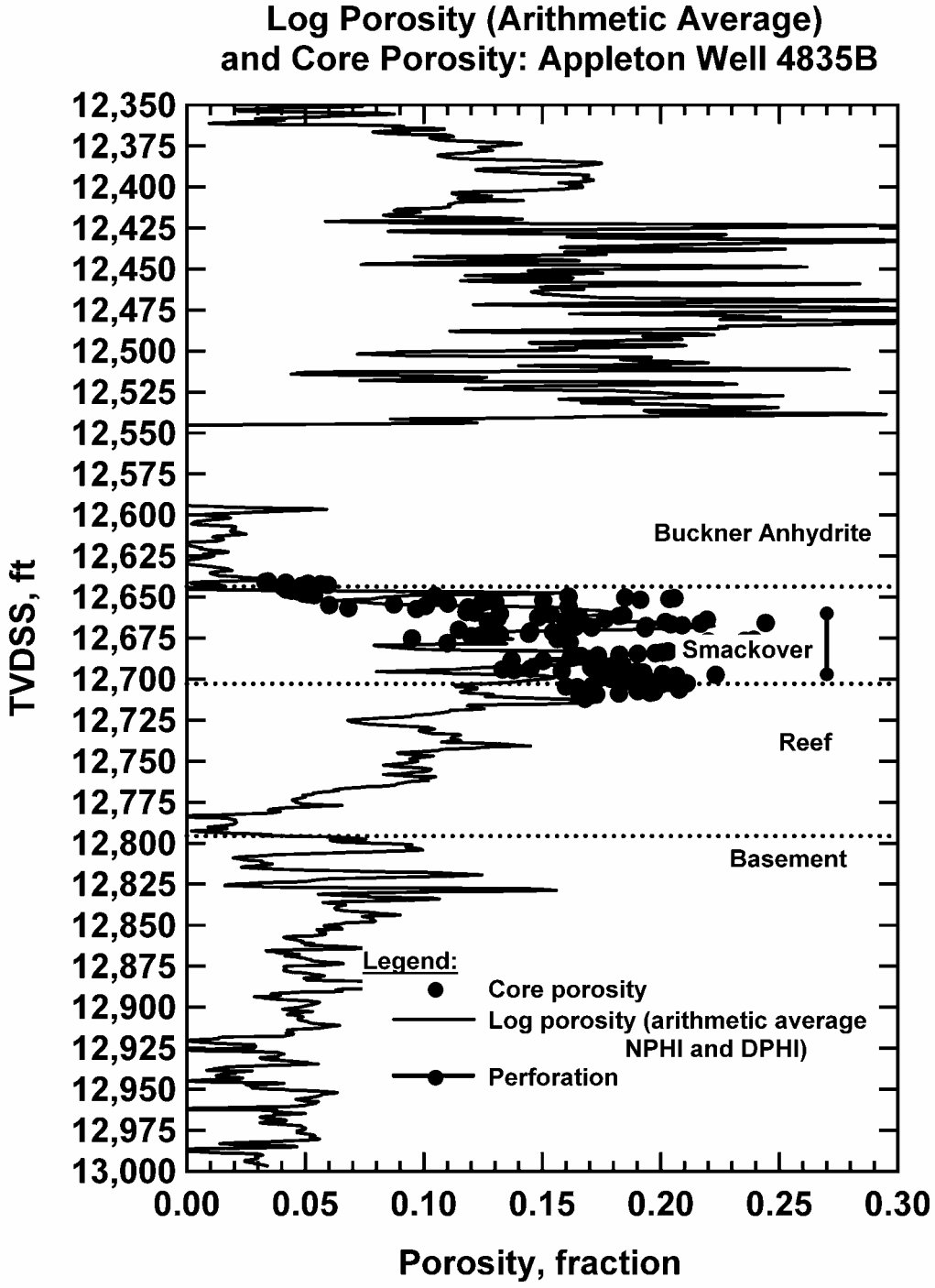


Fig. 66 — Porosity Variation with Depth, Appleton Well 4835B

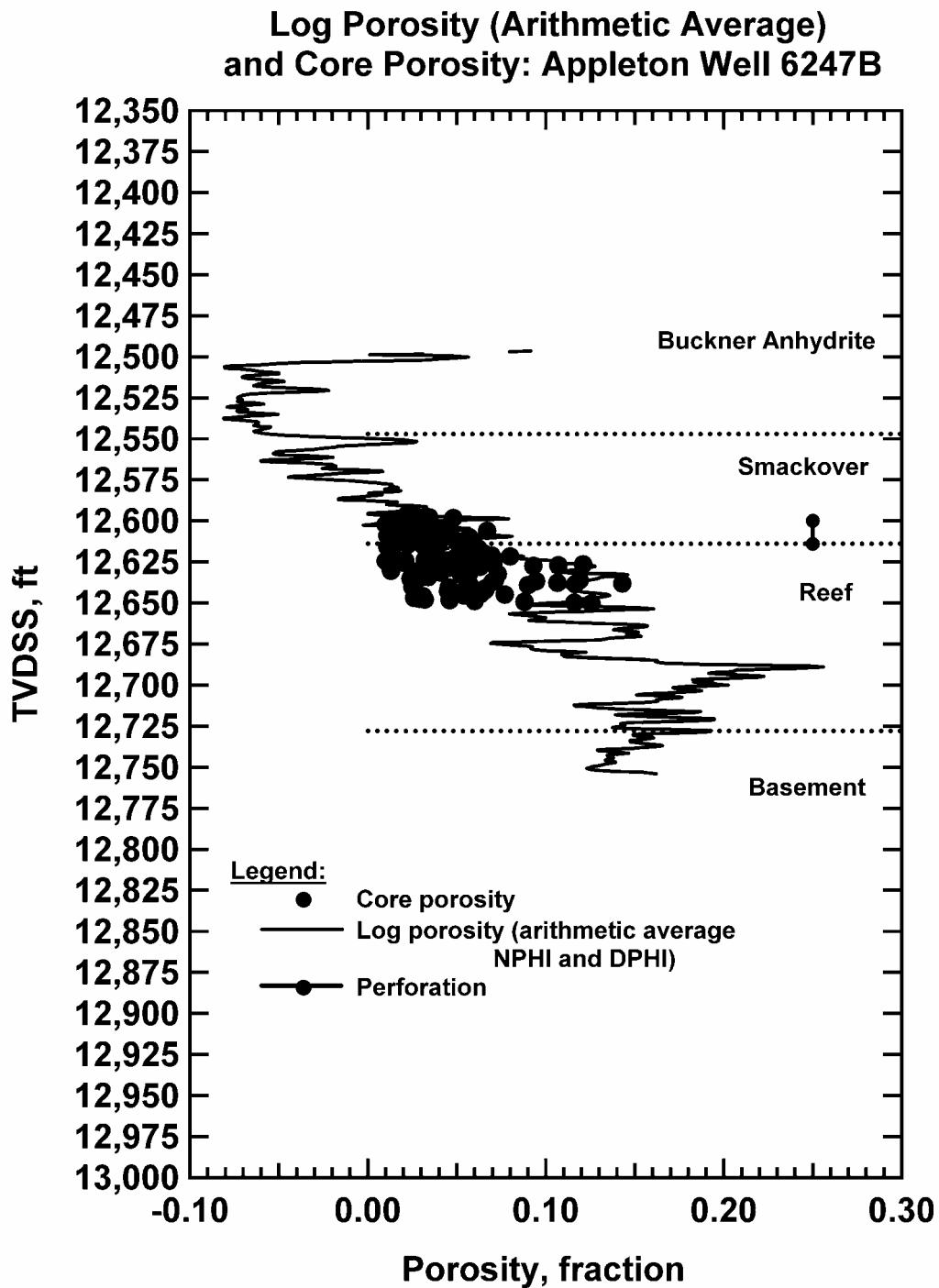


Fig. 67 — Porosity Variation with Depth, Appleton Well 6247B

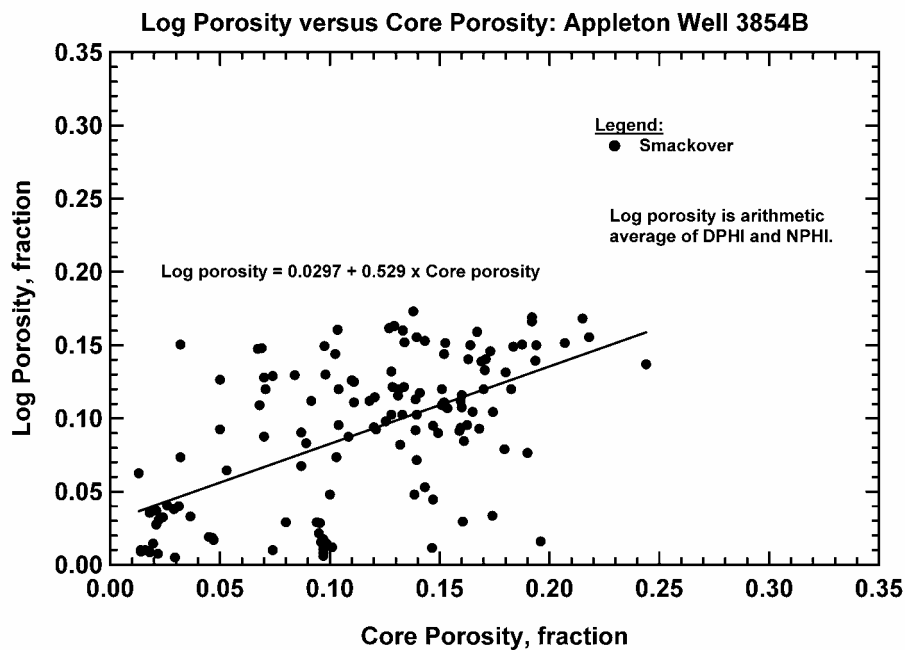


Fig. 68 — Log Porosity versus Core Porosity, Appleton Well 3854B

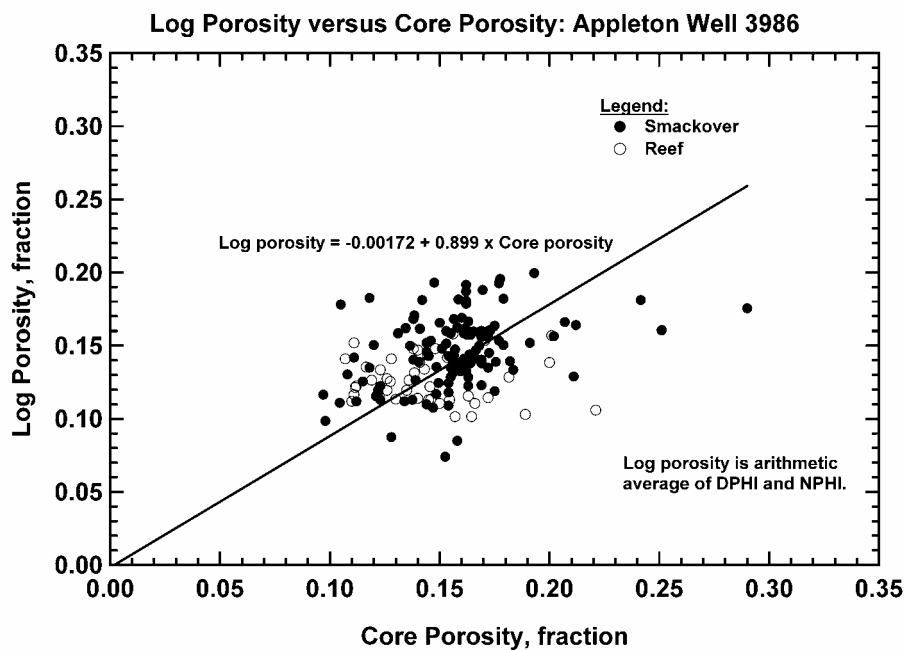


Fig. 69 — Log Porosity versus Core Porosity, Appleton Well 3986



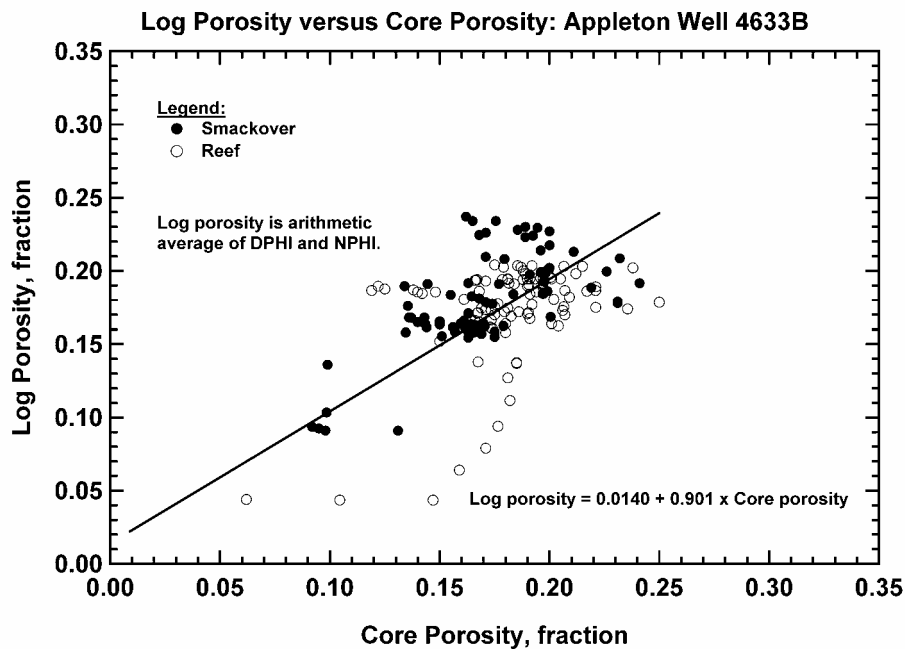


Fig. 70 — Log Porosity versus Core Porosity, Appleton Well 4633B

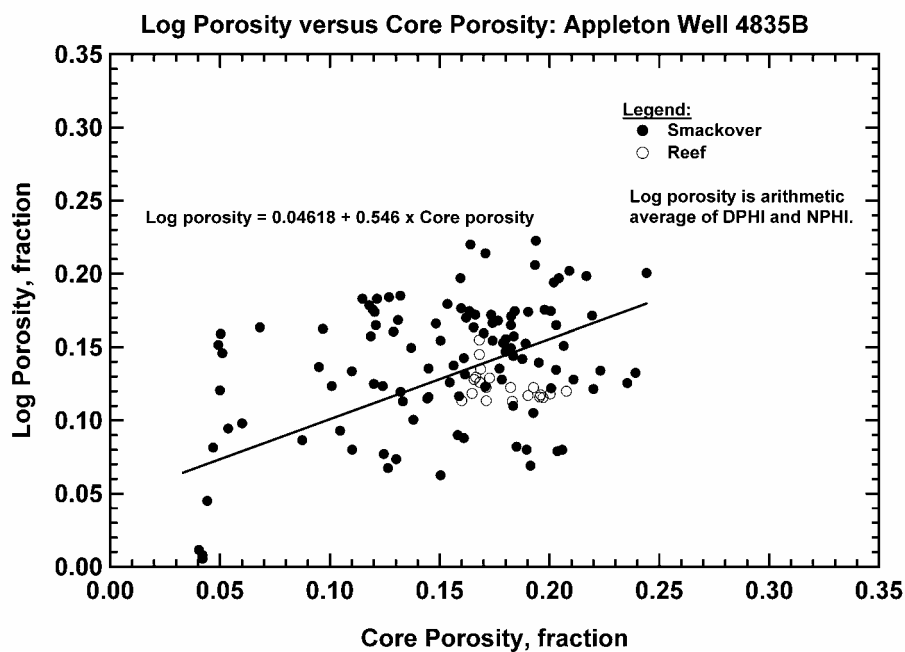


Fig. 71 — Log Porosity versus Core Porosity, Appleton Well 4835B

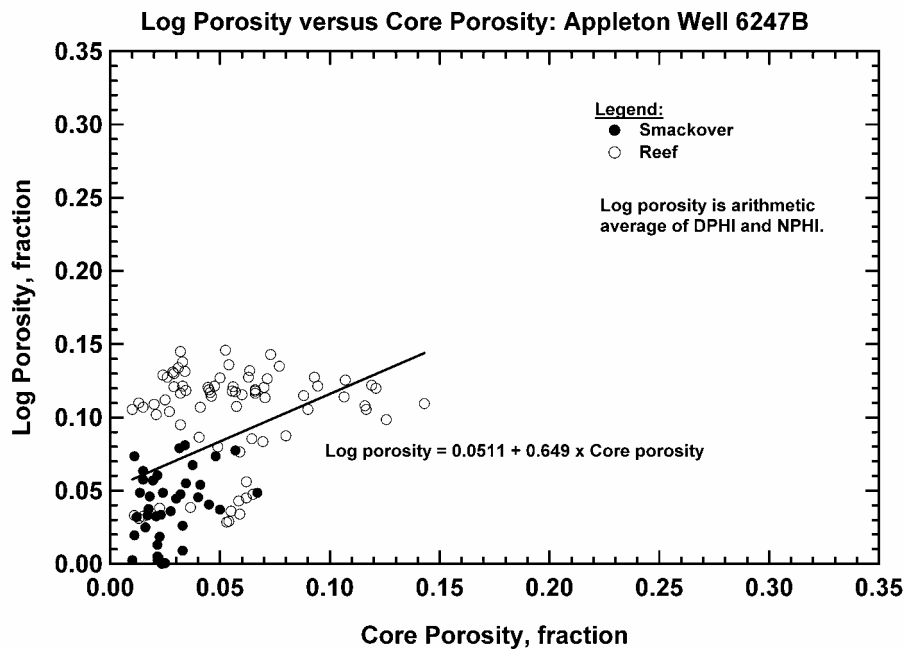


Fig. 72 — Log Porosity versus Core Porosity, Appleton Well 6247B

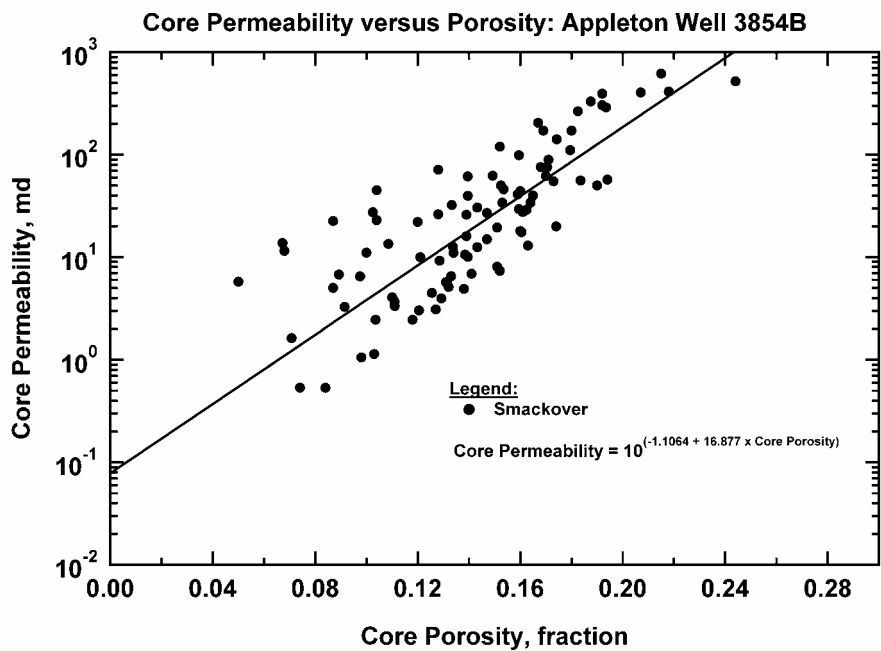


Fig. 73 — Core Permeability versus Core Porosity, Appleton Well 3854B.

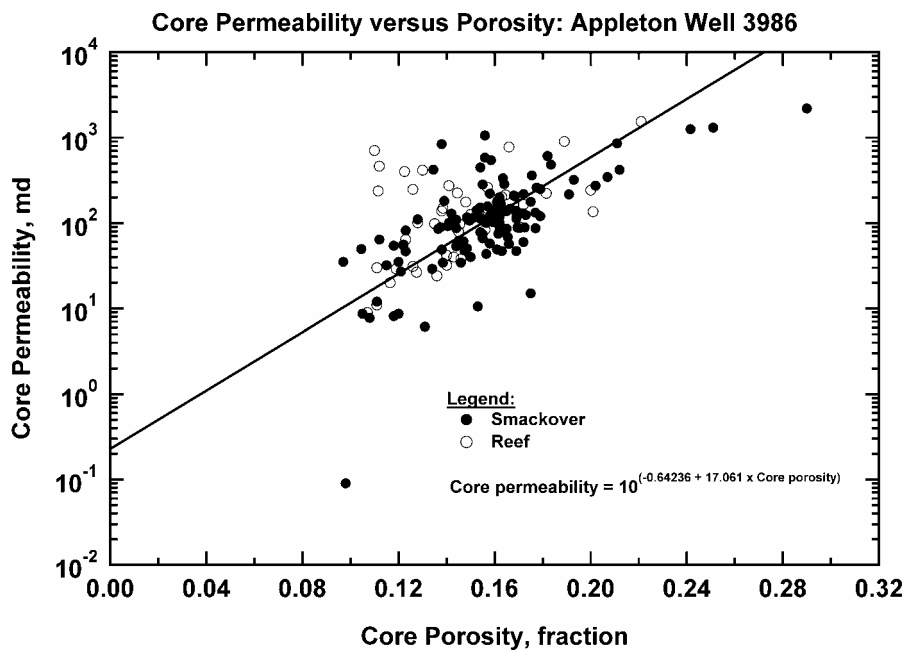


Fig. 74 — Core Permeability versus Core Porosity, Appleton Well 3986.

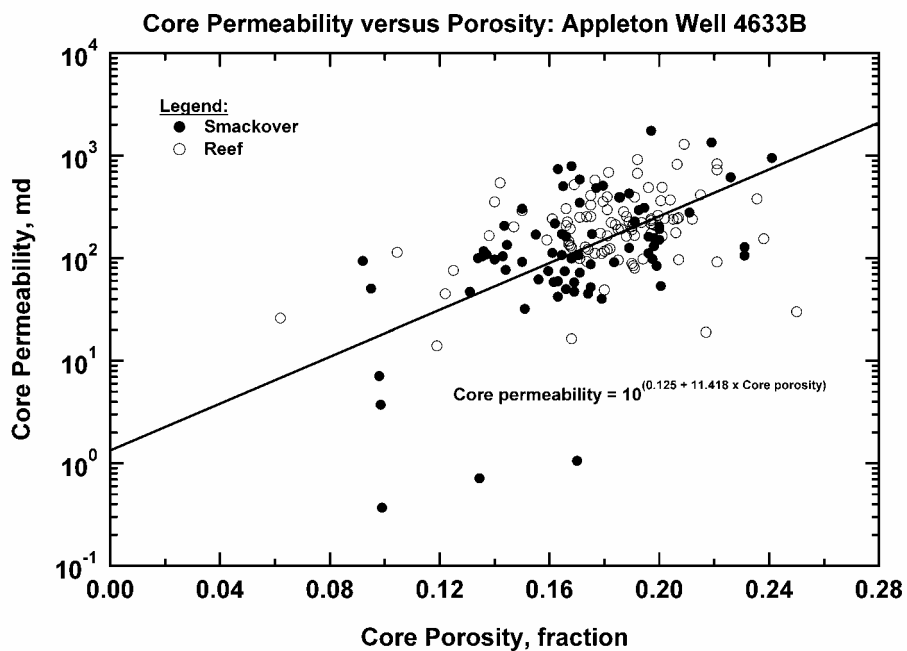


Fig. 75 — Core Permeability versus Core Porosity, Appleton Well 4633B.

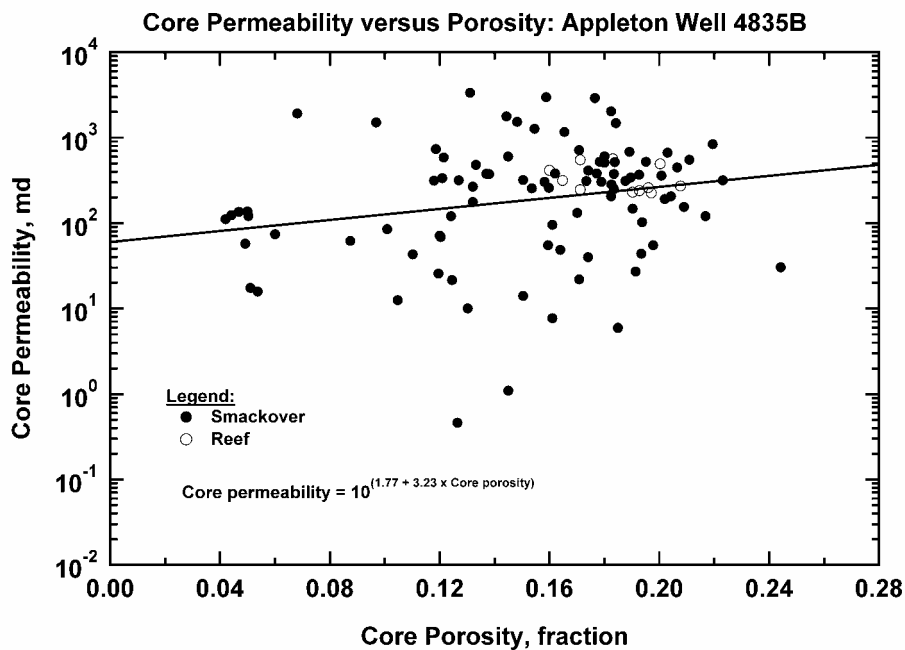


Fig. 76 — Core Permeability versus Core Porosity, Appleton Well 4835B.

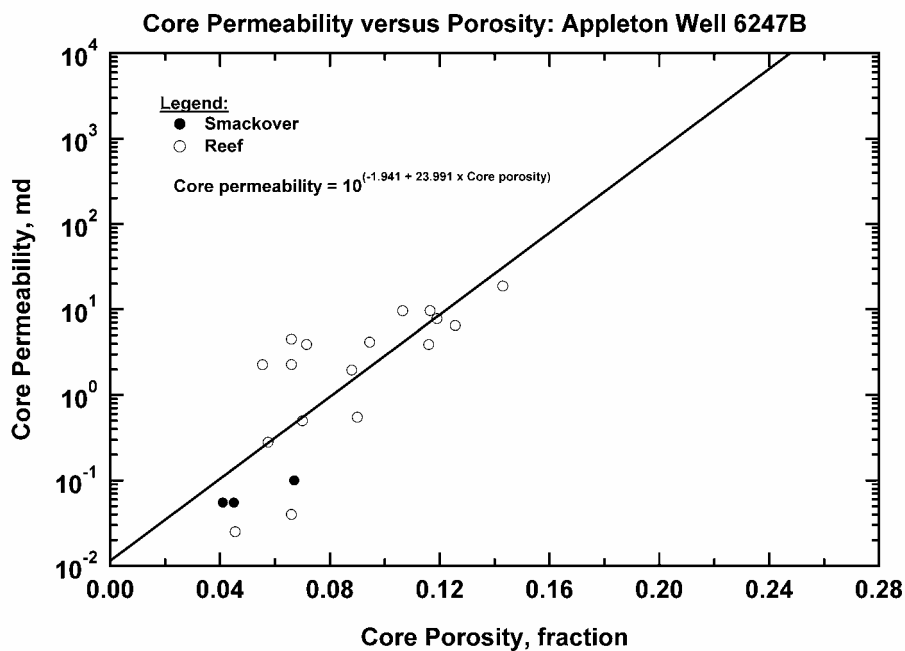


Fig. 77 — Core Permeability versus Core Porosity, Appleton Well 6247B.

Table 8 — Parameters Derived from Type Curve Analysis.

Well	$N_{c_t}$ (STB/ps i)	$N$ (MSTB)	$A$ (acres)	$k_o$ (md)	$s$ (dim-less)
3854B	471.6	25630	1600.5	1.14	-7.6
3986	50.1	2725	35.6	0.06	-5.7
4633B	510.1	27720	680.9	1.86	0.09
4835B	355.4	19320	617.6	3.00	0.12
6247B	62.8	3411	229.0	1.14	-4.7
Total		= 78806			

Well Id: Well 3854 Date: Sep 10,2002 Time: 16:10  
 Analyst: Archer/Blasingame/Chijuka

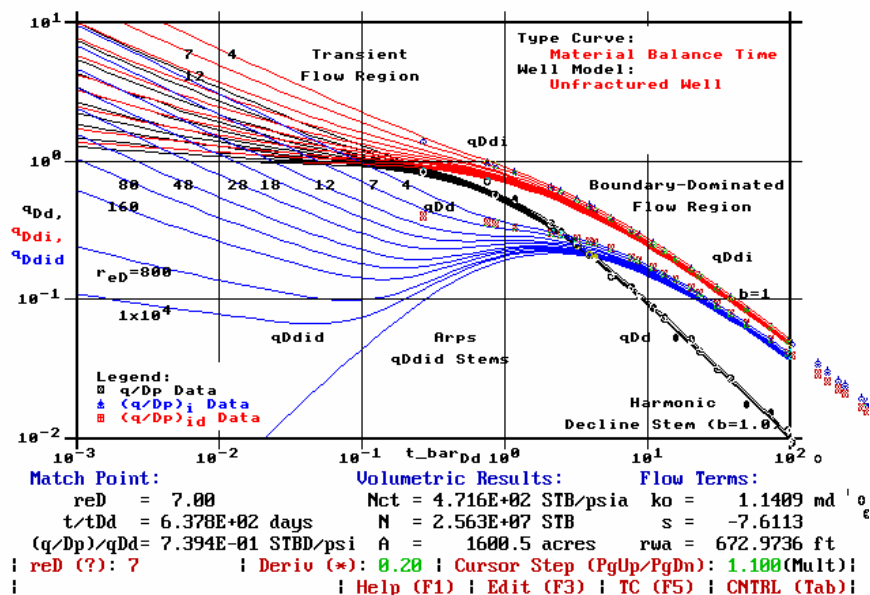


Fig. 78 — Type Curve Match, Appleton Well 3854.

Well Id: Well 3986 Date: Sep 10,2002 Time: 16:00  
 Analyst: Archer/Chijuka/Blasingame

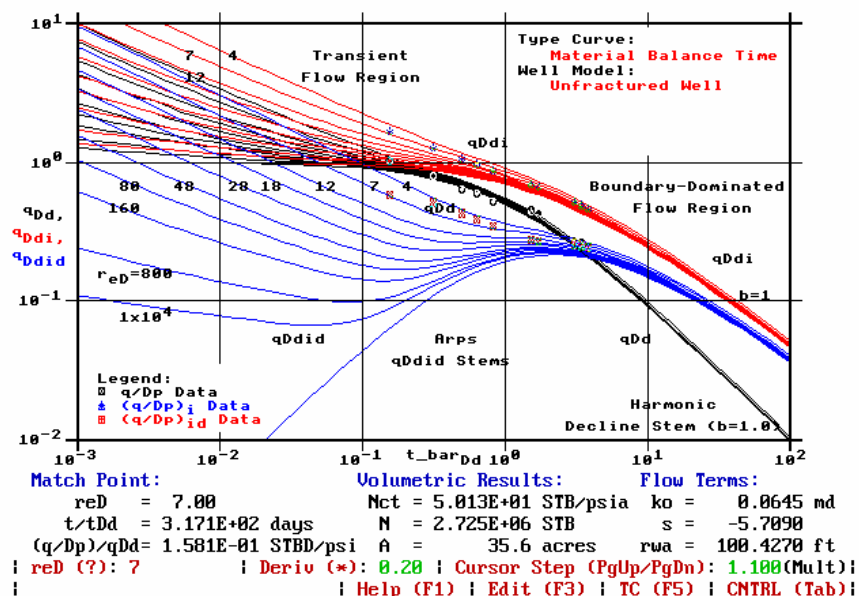


Fig. 79 — Type Curve Match, Appleton Well 3986.

Well Id: Well 4633 Date: Sep 10, 2002 Time: 20:00  
 Analyst: Archer/Blasingame/Chijuka

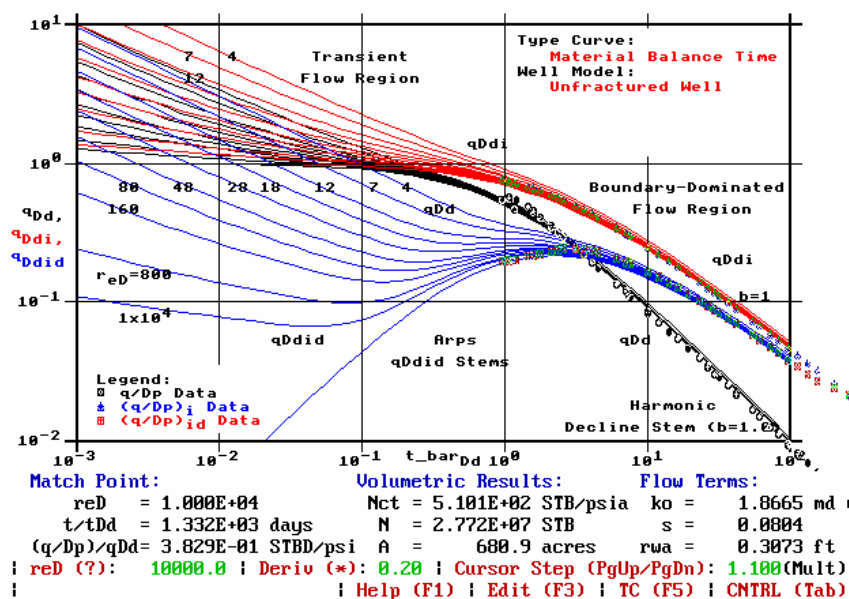


Fig. 80 — Type Curve Match, Appleton Well 4633B.

Well Id: Well 4835 Date: Sep 10, 2002 Time: 17:09  
 Analyst: Archer/Blasingame/Chijuka

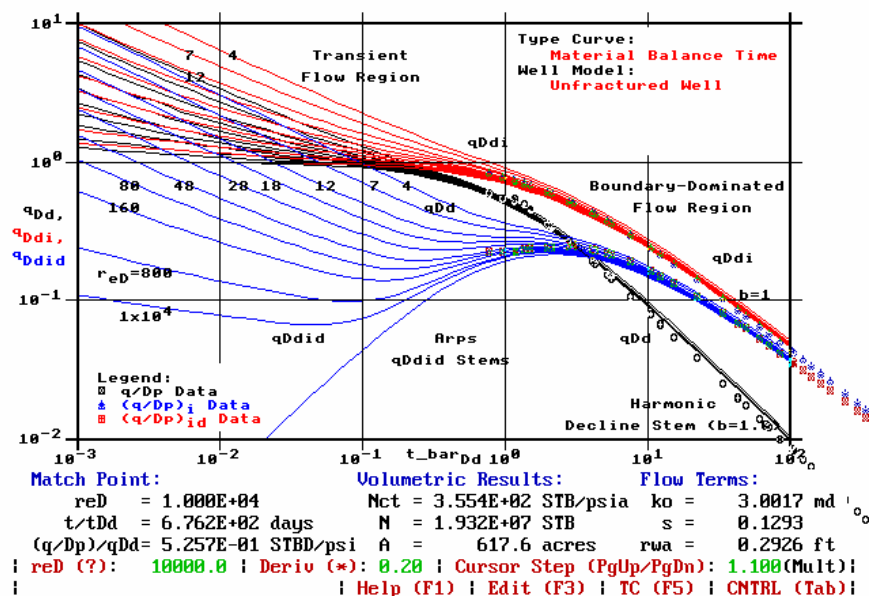


Fig. 81 — Type Curve Match, Appleton Well 4835B.

Well Id: Well 6247 Date: Sep 10, 2002 Time: 17:11  
 Analyst: Archer/Blasingame/Chijuka

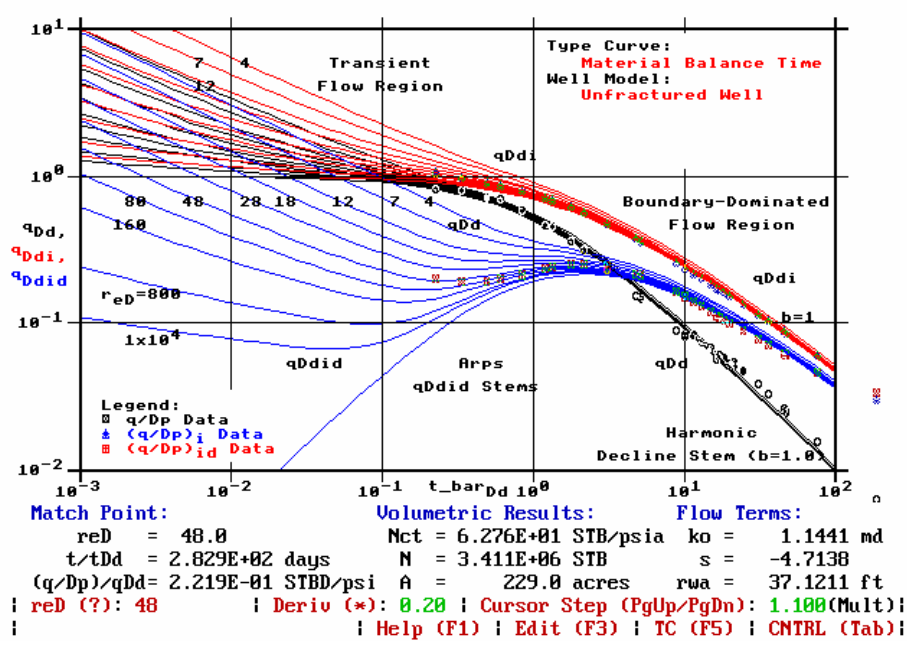


Fig. 82 — Type Curve Match, Appleton Well 6247B.



Date: Sep 10,2002 Time: 21:25

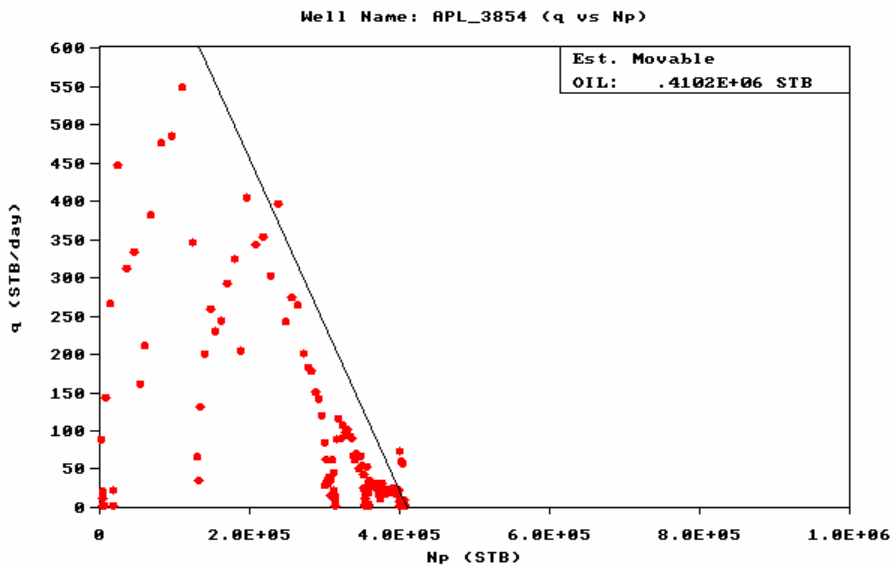


Fig. 83 — Estimate of Recoverable Oil, Appleton Well 3854B.

Date: Sep 15,2002 Time: 14:41

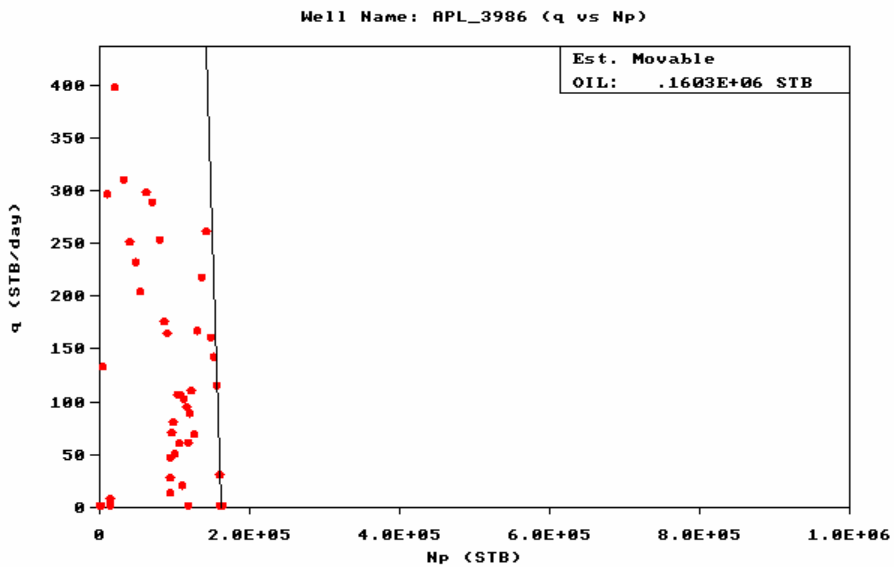


Fig. 84 — Estimate of Recoverable Oil, Appleton Well 3986.

Date: Sep 15,2002 Time: 15:09

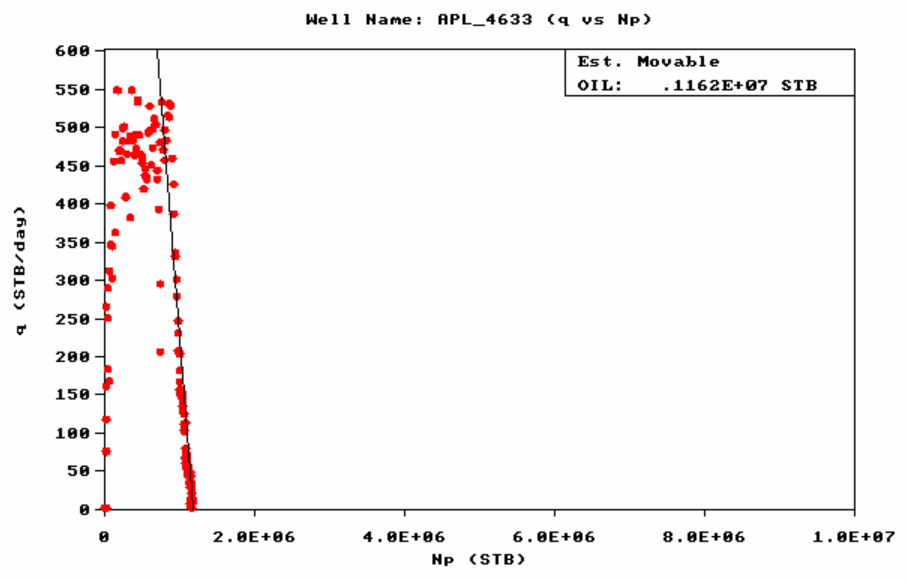


Fig. 85 — Estimate of Recoverable Oil, Appleton Well 4633B.

Date: Sep 15,2002 Time: 15:12

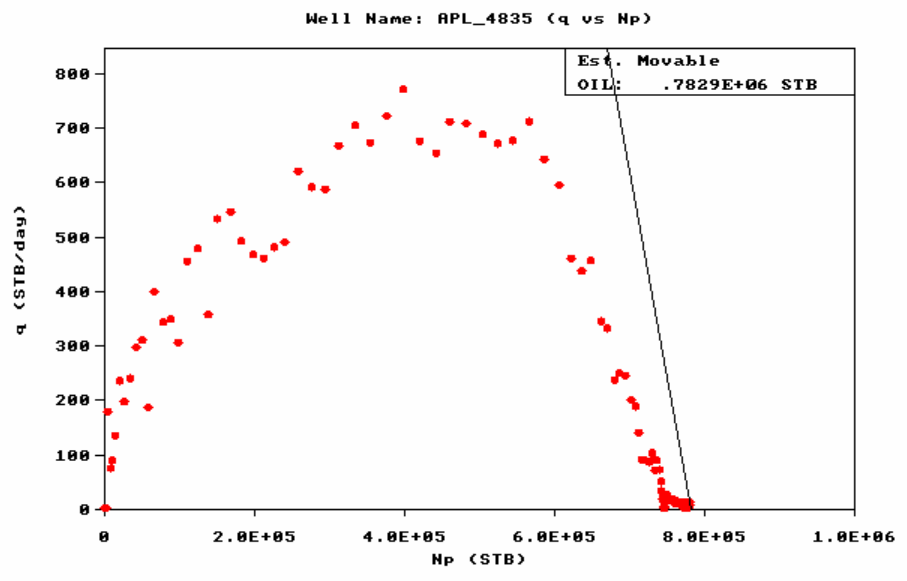


Fig. 86 — Estimate of Recoverable Oil, Appleton Well 4835B.

Date: Sep 15, 2002 Time: 15:15

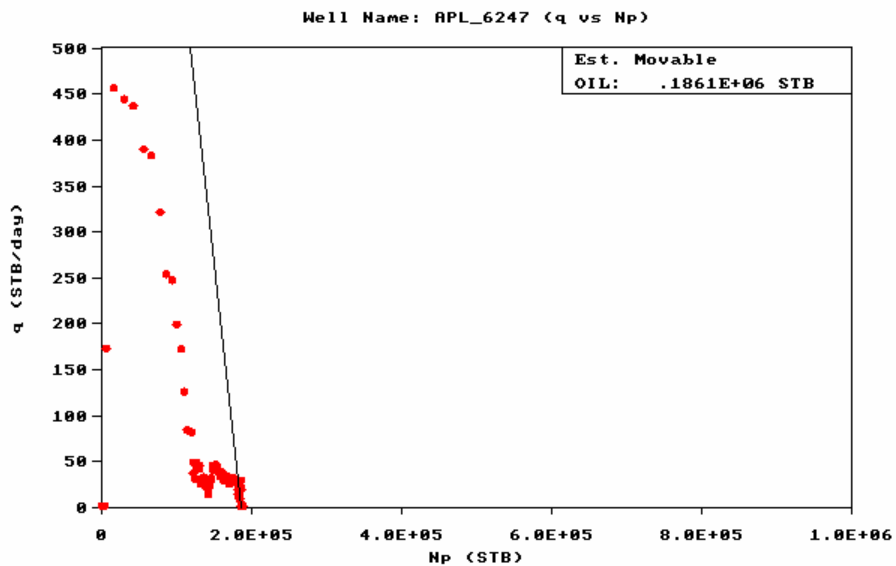


Fig. 87 — Estimate of Recoverable Oil, Appleton Well 6247B.

Table 9 – Oil Recovery and Recovery Factors.

Well	$N_{recoverable}$ (MSTB)	$N_p$ (MSTB)	$N$ (MSTB)	Recovery Factor $N_p/N$ (dim-less)
3854B	410	410	25630	0.016
3986	160	160	2725	0.059
4633B	1160	1150	27720	0.041
4835B	783	780	19320	0.040
6247B	186	180	3411	0.053
Total	= 2699	= 2680	= 78806	= 0.034

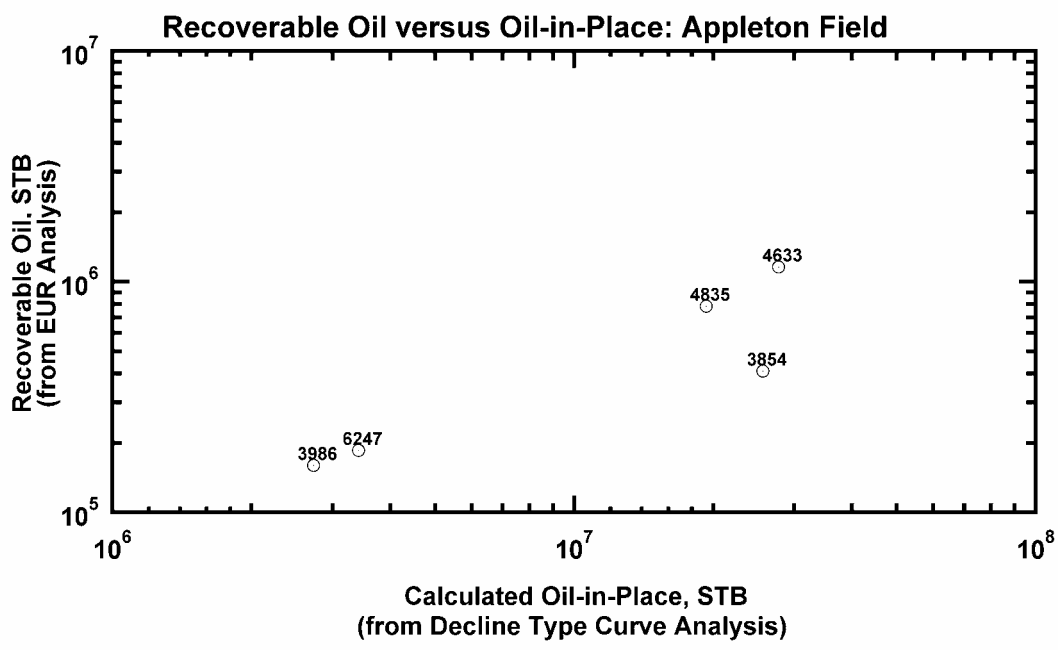


Fig. 88 — Recoverable Oil (*EUR* Analysis) versus Computed Original Oil-in-Place (Decline Type Curve Analysis), Appleton Oil Field.

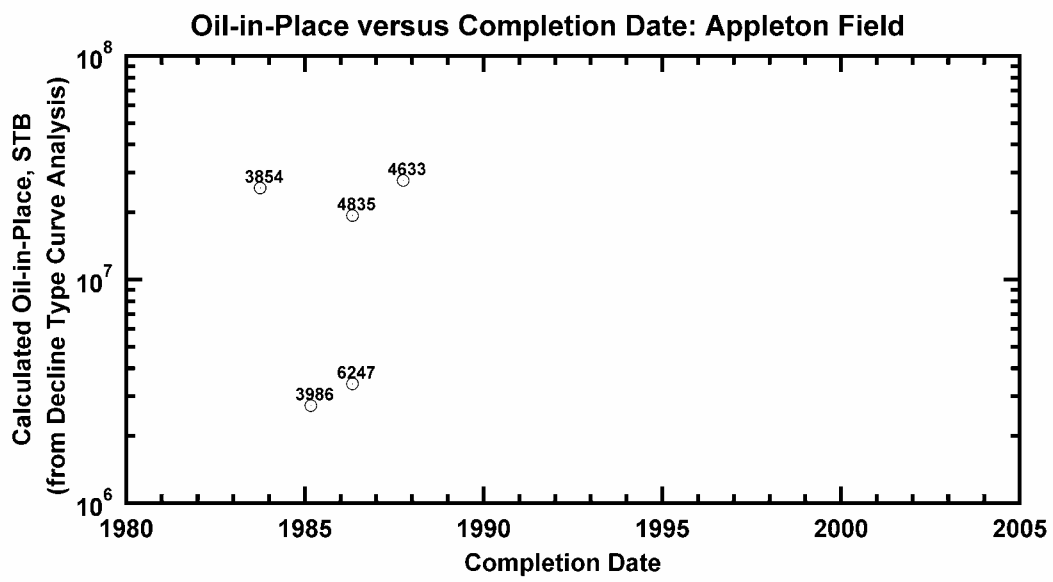


Fig. 89 — Computed Original Oil-in-Place versus Completion Date, Appleton Oil Field.

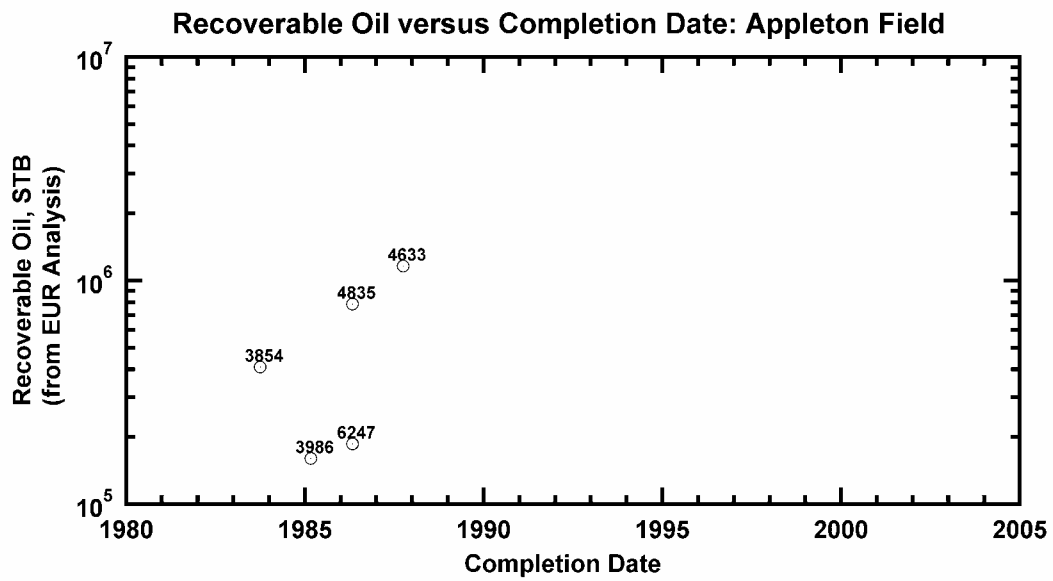


Fig. 90 — Recoverable Oil versus Completion Date, Appleton Oil Field.

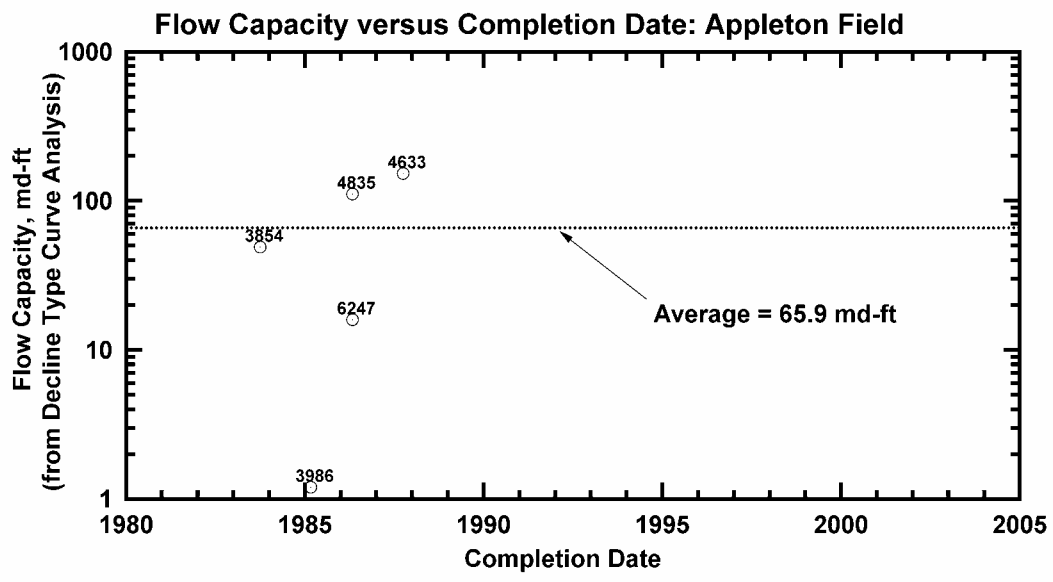


Fig. 91 — Flow Capacity versus Completion Date, Appleton Oil Field.

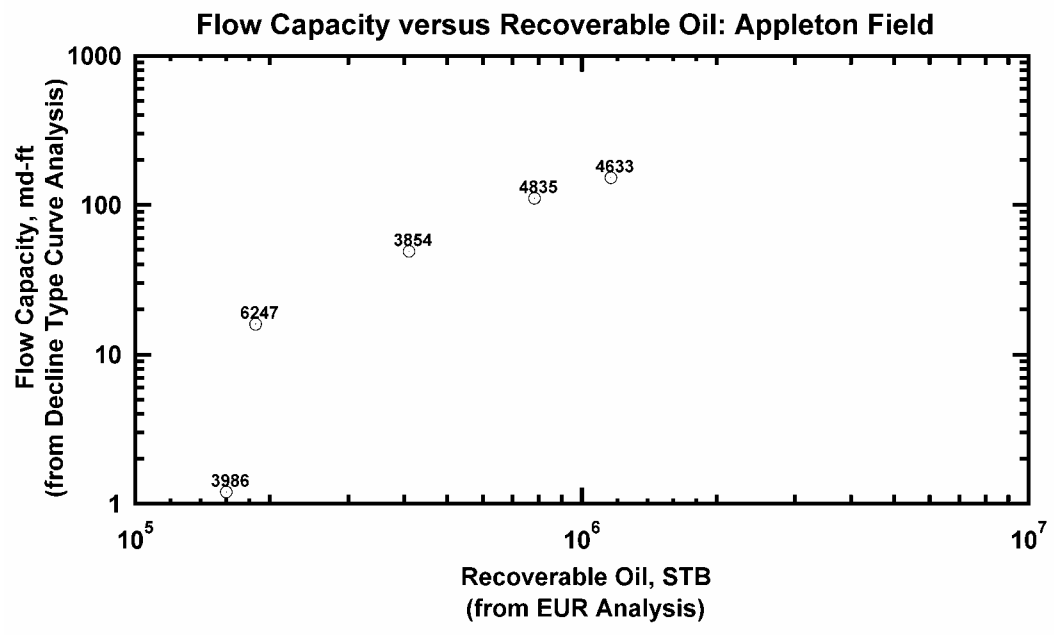


Fig. 92 — Flow Capacity versus Recoverable Oil, Appleton Oil Field.

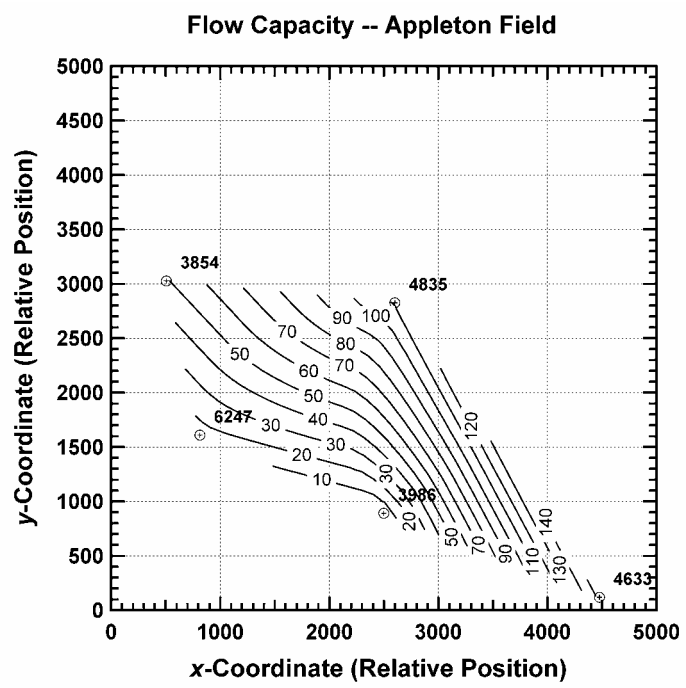


Fig. 93 — Contour Map of Flow Capacity, Appleton Oil Field.

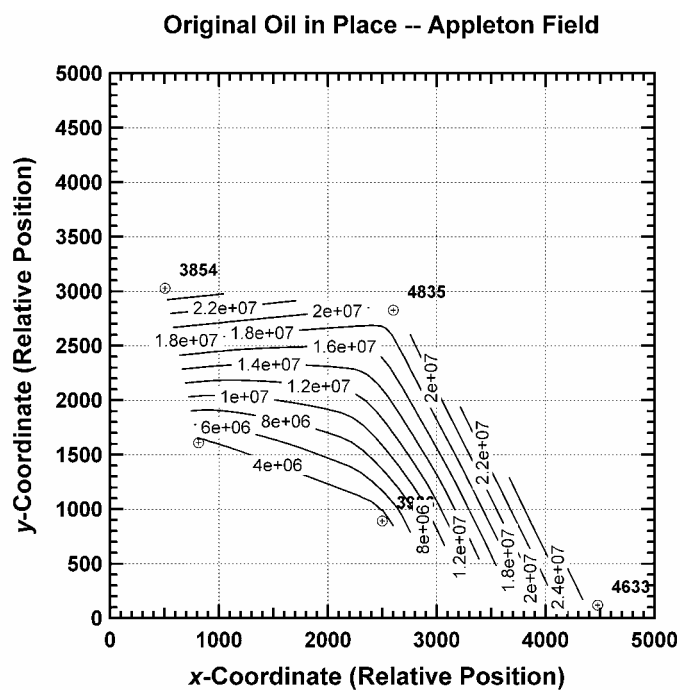


Fig. 94 — Contour Map of Original Oil-in-Place, Appleton Oil Field.

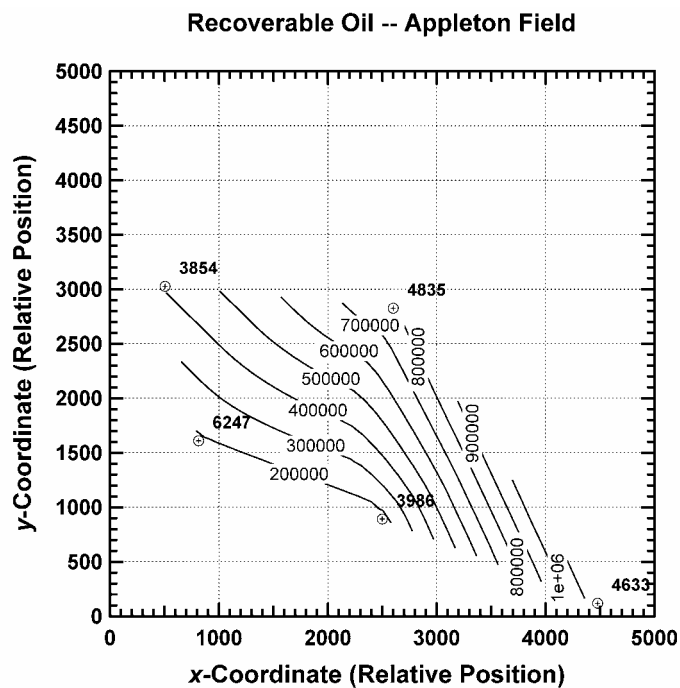


Fig. 95 — Contour Map of Recoverable Oil, Appleton Oil Field.



Table 10 — Porosity and permeability characteristics in the Sabkha Interval.

Well	Minimum Porosity, (percent)	Maximum Porosity, (percent)	Average Porosity, (percent)	Minimum Permeability ,(md)	Maximum Permeability ,(md)	Geometric Average Permeability ,(md)
1599	N/A	N/A	N/A	N/A	N/A	N/A
1830	N/A	N/A	N/A	N/A	N/A	N/A
2851	N/A	N/A	N/A	N/A	N/A	N/A
2935	N/A	N/A	N/A	N/A	N/A	N/A
3412	1.1	6.6	2.4	0.1	0.1	0.1
3739	N/A	N/A	N/A	N/A	N/A	N/A
4225	2.3	2.5	2.4	N/A	N/A	N/A
5779	N/A	N/A	N/A	N/A	N/A	N/A
11185	0.9	14.6	8.3	N/A	N/A	N/A

Table 11 — Porosity and permeability characteristics in the Tidal Flat Interval.

Well	Minimum Porosity, (percent)	Maximum Porosity, (percent)	Average Porosity, (percent)	Minimum Permeability ,(md)	Maximum Permeability ,(md)	Geometric Average Permeability ,(md)
1599	N/A	N/A	N/A	N/A	N/A	N/A
1830	14.6	23.6	21.3	5.9	162.0	56.6
2851	1.0	12.0	7.0	7.9	14.1	11.0
2935	N/A	N/A	N/A	N/A	N/A	N/A
3412	2.4	10.9	5.5	0.3	10.4	1.5
3739	3.7	8.6	5.1	9.0	9.0	9.0
4225	1.2	3.5	2.0	0.04	0.04	0.04
5779	2.1	3.7	2.9	N/A	N/A	N/A
11185	0.9	9.9	5.1	0.13	75.0	3.3

Table 12 — Porosity and permeability characteristics in the Shoal Complex Interval.

Well	Minimum Porosity, (percent)	Maximum Porosity, (percent)	Average Porosity, (percent)	Minimum Permeability, (md)	Maximum Permeability, (md)	Geometric Average Permeability, (md)
1599	N/A	N/A	N/A	N/A	N/A	N/A
1830	10.7	22.0	15.8	5.6	400.0	54.0
2851	2.1	20.1	9.9	0.02	1321.5	8.6
2935	1.6	15.3	9.7	0.05	57.0	4.5
3412	1.7	15.3	6.4	0.2	466.7	15.8
3739	1.6	13.7	7.9	0.04	18.0	1.8
4225	0.8	13.0	5.1	0.04	266.0	1.8
5779	2.7	21.9	13.3	0.04	1263.0	44.7
11185	N/A	N/A	N/A	N/A	N/A	N/A

Table 13 — Porosity and permeability characteristics in the Lagoon Interval.

Well	Minimum Porosity, (percent)	Maximum Porosity, (percent)	Average Porosity, (percent)	Minimum Permeability, (md)	Maximum Permeability, (md)	Geometric Average Permeability ,(md)
1599	8.0	19.0	12.5	2.8	1119.2	31.3
1830	2.5	15.3	7.6	0.3	57.0	4.1
2851	N/A	N/A	N/A	N/A	N/A	N/A
2935	N/A	N/A	N/A	N/A	N/A	N/A
3412	1.7	11.1	4.3	0.2	8.6	1.1
3739	1.8	14.0	5.7	0.02	50.0	1.4
4225	2.0	7.5	3.4	0.02	0.2	0.06
5779	1.9	8.1	2.7	0.02	2.2	0.1
11185	N/A	N/A	N/A	N/A	N/A	N/A

Table 14 — Porosity and permeability characteristics in the Reef Interval.

Well	Minimum Porosity, (percent)	Maximum Porosity, (percent)	Average Porosity, (percent)	Minimum Permeability ,(md)	Maximum Permeability, (md)	Geometric Average Permeability ,(md)
1599	2.5	33.6	9.3	0.8	5730.0	71.9
1830	5.2	18.6	12.1	0.3	196.0	12.0
2851	2.7	24.9	12.3	0.06	740.0	29.2
2935	3.2	18.3	8.2	0.02	332.0	5.8
3412	N/A	N/A	N/A	N/A	N/A	N/A
3739	1.7	7.8	5.5	2.7	68.0	10.3
4225	N/A	N/A	N/A	N/A	N/A	N/A
5779	N/A	N/A	N/A	N/A	N/A	N/A
11185	N/A	N/A	N/A	N/A	N/A	N/A

permeability characteristics of Smackover facies have been analyzed for each well using porosity histograms (Figures 96-104), permeability histograms (Figures 105-113) and porosity versus depth plots (Figures 114-122). Log porosity versus core porosity for wells in the field have been prepared (Figures 123-131). Porosity versus permeability cross plots for wells (Figures 132-139) and for Smackover facies have been prepared (Figures 140-143). Well performance studies through type curve (Figures 144-153 and Table 15) and decline curve analyses (Figures 154-163) have been completed for the wells in the field. Figure 164 presents an alternative calculation of recoverable oil. The original oil in place and recoverable oil remaining for the field have been calculated (Table 16 and Figures 165-172).

**Task 4—Data Integration.**--This task will integrate the geological, geophysical, petrophysical and engineering data into a comprehensive digital database for reservoir characterization, modeling and simulation. Separate databases will be constructed for Appleton and Vocation Fields. This task serves as a critical effort to the project because the construction of a digital database is an essential tool for the integration of large volumes of data. This task also serves as a means to begin the process of synthesizing concepts. The task will involve entering geologic data and merging these data with geophysical imaging information. Individual well logs will serve as the standard from which the data are entered and compared. The data will be entered at 1-foot intervals. All well logs in the fields will be utilized. The researchers will resolve any apparent inconsistencies among data sets through an iterative approach. This task also will involve entering petrophysical data, rock and fluid property data, production data, including oil, gas and water production, and well completion data, including perforated intervals, completion parameters, well stimulation information, etc. A validation effort will be conducted to resolve any apparent inconsistencies among data sets through an iterative approach.

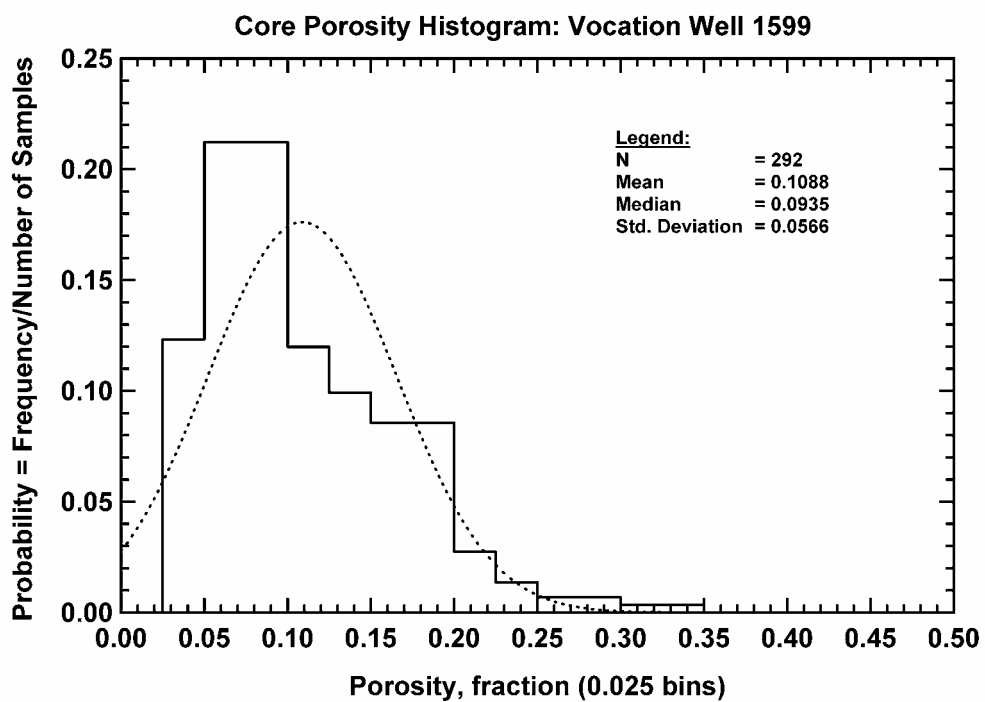


Fig. 96 — Core Porosity Histogram, Vocation Well 1599.

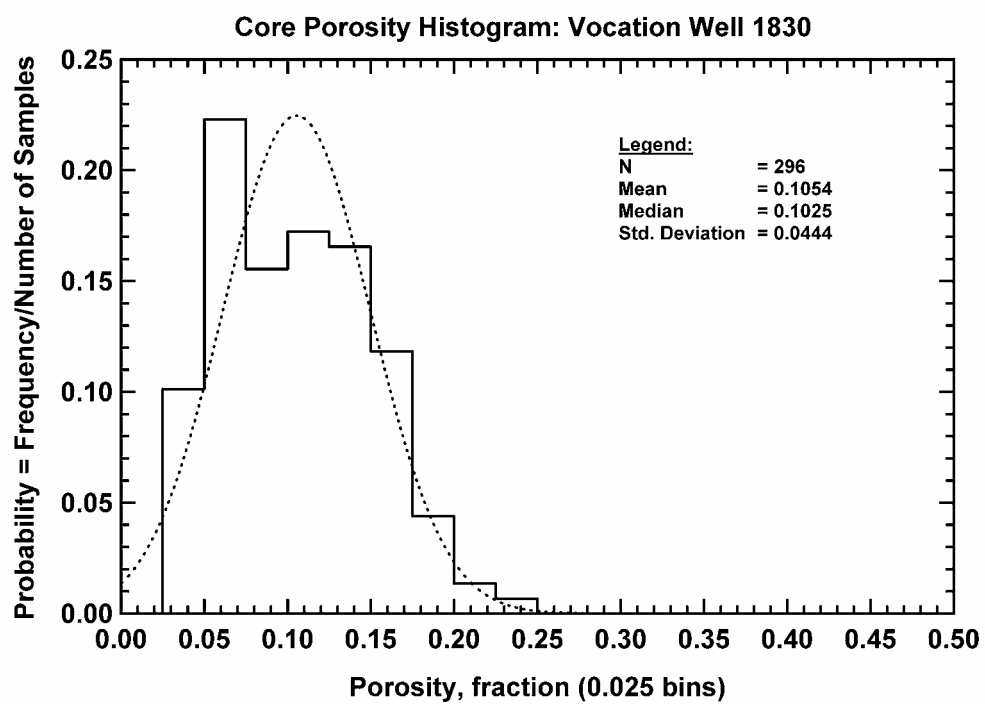


Fig. 97 — Core Porosity Histogram, Vocation Well 1830.

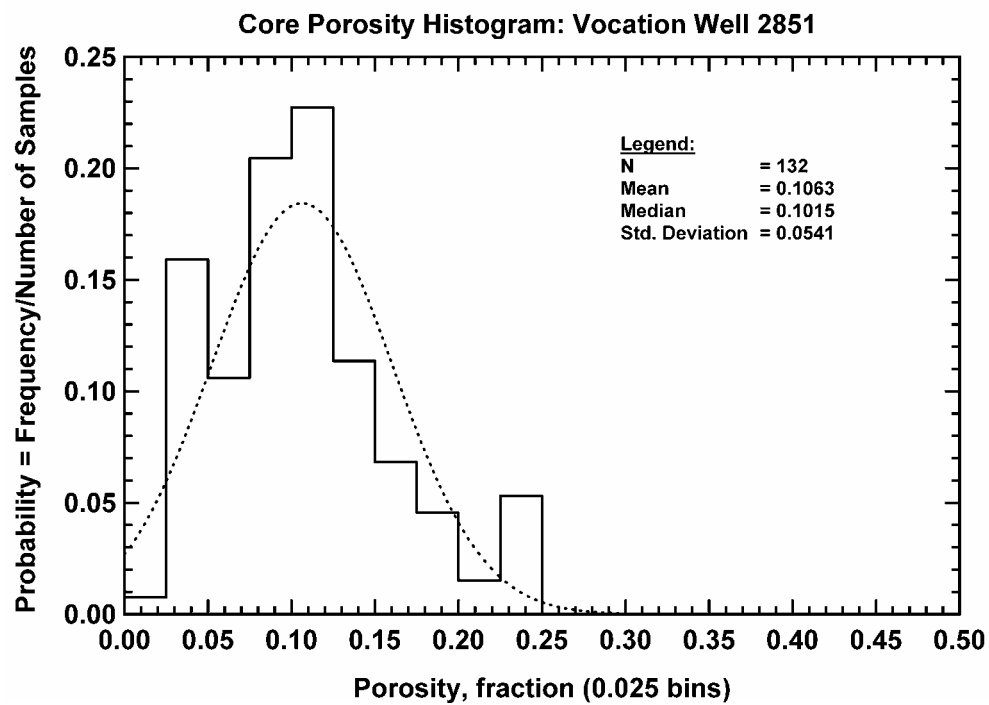


Fig. 98 — Core Porosity Histogram, Vocation Well 2851.

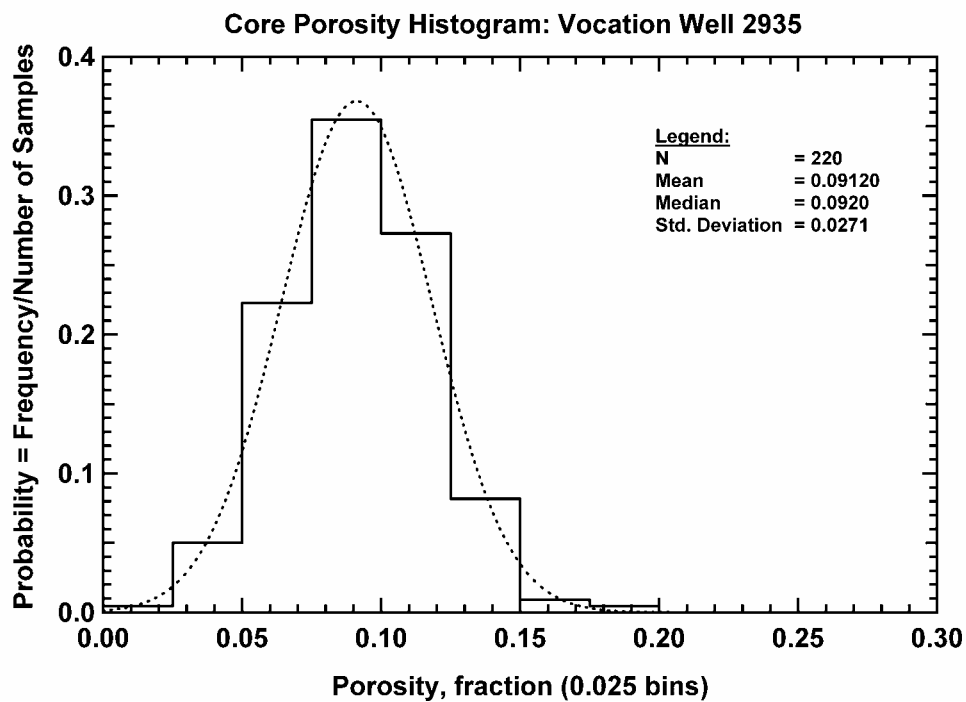


Fig. 99 — Core Porosity Histogram, Vocation Well 2935.

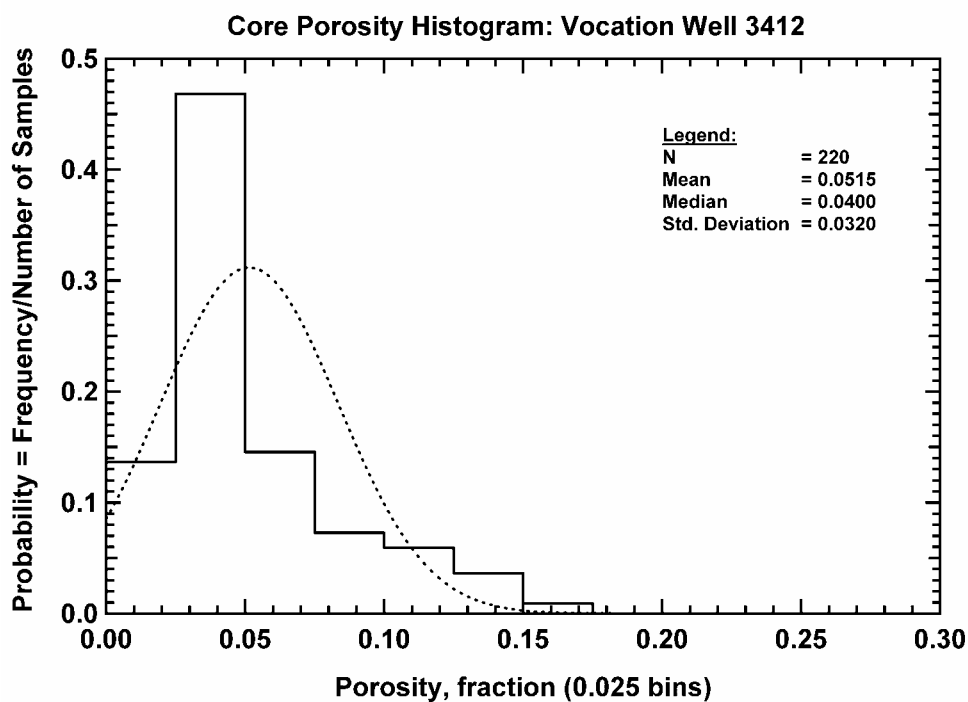


Fig. 100 — Core Porosity Histogram, Vocation Well 3412.

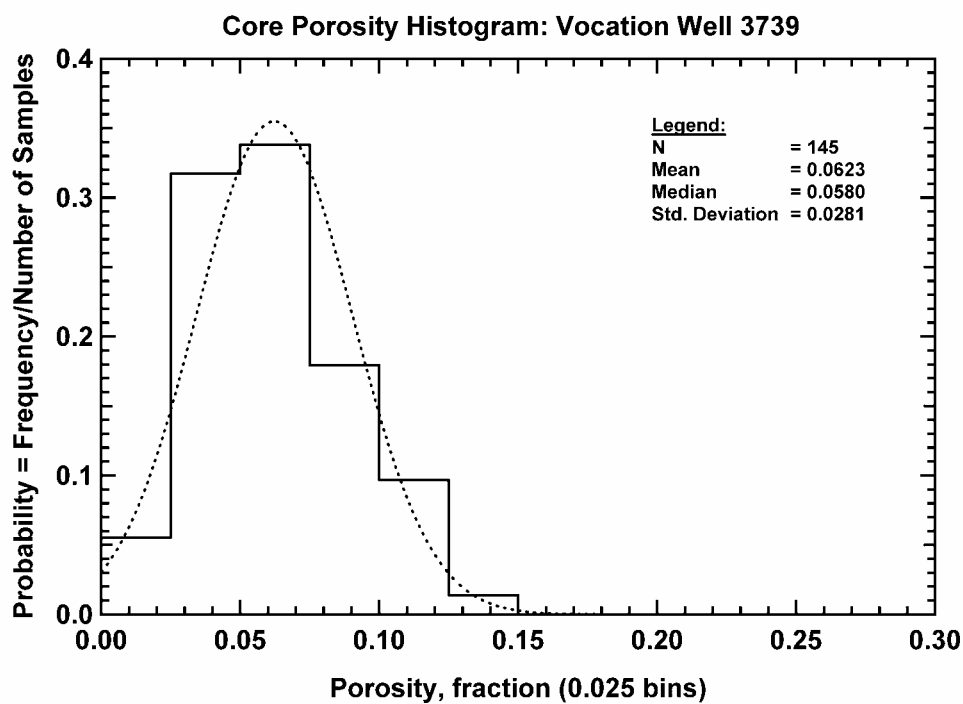


Fig. 101 — Core Porosity Histogram, Vocation Well 3739.

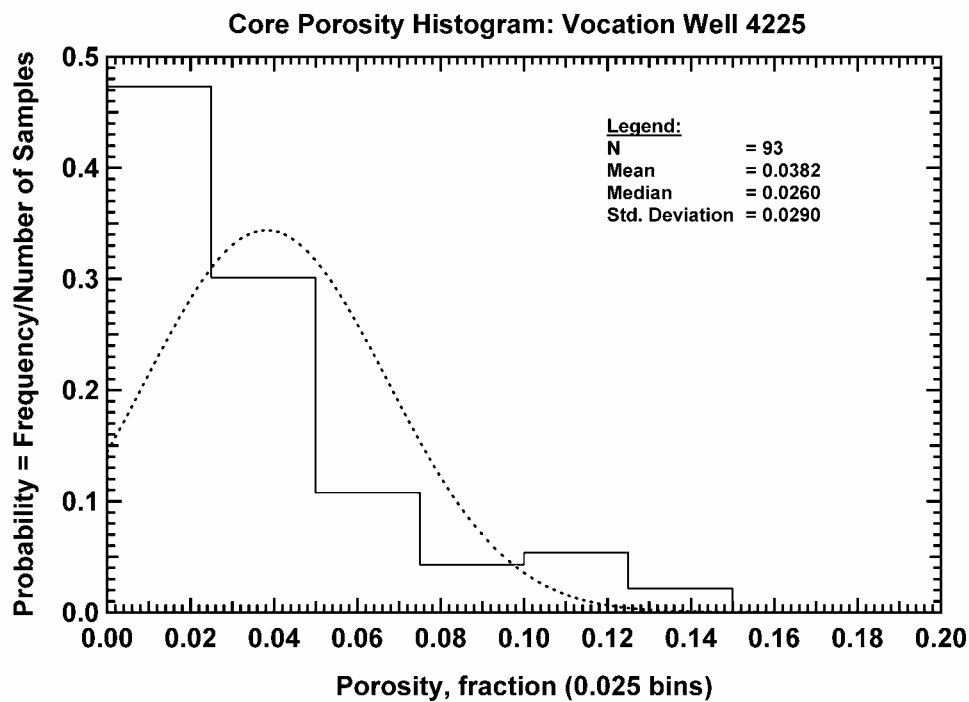


Fig. 102 — Core Porosity Histogram, Vocation Well 4225.

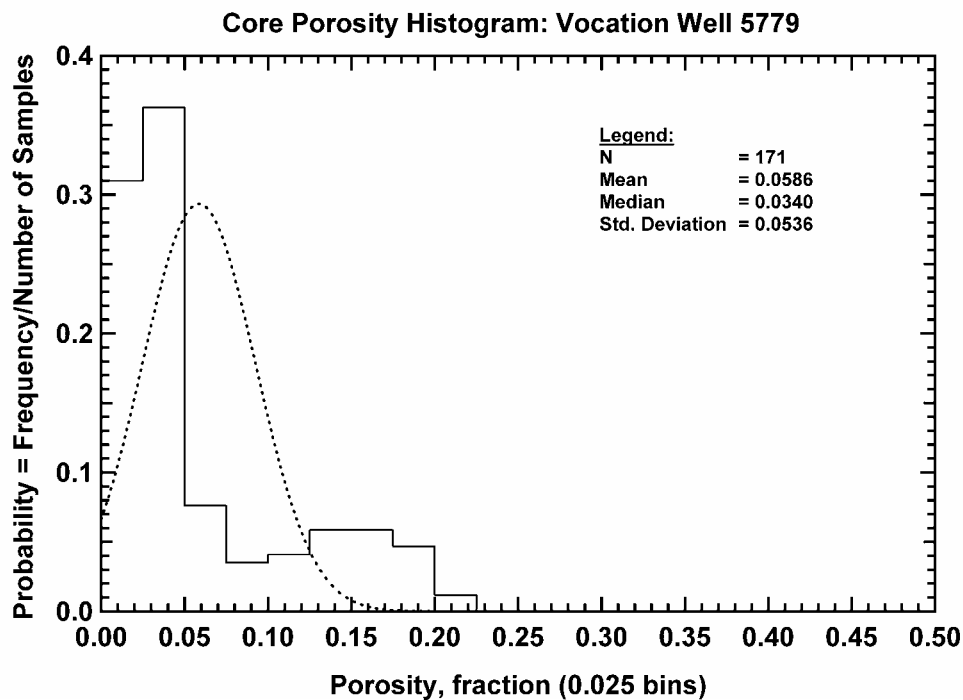


Fig. 103 — Core Porosity Histogram, Vocation Well 5779.



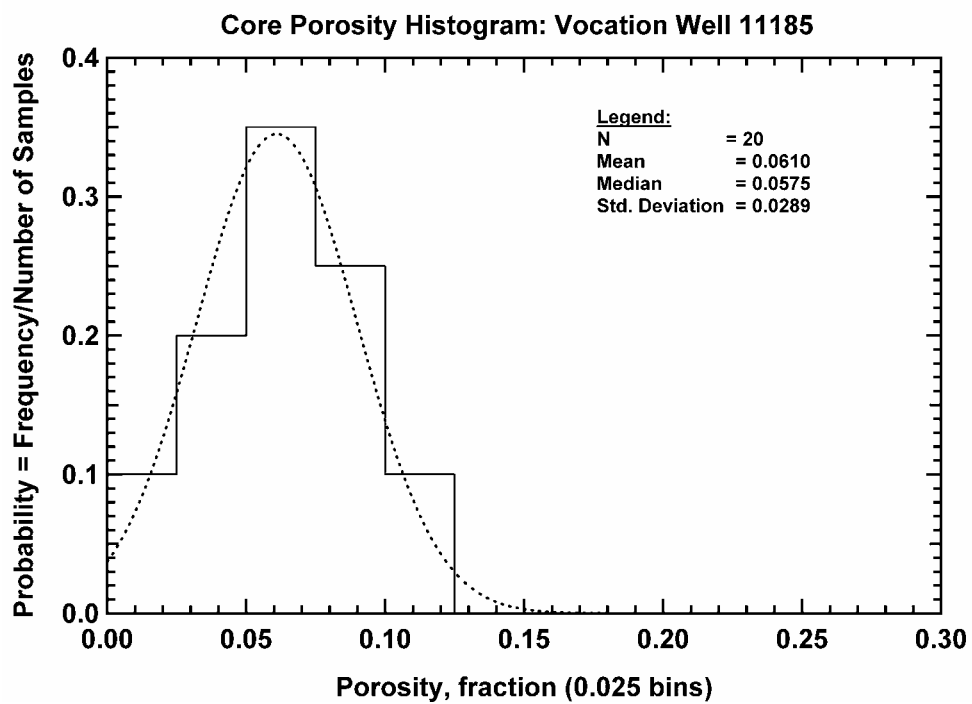


Fig. 104 — Core Porosity Histogram, Vocation Well 11185.

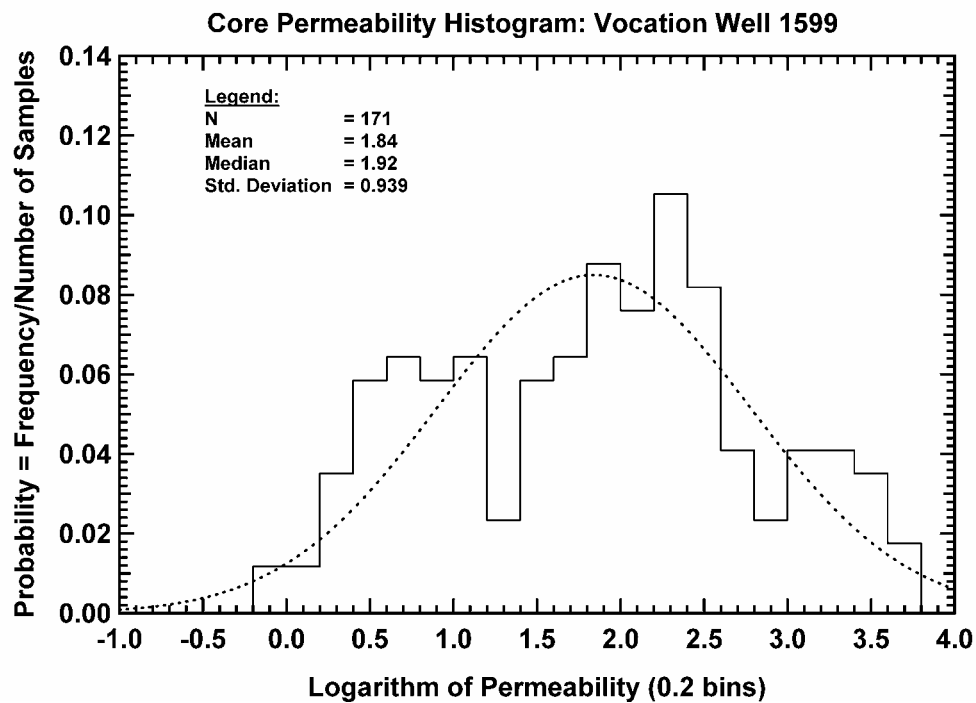


Fig. 105 — Core Permeability Histogram, Vocation Well 1599.

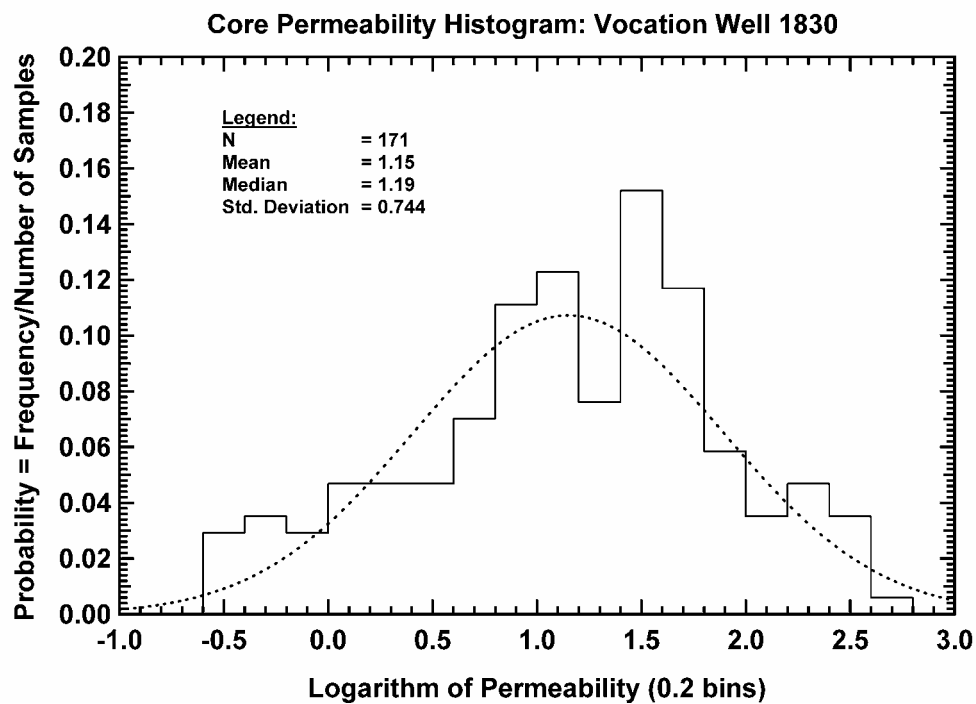


Fig. 106 — Core Permeability Histogram, Vocation Well 1830.

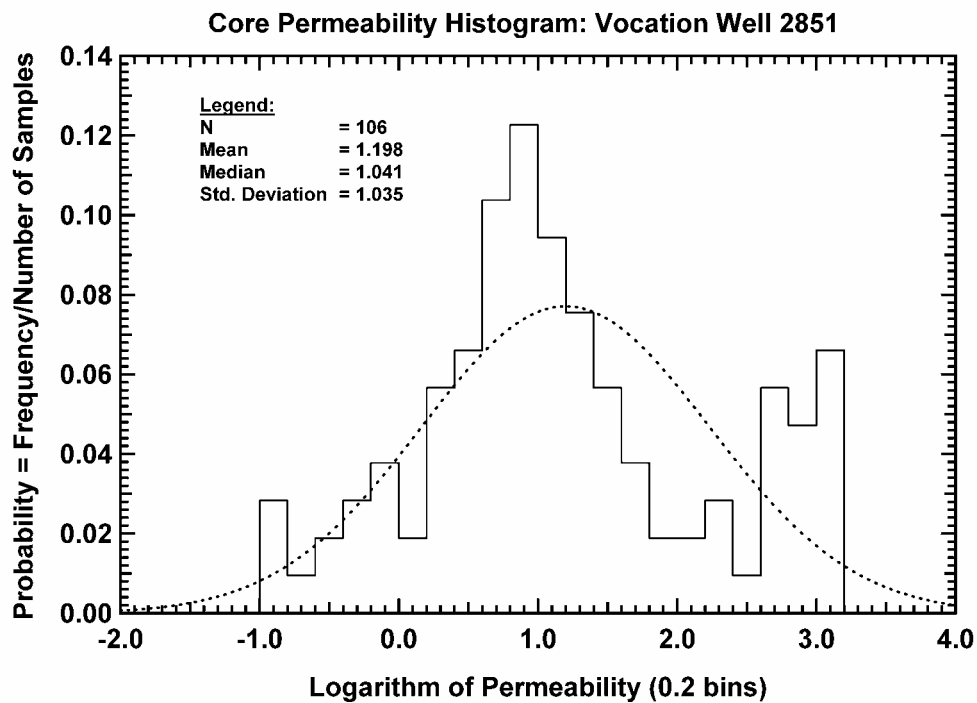


Fig. 107 — Core Permeability Histogram, Vocation Well 2851.

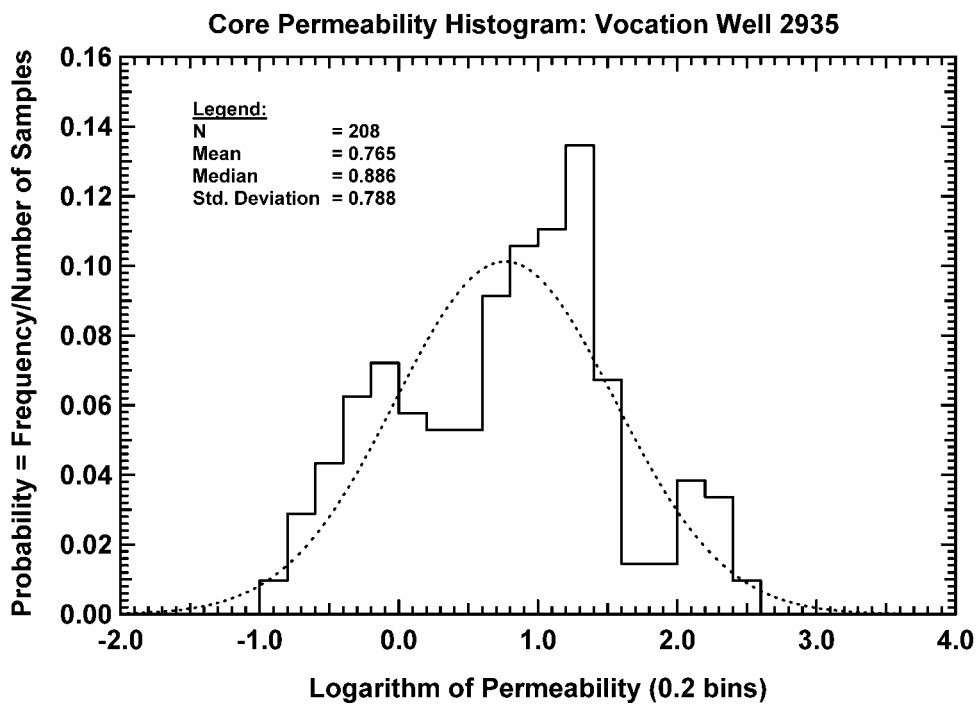


Fig. 108 — Core Permeability Histogram, Vocation Well 2935.

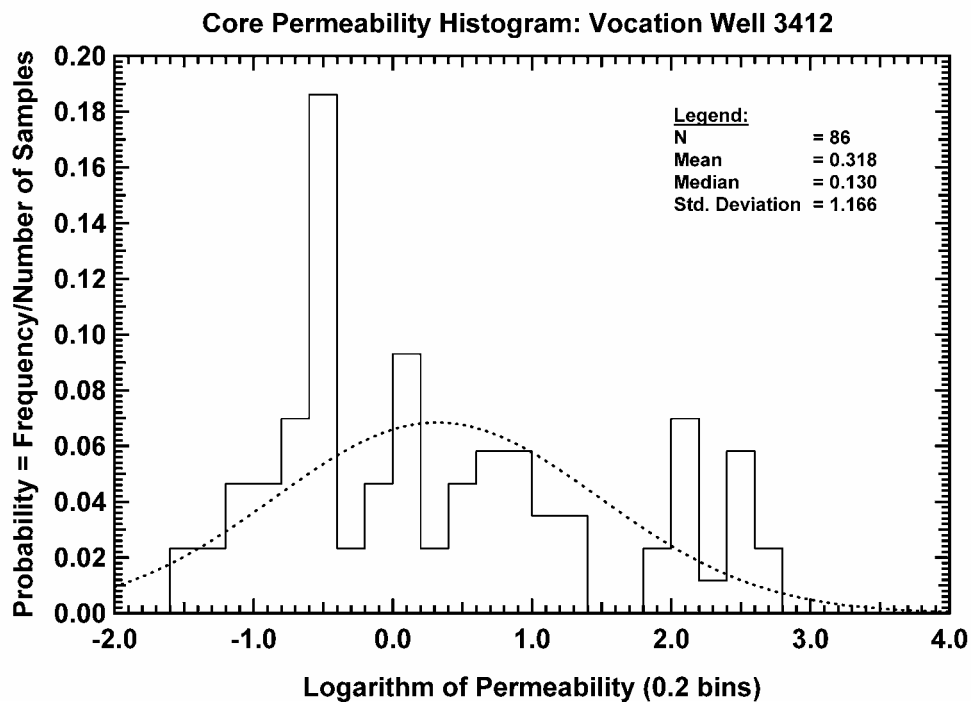


Fig. 109 — Core Permeability Histogram, Vocation Well 3412.

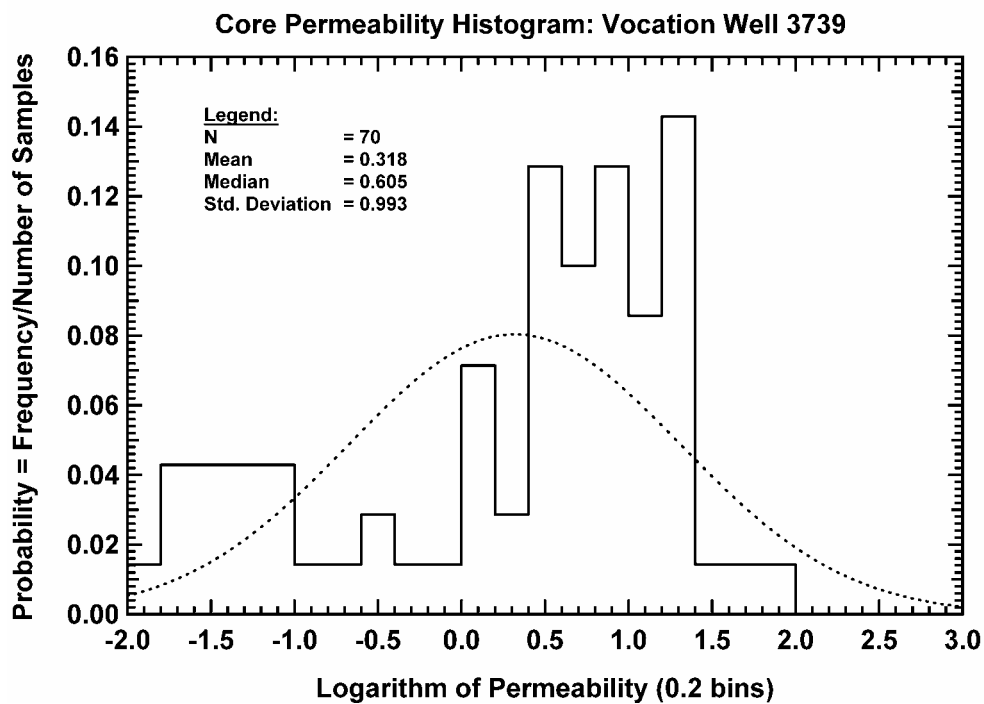


Fig. 110 — Core Permeability Histogram, Vocation Well 3739.

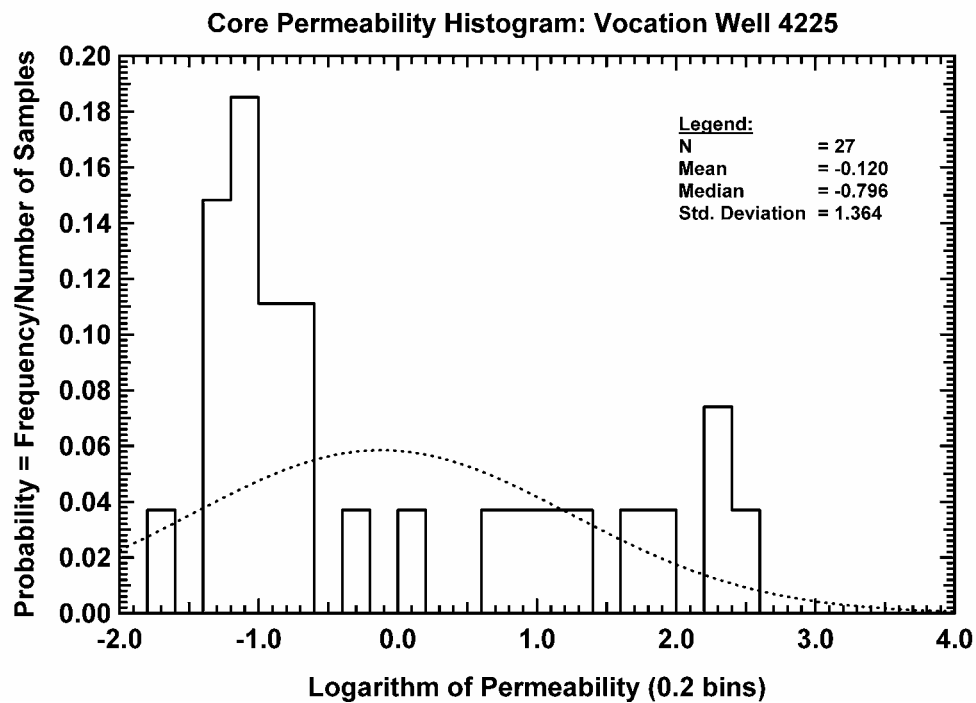


Fig. 111 — Core Permeability Histogram, Vocation Well 4225.

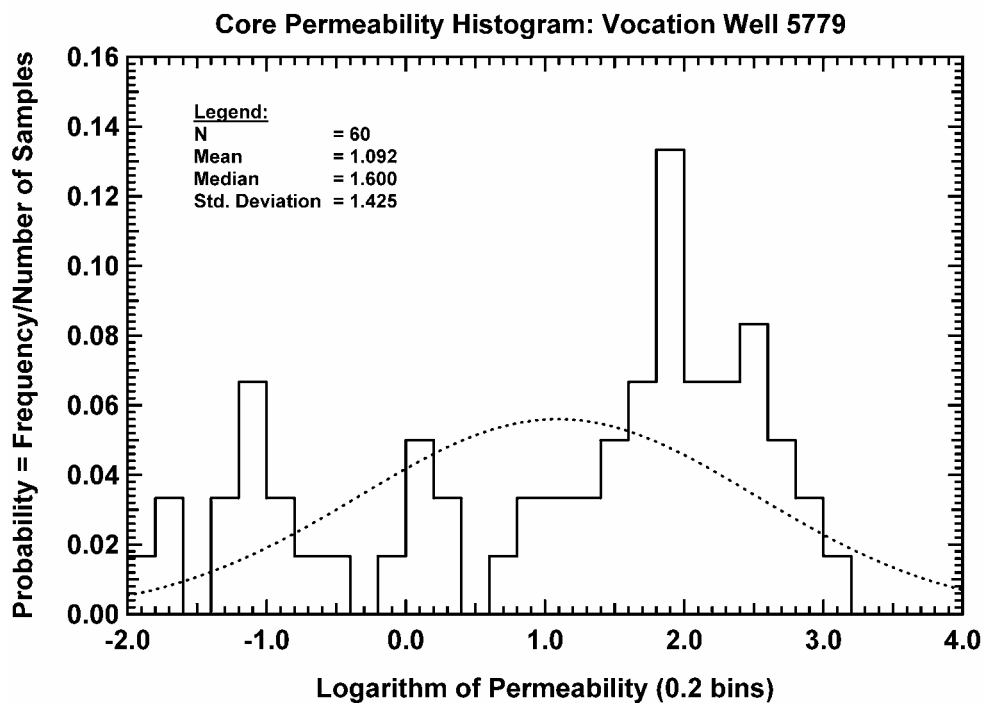


Fig. 112 — Core Permeability Histogram, Vocation Well 5779.

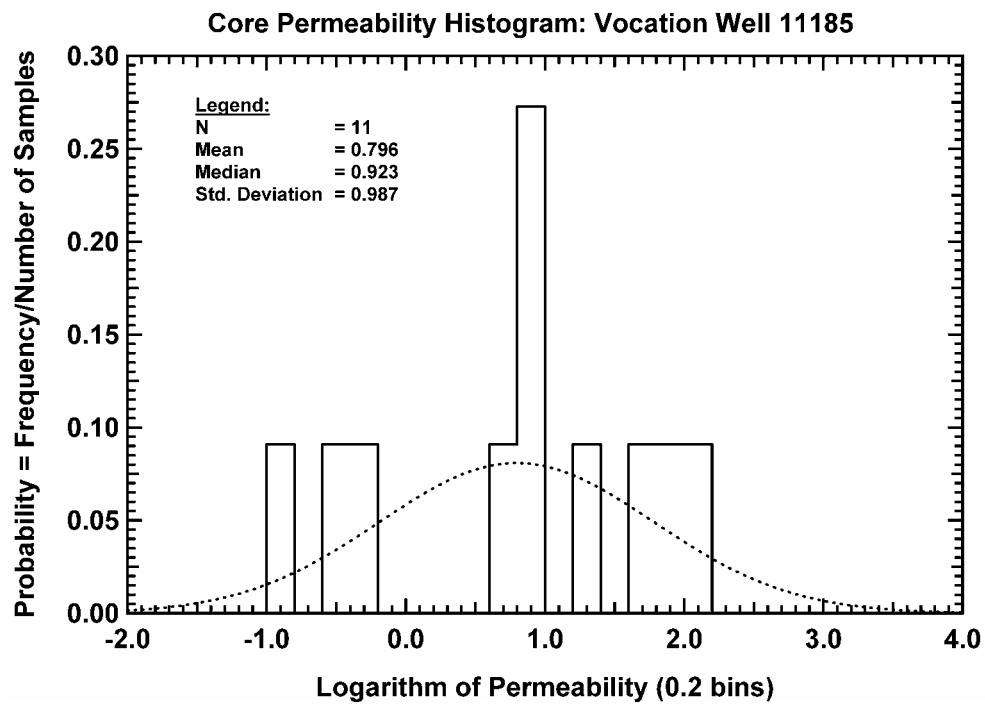


Fig. 113 — Core Permeability Histogram, Vocation Well 11185.

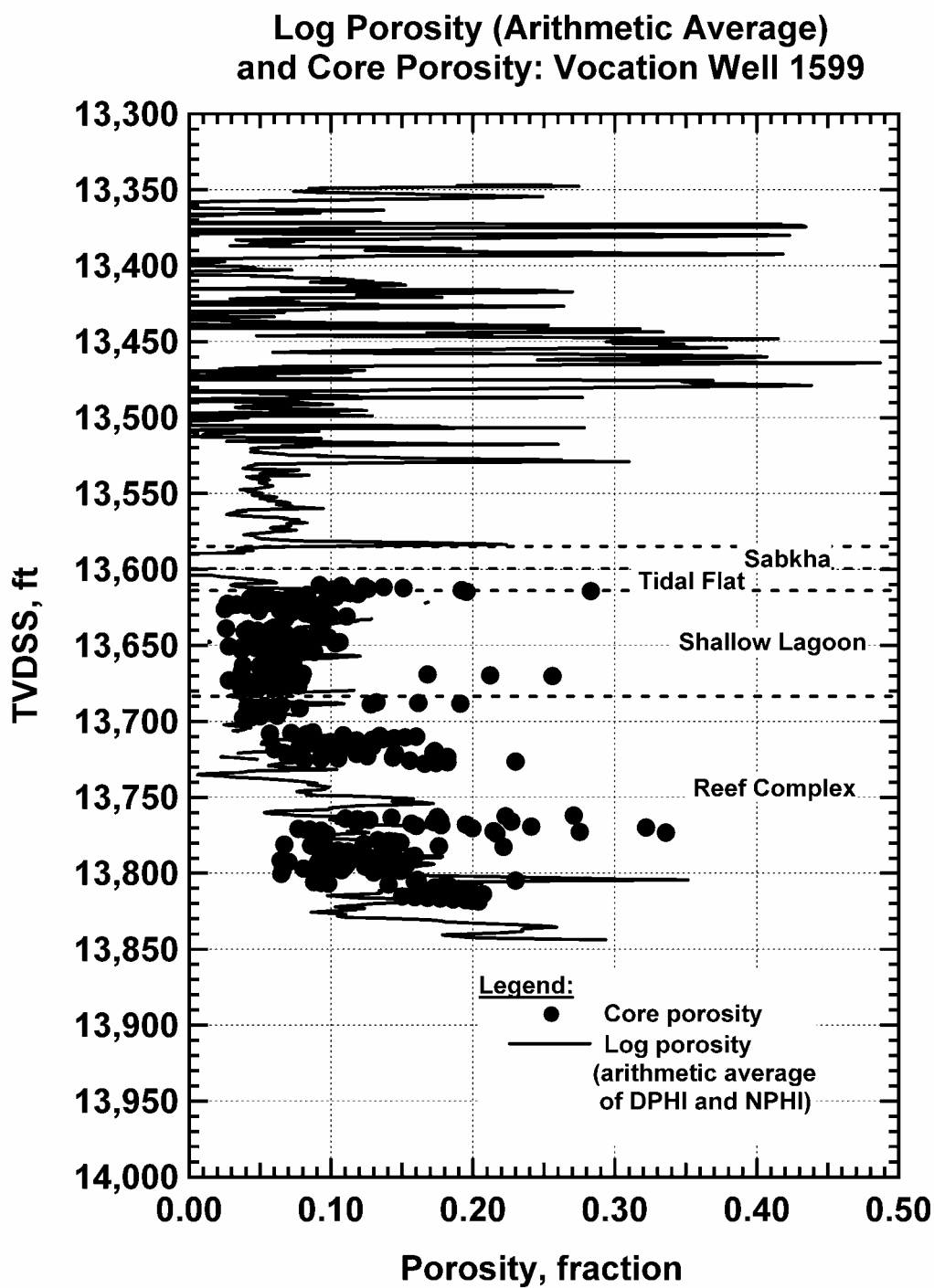


Fig. 114 — Porosity Variation with Depth, Vocation Well 1599.

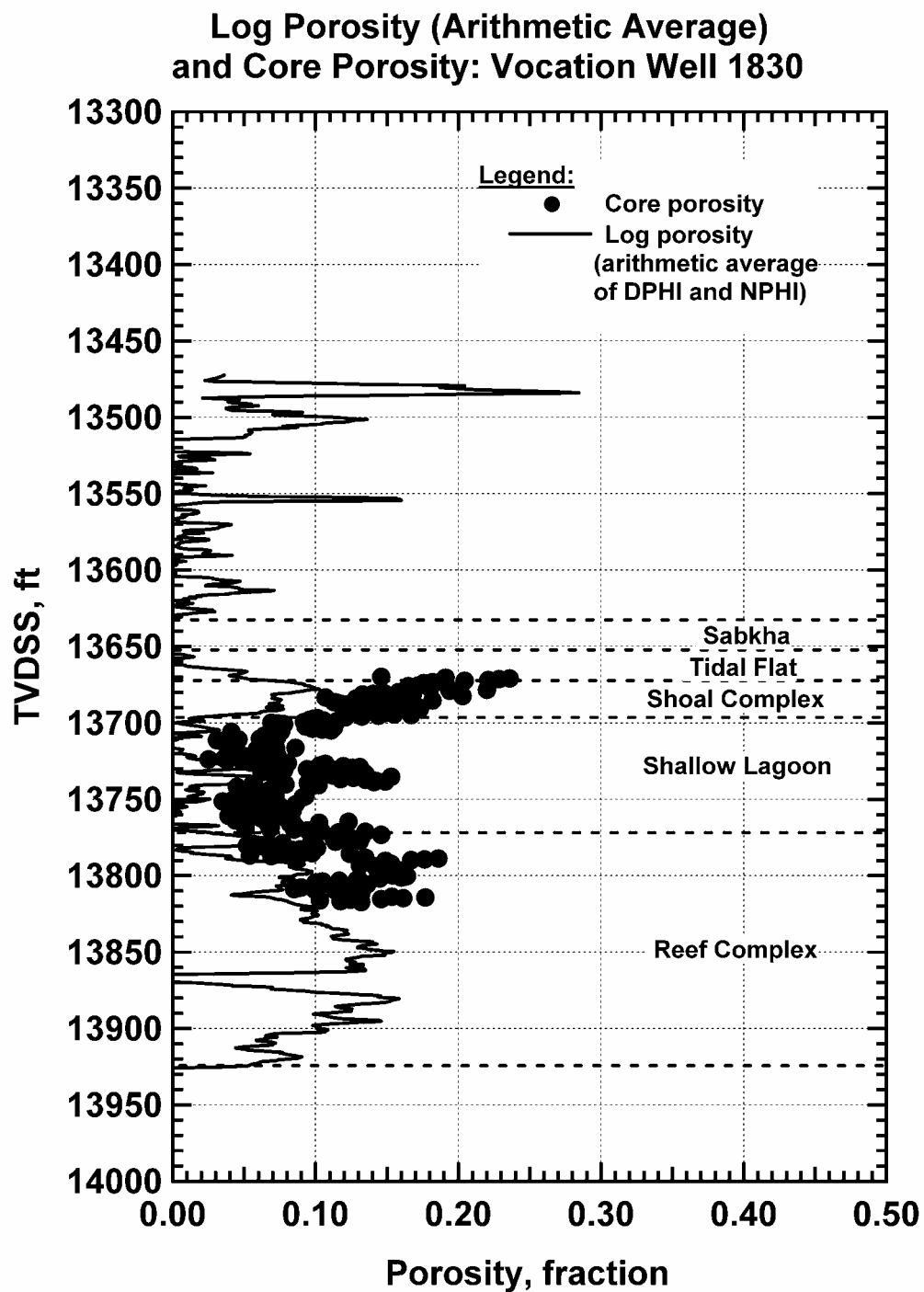


Fig. 115 — Porosity Variation with Depth, Vocation Well 1830.



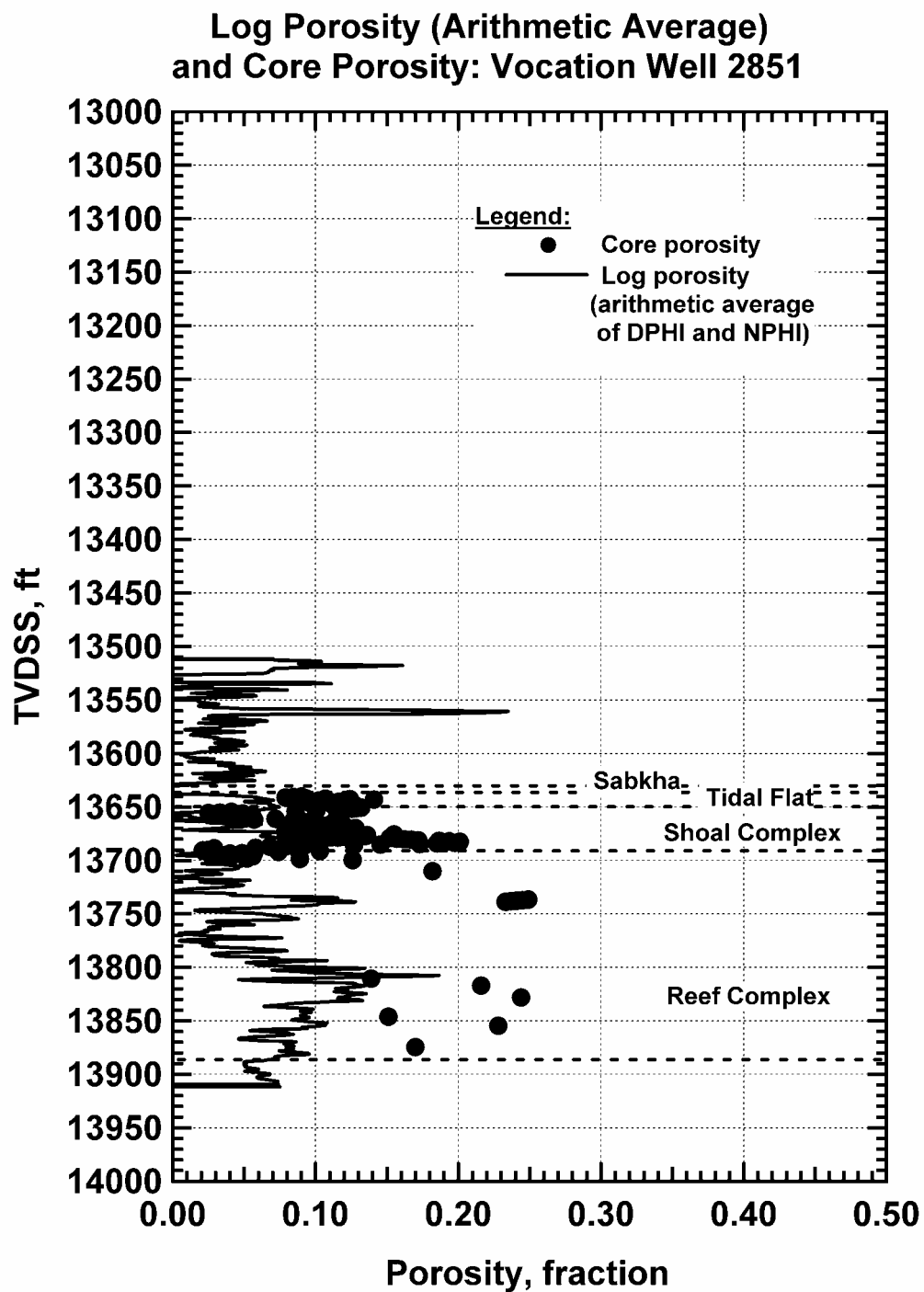


Fig. 116 — Porosity Variation with Depth, Vocation Well 2851.

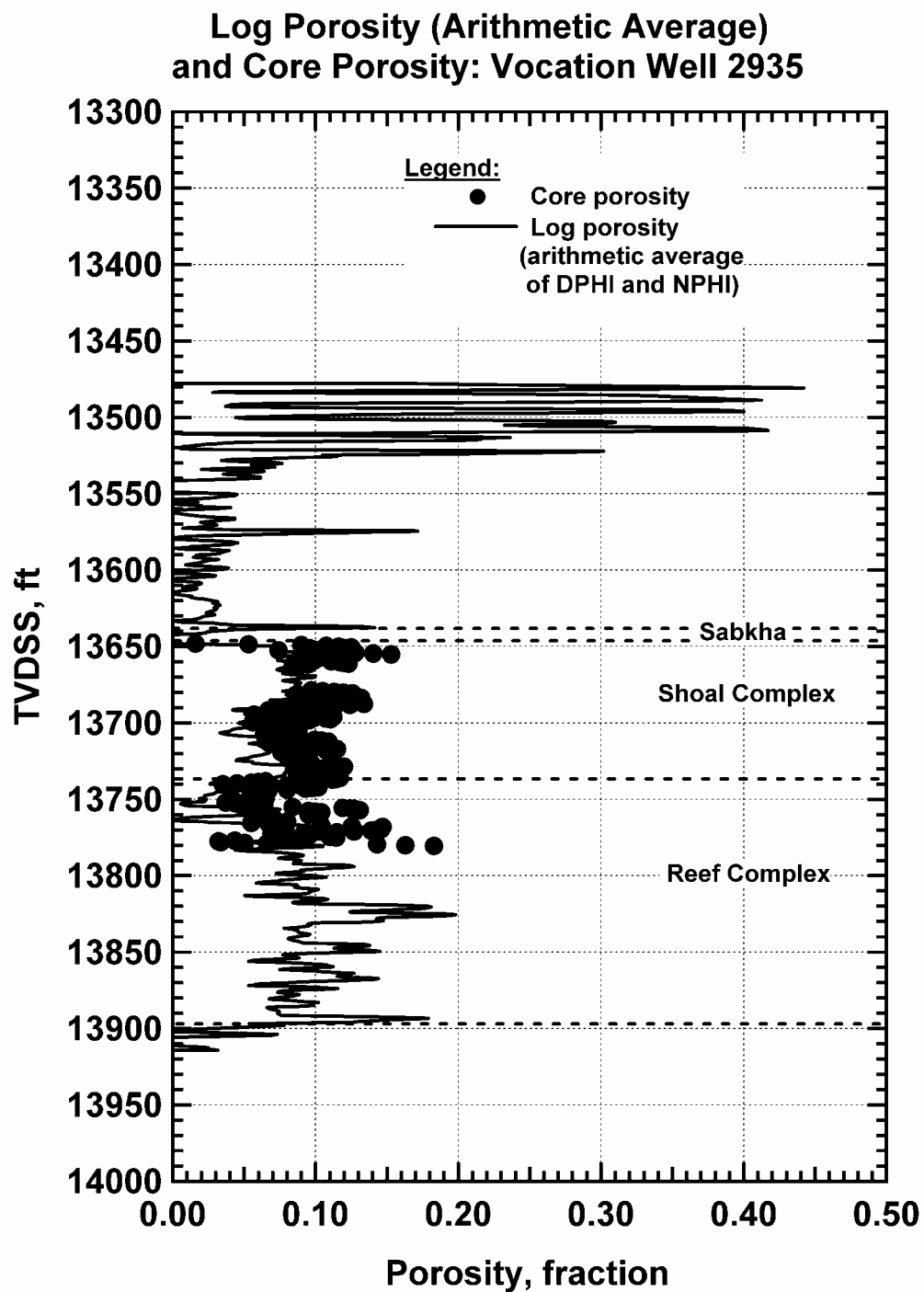


Fig. 117 — Porosity Variation with Depth, Vocation Well 2935.

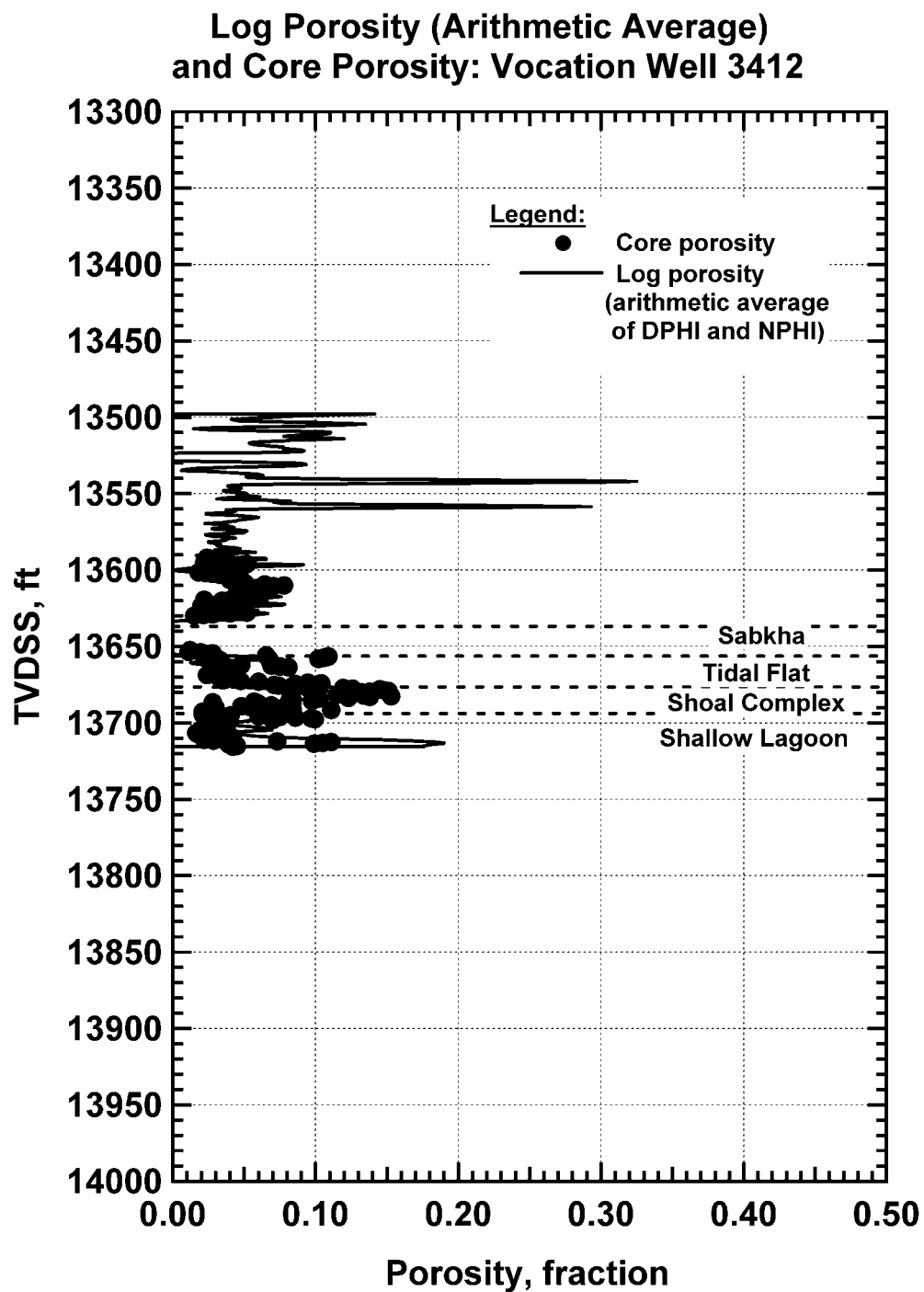


Fig. 118 — Porosity Variation with Depth, Vocation Well 3412.

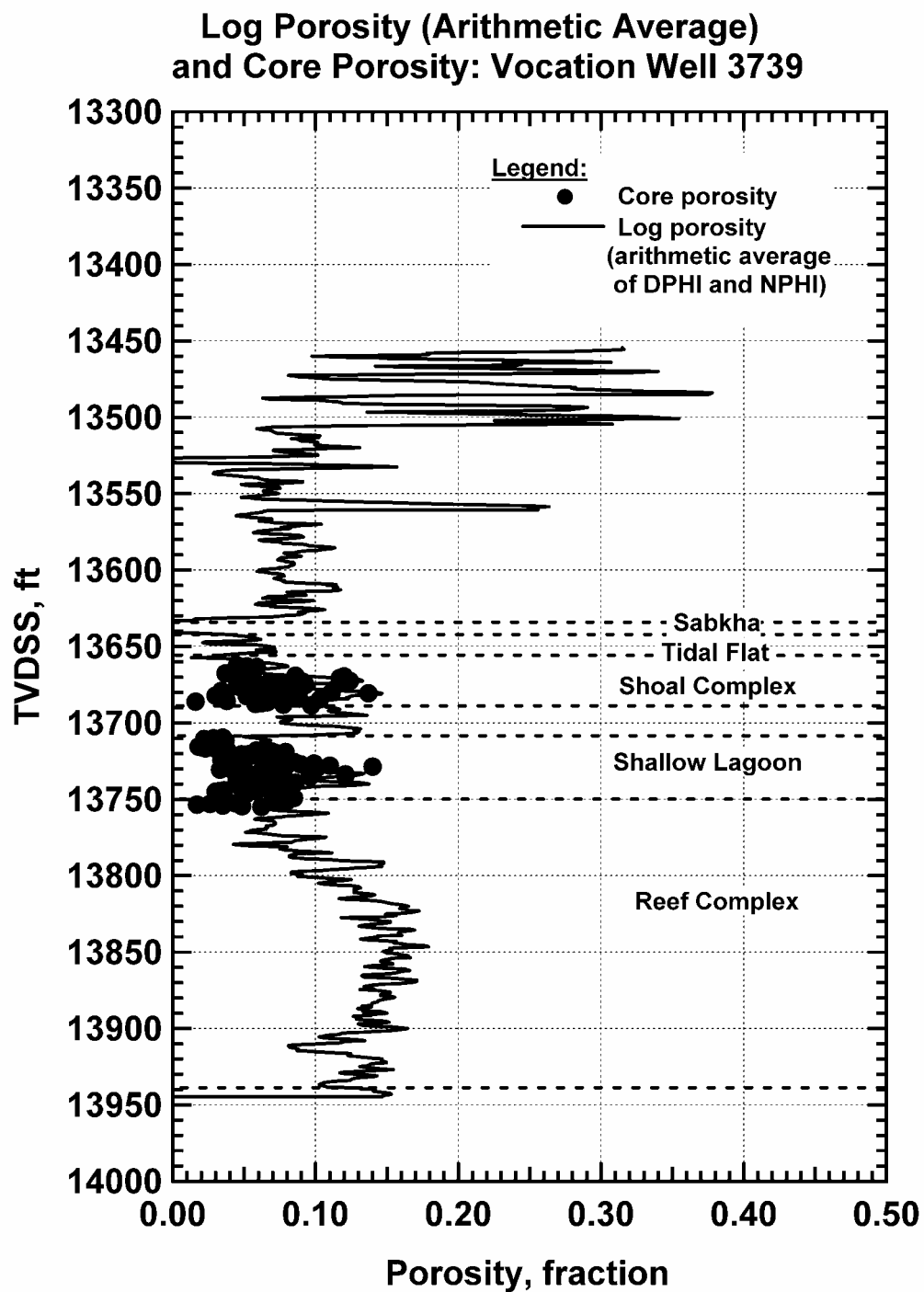


Fig. 119 — Porosity Variation with Depth, Vocation Well 3739.

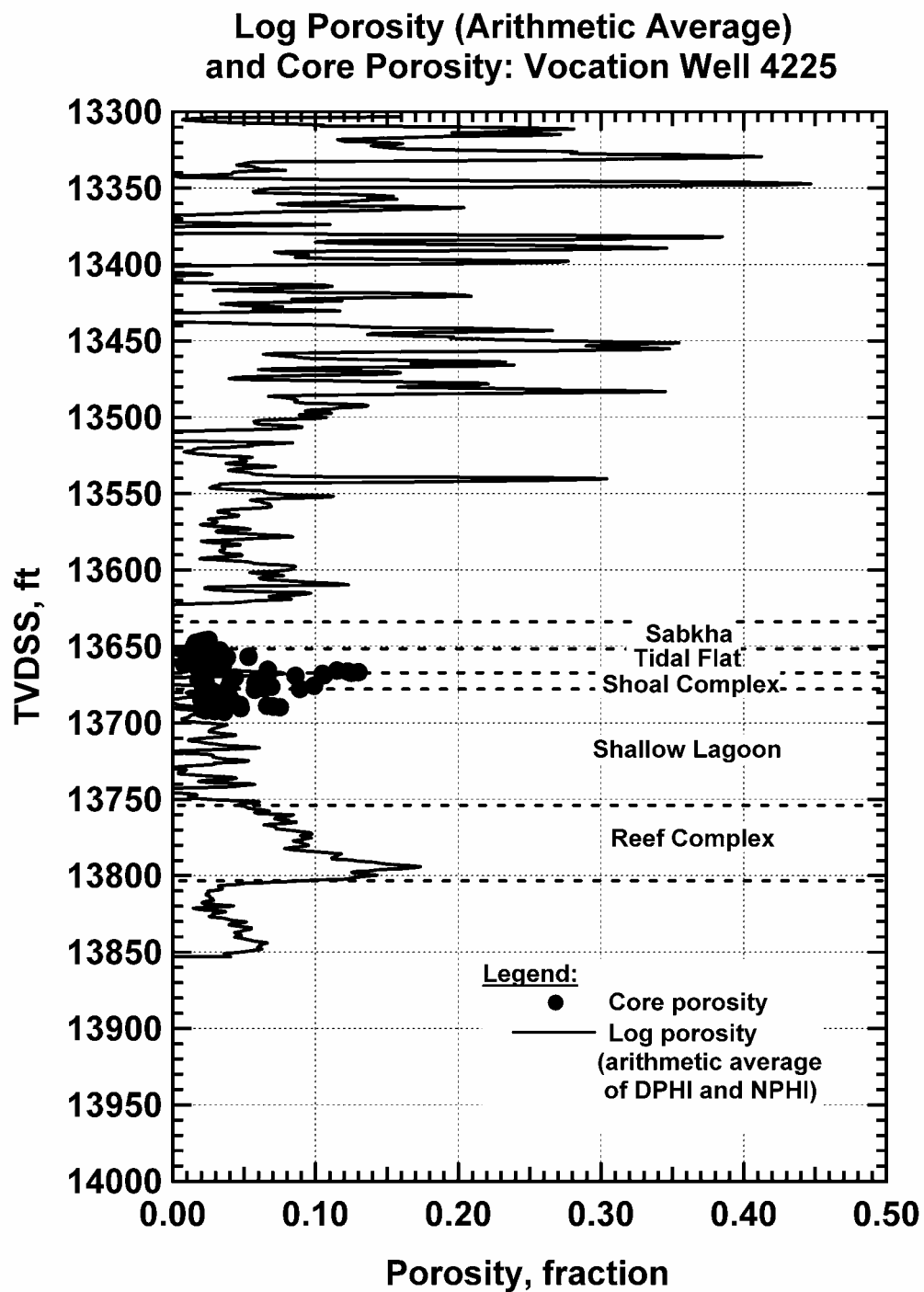


Fig. 120 — Porosity Variation with Depth, Vocation Well 4225.

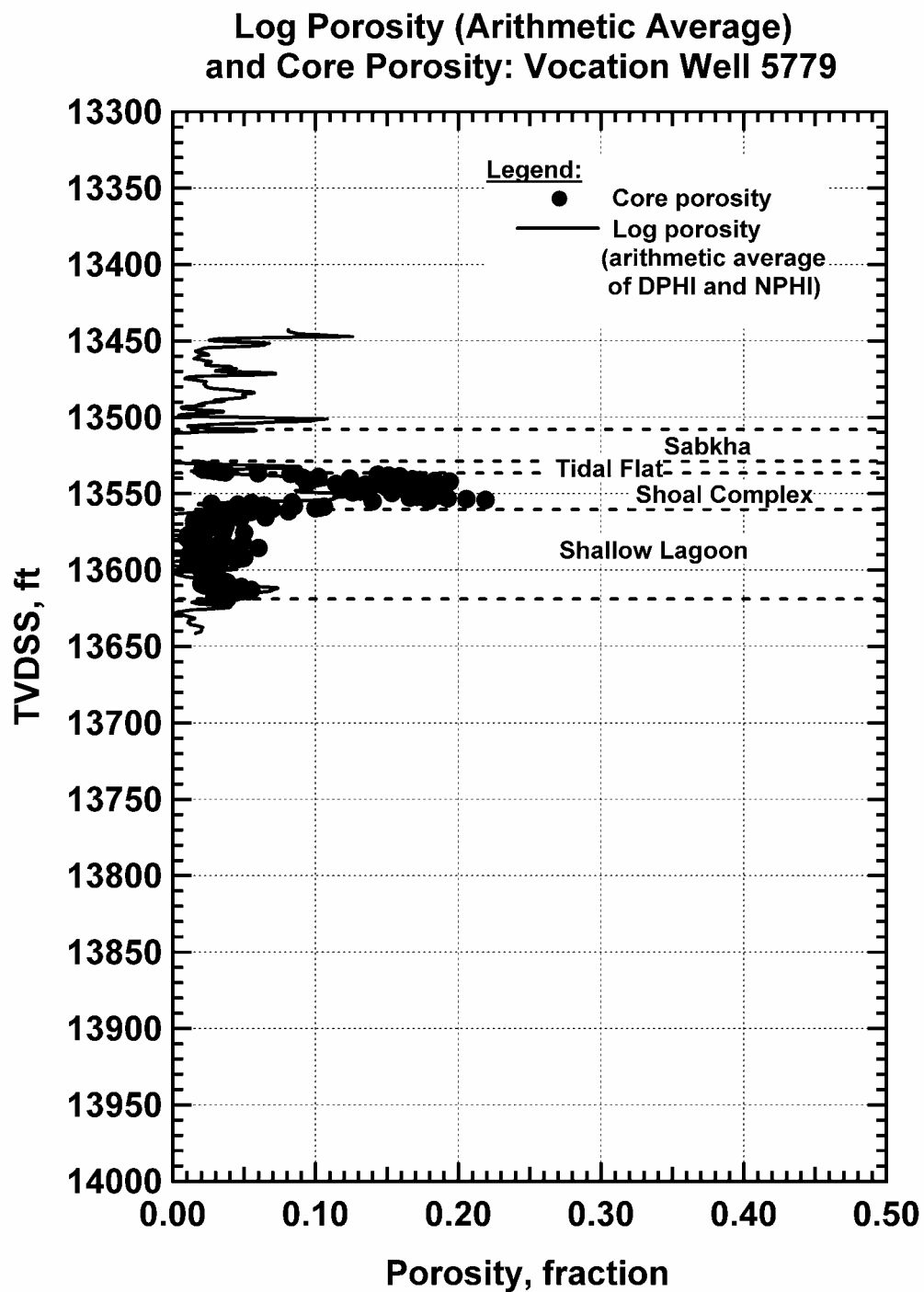


Fig. 121 — Porosity Variation with Depth, Vocation Well 5779.

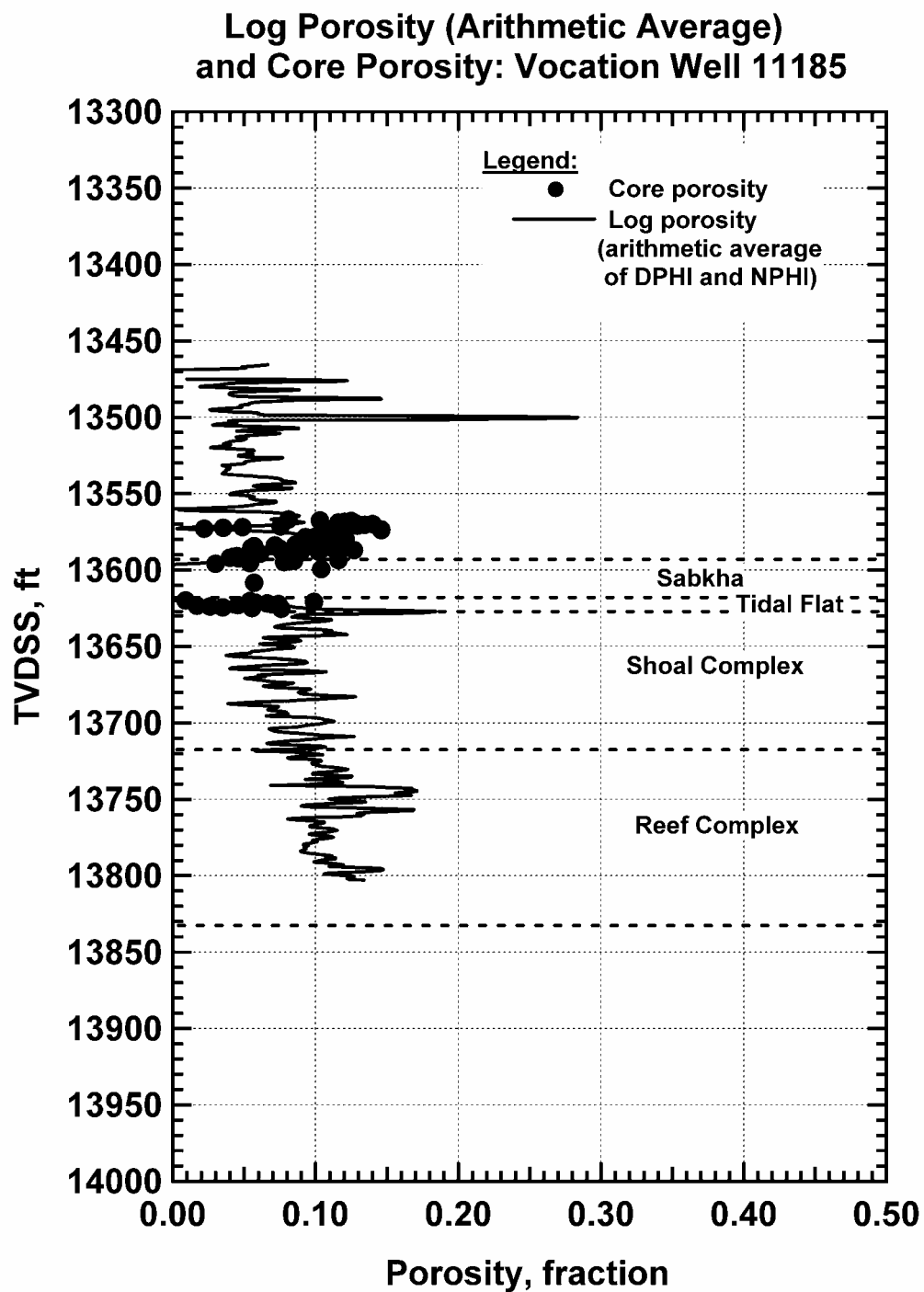


Fig. 122 — Porosity Variation with Depth, Vocation Well 11185.

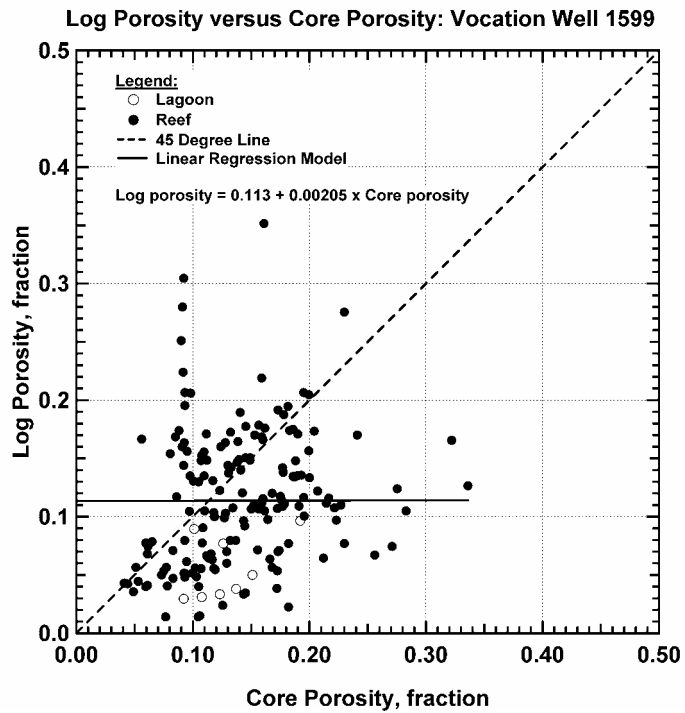


Fig. 123 — Log Porosity versus Core Porosity, Vocation Well 1599.

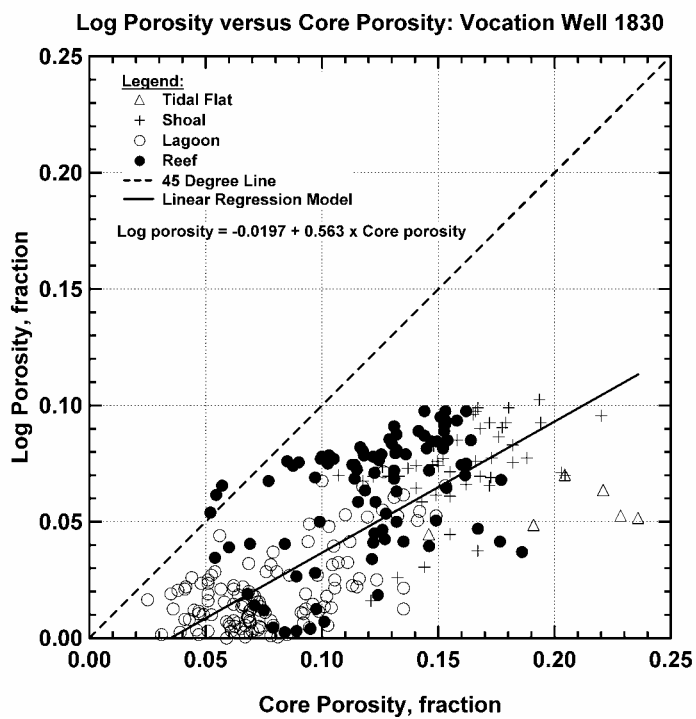


Fig. 124 — Log Porosity versus Core Porosity, Vocation Well 1830.



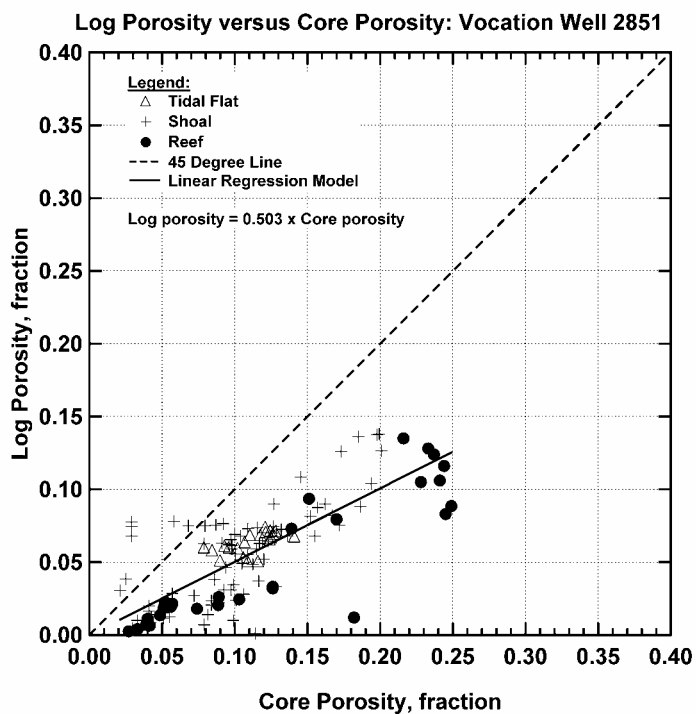


Fig. 125 — Log Porosity versus Core Porosity, Vocation Well 2851.

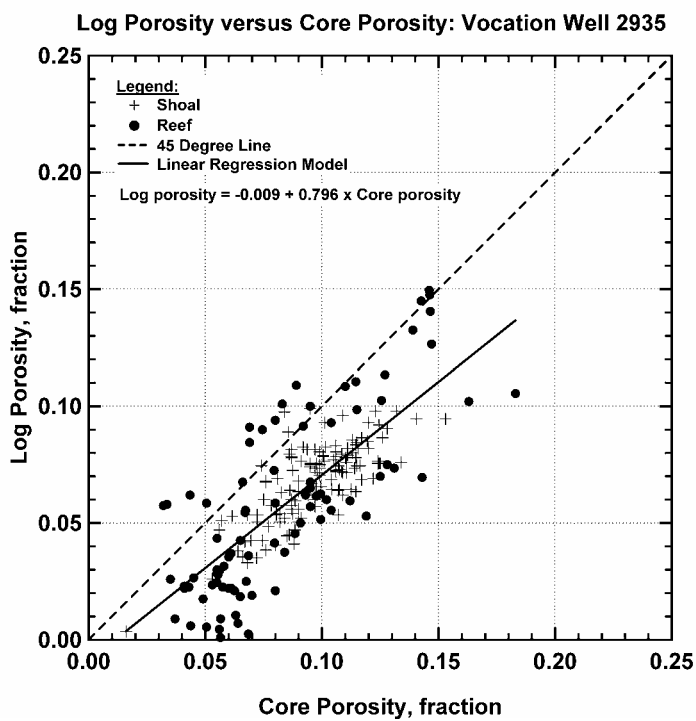


Fig. 126 — Log Porosity versus Core Porosity, Vocation Well 2935.

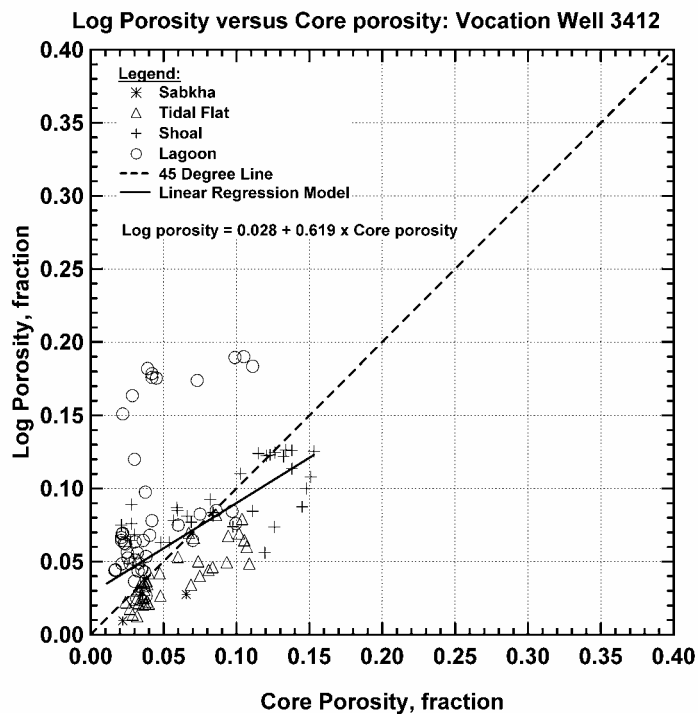


Fig. 127 — Log Porosity versus Core Porosity, Vocation Well 3412.

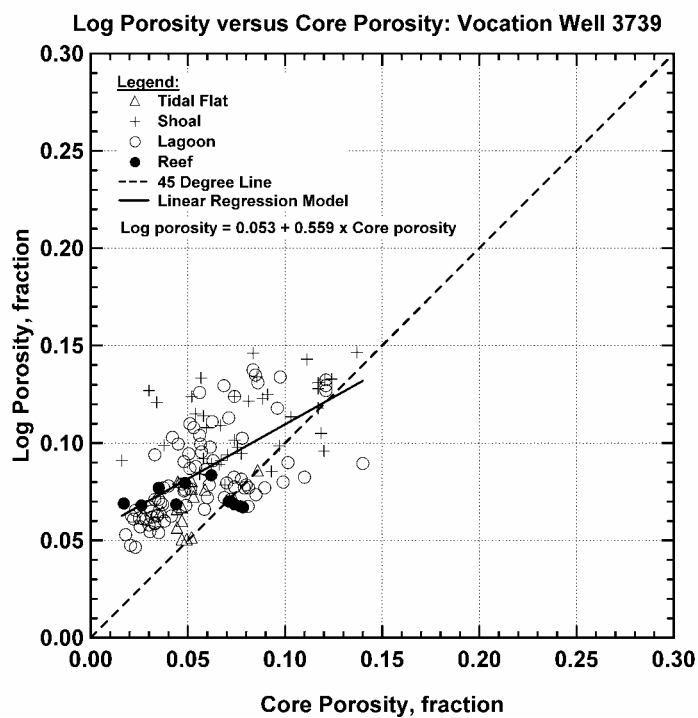


Fig. 128 — Log Porosity versus Core Porosity, Vocation Well 3739.

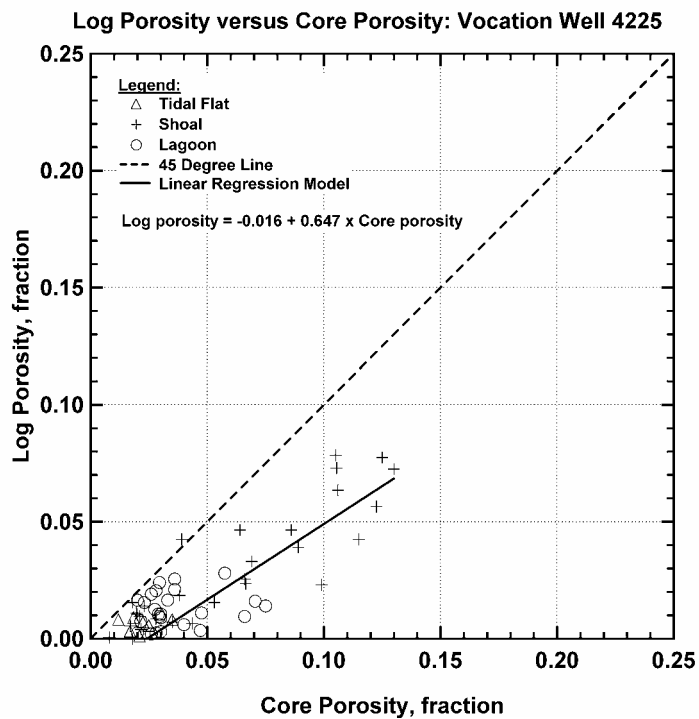


Fig. 129 — Log Porosity versus Core Porosity, Vocation Well 4225.

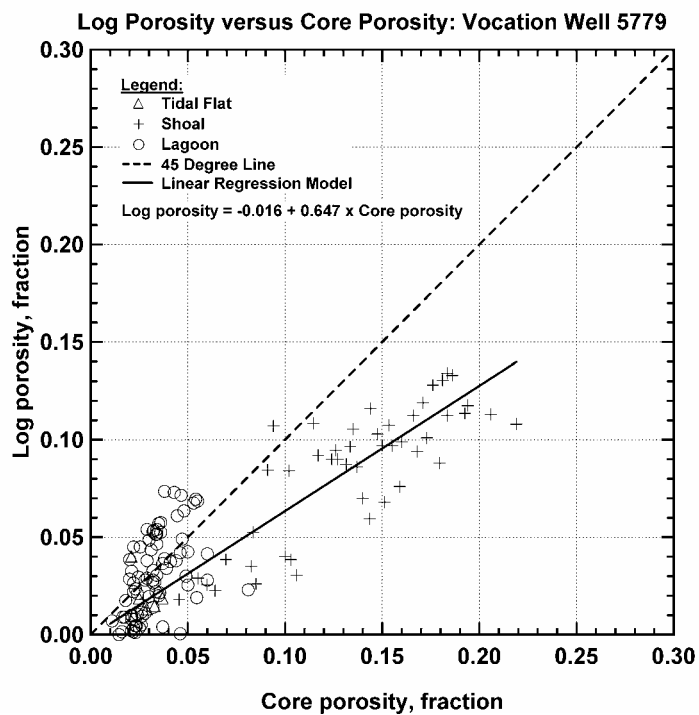


Fig. 130 — Log Porosity versus Core Porosity, Vocation Well 5779.

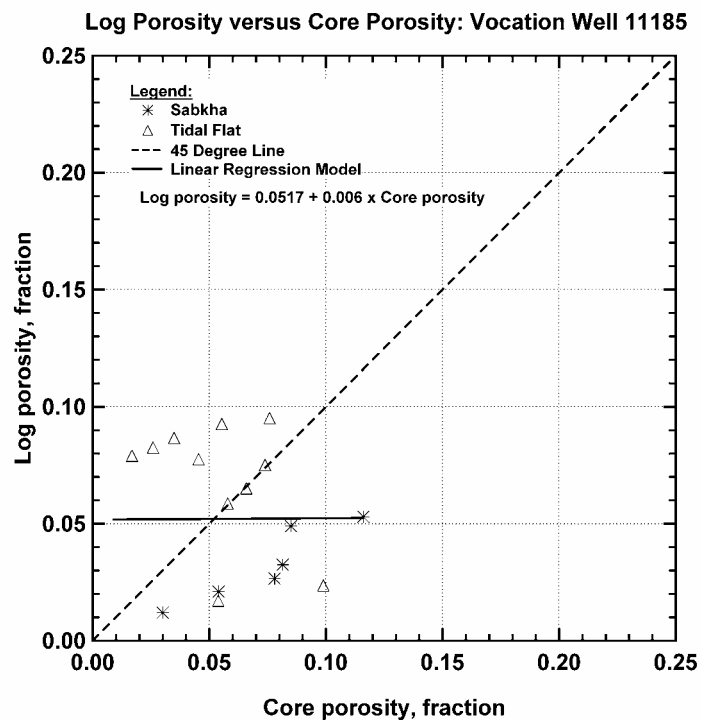


Fig. 131 — Log Porosity versus Core Porosity, Vocation Well 11185.

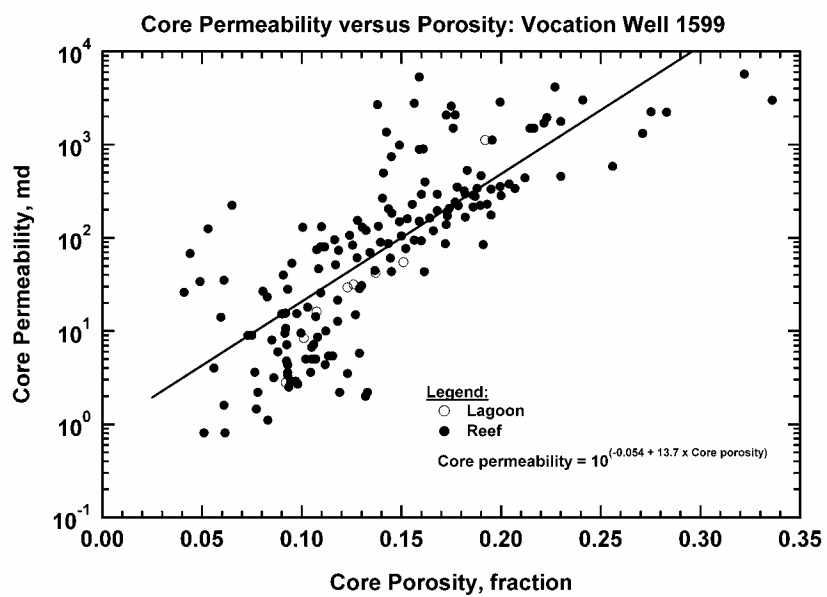


Fig. 132 — Core Permeability versus Core Porosity, Vocation Well 1599.

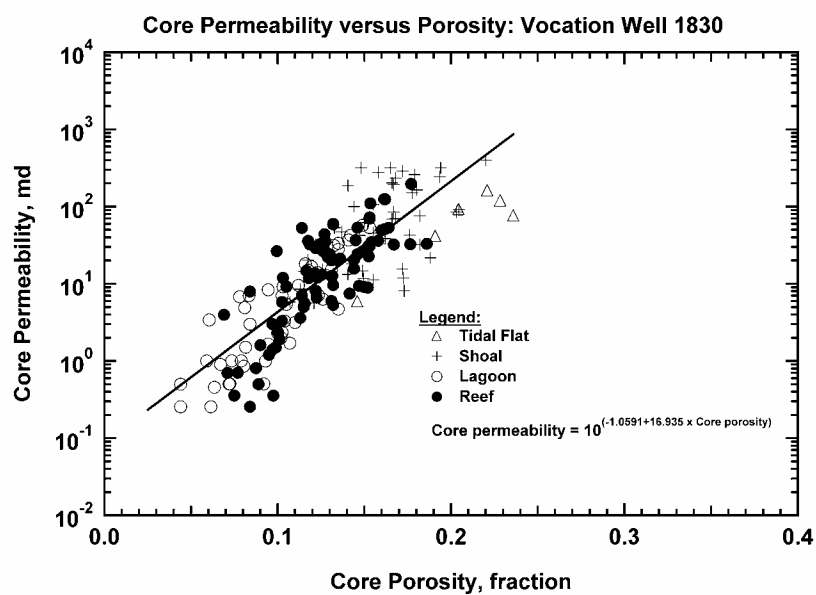


Fig. 133 — Core Permeability versus Core Porosity, Vocation Well 1830.

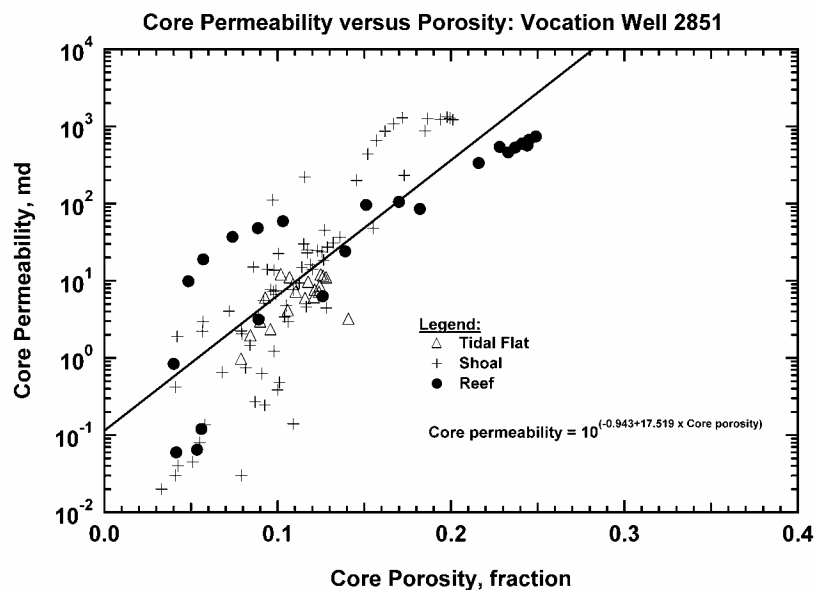


Fig. 134 — Core Permeability versus Core Porosity, Vocation Well 2851.

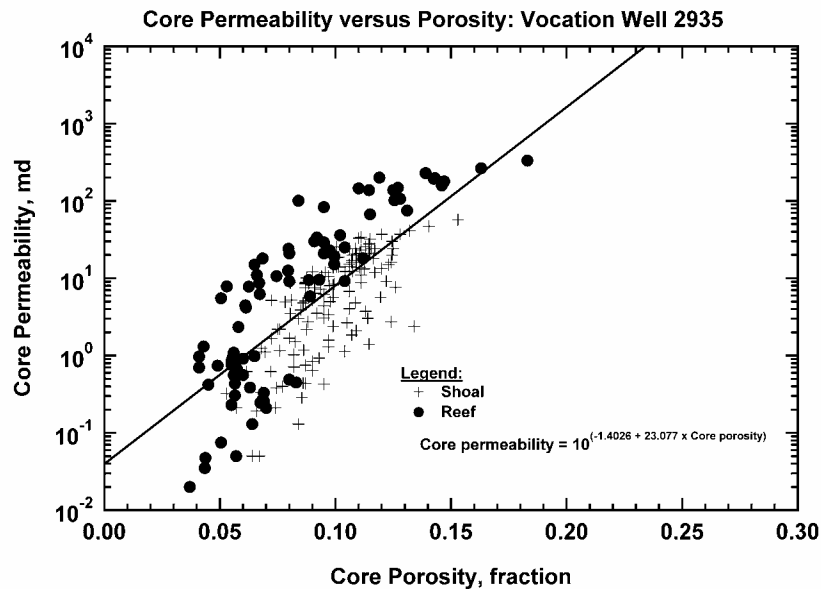


Fig. 135 — Core Permeability versus Core Porosity, Vocation Well 2935.

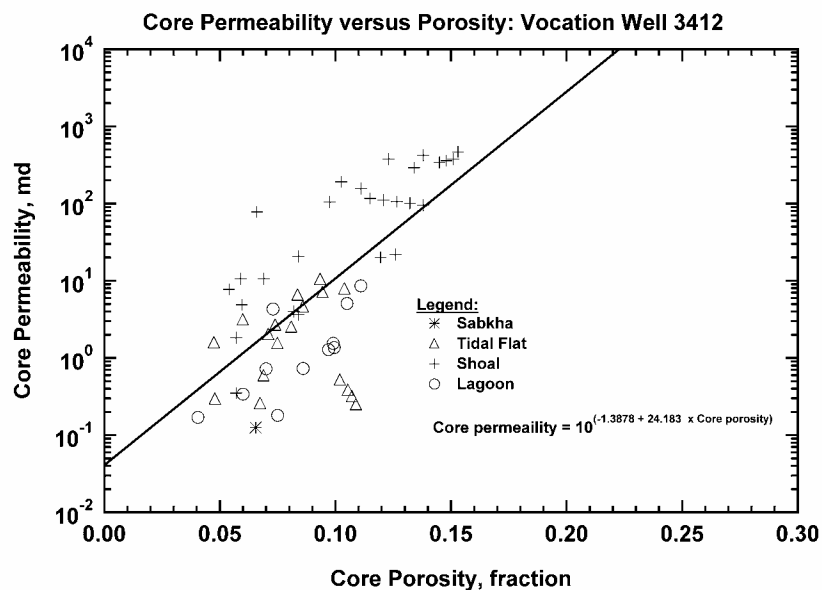


Fig. 136 — Core Permeability versus Core Porosity, Vocation Well 3412.

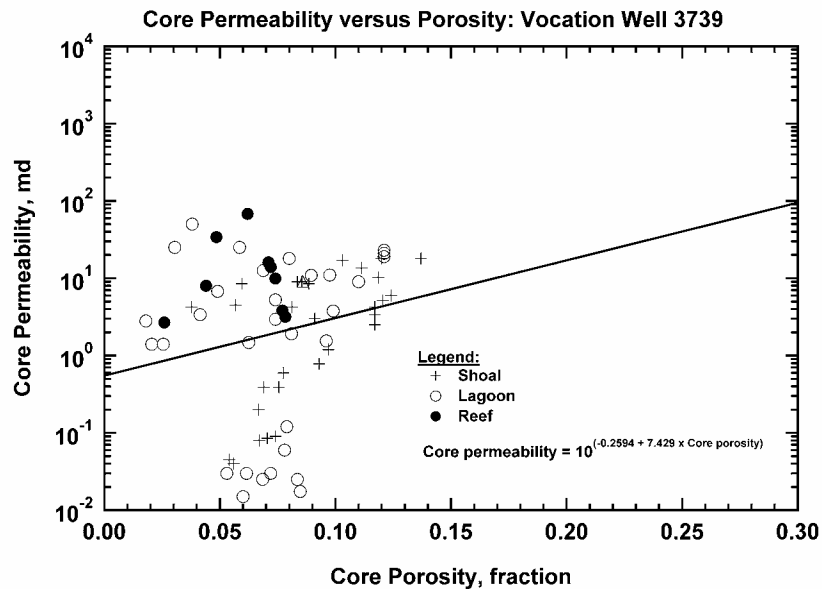


Fig. 137 — Core Permeability versus Core Porosity, Vocation Well 3739

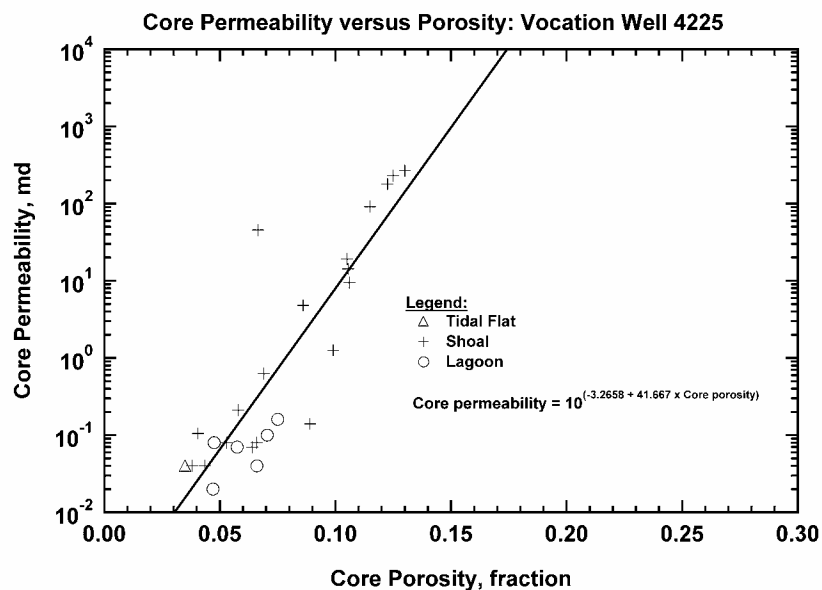


Fig. 138 — Core Permeability versus Core Porosity, Vocation Well 4225.

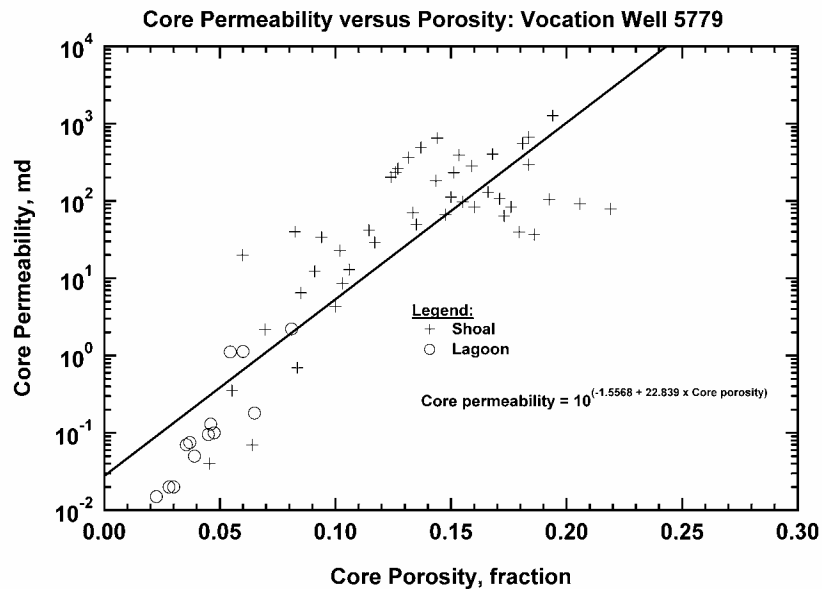


Fig. 139 — Core Permeability versus Core Porosity, Vocation Well 5779.



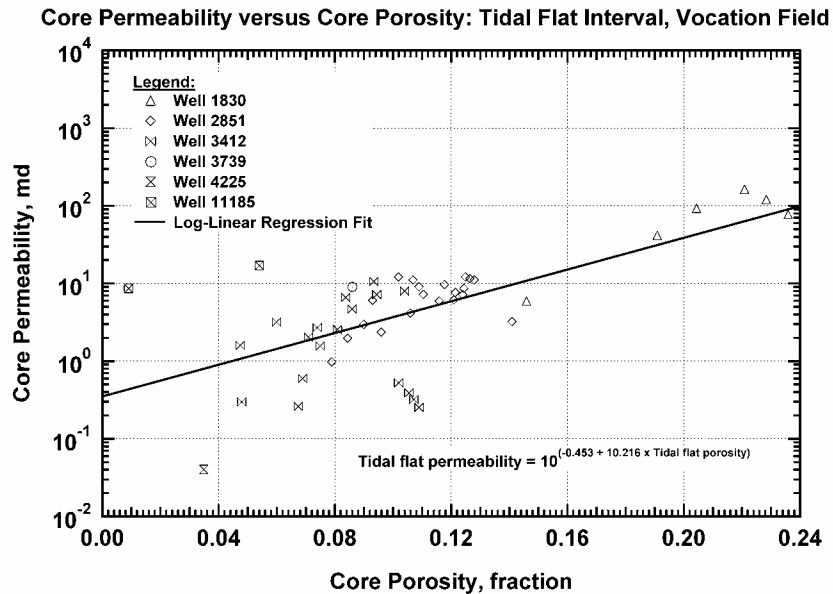


Fig. 140 — Core Permeability versus Core Porosity, Tidal Flat.

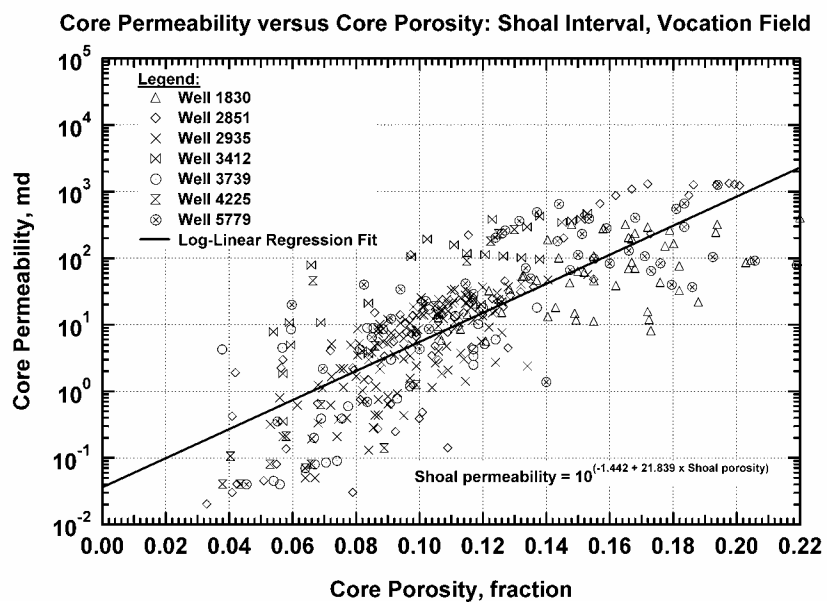


Fig. 141 — Core Permeability versus Core Porosity, Shoal.

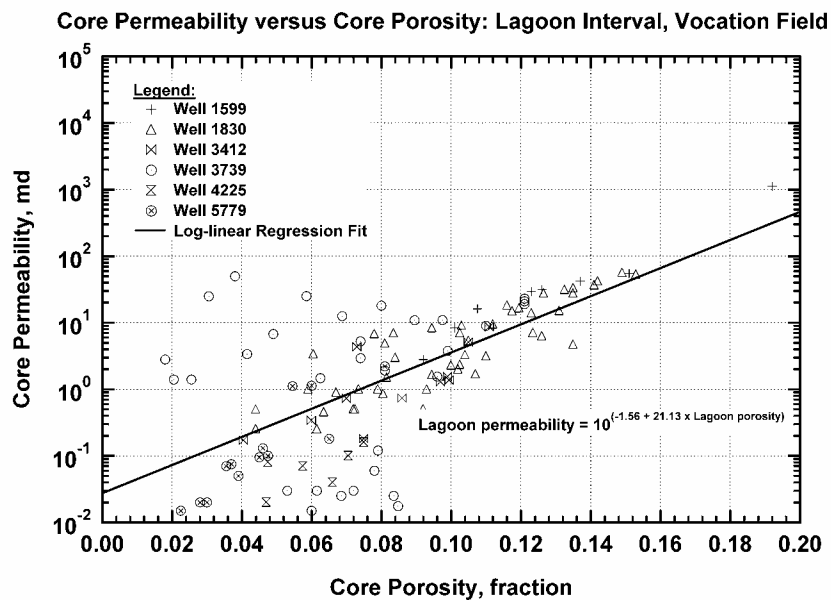


Fig. 142 — Core Permeability versus Core Porosity, Lagoon.

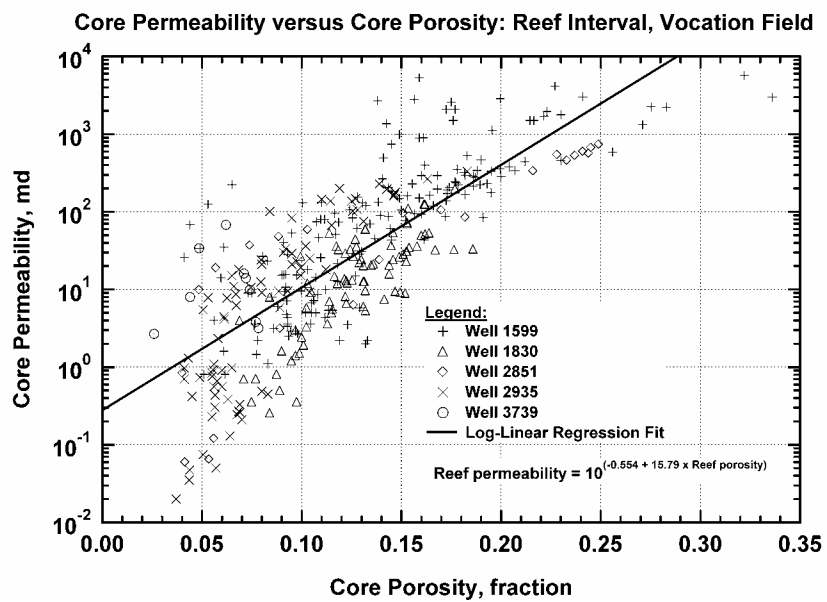


Fig. 143 — Core Permeability versus Core Porosity, Reef.

Well Id: Vocation Well 1599 Date: Aug 24,2002 Time: 16:01  
 Analyst: Archer/Blasingame

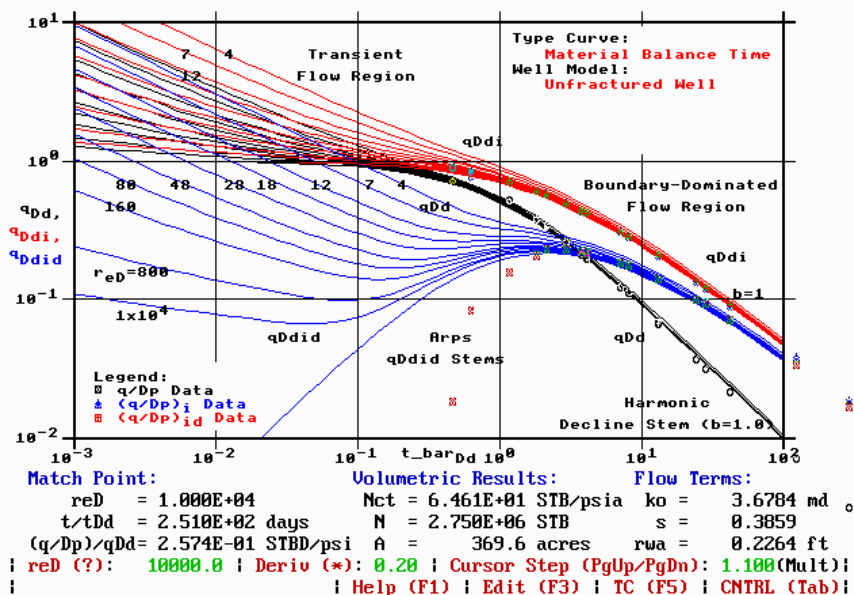


Fig. 144 — Type Curve Match, Vocation Well 1599.

Well Id: Vocation Well 1830 Date: Aug 24,2002 Time: 16:13  
 Analyst: Archer/Blasingame

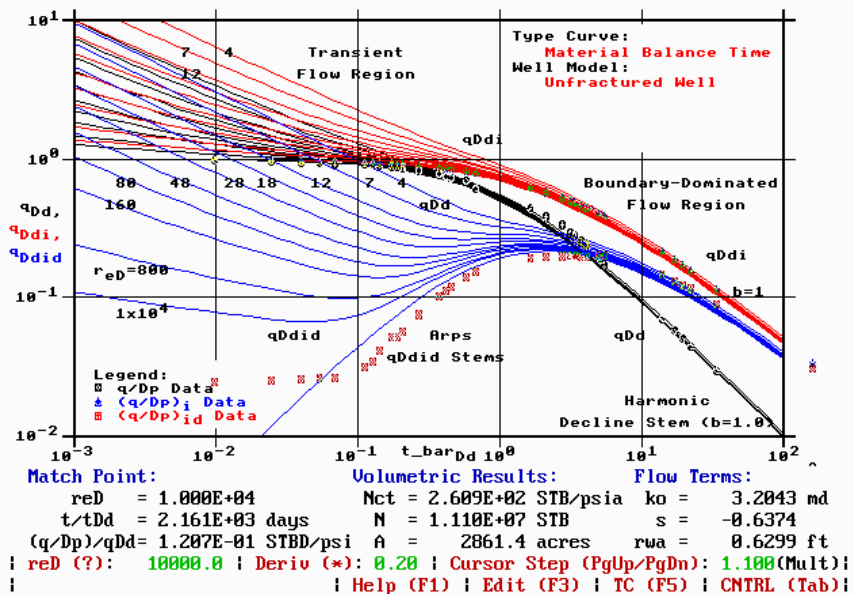


Fig. 145 — Type Curve Match, Vocation Well 1830.

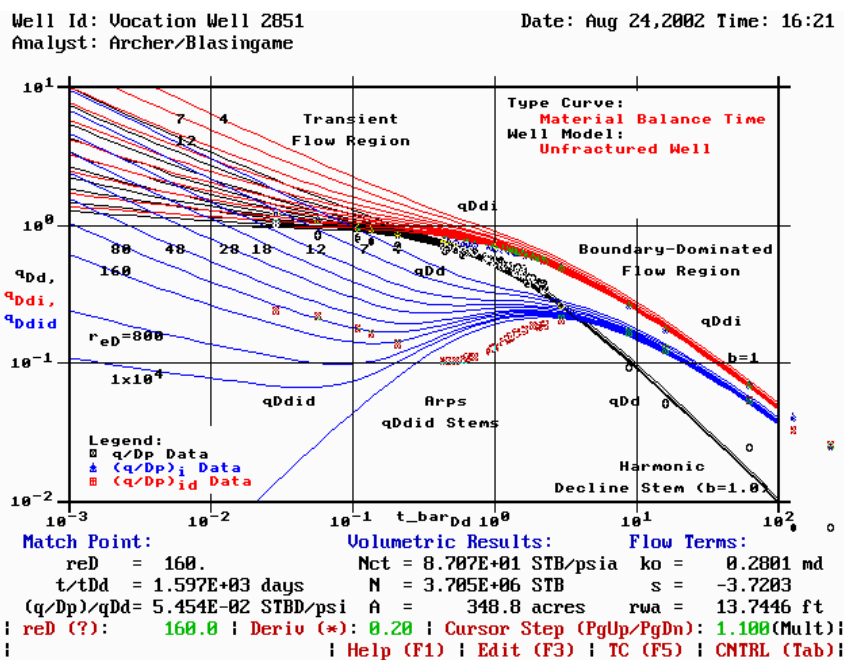


Fig. 146 — Type Curve Match, Vocation Well 2851.

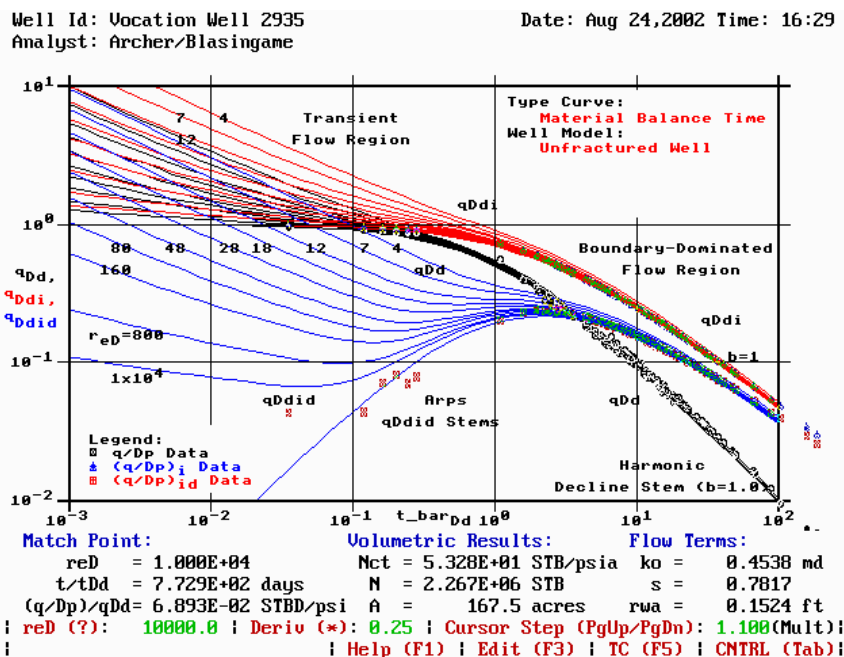


Fig. 147 — Type Curve Match, Vocation Well 2935.

Well Id: Vocation Well 3412 Date: Aug 24,2002 Time: 16:37  
 Analyst: Archer/Blasingame

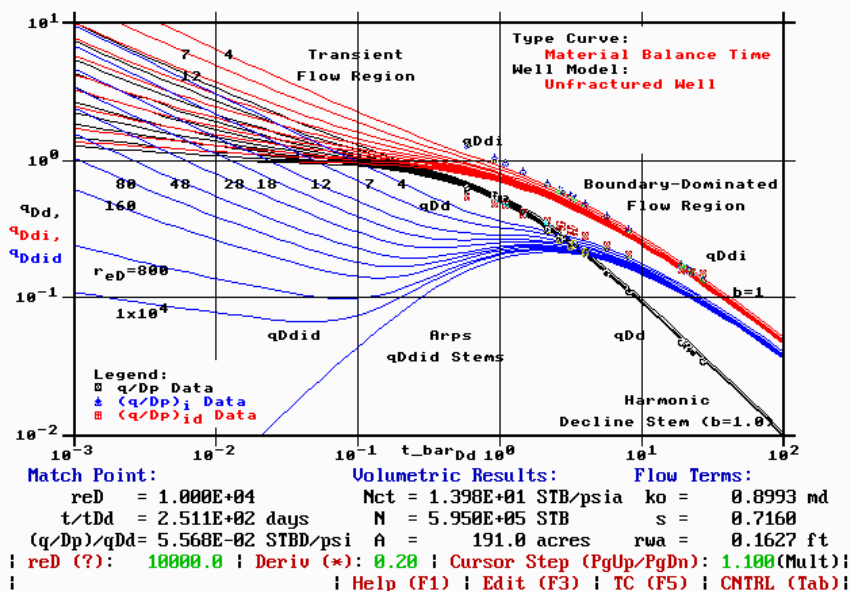


Fig. 148 — Type Curve Match, Vocation Well 3412.

Well Id: Vocation Well 3739 Date: Aug 24,2002 Time: 16:44  
 Analyst: Archer/Blasingame

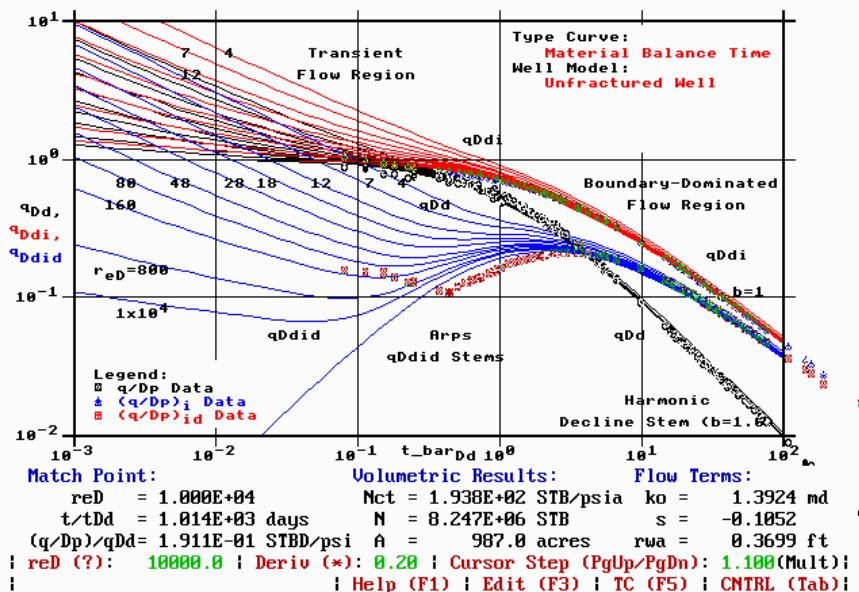


Fig. 149 — Type Curve Match, Vocation Well 3739.

Well Id: Vocation Well 4225 Date: Aug 24,2002 Time: 17:34  
 Analyst: Archer/Blasingame

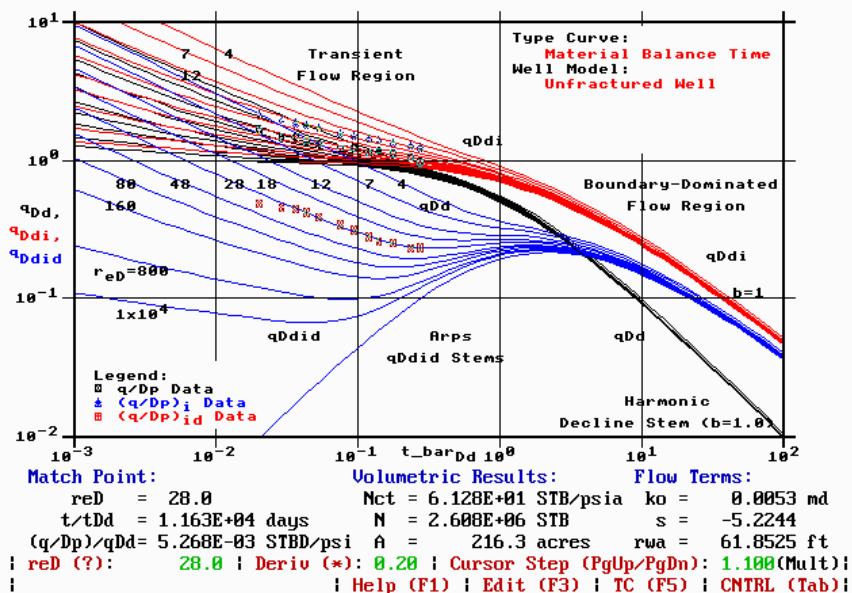


Fig. 150 — Type Curve Match, Vocation Well 4225.

Well Id: Vocation Well 4225B Date: Aug 24,2002 Time: 17:07  
 Analyst: Archer/Blasingame

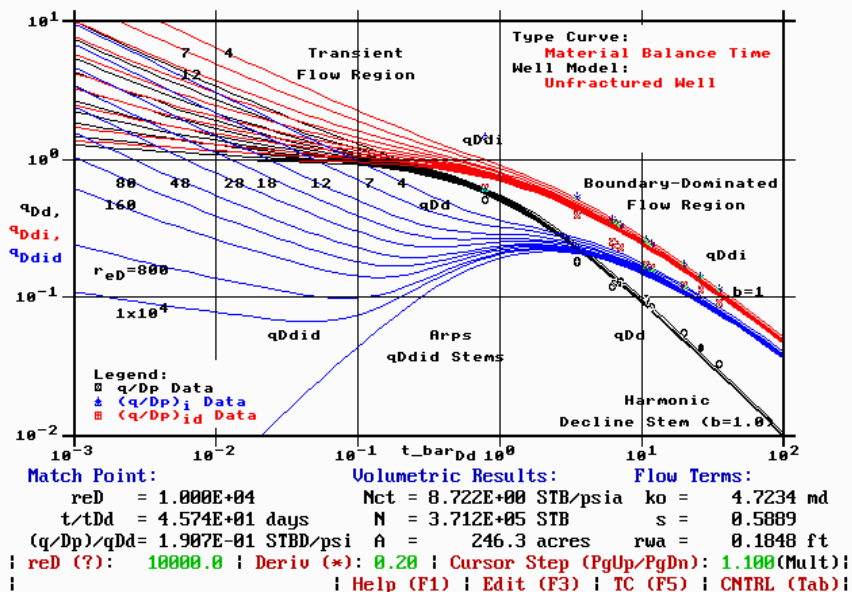


Fig. 151 — Type Curve Match, Vocation Well 4225B.

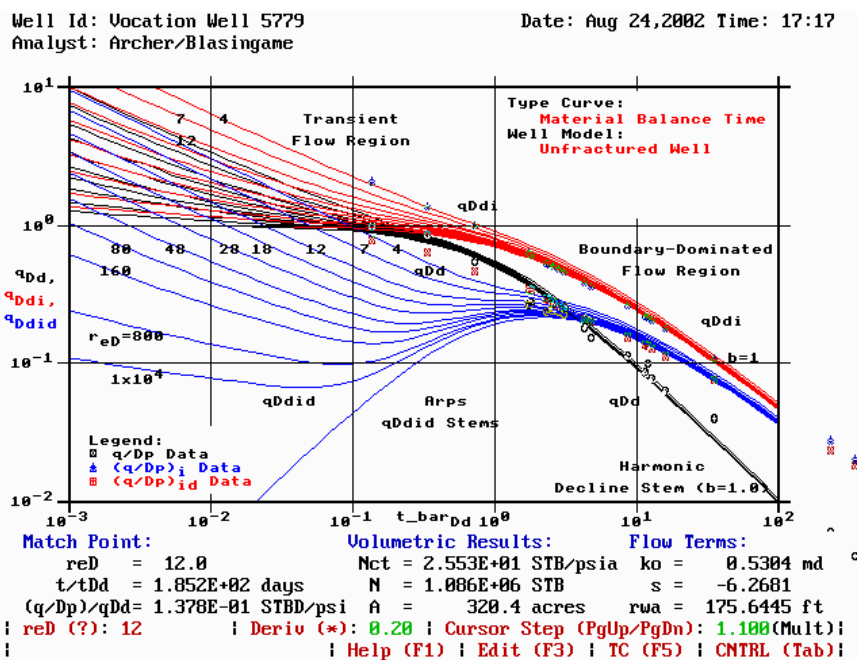


Fig. 152 — Type Curve Match, Vocation Well 5779.

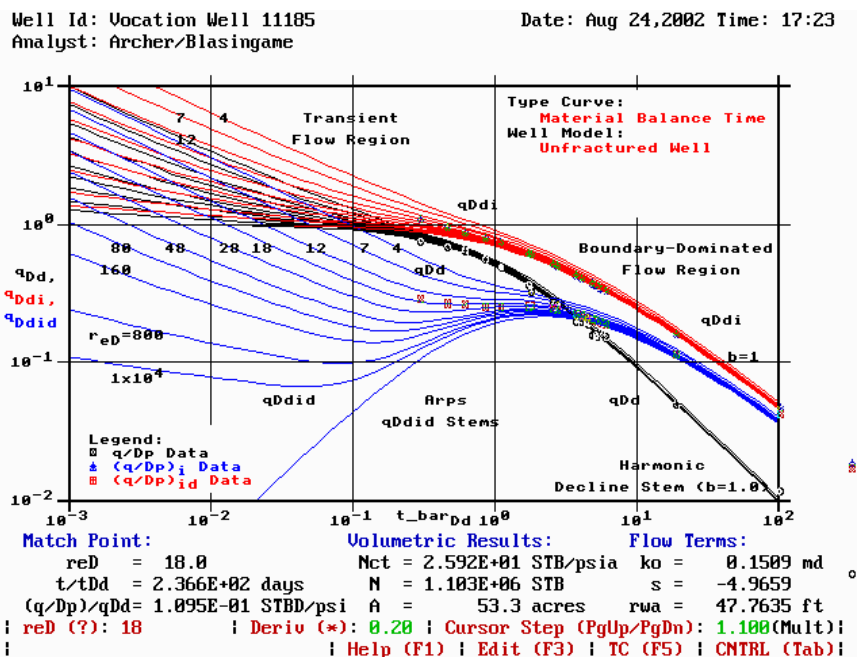


Fig. 153 — Type Curve Match, Vocation Well 11185.

Table 15 — Parameters Derived from Type Curve Analysis.

Well	$Nc_t$ (STB/psi)	$N$ (MSTB)	$A$ (acres)	$k_o$ (md)	$s$ (dim-less)
1599	64.6	2,750	369.6	3.68	0.38
1830	260.9	11,100	2861.4	3.20	0.63
2851	87.0	3,705	348.8	0.28	-3.72
2935	53.3	2,267	167.5	0.45	0.78
3412	13.9	595	191.0	0.90	0.72
3739	193.8	8,247	987.0	1.39	-0.10
4225	61.3	2,608	216.3	0.005	-5.2
4225B	8.7	371	246.3	4.72	0.58
5779	25.5	1,086	328.4	0.53	-6.26
11185	25.9	1,103	53.3	0.15	-4.96
Total		= 33,382			



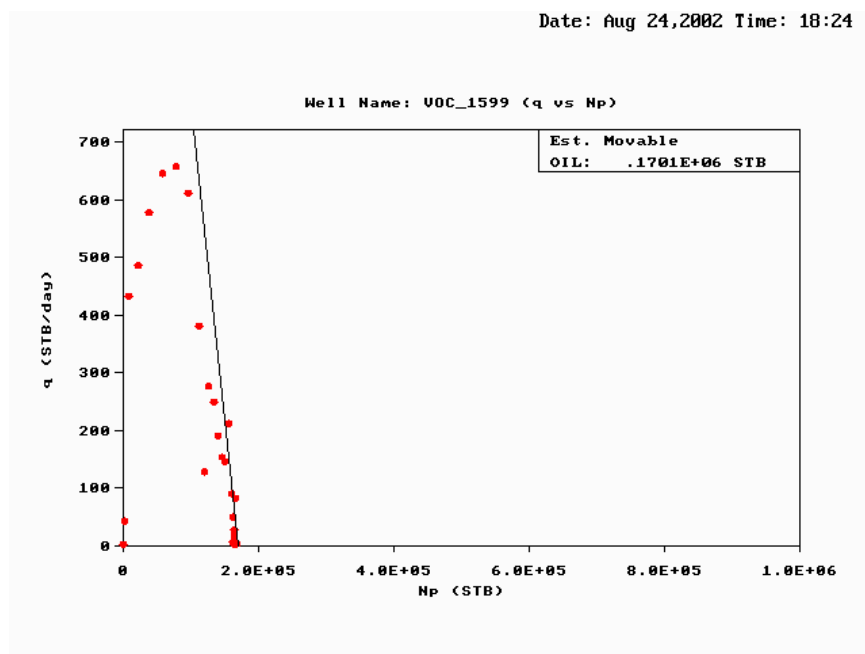


Fig. 154 — Calculation of Recoverable Oil, Vocation Well 1599.

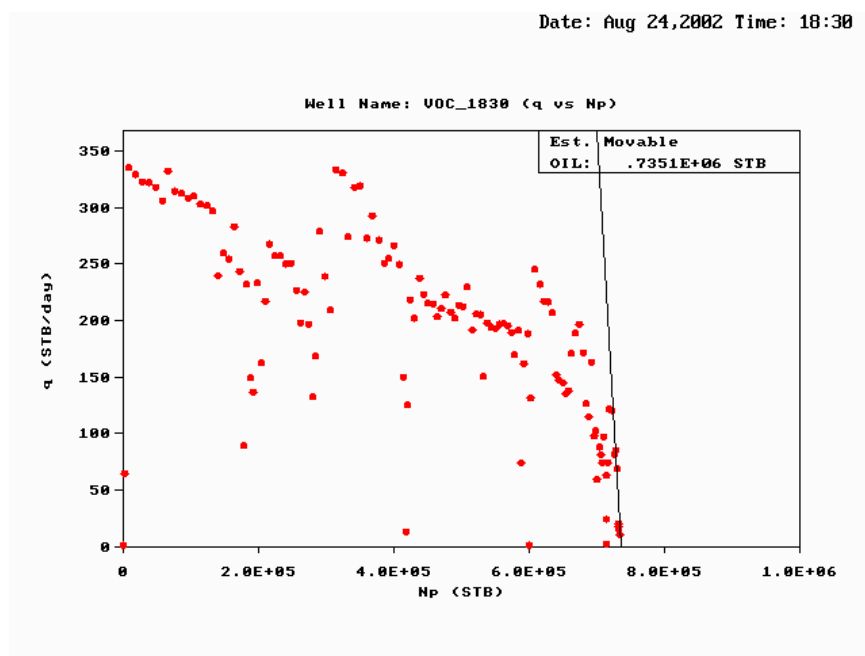


Fig. 155 — Calculation of Recoverable Oil, Vocation Well 1830.

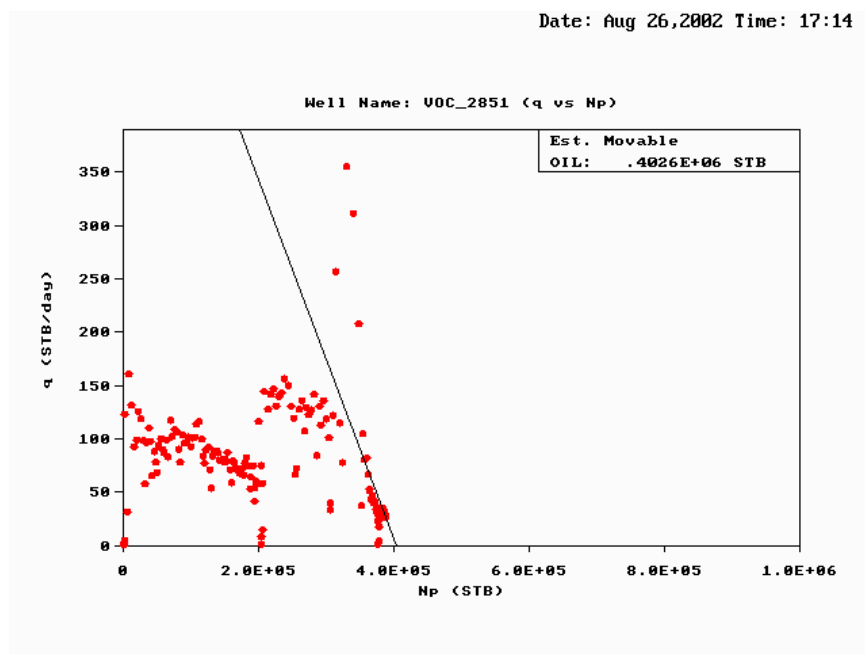


Fig. 156 — Calculation of Recoverable Oil, Vocation Well 2851.

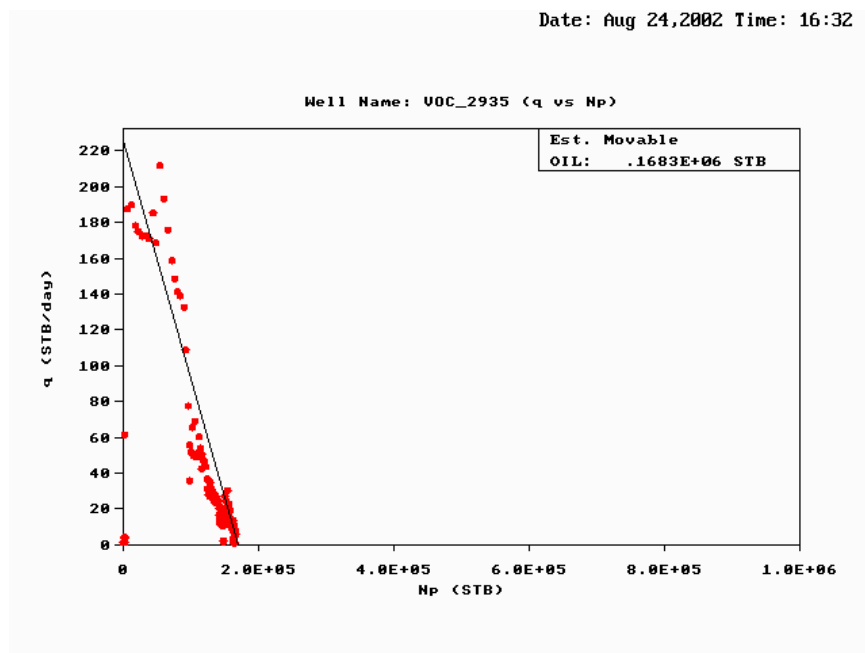


Fig. 157 — Calculation of Recoverable Oil, Vocation Well 2935.

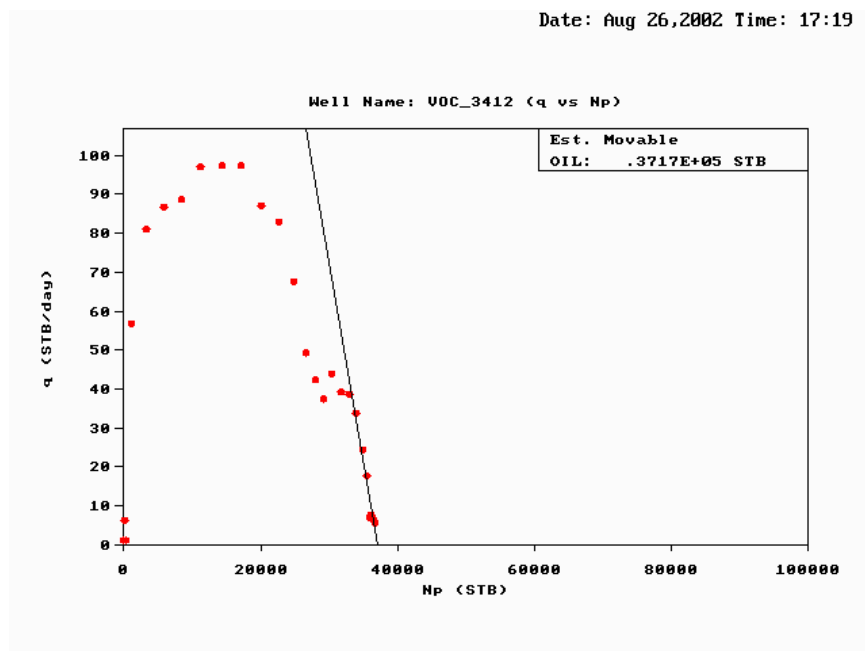


Fig. 158 — Calculation of Recoverable Oil, Vocation Well 3412.

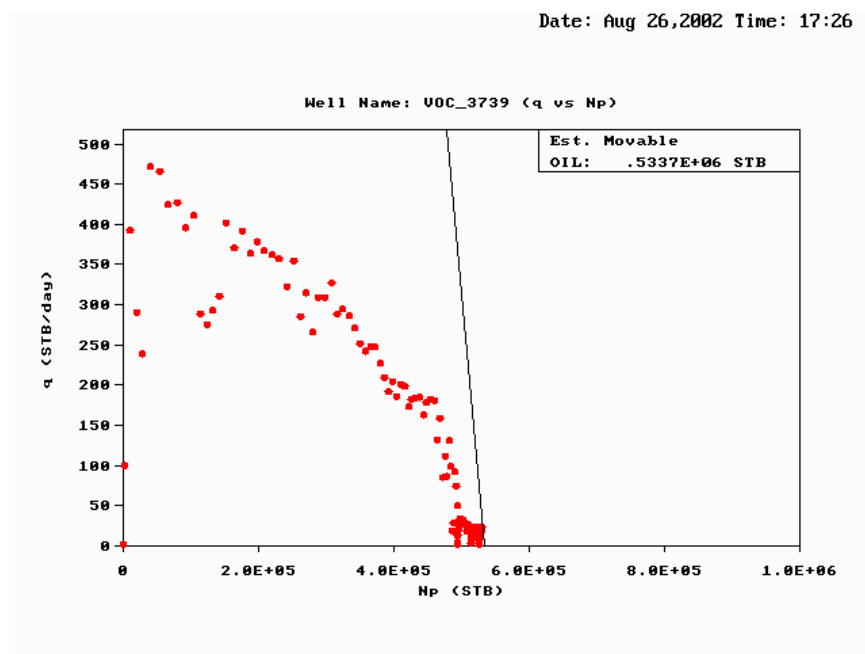


Fig. 159 — Calculation of Recoverable Oil, Vocation Well 3739.

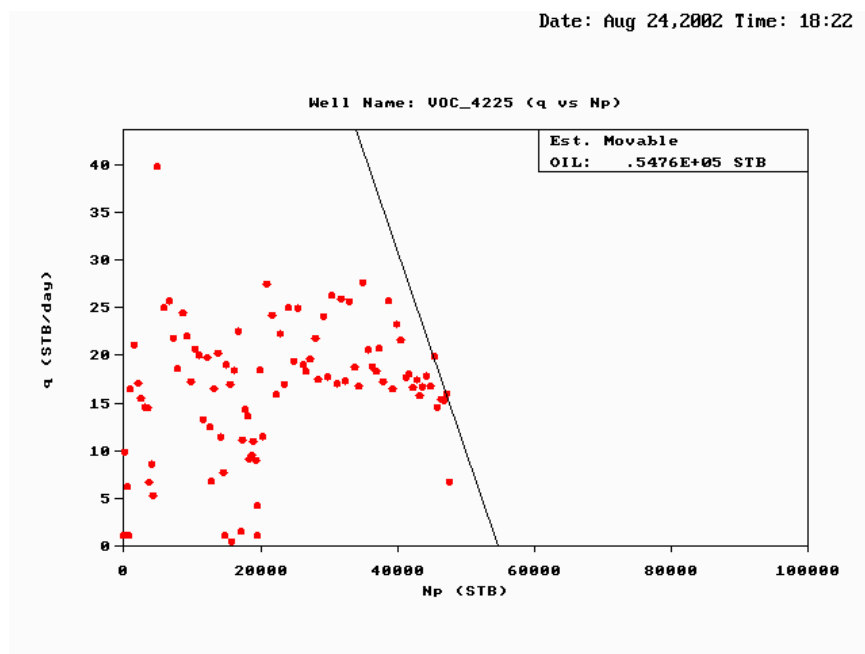


Fig. 160 — Calculation of Recoverable Oil, Vocation Well 4225.

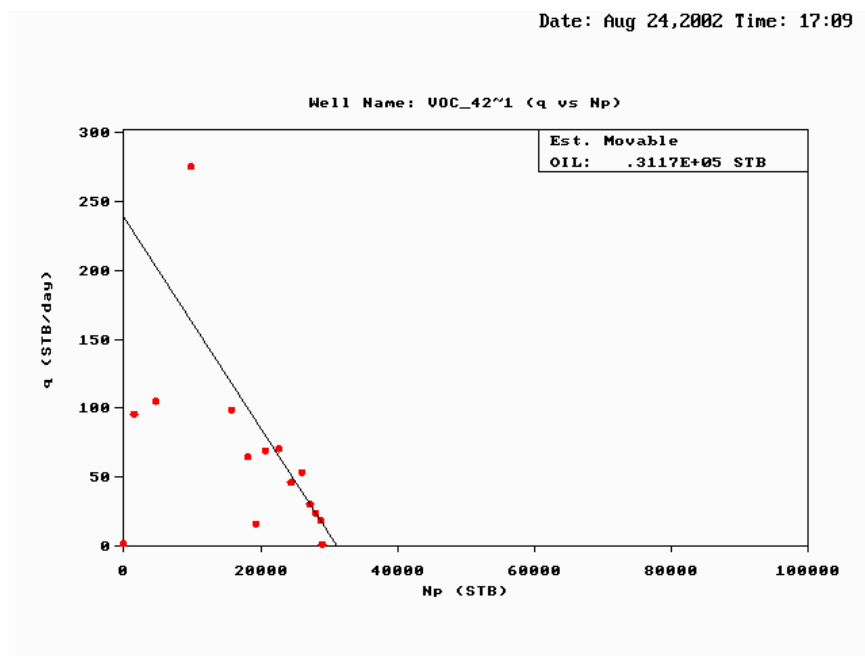


Fig. 161 — Calculation of Recoverable Oil, Vocation Well 4225B.

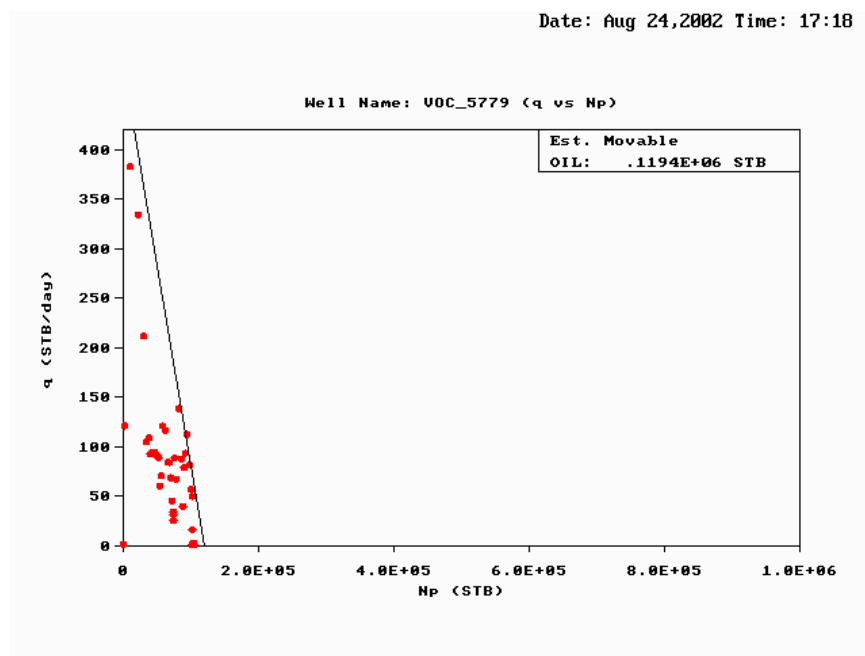


Fig. 162 — Calculation of Recoverable Oil, Vocation Well 5779.

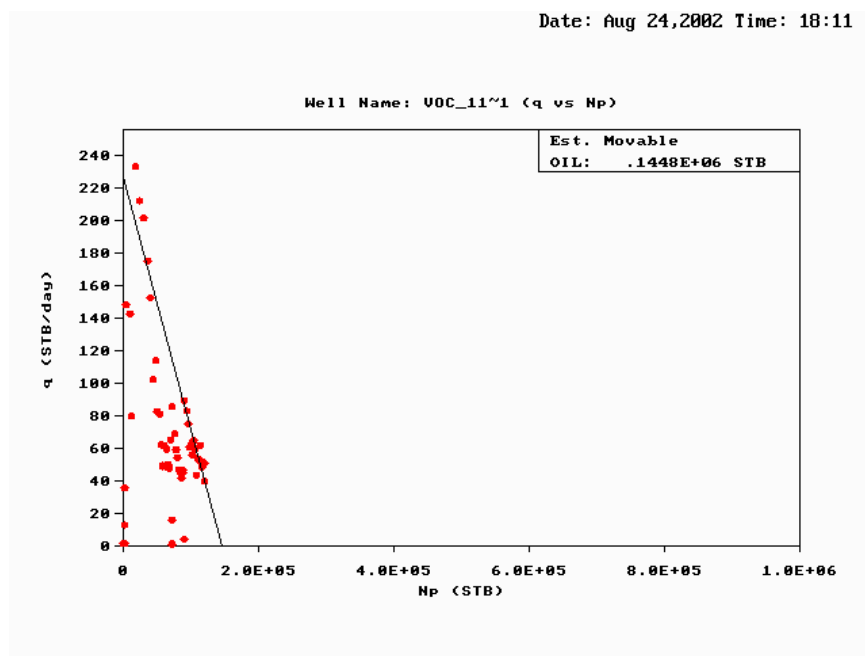


Fig. 163 — Calculation of Recoverable Oil, Vocation Well 11185.

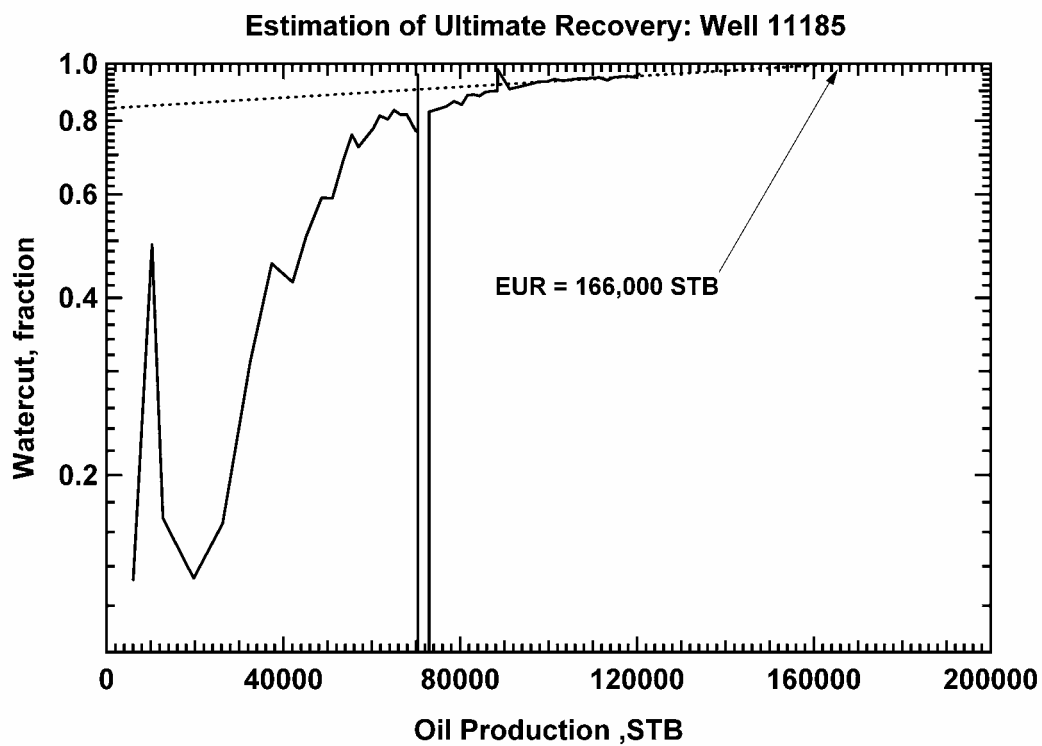


Fig. 164 — Alternative Calculation of Recoverable Oil, Vocation Well 11185.

Table 16 – Oil Recovery and Recovery Factors.

Well	$N_{recoverable}$ (MSTB)	$N_p$ (MSTB)	$N$ (MSTB)	Recovery Factor $N_p/N$ (dim-less)
1599	170	169	2,750	0.061
1830	735	733	11,100	0.066
2851	402	388	3,705	0.105
2935	168	165	2,267	0.072
3412	37	36	595	0.061
3739	534	529	8,247	0.064
4225	55	47	2,608	0.018
4225B	31	29	371	0.078
5779	119	102	1,086	0.094
11185	145	120	1,103	0.109
Total	= 2,331	= 2,318	= 33,832	= 0.069

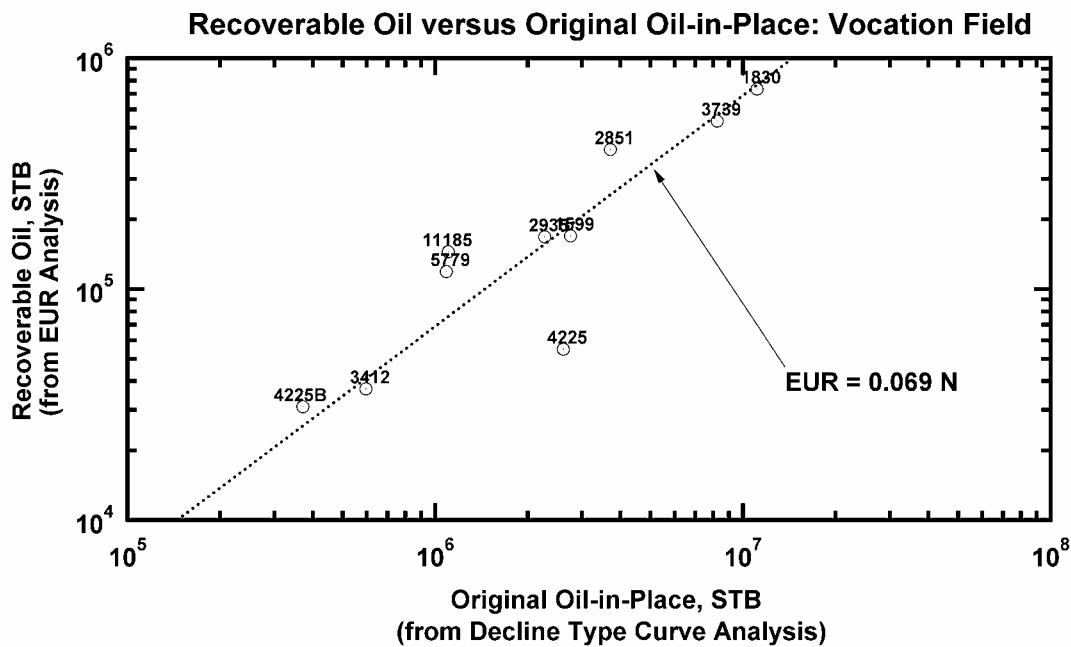


Fig. 165 — Recoverable Oil (*EUR* Analysis) versus Computed Original Oil-in-Place (Decline Type Curve Analysis), Vocation Oil Field.

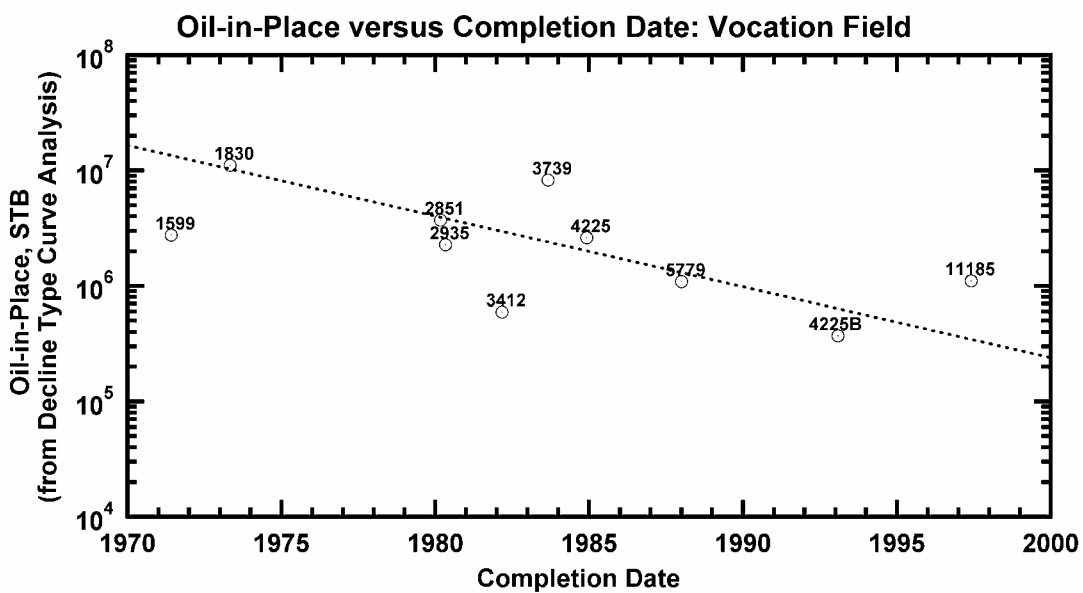


Fig. 166 — Computed Original Oil-in-Place versus Completion Date, Vocation Oil Field.



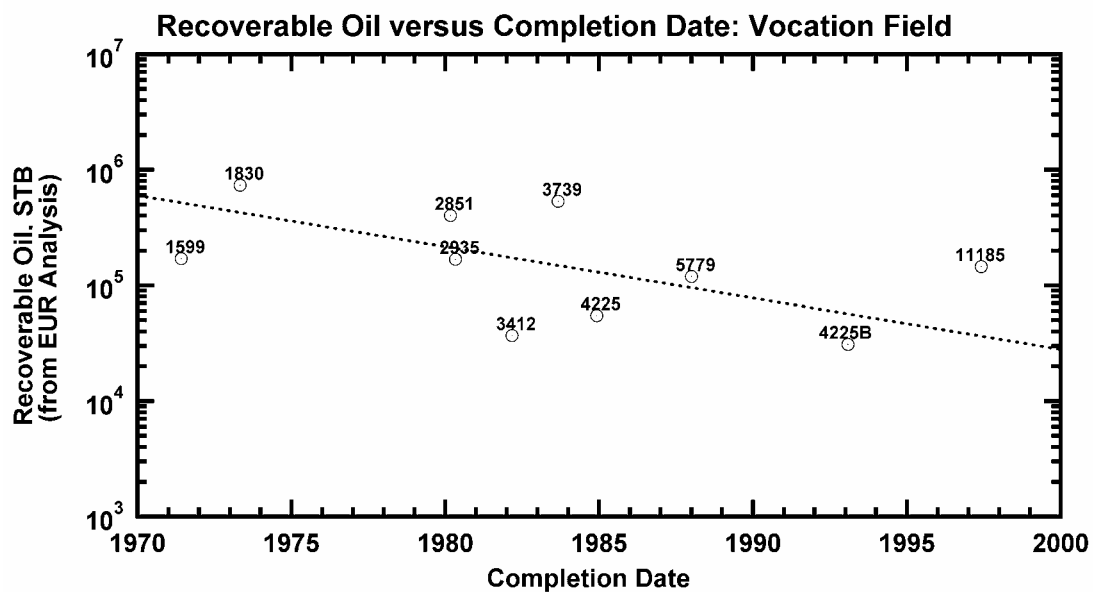


Fig. 167 — Recoverable Oil versus Completion Date, Vocation Oil Field.

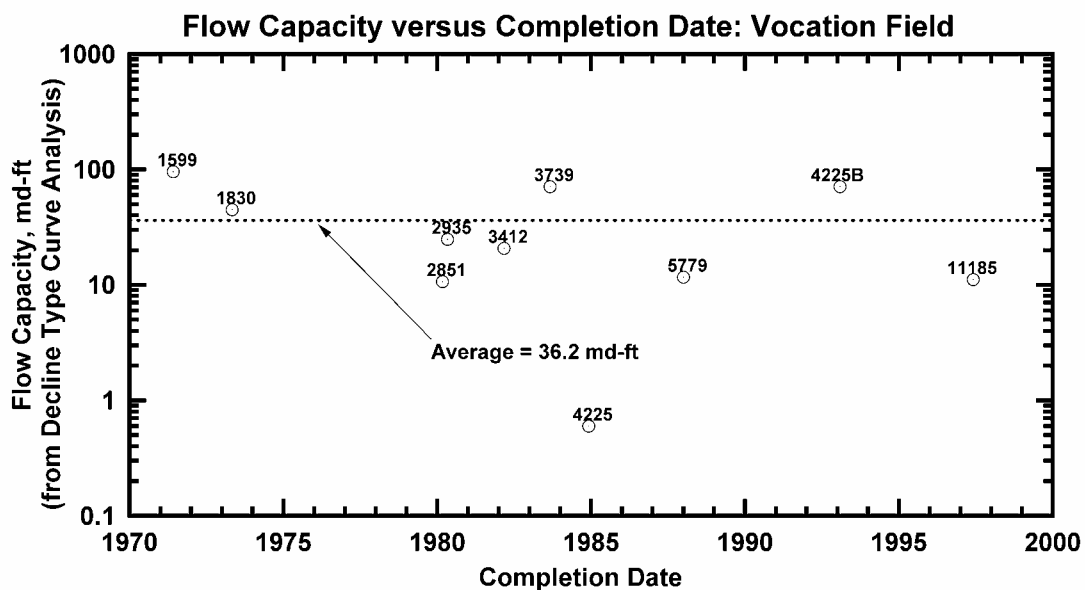


Fig. 168 — Flow Capacity versus Completion Date, Vocation Oil Field.

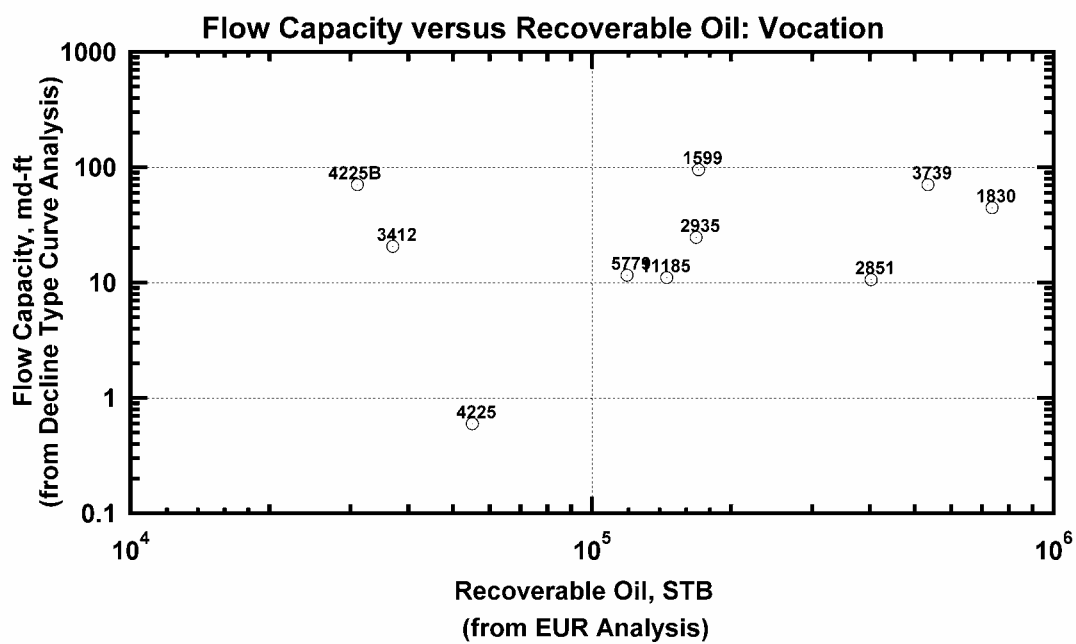


Fig. 169 — Flow Capacity versus Recoverable Oil, Vocation Oil Field.

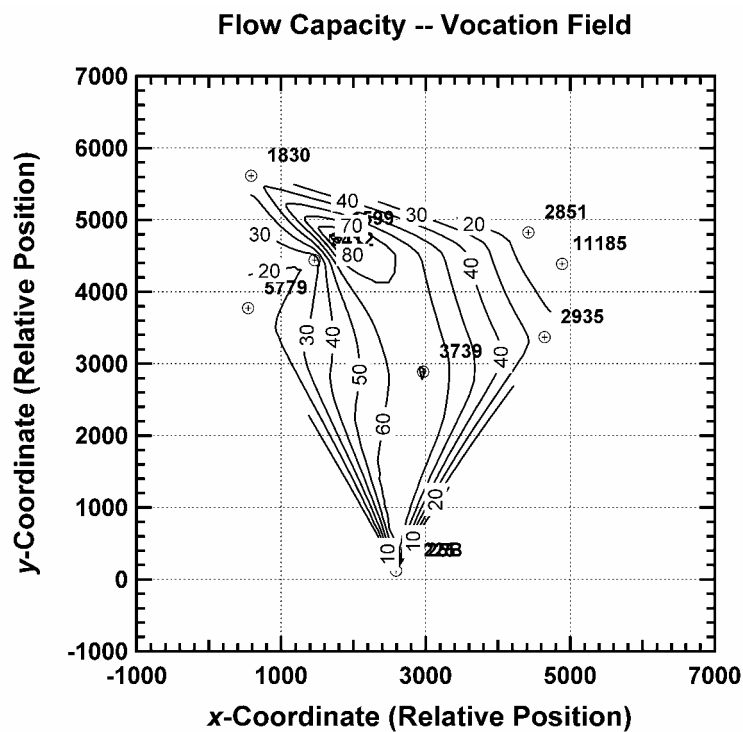


Fig. 170 — Contour Map of Flow Capacity, Vocation Oil Field.

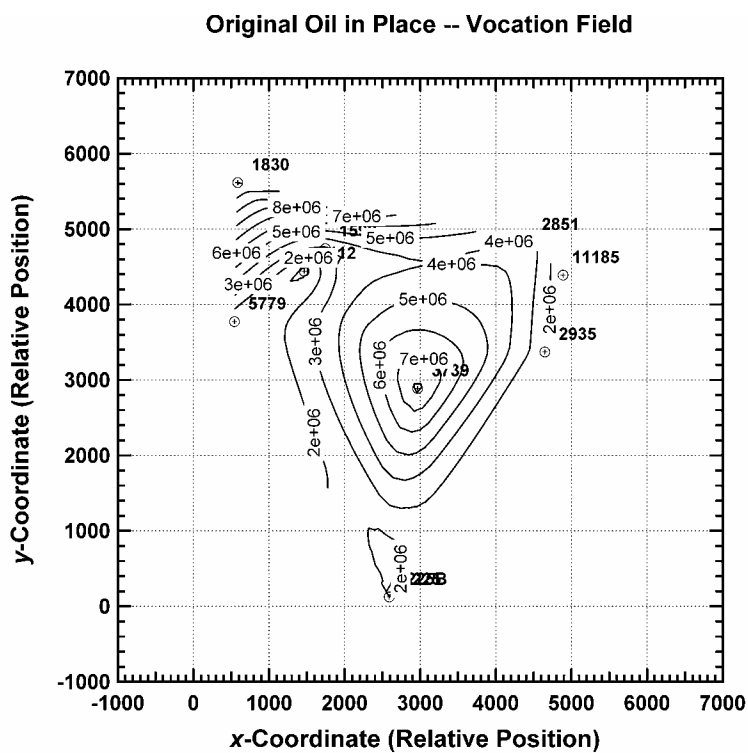


Fig. 171 — Contour Map of Original Oil-in-Place, Vocation Oil Field.

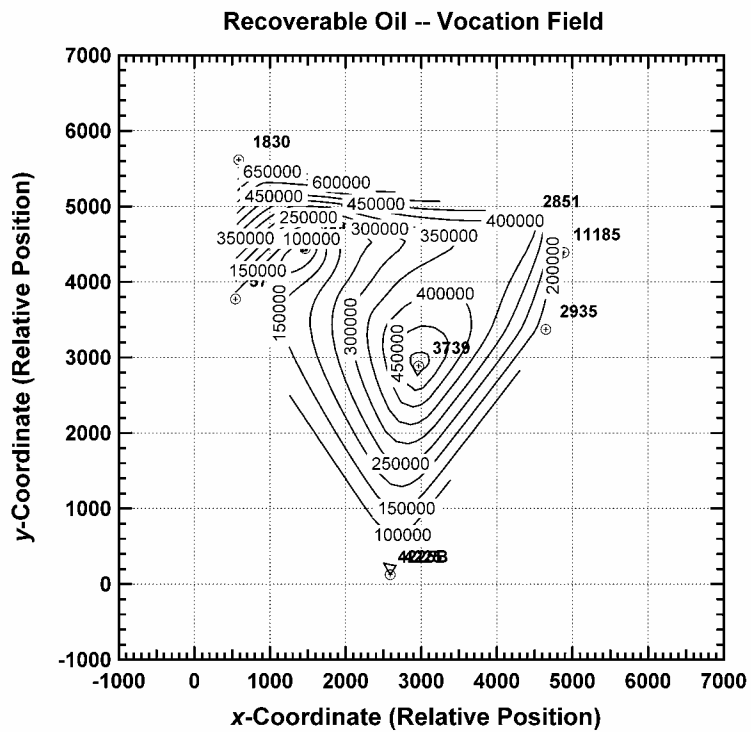


Fig. 172 — Contour Map of Recoverable Oil, Vocation Oil Field.

All geological, geophysical, petrophysical and engineering data generated to date from this study have been entered and integrated into digital databases for Appleton and Vocation Fields.

### ***3-D Modeling (Phase 2)***

**Task 5—3-D Geologic Model.**--This task involves using the integrated database which includes the information from the reservoir characterization tasks to build a 3-D stratigraphic and structural model(s) for Appleton and Vocation Fields. For Appleton Field, the existing, but independently completed, geological and geophysical studies will be integrated and used in combination with the new information from the drilling and producing of the sidetrack well in the field and from the study of the additional five cores and additional 3-D seismic data from the field area to revise, as needed, the current Appleton geologic model. The Appleton reef-shoal paleohigh (low-relief) model will be applied to Vocation Field (high-relief paleohigh). The application of the Appleton model to Vocation Field could result in the Appleton model being reasonable for modeling the Vocation reservoir or could result in the need to modify the Appleton model to honor the characteristics of the Vocation reservoir and structure. The result, therefore, could be a single geologic model for reef-shoal reservoirs associated with basement paleohighs of varying degrees of relief or two geologic models—one for reef-shoal reservoirs associated with low-relief paleohighs and one for reef-shoal reservoirs associated with high-relief paleohighs. This task also provides the framework for the reservoir simulation modeling in these fields. Geologic modeling sets the stage for reservoir simulation and for the recognition of flow units, barriers to flow and flow patterns in the respective fields. Sequence stratigraphy in association with structural interpretation will form the framework for the model(s). The model(s) will incorporate data and interpretations from sequence stratigraphic, depositional history and structural studies, core and well log analysis, petrographic and diagenetic studies, and pore

system and petrophysical analysis. The model(s) will also incorporate the geologic observations and interpretations made from studying stratigraphic and spatial lithofacies relationships observed in Late Jurassic microbial reefs in outcrops. The purpose of the 3-D geologic model(s) is to provide an interpretation for the interwell distribution of systems tracts, lithofacies, and reservoir-grade rock. This work is designed to improve well-to-well predictability with regard to reservoir parameters, such as lithofacies, diagenetic rock-fluid alterations, pore types and systems, and heterogeneity. The geologic model(s) and integrated database become effective tools for cost-effective reservoir management for making decisions regarding operations in these fields. Accepted industry software, such as Stratamodel and GeoSec, will be used to build the 3-D geologic model(s). GeoSec software will be used in the 3-D structural interpretation and Stratamodel software will be used to construct the geologic model(s).

3-D geologic modeling of the structures and reservoirs at Appleton and Vocation Fields has been completed. The model for the structure and reservoir characteristics at Appleton Field are illustrated in Figures 173-174 and Figures 175-176, respectively. The model for the structure and reservoirs at Vocation Field are shown in Figures 177-178 and Figures 179-180, respectively. The model represents an integration of geological, petrophysical and seismic data.

**Task 6—3-D Reservoir Simulation Model.**--This task focuses on the construction, implementation and validation of a numerical simulation model(s) for Appleton and Vocation Fields that is based on the 3-D geologic model(s), petrophysical properties, fluid (PVT) properties, rock-fluid properties, and the results of the well performance analysis. The geologic model(s) will be coupled with the results of the well performance analysis to determine flow units, as well as reservoir-scale barriers to flow. Reservoir simulation will be performed

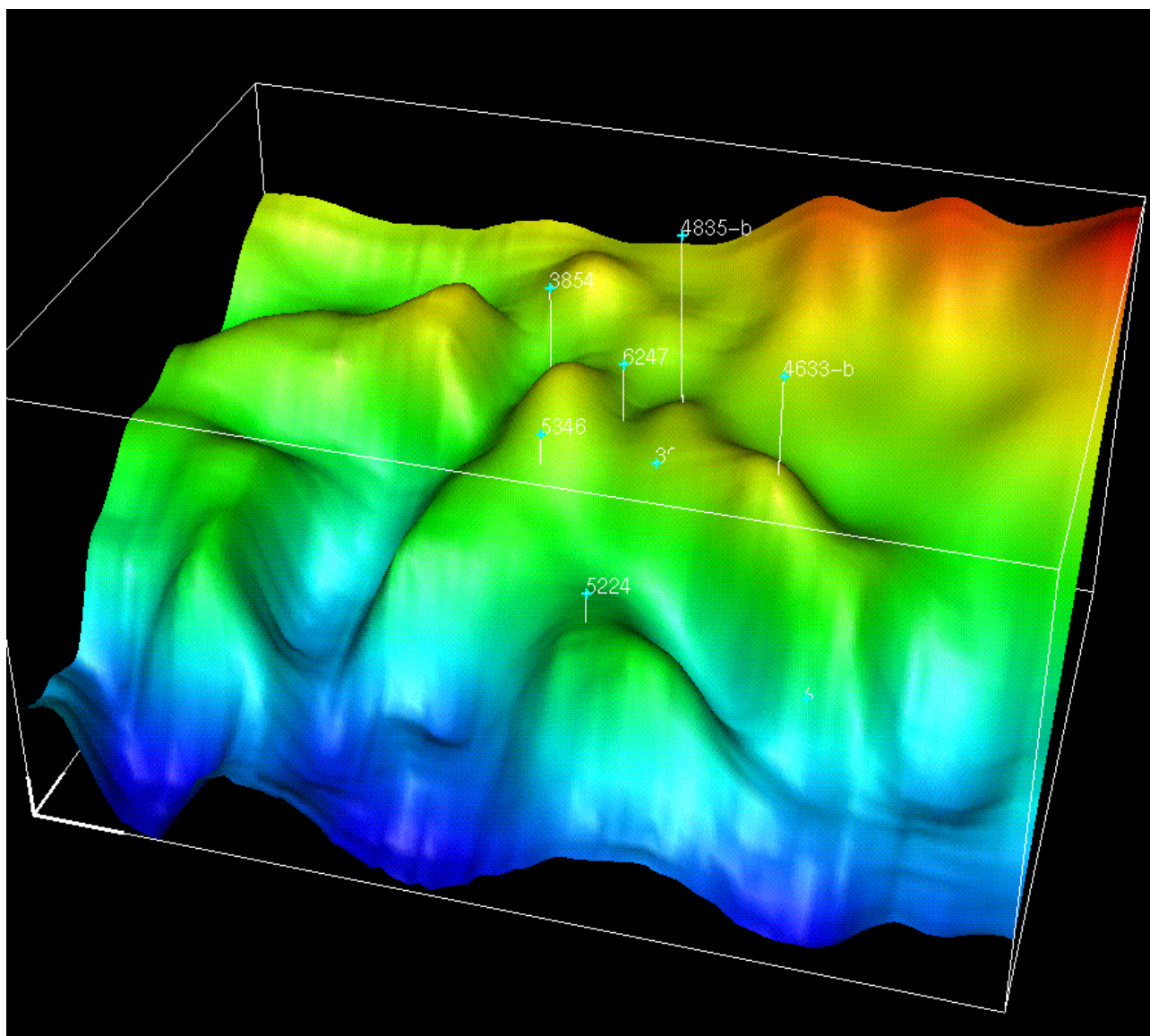


Fig. 173 – 3-D model of Appleton Field structure on top of the Smackover/Buckner.

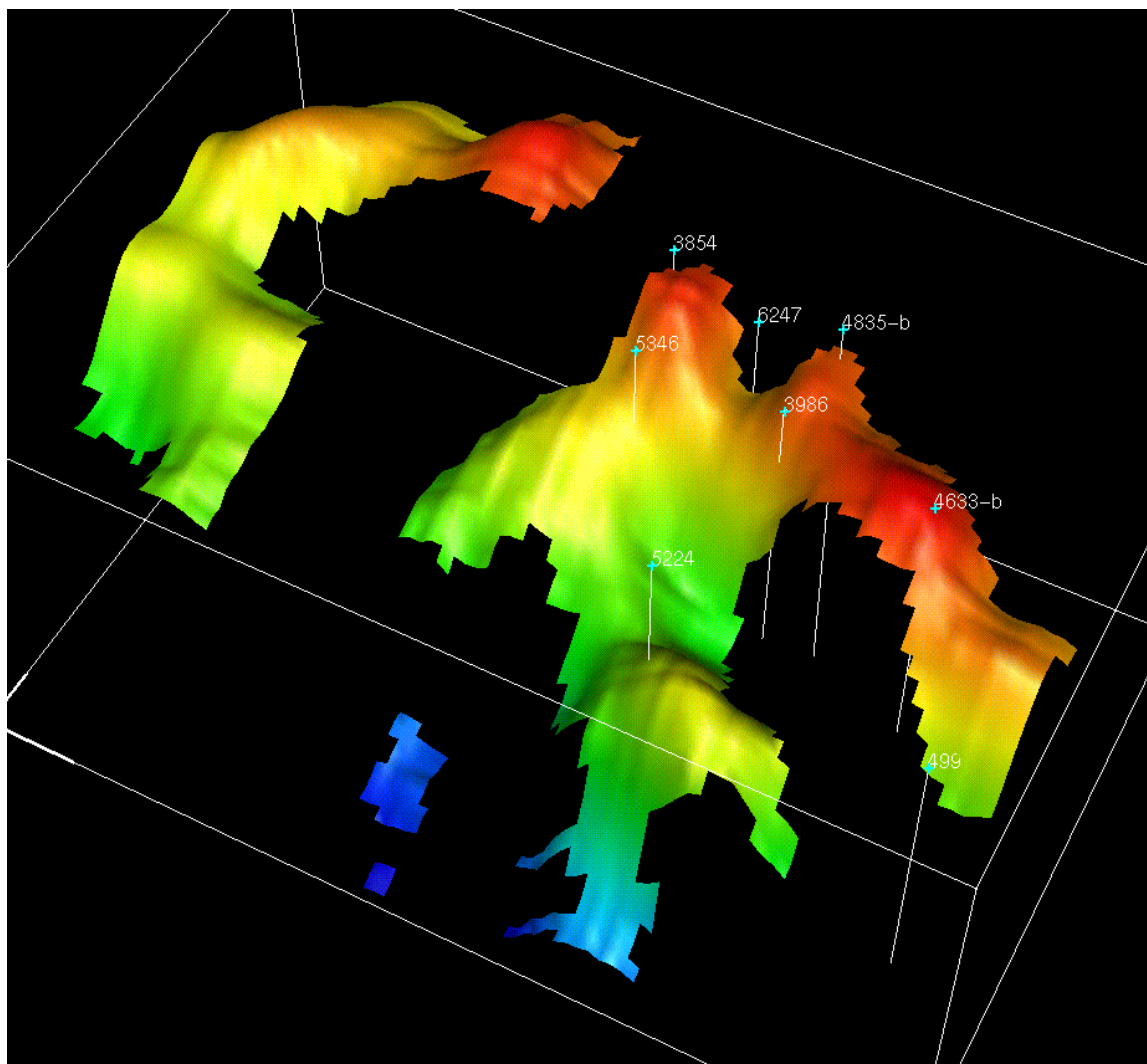


Figure 174. 3-D model of Appleton Field structure on top of the reef interval.



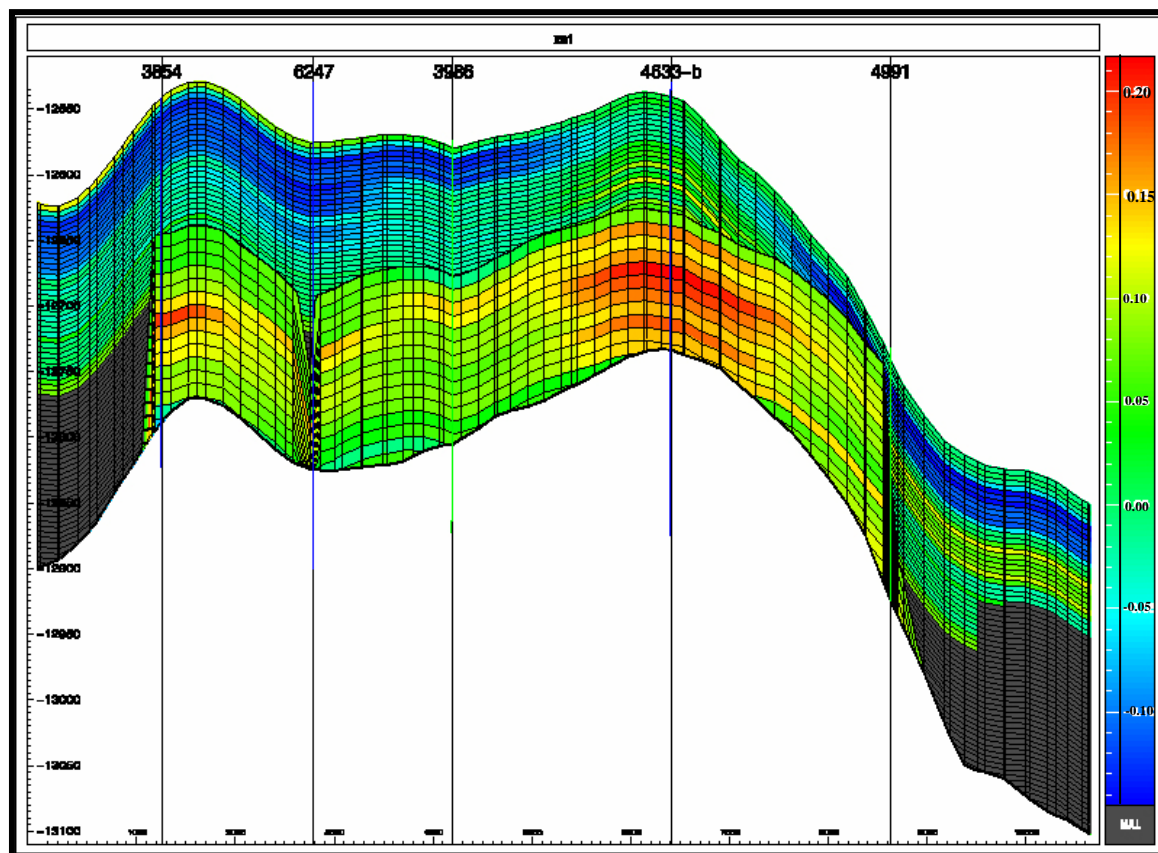


Fig. 175 –Cross section showing reservoir porosity at Appleton Field.

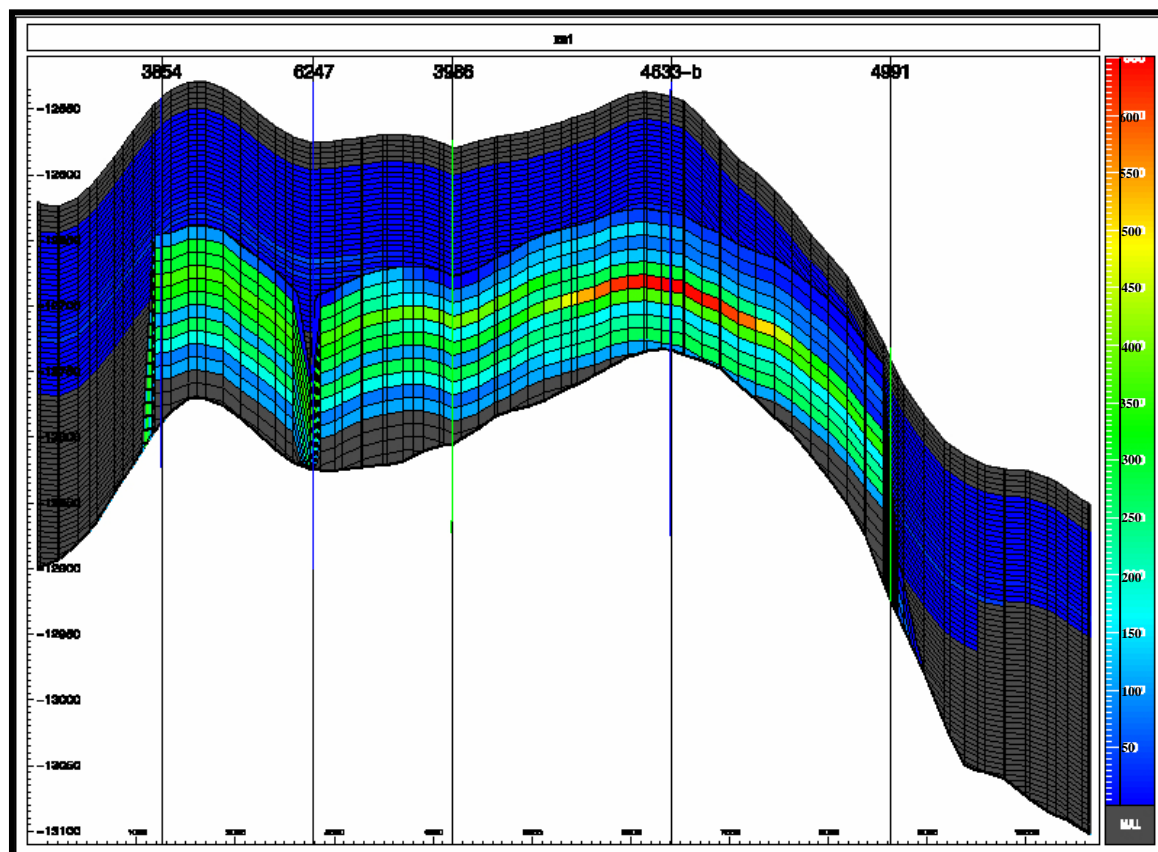
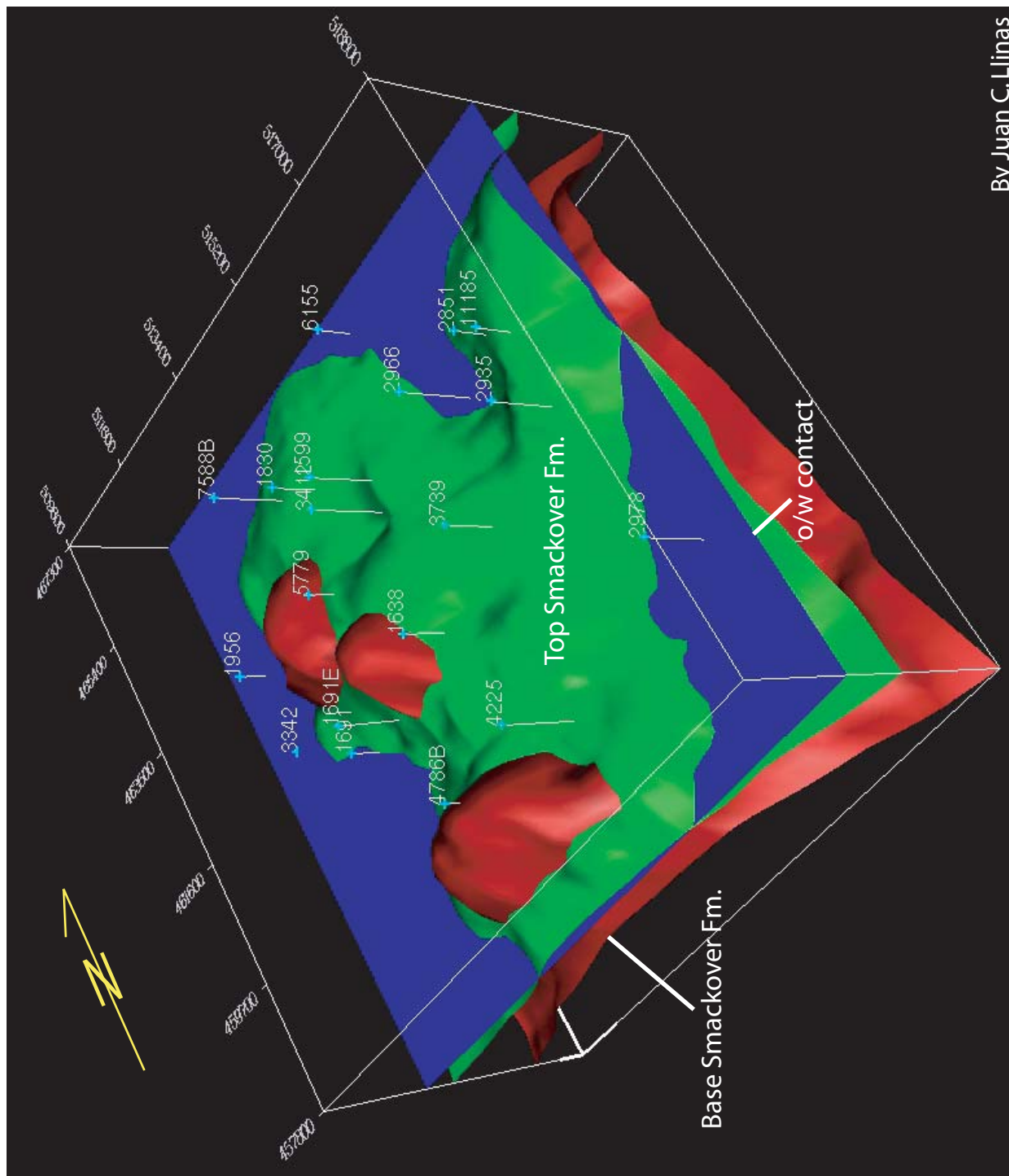


Fig. 176 –Cross section showing permeability at Appleton Field.



By Juan C. Llinas

Figure 177. 3-D model of the Smackover Formation in Vocation Field.

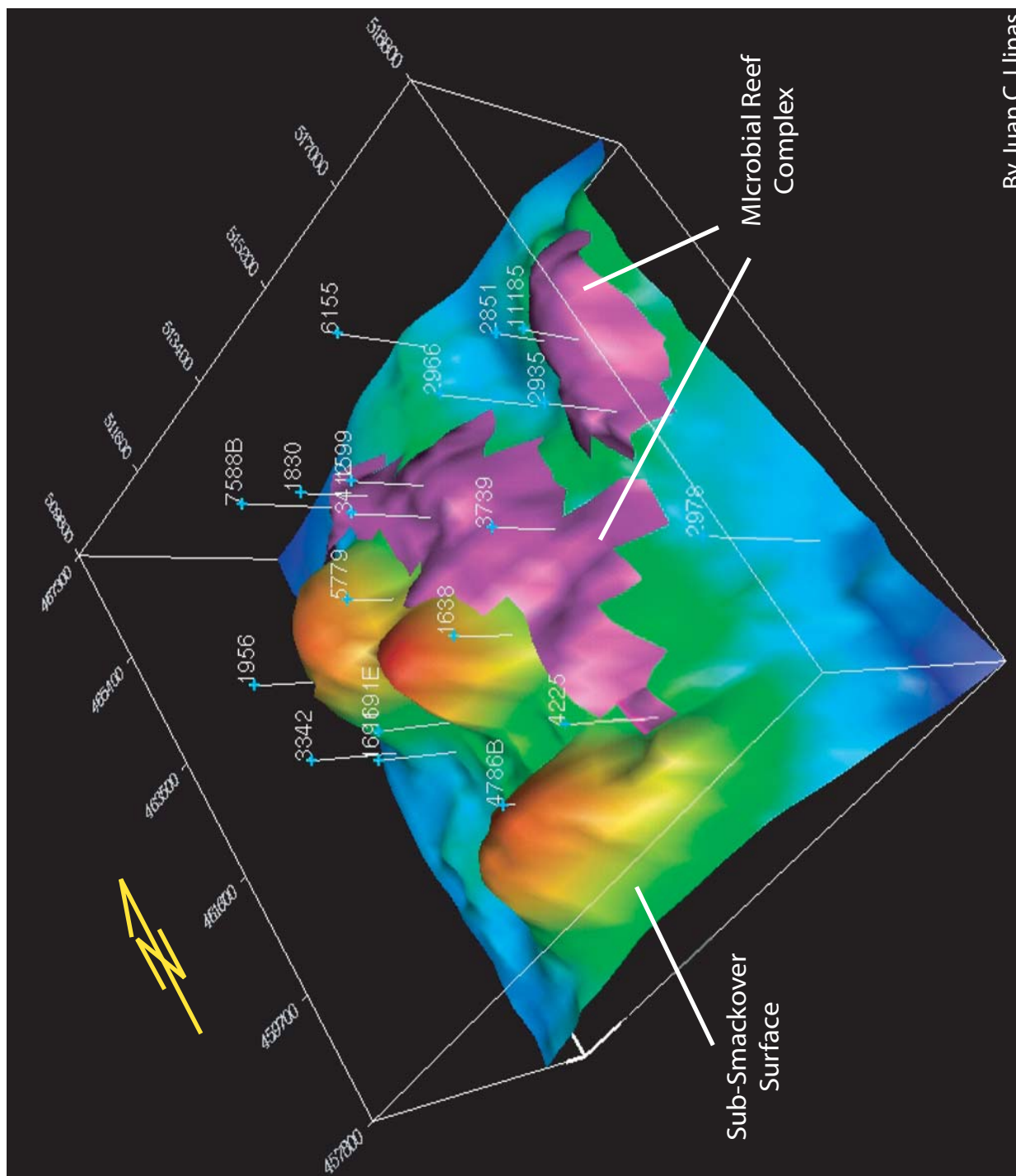


Figure 178. Distribution of microbial reef complex facies in Vocation Field.

By Juan C. Llinas

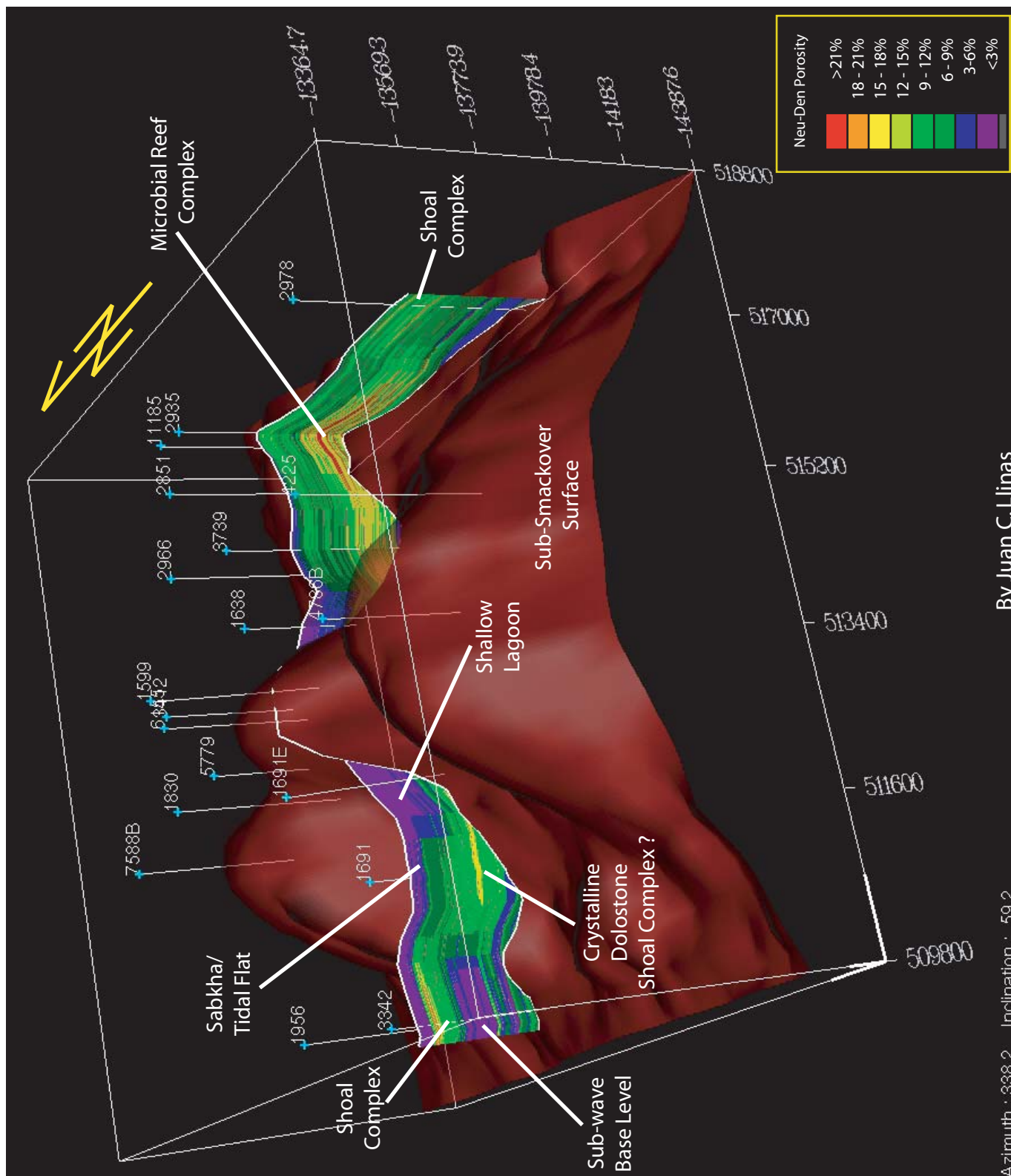


Figure 179. Depositional facies of the Smackover facies.

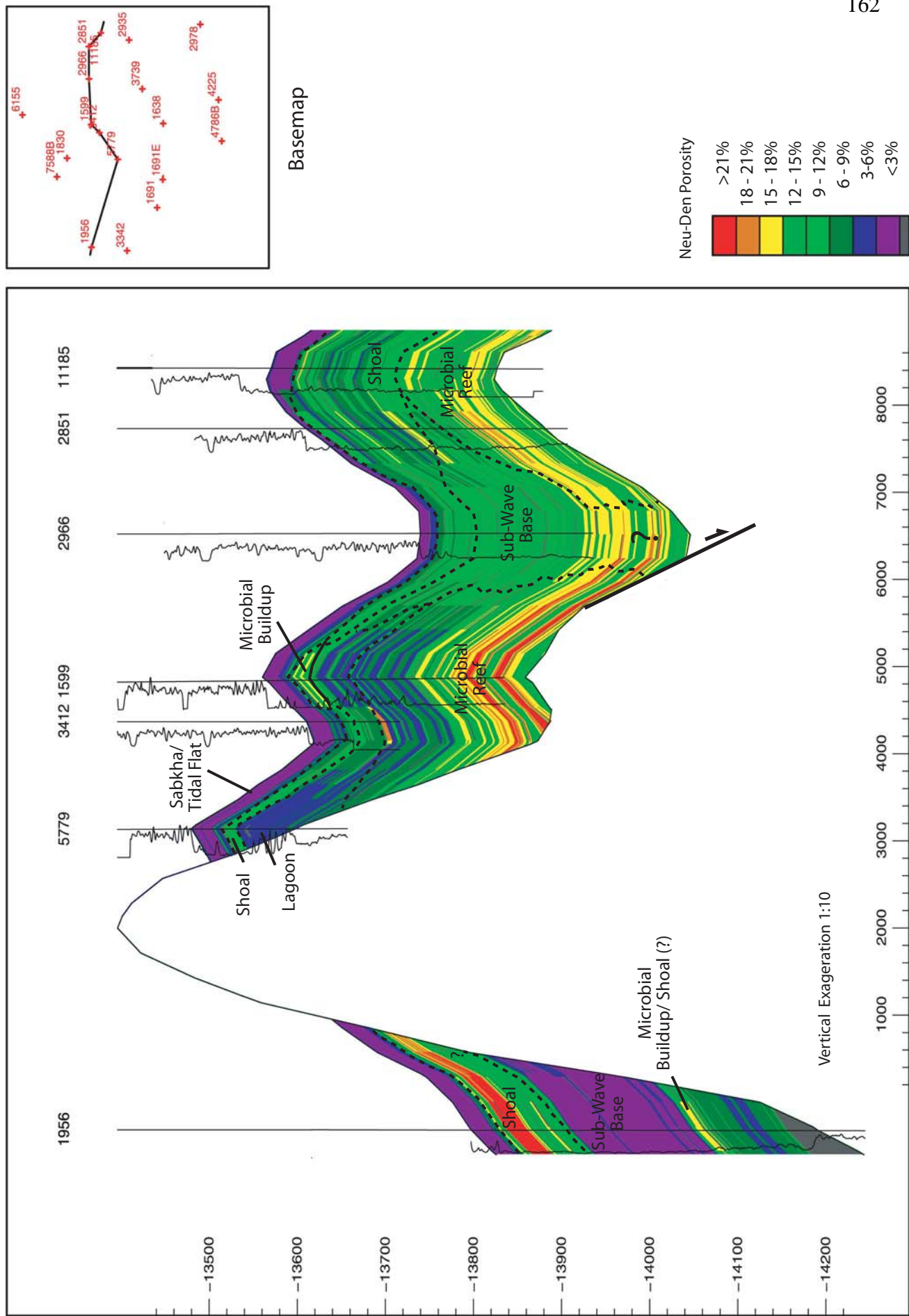


Figure 180. Cross section in Vocation Field.

separately for cases of the Appleton and Vocation Fields to determine if a single simulation model can represent these reef-shoal reservoirs. However, because these reservoirs are associated with basement paleohighs of varying degrees of relief, two simulation models may be required—one for reef-shoal reservoirs associated with low-relief paleohighs (Appleton) and one for reef-shoal reservoirs associated with high-relief paleohighs (Vocation). The purpose of this work is to validate the reservoir model with history-matching, then build forecasts that consider the following scenarios: 1) base case (continue field management as is); 2) optimization of production practices (optimal well completions, including stimulation); 3) active reservoir management (new replacement and development wells); and 4) initiation of new recovery methodologies (targeted infill drilling program and/or possible enhanced oil recovery scenarios). The purposes of reservoir simulation are to forecast expected reservoir performance, to forecast ultimate recovery, and to evaluate different production development scenarios. We will use reservoir simulation to validate the reef-shoal reservoir model, then extend the model to predict performance for a variety of scenarios (as listed above). Our ultimate goals in using reservoir simulation are to establish the viability of a simulation model for a particular reservoir, then make optimal performance predictions. Probably the most important aspect of the simulation work will be the setup phase. The Smackover is well known as a geologically complex system, and our ability to develop a representative numerical model for both the Appleton and Vocation Fields is linked not only to the engineering data, but also to the geological, petrophysical, and geophysical data. We expect to gain considerable understanding regarding carbonate reservoir architecture and heterogeneity, especially with regard to large-scale fluid flow from our reservoir simulation work.

This task requires a setup phase which will be performed in conjunction with the creation and validation of the integrated reservoir description. However, this work has more specific goals than simply building the reservoir simulation model; considerable effort will go into the validation of the petrophysical, fluid (PVT), and rock-fluid properties in order to establish a benchmark case, as well as bounds (uncertainty ranges) on these data. In addition, well performance data will be thoroughly reviewed for accuracy and appropriateness.

The history matching phase in this task will involve refining and adjusting data similar to previous tasks, but in this work our sole focus will be to establish the most representative numerical model for both the Appleton and Vocation Fields. Adjustments will undoubtedly be made to all data types, but as a means to ensure appropriateness, these adjustments will be made in consultation and collaboration with the geoscientists on the technical team. Our goal is to obtain a reasonable match of the model and the field data, and to scale-up the small-scale information (core, logs, etc.) in order to yield a representative reservoir simulation model. We will use a black oil formulation for this work.

3-D reservoir simulations of the reservoirs at Appleton and Vocation Fields have been completed. Fluid data (Figures 181-183 and Tables 17-20), rock properties (Figures 184-185), historical production (Table 21 and Figures 186-187), phase flowrates (Figures 188-189), cumulative production (Figure 190), gas-oil ratio profile (Figure 191), watercut profile (Figure 192), oil production rate history match (Figure 193), water production rate history match (Figure 194), gas production history match (Figure 195) and water production rate history match per well (Figures 196-200) were used in the simulation model for Appleton Field. The results of the simulation for Appleton Field are illustrated in Figures 201-205. Fluid data (Figures 206-207 and



<b>Permit #:</b>	3854			<b>Full Wellstream Recombination</b>	
<b>Well Name:</b>	APPLETON UNIT 2-14 #1			<b>Component</b>	<b>MOL %</b>
<b>Field:</b>	APPLETON-OIL			<b>H2S</b>	1.75
<b>Pool:</b>	SMACKOVER			<b>N2</b>	1.38
<b>County :</b>	ESCAMBIA			<b>CO2</b>	5.7
<b>Date:</b>	25-10-1983			<b>C1</b>	42.01
<b>Pi (PSIA):</b>	6264	<b>Boi (RBBL/STB):</b>	2.4676	<b>C2</b>	10.06
<b>Pb (PSIA):</b>	3416	<b>Bob (Rbbl/STB):</b>	2.755	<b>C3</b>	7.49
<b>T:</b>	245.3	<b>Rsi (SCF/STB):</b>	2479.0	<b>C4i</b>	2.51
<b>API:</b>	48.3	<b>Rsib (SCF/STB):</b>	900.0	<b>C4n</b>	5.06
				<b>C5i</b>	2.37
				<b>C5n</b>	3.05
				<b>C6</b>	3.06
				<b>C7</b>	15.56
<b>Comments:</b>					-----
				<b>Total</b>	100.

Fig. 181 — Fluid Report Well 3854, Appleton Oil Field.<sup>12</sup>

<b>Permit #:</b>	3986			<b>Full Wellstream Recombination</b>	
<b>Well Name:</b>	APL UNIT TR 5:MCMILLAN TRUST 11-1 #2			<b>Component</b>	<b>MOL %</b>
<b>Field:</b>	APPLETON-OIL			<b>H2S</b>	1.6
<b>Pool:</b>	SMACKOVER			<b>N2</b>	4.03
<b>County :</b>	ESCAMBIA			<b>CO2</b>	1.19
<b>Date:</b>	19-03-1984			<b>C1</b>	38.07
<b>Pi (PSIA):</b>	6270	<b>Boi (RBBL/STB):</b>	2.2721	<b>C2</b>	9.86
<b>Pb (PSIA):</b>	3028	<b>Bob (Rbbl/STB):</b>	2.5398	<b>C3</b>	7.83
<b>T:</b>	252.0	<b>Rsi (SCF/STB):</b>	2062.0	<b>C4i</b>	2.64
<b>API:</b>	46.4	<b>Rsib (SCF/STB):</b>	812.0	<b>C4n</b>	5.44
				<b>C5i</b>	2.6
				<b>C5n</b>	3.36
				<b>C6</b>	2.81
				<b>C7</b>	20.57
<b>Comments:</b>					-----
				<b>Total</b>	100.

Fig. 182 — Fluid Report Well 3986, Appleton Oil Field.<sup>12</sup>

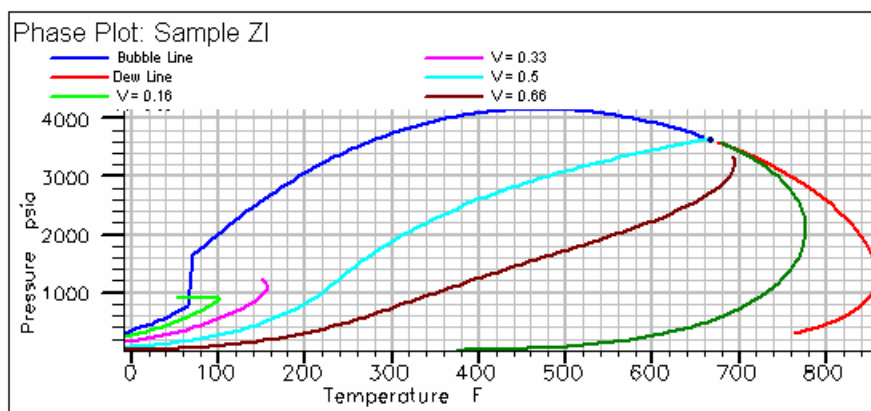


Fig. 183 – Phase Envelope, Appleton Oil Field.

Table 17 — Pseudocomponent Grouping, Appleton Field.

<u>Pseudocomponent</u>	<u>Components</u>
Group 1	H <sub>2</sub> S
Group 2	C <sub>1</sub> + N <sub>2</sub>
Group 3	C <sub>2</sub> + CO <sub>2</sub>
Group 4	C <sub>3</sub> +C <sub>4</sub> +C <sub>5</sub>
Group 5	C <sub>6</sub> + C <sub>7</sub>

Table 18 — Pseudocomponent Properties, Appleton Field.

<u>Component</u>	<u>Molecular Weight (dim-less)</u>	<u>Critical Temperature (deg R)</u>	<u>Critical Pressure, (psia)</u>	<u>Critical z-Factor (dim-less)</u>	<u>Acentric Factor (dim-less)</u>
Group 1	34.07	672.48	1296.18	0.2820	0.0642
Group 2	16.42	339.39	662.20	0.2847	0.0089
Group 3	35.11	549.29	839.63	0.2931	0.0927
Group 4	56.71	744.35	555.77	0.2790	0.1232
Group 5	179.62	1216.73	289.19	0.2524	0.3783

Table 19 — Pseudocomponent Properties, Appleton Field (continued).

<u>Component t</u>	<u><math>\Omega_a</math> (dim-less)</u>	<u><math>\Omega_b</math> (dim-less)</u>	<u><math>V_s</math> (dim-less)</u>
Group 1	0.4898	0.0749	-0.000642
Group 2	1.0288	0.1109	-0.000887
Group 3	0.9591	0.1235	-0.000501
Group 4	0.6951	0.0965	-0.000362
Group 5	0.6951	0.0717	0.000663

Table 20 — Binary Interaction Coefficients, Appleton Field.

	<u>Group 1</u>	<u>Group 2</u>	<u>Group 3</u>	<u>Group 4</u>	<u>Group 5</u>
Group 1	0.0	-	-	-	-
Group 2	0.0540	0.0	-	-	-
Group 3	0.0622	0.0369	0.0	-	-
Group 4	0.0684	0.0011	0.0332	0.0	-
Group 5	0.0684	0.016	0.0044	0.0062	0.0

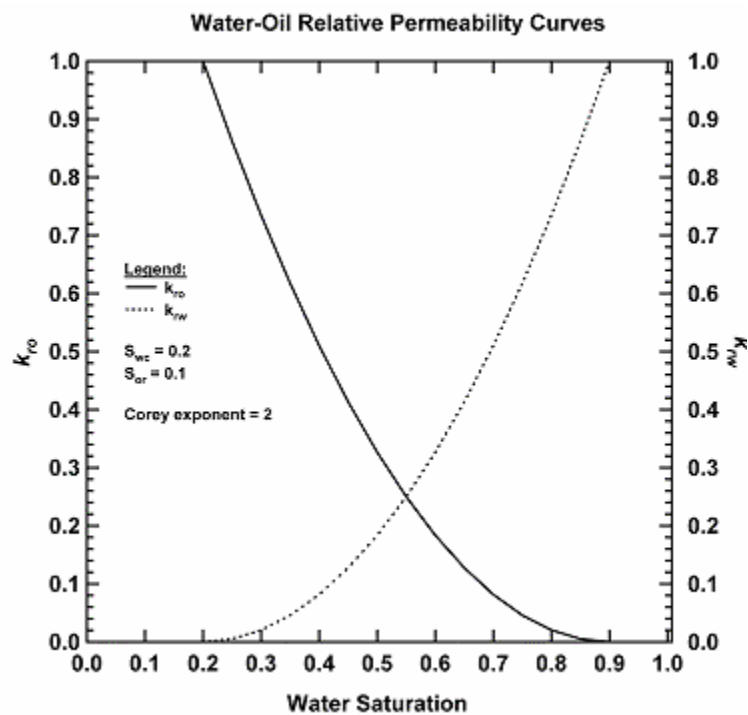


Fig. 184 — Oil-Water Relative Permeability Curves used in the Simulation Study.

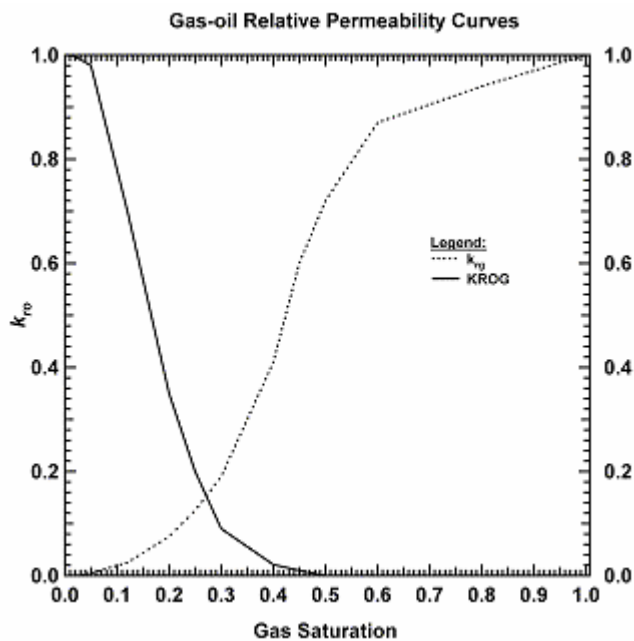


Fig. 185 – Gas-Oil Relative Permeability Curves used in the Simulation Study.

Table 21 – Reported Cumulative Production per Well, Appleton Oil Field.

Well	Oil Production (MSTB)	Water Production (MSTB)	Gas Production (MMSCF)
3854	405	1,246	850
3986	158	141	309
3986B	41	32	86
4633B	1,149	1,618	1,781
4835B	778	738	1,468
6247B	184	334	280

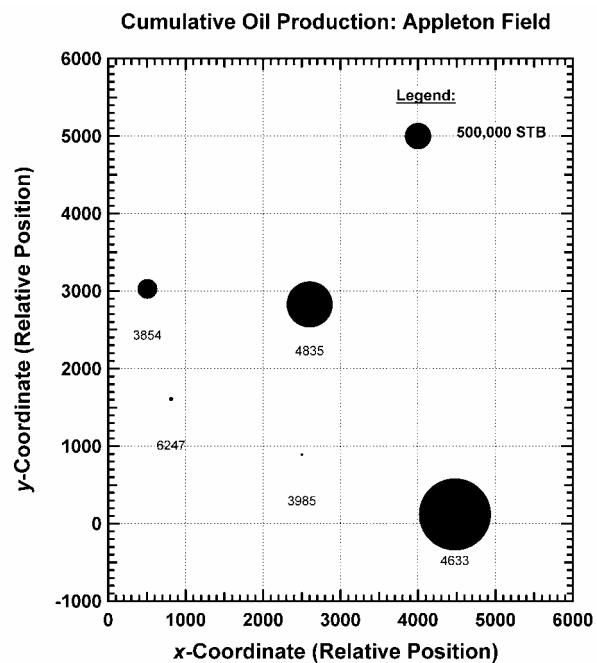


Fig. 186 — Oil Production as a Function of Well Location, Appleton Field.

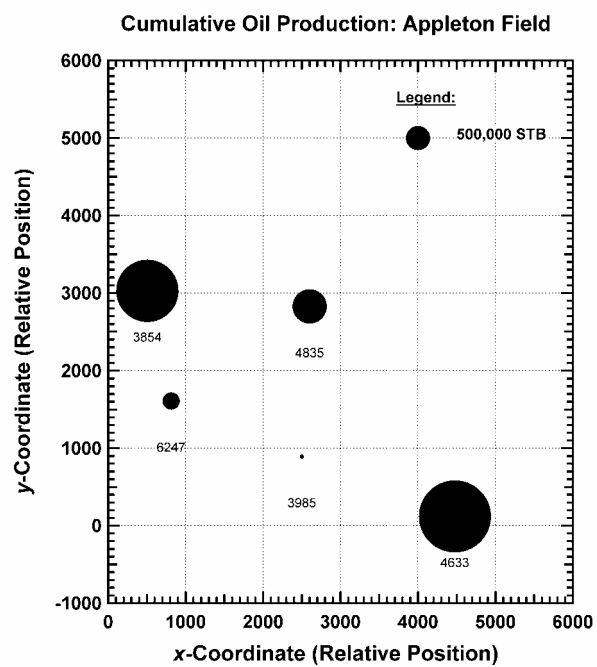


Fig. 187 — Water Production as a Function of Well Location, Appleton Field.

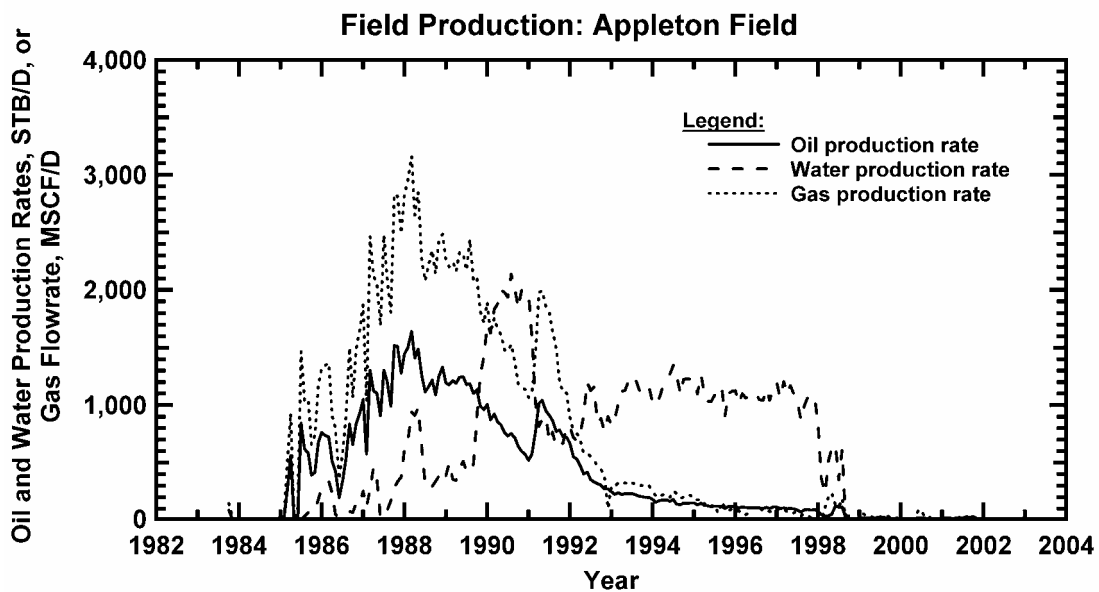


Fig. 188 — Individual Phase Flowrates, Appleton Field (Cartesian Format).

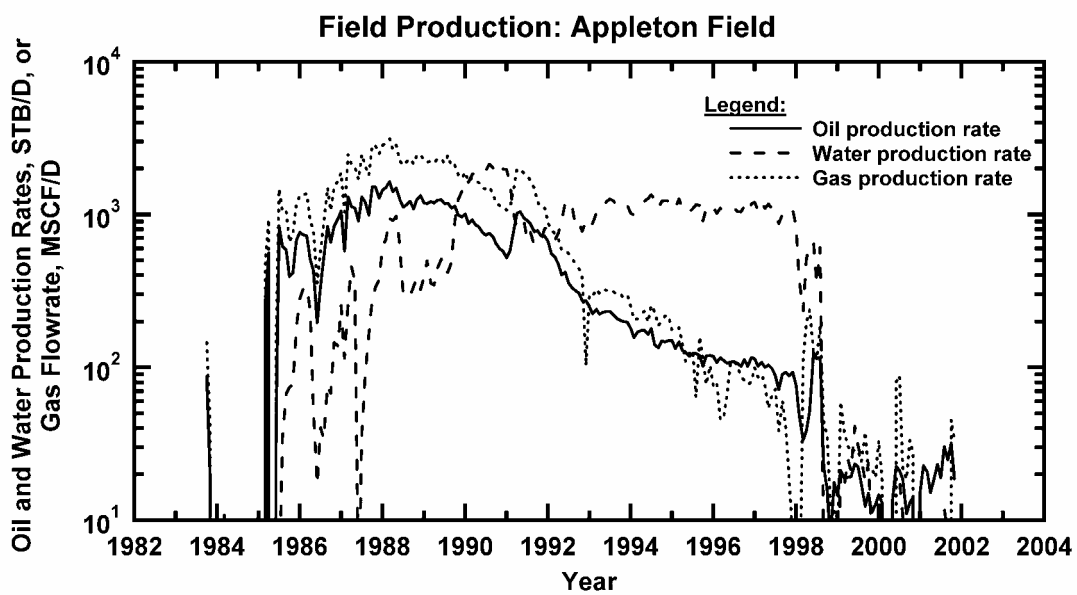


Fig. 189 — Individual Phase Flowrates, Appleton Field (Semilog Format).

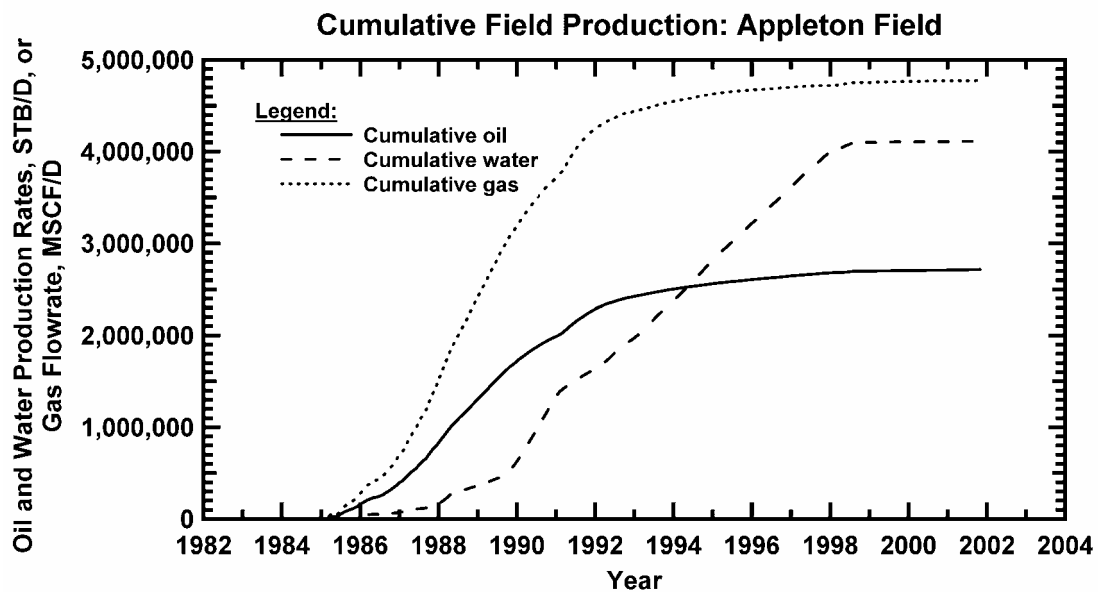


Fig. 190 — Cumulative Production Profiles, Appleton Field.

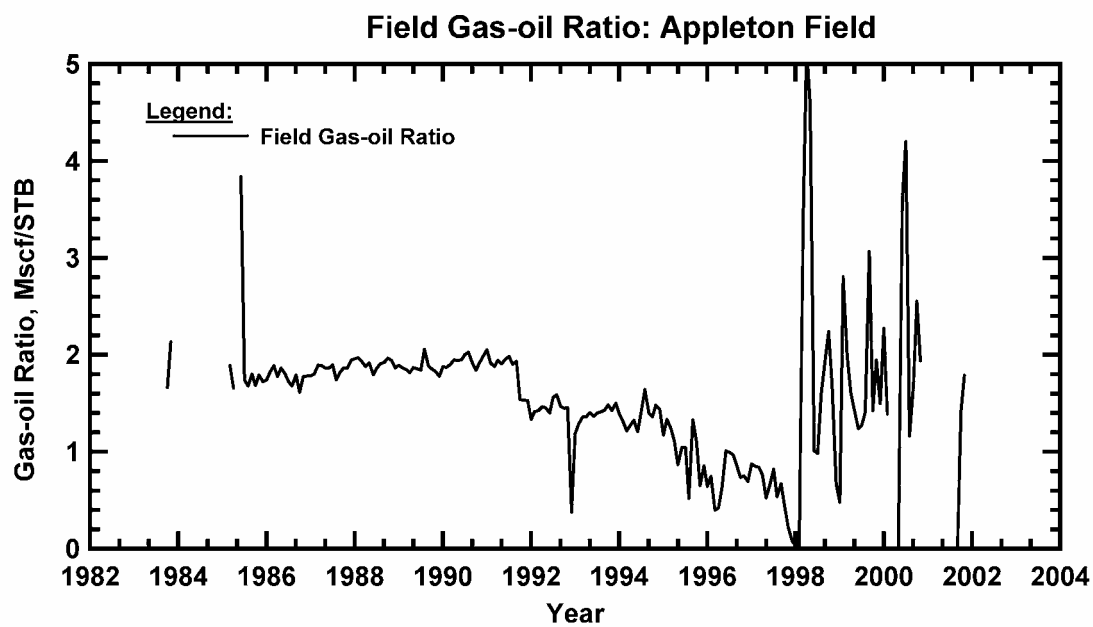


Fig. 191 — Gas-Oil Ratio Profile, Appleton Field.

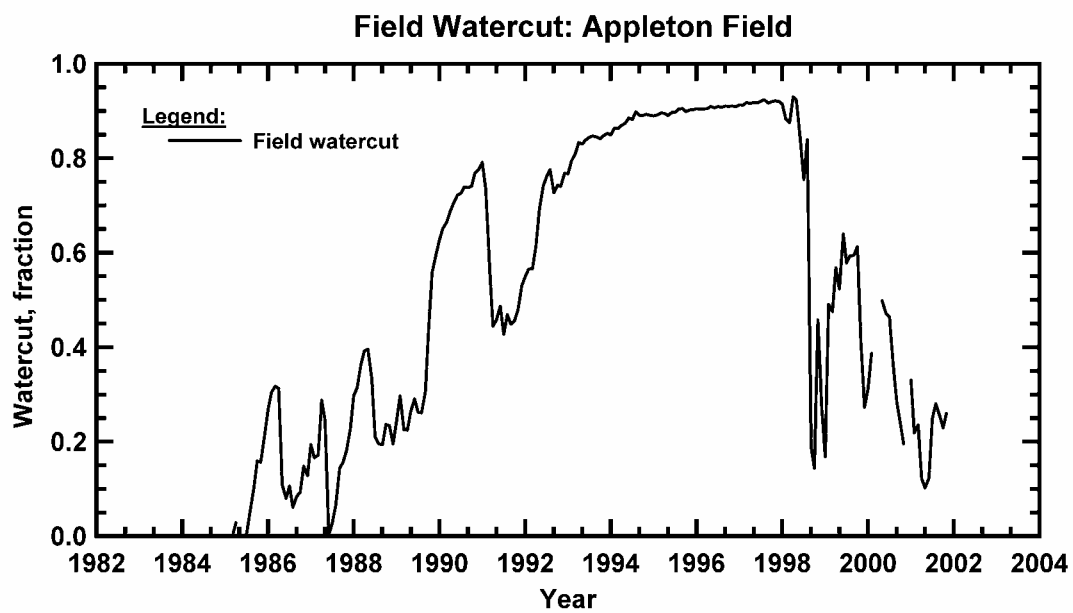


Fig. 192 — Watercut Profile, Appleton Field.



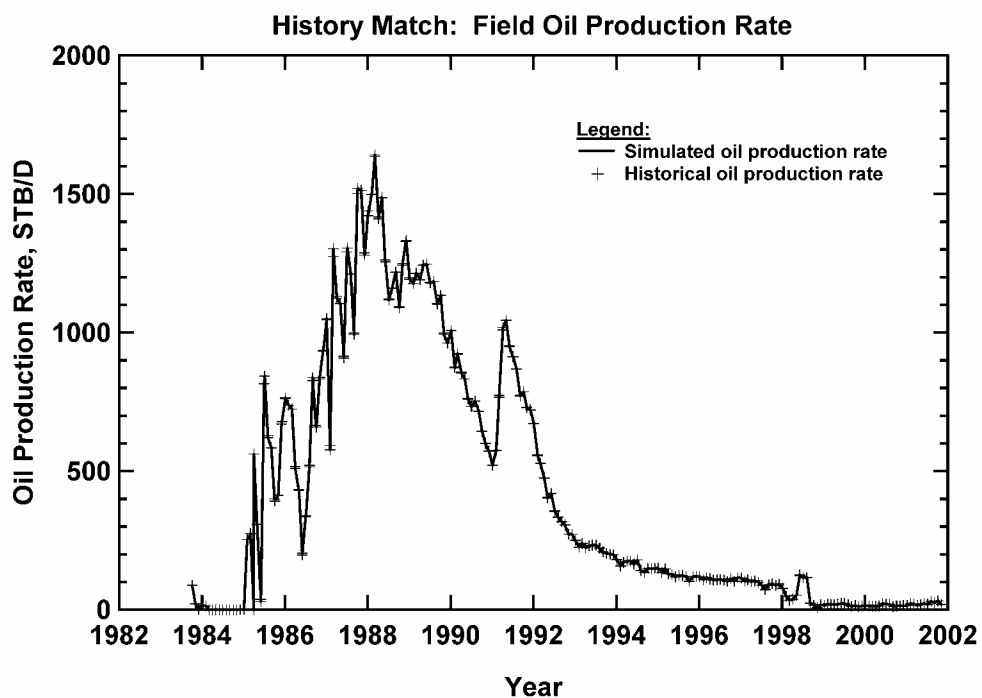


Fig. 193 — Oil Production Rate History Match, Appleton Field.

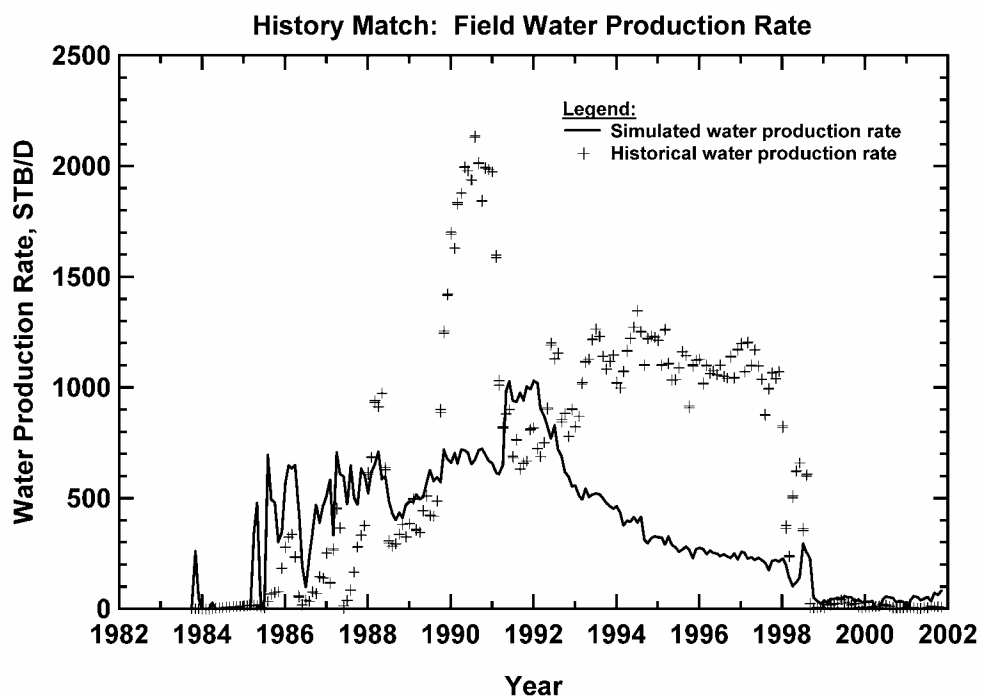


Fig. 194 — Water Production Rate History Match, Appleton Field

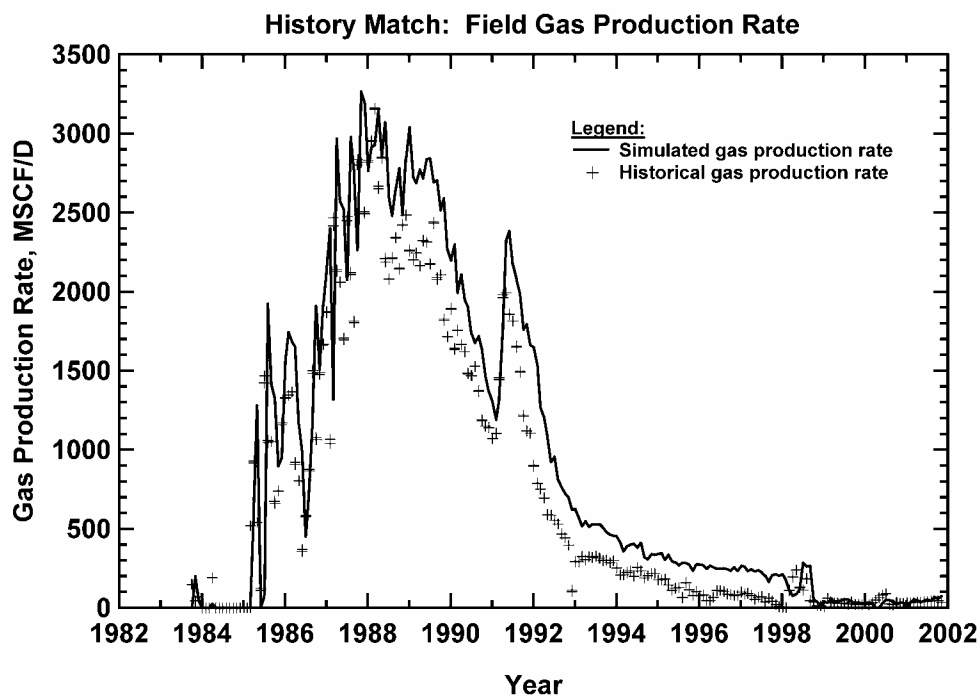


Fig. 195 — Gas Production Rate History Match, Appleton Field.

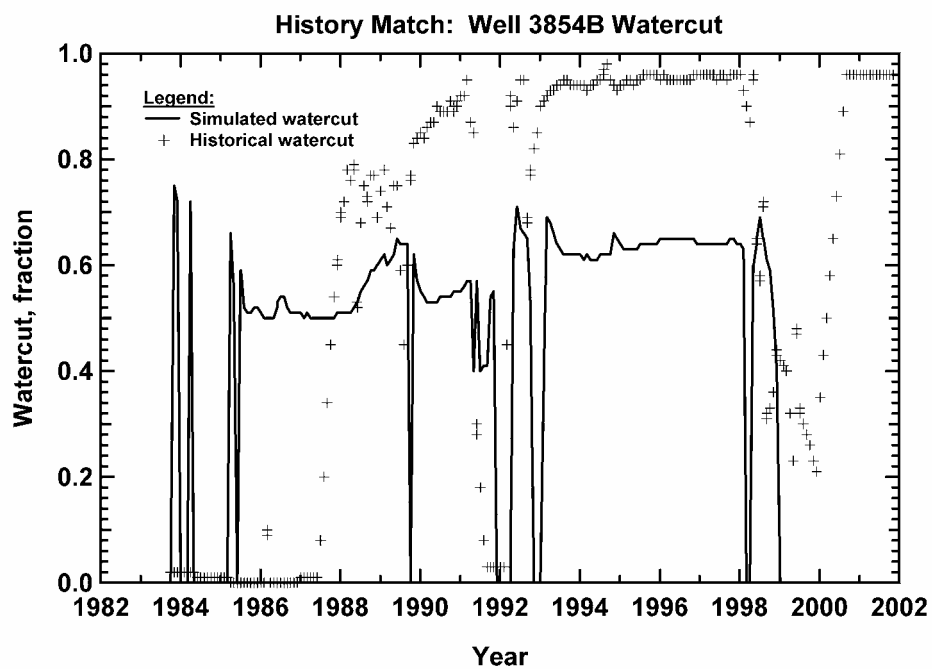


Fig. 196 — Water Production History Match, Appleton Well 3854B.

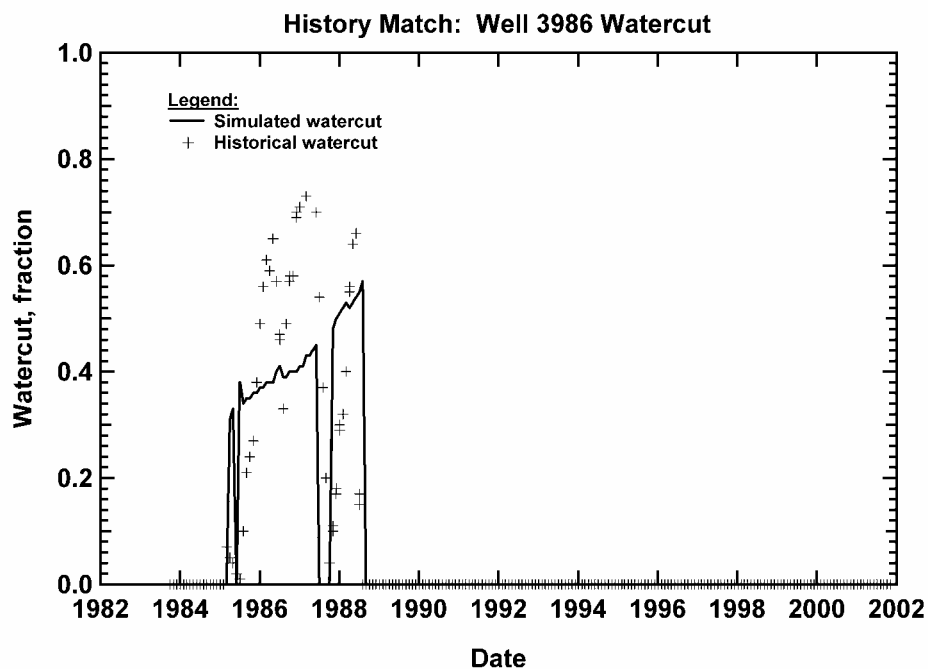


Fig. 197 — Water Production History Match, Appleton Well 3986.

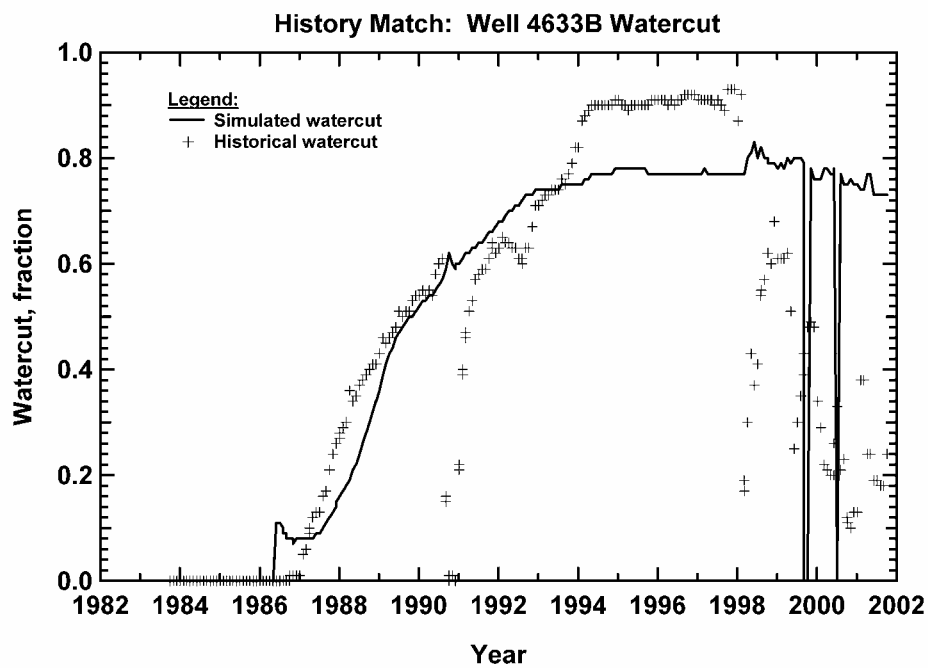


Fig. 198 — Water Production History Match, Appleton Well 4633B.

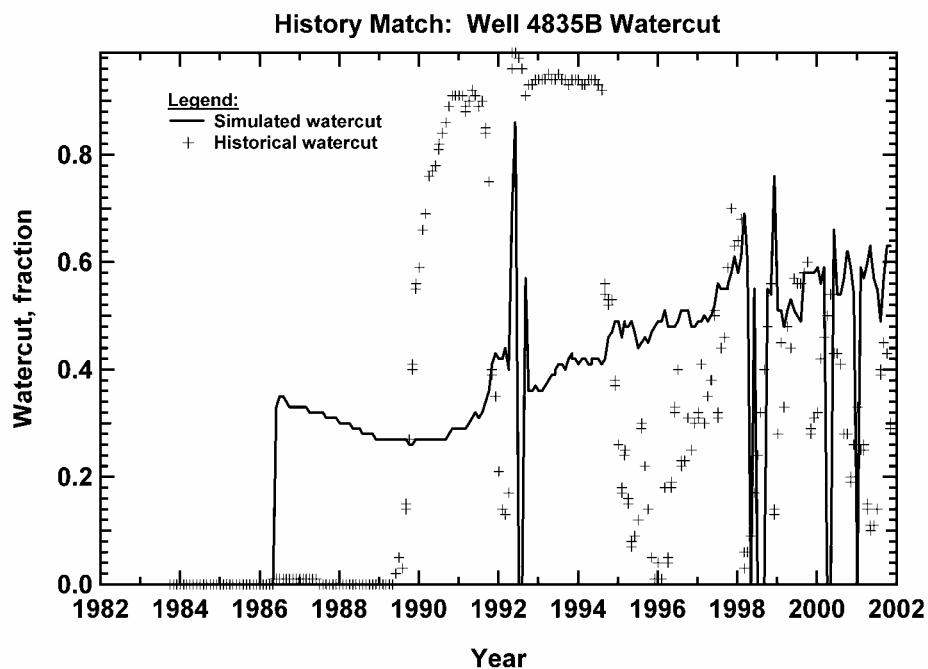


Fig. 199 — Water Production History Match, Appleton Well 4835B.

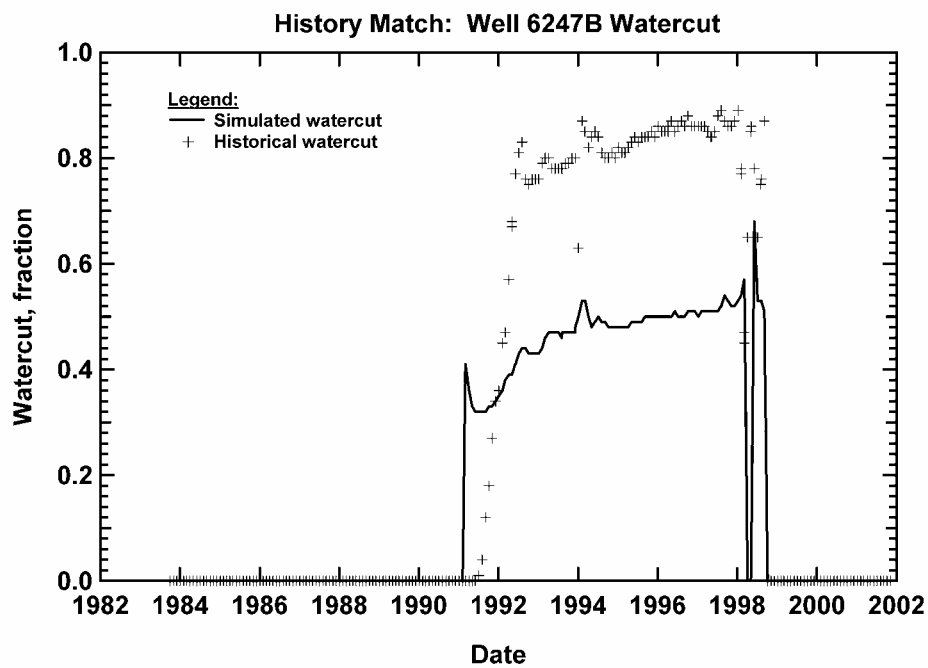


Fig. 200 — Water Production History Match, Appleton Well 6247B.

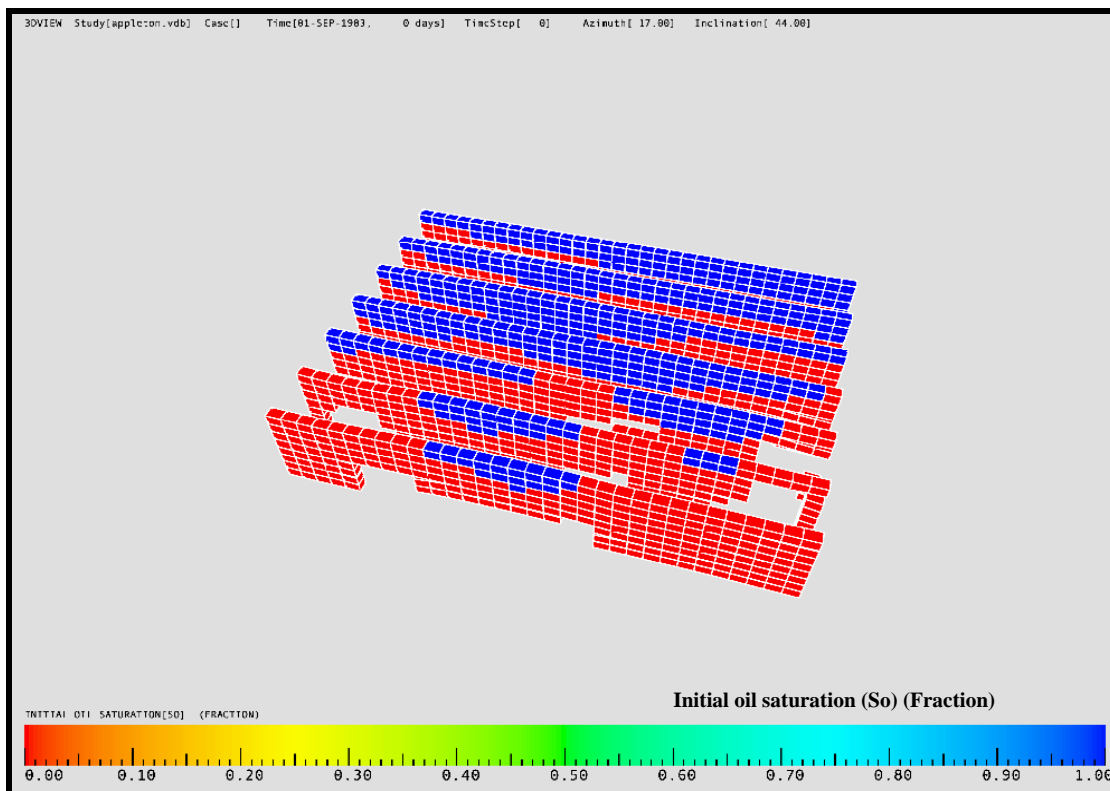


Fig. 201 - Initial Oil Saturation Profile as Loaded into VIP-CORE<sup>®</sup>

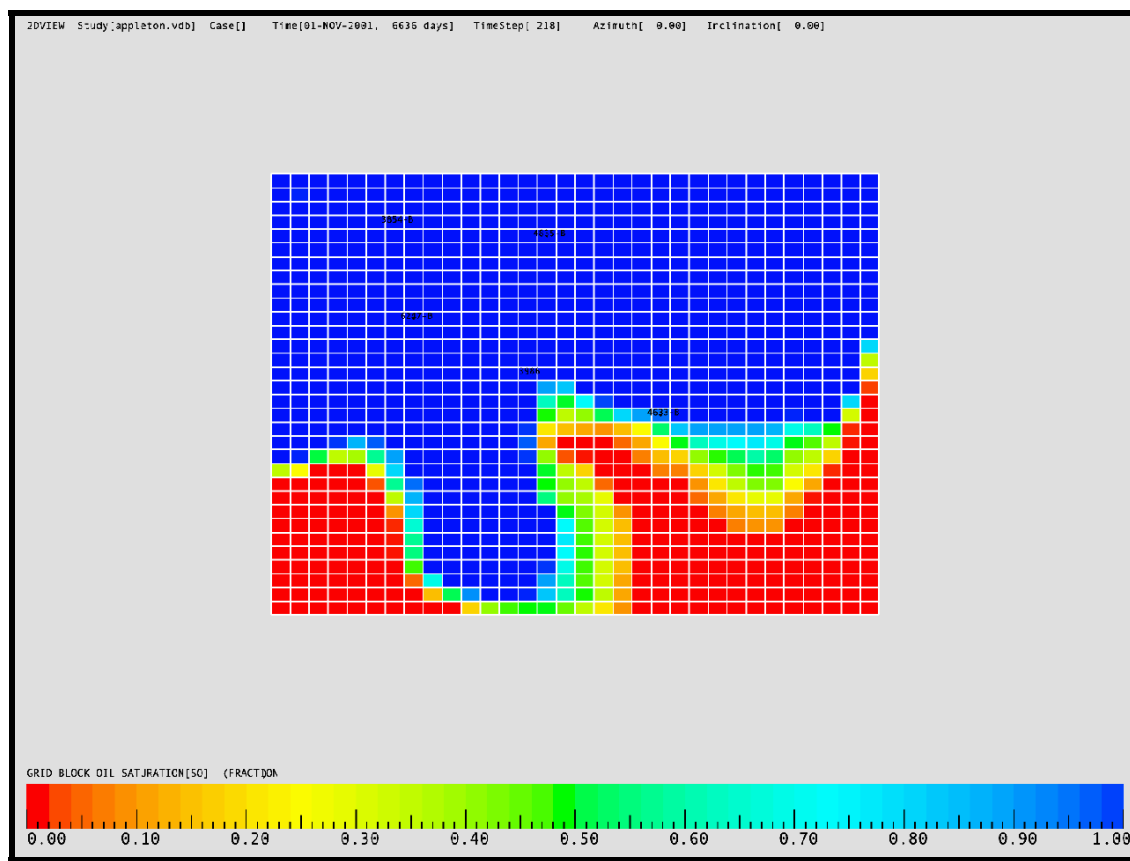


Fig. 202 – Simulated Unswept Area in the Appleton Oil Field Simulation Layer 1

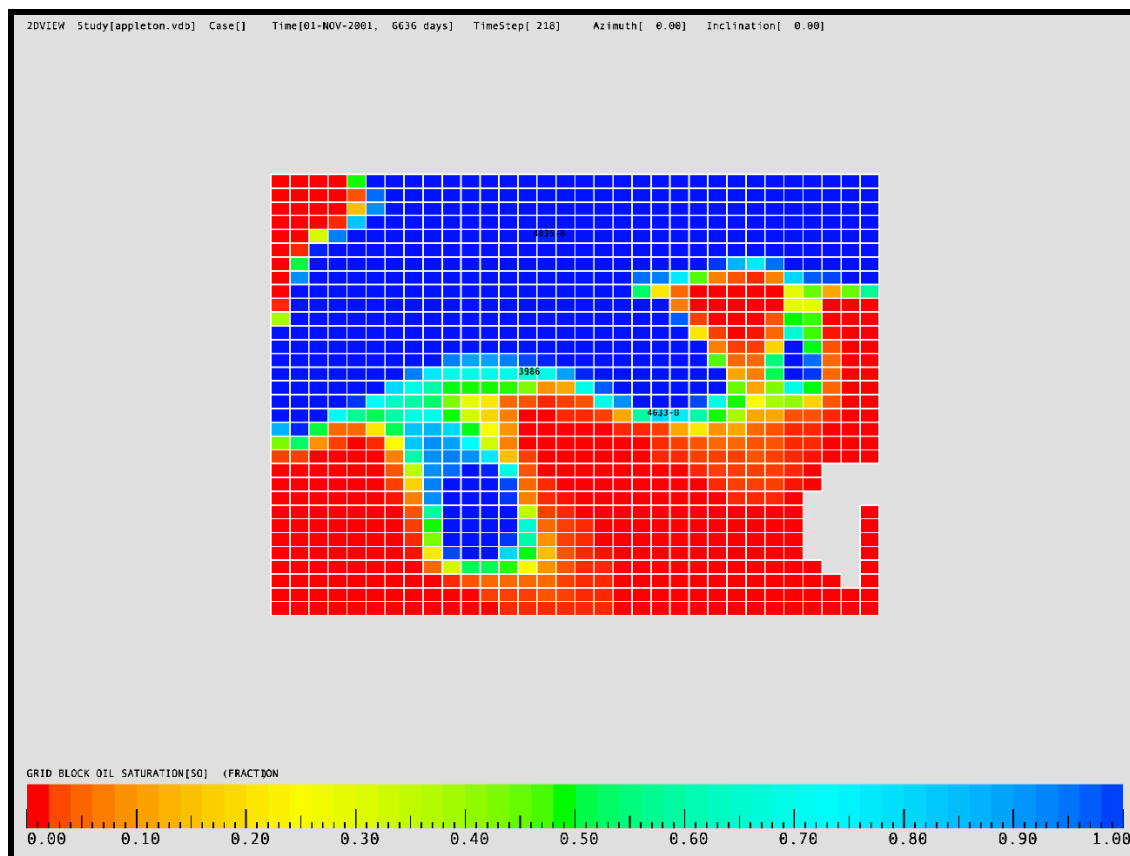


Fig. 203 – Simulated Unswept Area in the Appleton Oil Field Simulation Layer 2

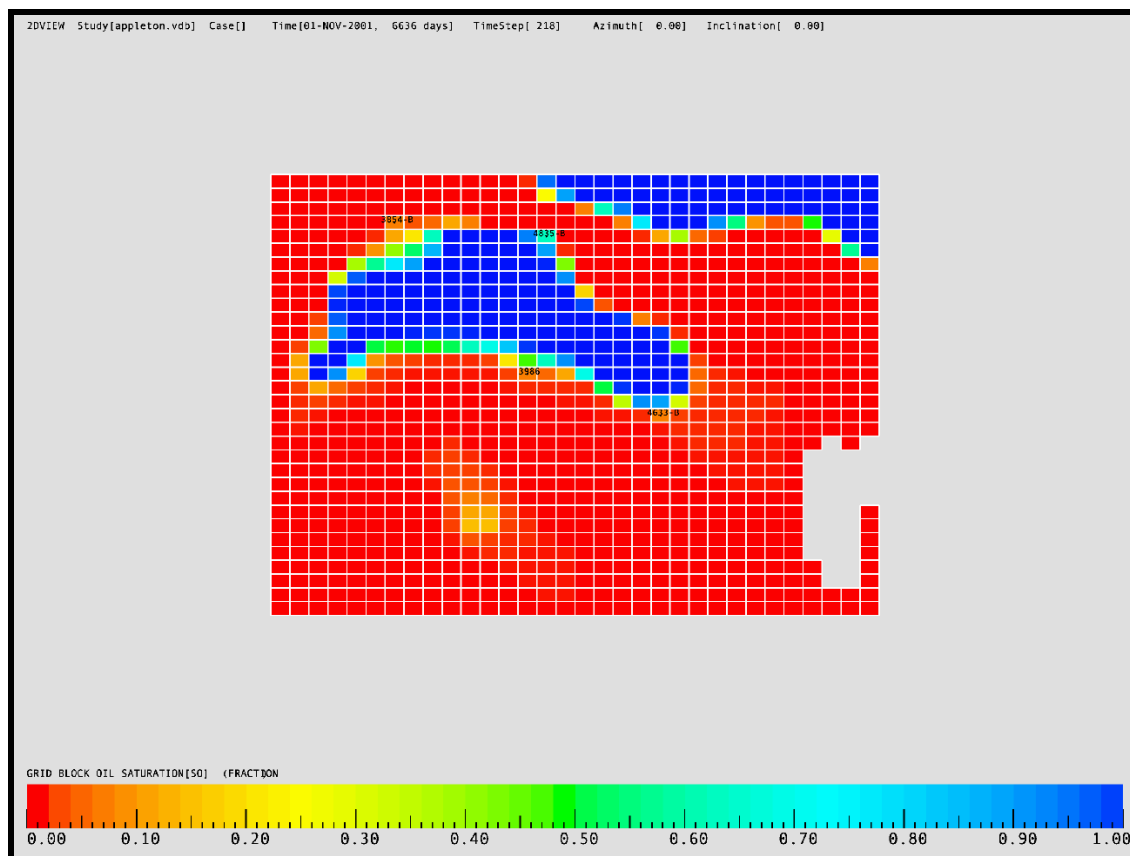


Fig. 204 – Simulated Unswept Area in the Appleton Oil Field Simulation Layer 3



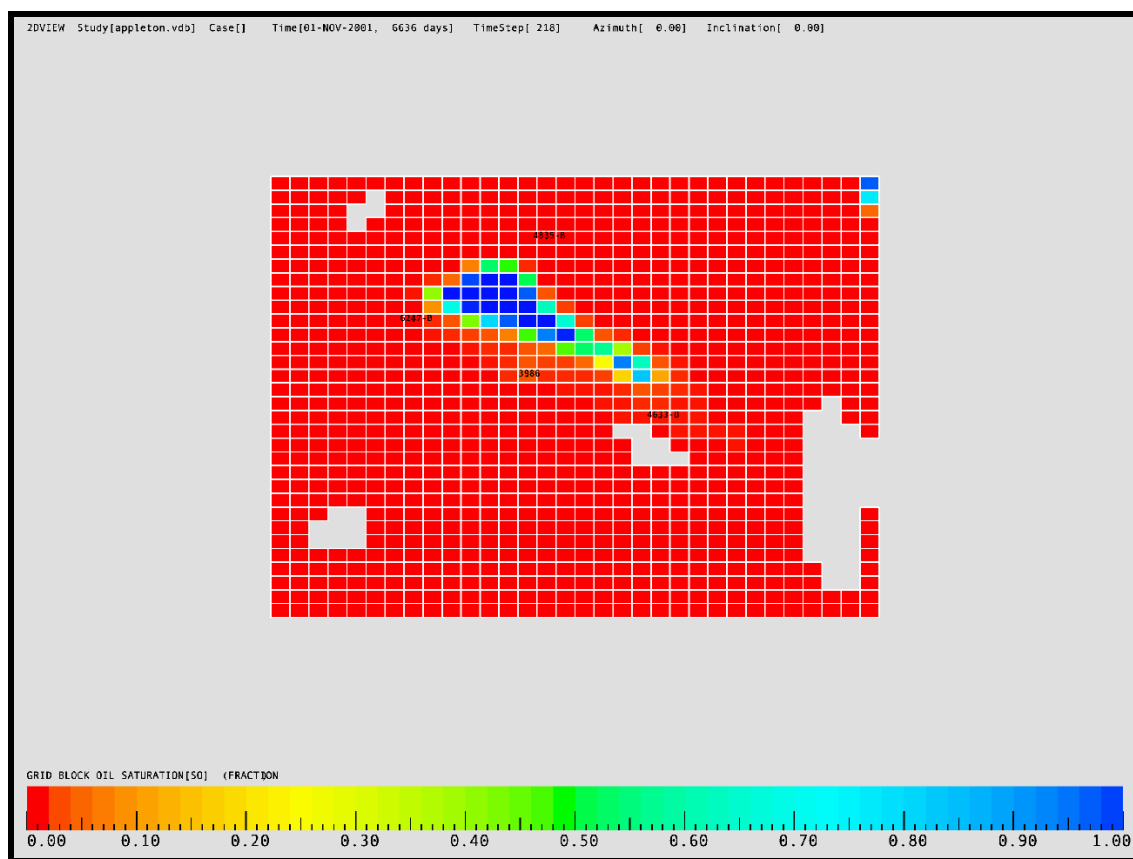


Fig. 205 – Simulated Unswept Area in the Appleton Oil Field Simulation Layer 4

<b>Permit #:</b>	1599-SWD-77-151-7			<b>Full Wellstream Recombination</b>	
<b>Well Name:</b>	B.C. QUIMBY 27-15 SWD #1			<b>Component</b>	<b>MOL %</b>
<b>Field:</b>	VOCATION-OIL			H2S	0.0
<b>Pool:</b>				N2	7.11
<b>County :</b>	MONROE			CO2	0.63
<b>Date:</b>	11-05-1971			C1	45.99
<b>Pi (PSIA):</b>	6837	<b>Boi (RBBL/STB):</b>	2.1868	C2	6.73
<b>Pb (PSIA):</b>	3475	<b>Bob (Rbbl/STB):</b>	2.529	C3	6.28
<b>T:</b>	245.0	<b>Rsi (SCF/STB):</b>	0.0	C4i	2.21
<b>API:</b>	55.3	<b>Rsib (SCF/STB):</b>	0.0	C4n	4.87
				C5i	1.93
				C5n	2.95
				C6	4.51
				C7	16.79
<b>Comments:</b>				<b>Total</b>	100.

Fig. 206 — Fluid Report Well 1599, Vocation Oil Field.<sup>13</sup>

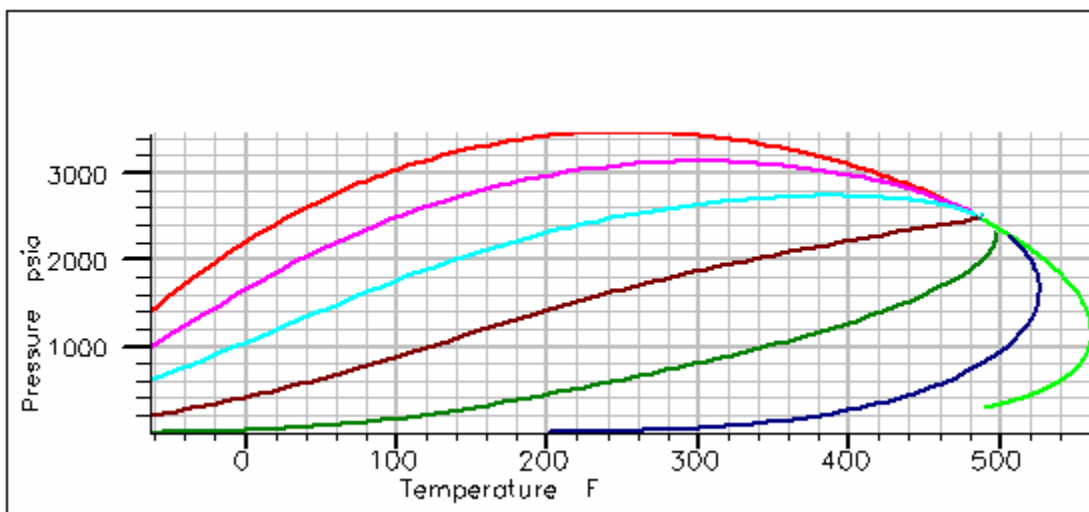


Fig. 207 – Phase Envelope, Vocation Field.

Tables 22-25), rock properties (Figures 208-209), historical production (Table 26 and Figures 210-211), phase flowrates (Figures 212-213), cumulative production (Figure 214), gas-oil ratio profile (Figure 215), watercut profile (Figure 216), oil production rate history match (Figure 217), water production rate history match (Figure 218), gas production rate history match (Figure 219) and water production history match per well (Figures 220-229) were used in the simulation for Vocation Field. The results of the simulation for the field are illustrated in Figures 230-232. The 3-D geologic model served as the framework for these simulations. The acquisition of additional pressure data would improve the simulation models.

### **Work Planned for Year 3**

**Task 7—Geologic-Engineering Model.** This task (Table 27) builds an integrated geologic and engineering model(s) for reef and shoal reservoirs associated with petroleum traps in Smackover fields represented by varying degrees of relief on pre-Mesozoic basement paleohighs. The Appleton case study (low-relief) and the Vocation case study (high-relief) are the basis for the model(s). The geologic model(s) is constructed utilizing the geological and geophysical characterization data for the reef-shoal reservoir and structure at Appleton and Vocation Fields. While these data will serve as the basis for the geologic-engineering model(s), many types and scales of engineering data will be incorporated into the model(s) as well. In Task 6, the geologic model(s) for these fields was used as the underlying framework for flow simulation of the Appleton and Vocation reservoirs. In this task, the reservoir simulation model(s) from these fields is used to refine and adjust the geologic model(s) for Appleton and Vocation Fields by integrating the results from the reservoir simulation modeling into the geologic model(s). Geologic and geophysical data are critical for building our representative geologic model(s) which will characterize, model and predict reservoir architecture, heterogeneity and quality.

Table 22 — Pseudocomponent Grouping, Vocation Field.

<u>Pseudocomponent</u>	<u>Components</u>
Group 1	C <sub>1</sub> + N <sub>2</sub>
Group 2	C <sub>2</sub> + CO <sub>2</sub>
Group 3	C <sub>3</sub>
Group 4	C <sub>4</sub> + C <sub>5</sub>
Group 5	C <sub>6</sub> + C <sub>7</sub>

Table 23 — Pseudocomponent Properties, Vocation Field.

<u>Component</u>	<u>Molecular Weight (dim-less)</u>	<u>Critical Temperature (deg R)</u>	<u>Critical Pressure, (psia)</u>	<u>Critical z-Factor (dim-less)</u>	<u>Acentric Factor (dim-less)</u>
Group 1	17.64	327.89	644.28	0.2845	0.0166
Group 2	31.26	549.99	739.41	0.2878	0.1094
Group 3	44.10	665.97	615.75	0.2762	0.1524
Group 4	63.85	789.93	521.87	0.2751	0.2145
Group 5	160.13	1169.96	293.41	0.2629	0.4918

Table 24 — Pseudocomponent Properties, Vocation Field (continued).

<u>Component</u>	<u><math>\Omega_a</math> (dim-less)</u>	<u><math>\Omega_b</math> (dim-less)</u>	<u><math>V_s</math> (dim-less)</u>
Group 1	0.6951	0.0717	-0.1425
Group 2	0.4898	0.0749	-0.0981
Group 3	1.0288	0.1109	-0.0775
Group 4	0.9591	0.1235	-0.0477
Group 5	0.6951	0.0965	0.2561

Table 25 — Binary Interaction Coefficients, Vocation Oil Field.

	<u>Group 1</u>	<u>Group 2</u>	<u>Group 3</u>	<u>Group 4</u>	<u>Group 5</u>
Group 1	0.0	-	-	-	-
Group 2	0.019519	0.0	-	-	-
Group 3	0.013889	0.008559	0.0	-	-
Group 4	0.013889	0.008559	0.0	0.0	-
Group 5	0.049655	0.017704	0.013889	0.0	0.0

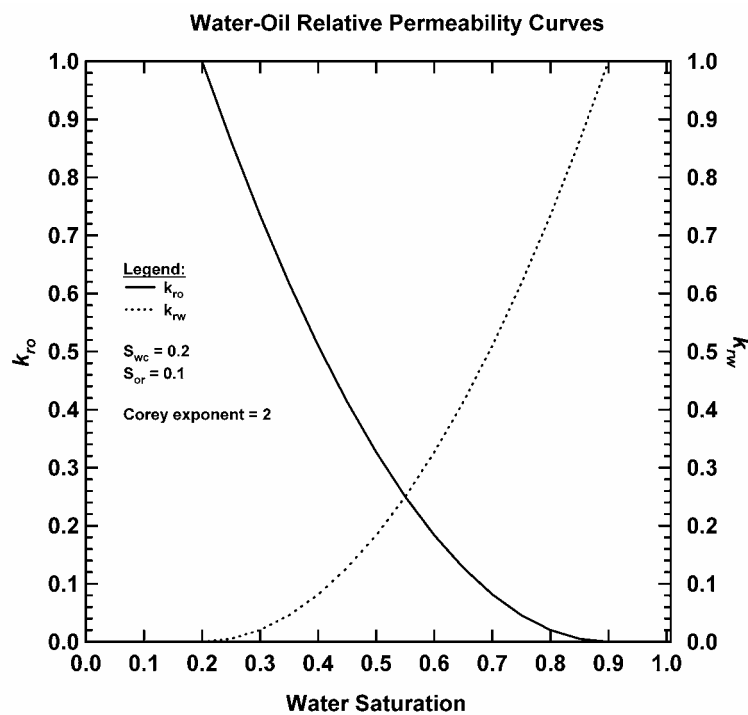


Fig. 208 — Oil-Water Relative Permeability Curves used in the Simulation Study.

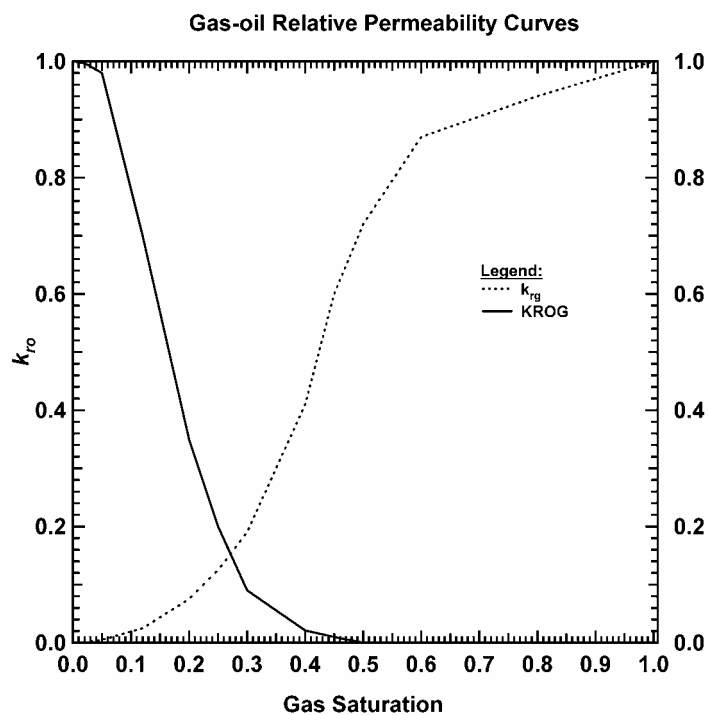


Fig. 209 – Gas-Oil Relative Permeability Curves used in the Simulation Study.

Table 26 – Reported Cumulative Production per Well, Vocation Oil Field.

Well	Oil Production (MSTB)	Water Production (MSTB)	Gas Production (MMSCF)
1599	168	0	532
1830	733	332	1750
2851	388	1810	530
2935	165	817	284
3412	36	84	60
3739	529	163	1286
4225A	47	28	79
4225B	29	50	71
5779	102	50	226
11185	120	0.6	194

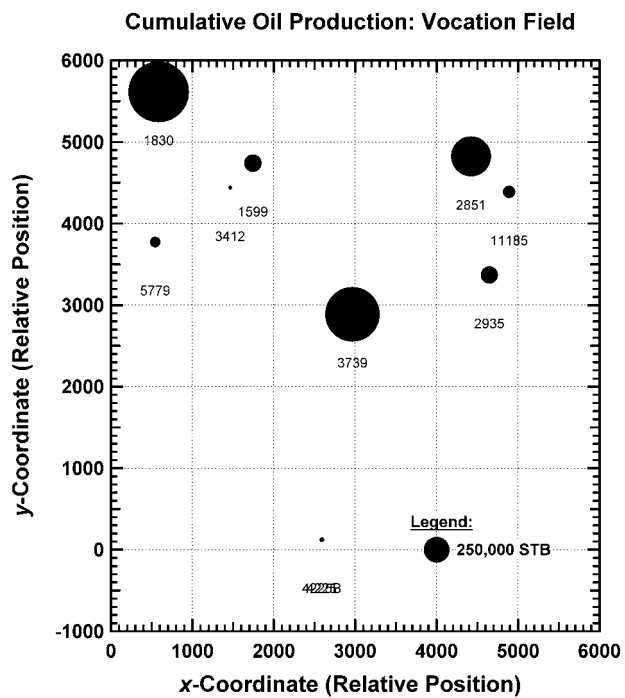


Fig. 210 — Oil Production as a Function of Well Location, Vocation Field.

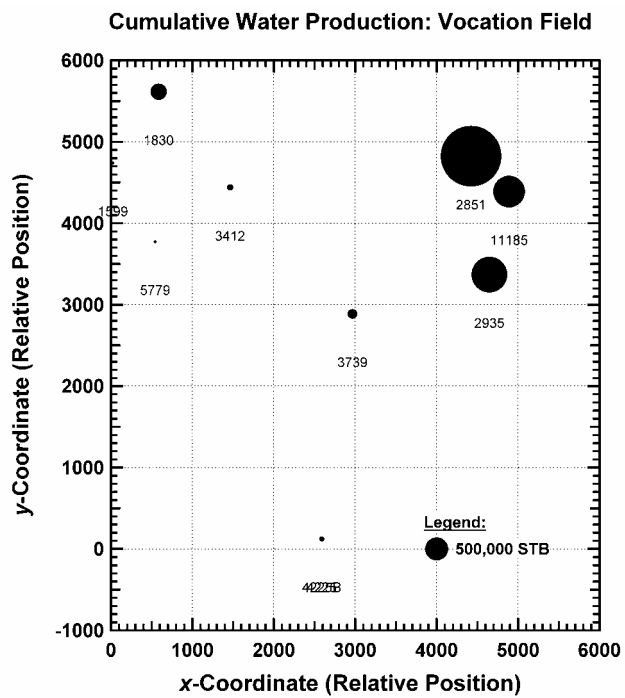


Fig. 211 — Water Production as a Function of Well Location, Vocation Field.

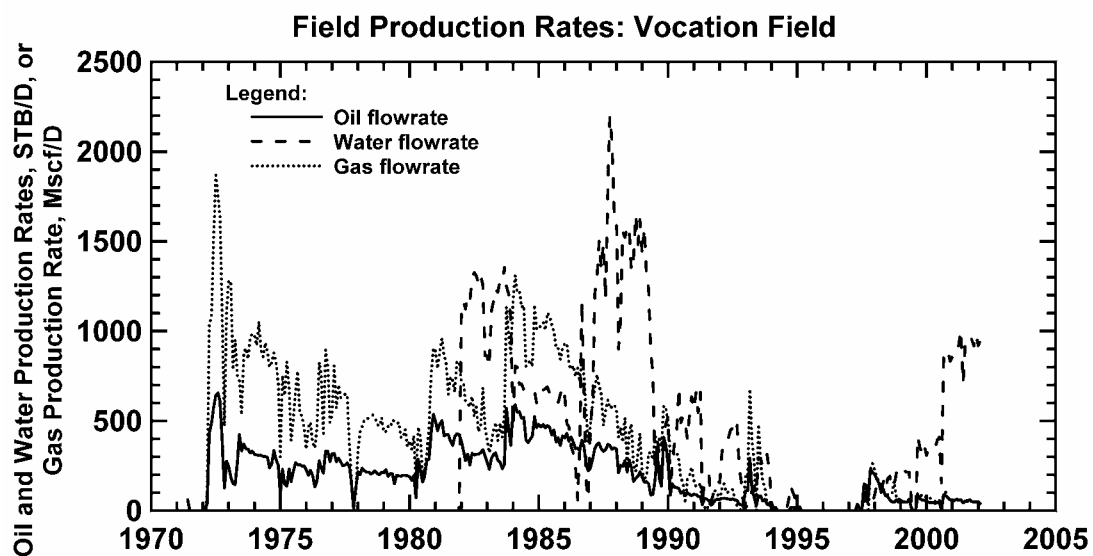


Fig. 212 — Individual Phase Flowrates, Vocation Field (Cartesian Format).

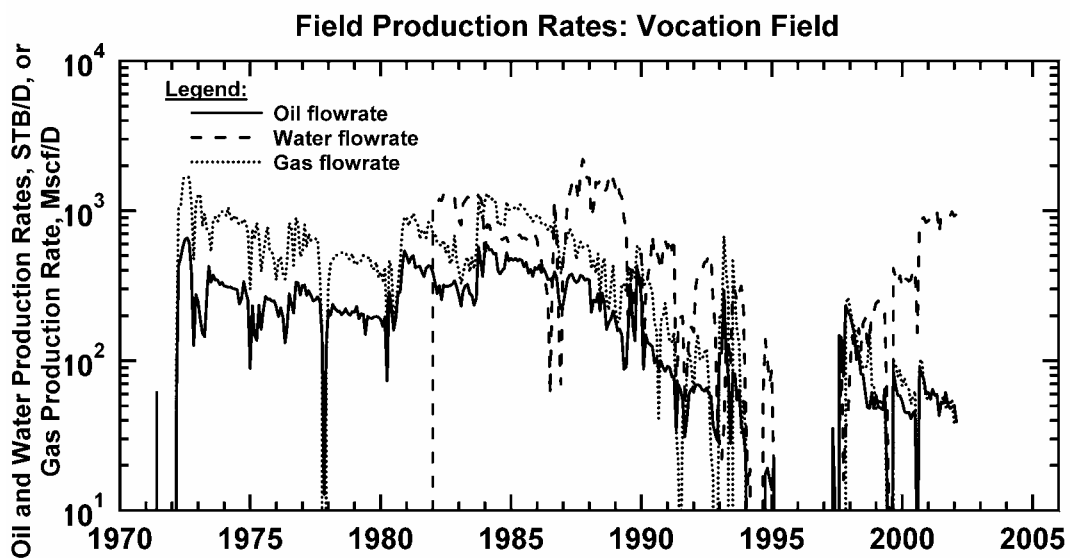


Fig. 213 — Individual Phase Flowrates, Vocation Field (Semilog Format).



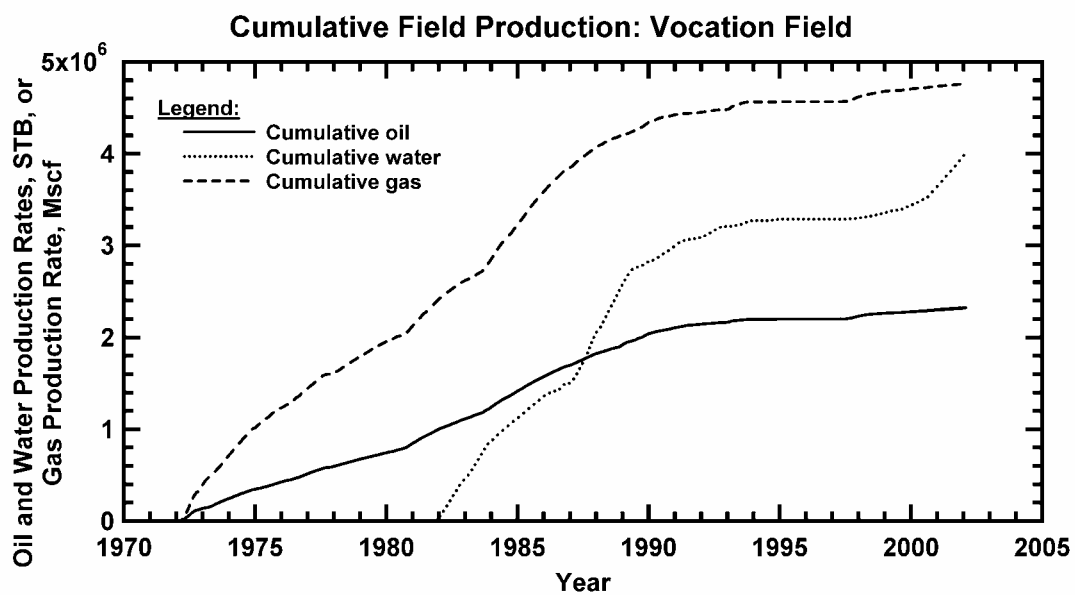


Fig. 214 — Cumulative Production Profiles, Vocation Field.

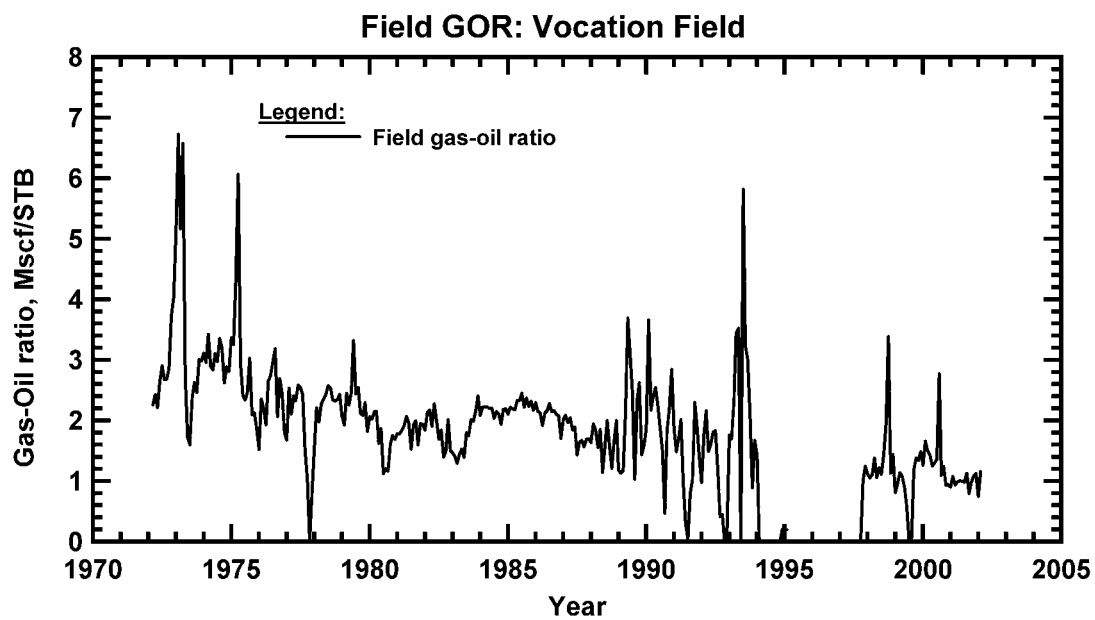


Fig. 215 — Gas-Oil Ratio Profile, Vocation Field.

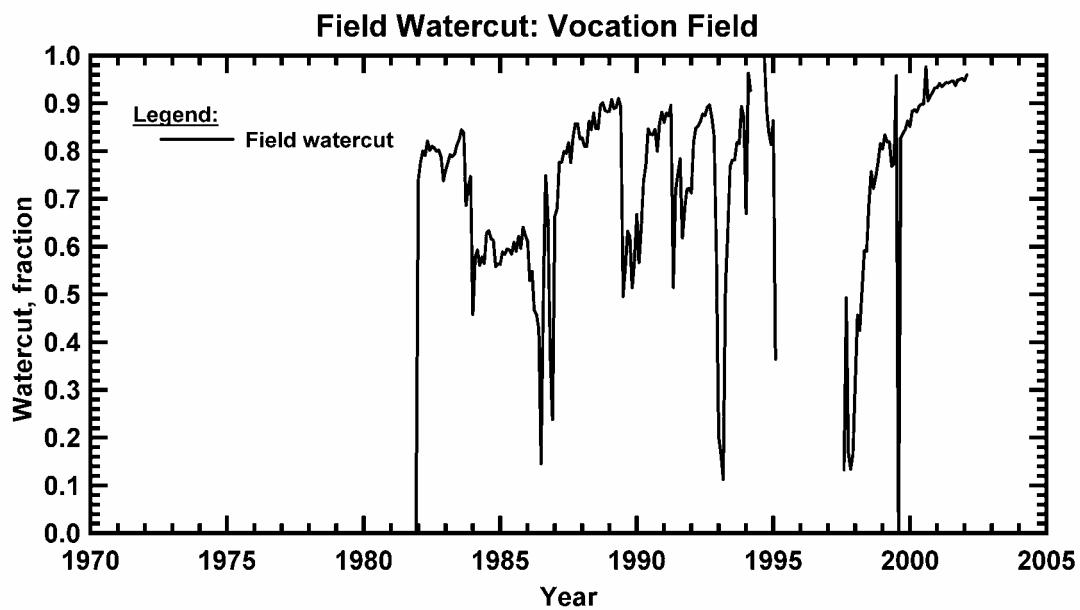


Fig. 216 — Watercut Profile, Vocation Field.

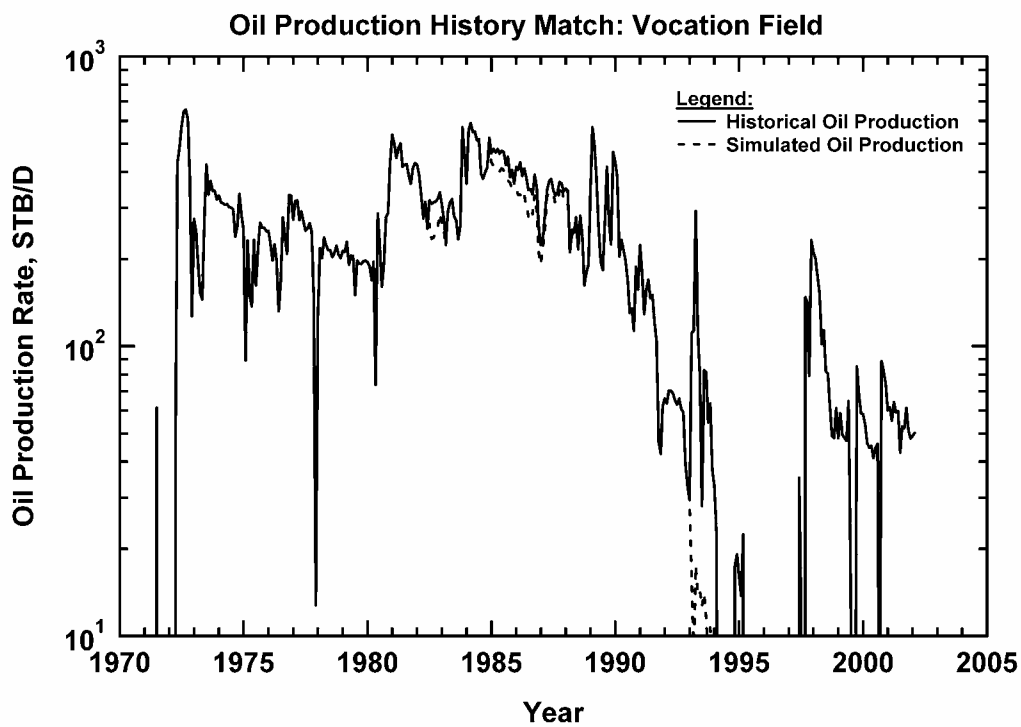


Fig. 217 — Oil Production Rate History Match, Vocation Field.

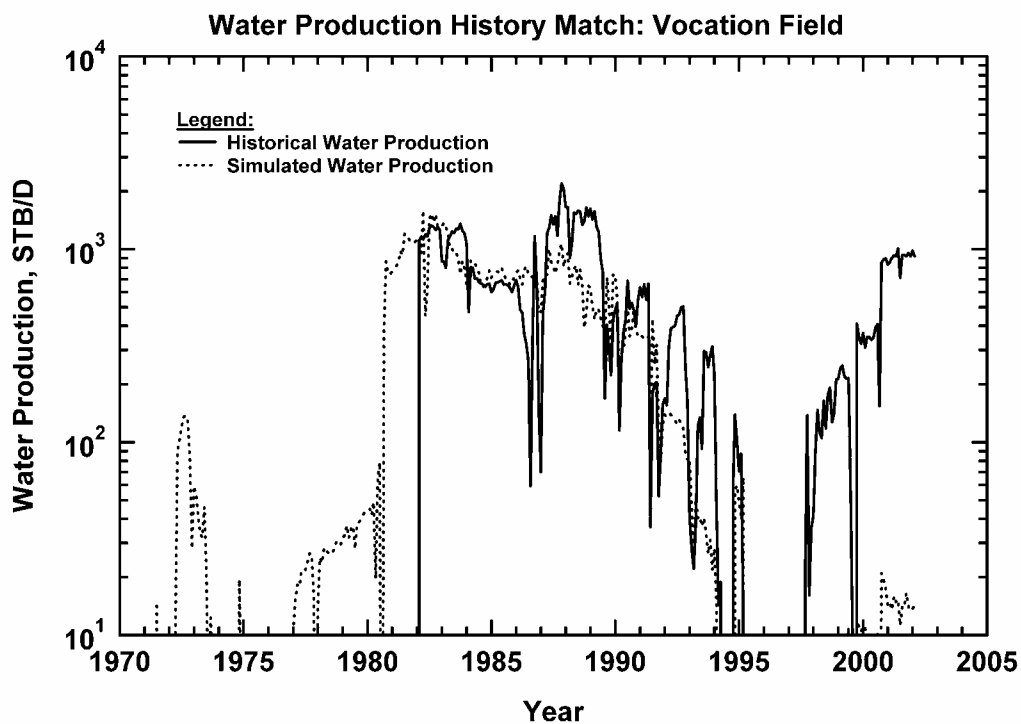


Fig. 218 — Water Production Rate History Match, Vocation Field.

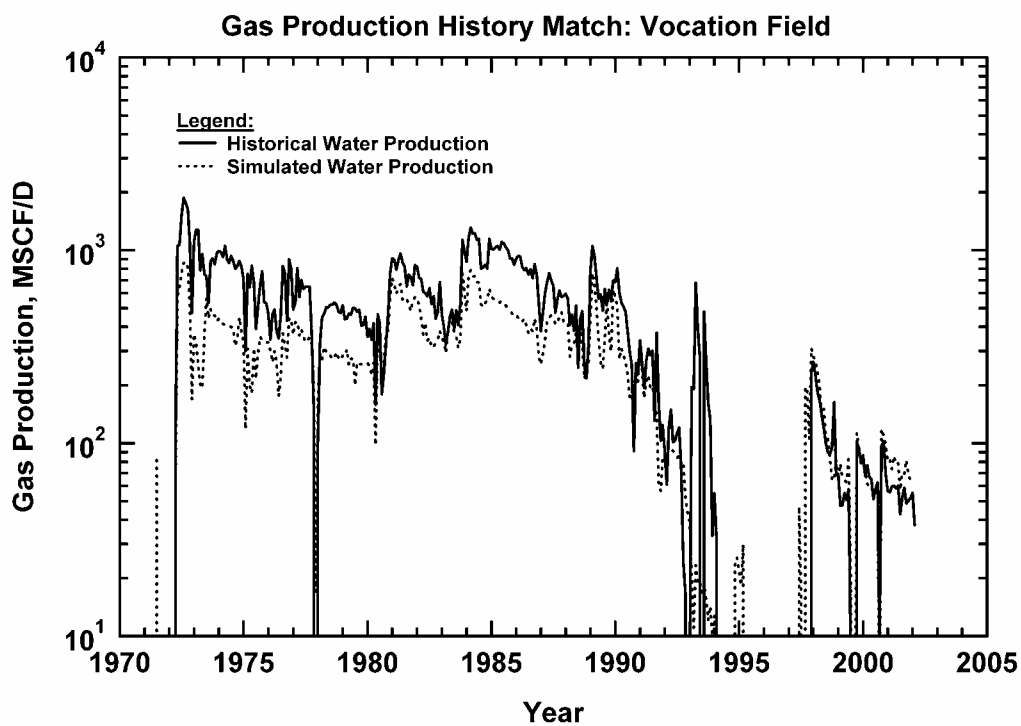


Fig. 219 — Gas Production Rate History Match, Vocation Field.

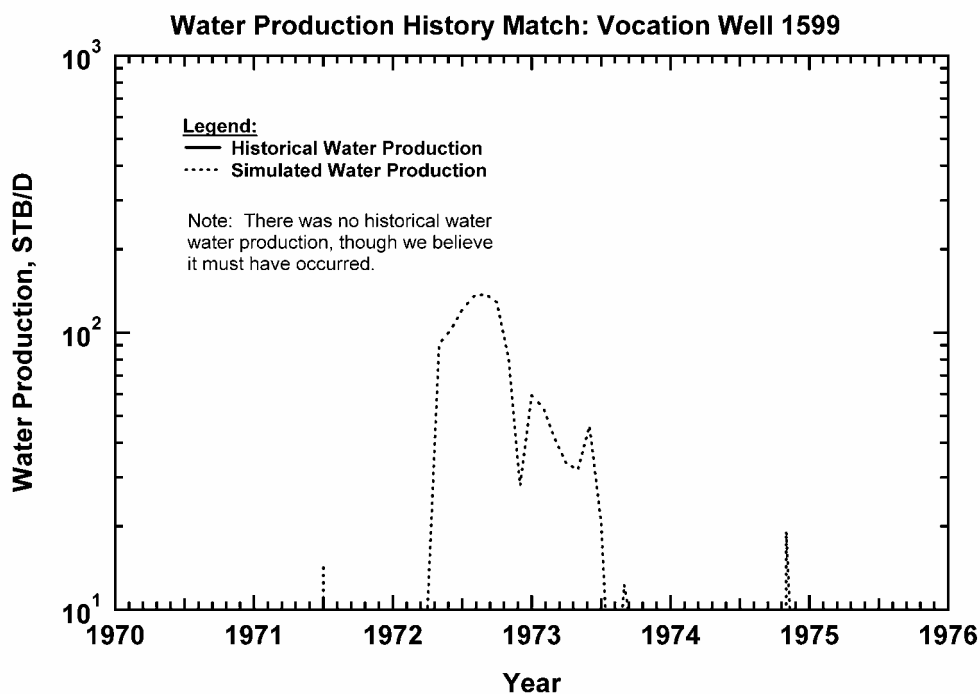


Fig. 220 — Water Production History Match, Vocation Well 1599.

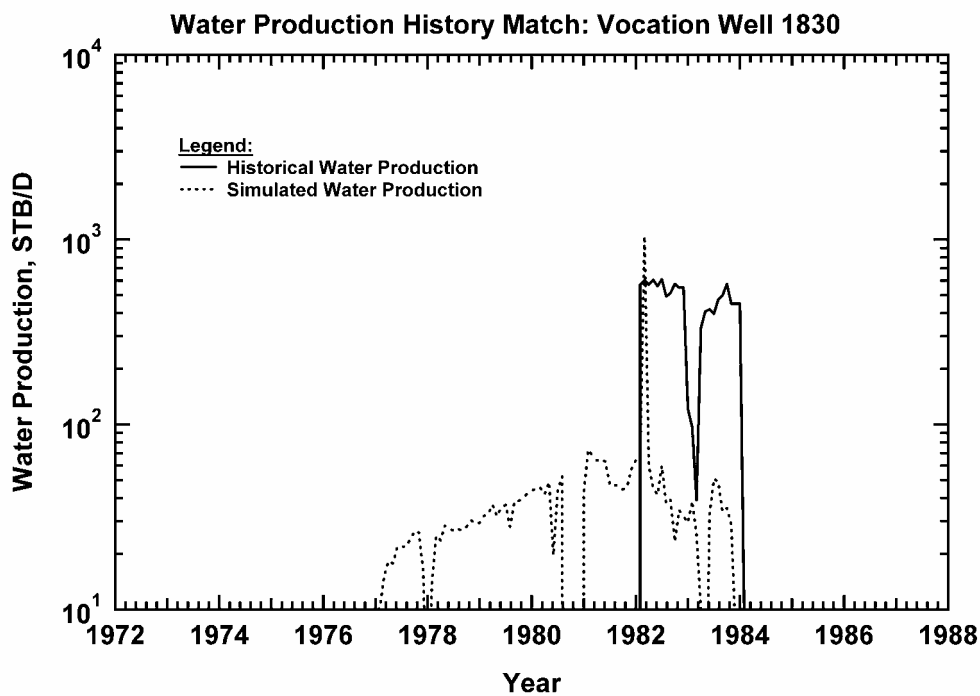


Fig. 221 — Water Production History Match, Vocation Well 1830.

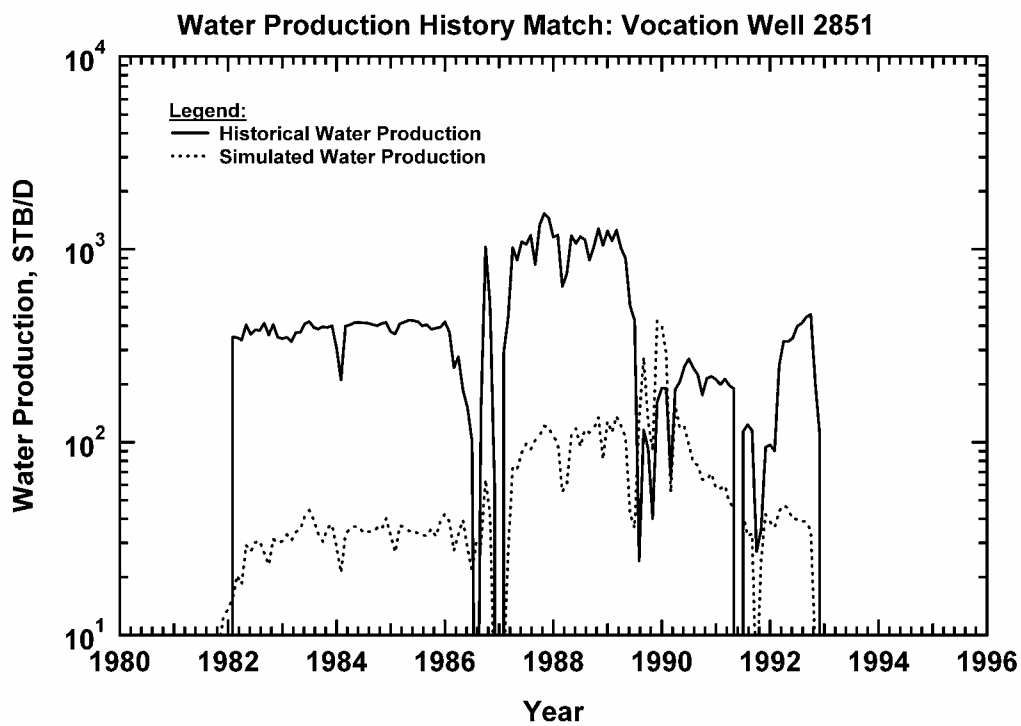


Fig. 222 — Water Production History Match, Vocation Well 2851.

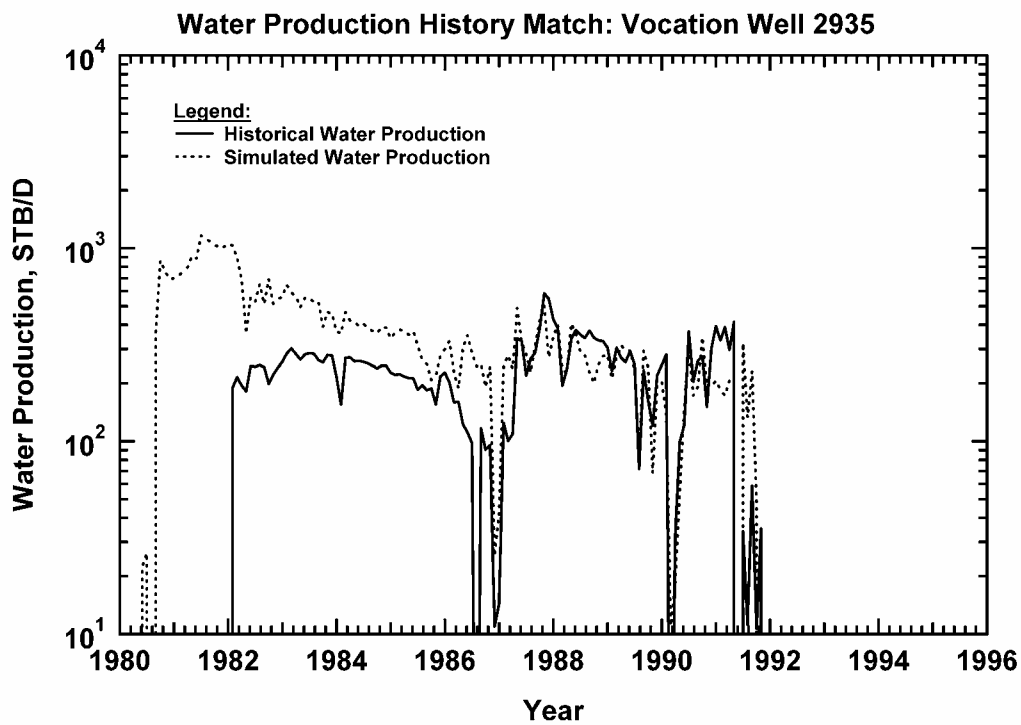


Fig. 223 — Water Production History Match, Vocation Well 2935.

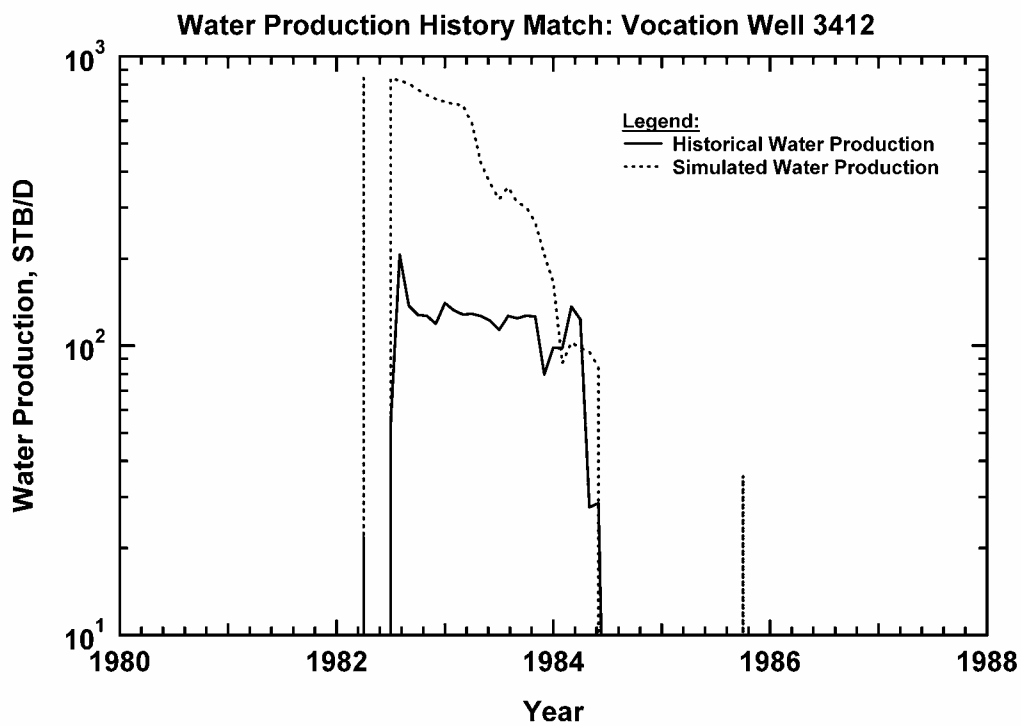


Fig. 224 — Water Production History Match, Vocation Well 3412.

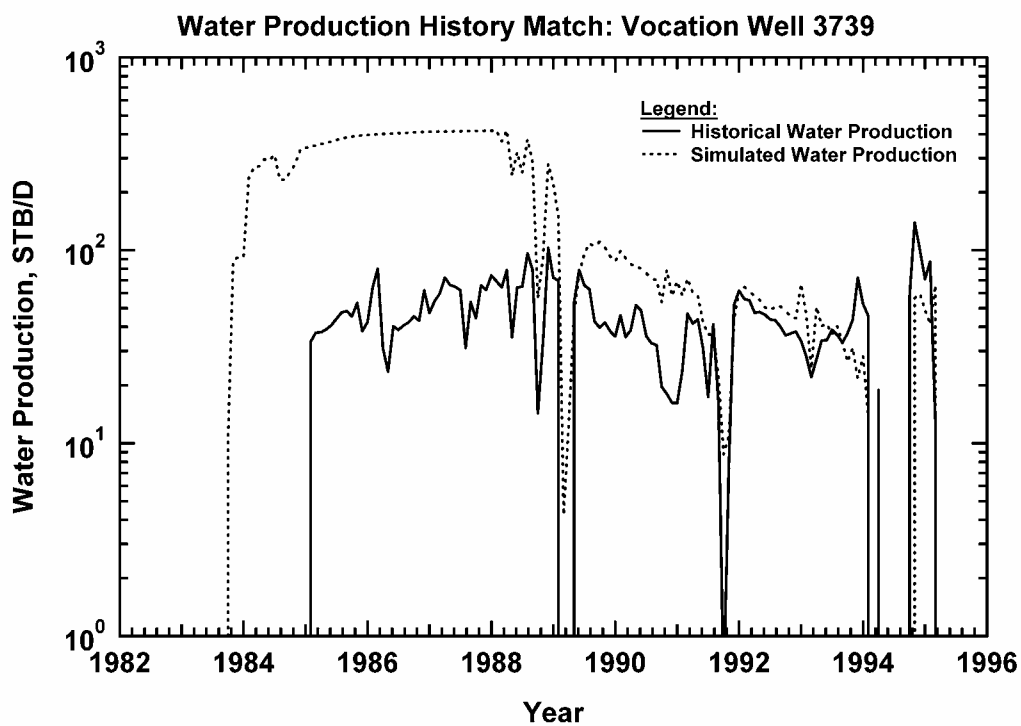


Fig. 225 — Water Production History Match, Vocation Well 3739.

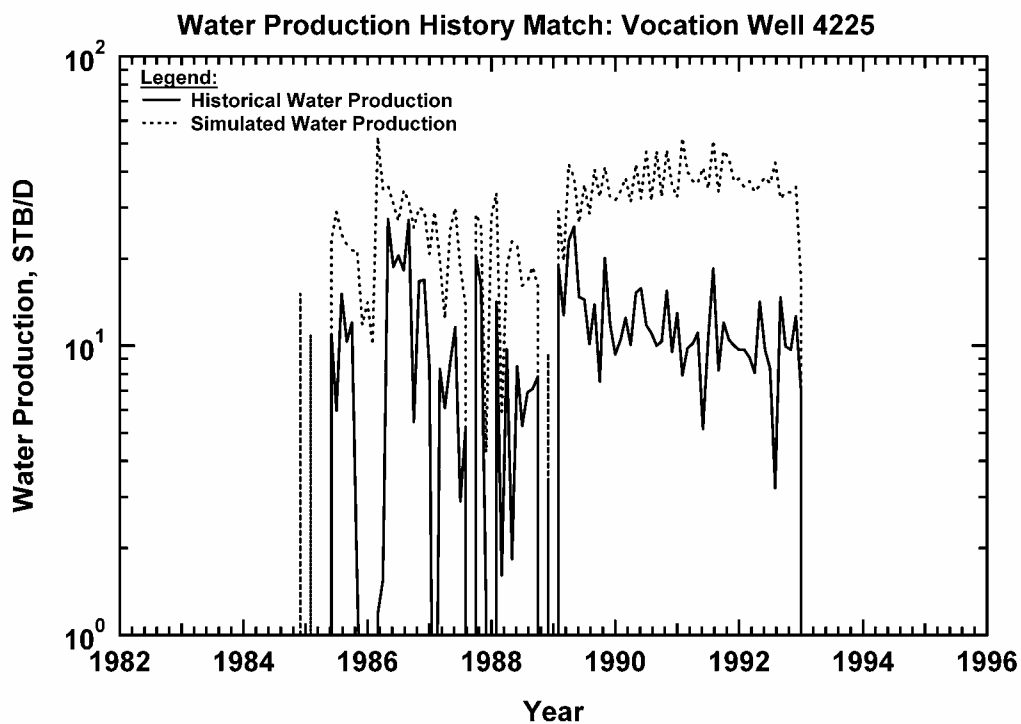


Fig. 226 — Water Production History Match, Vocation Well 4225.

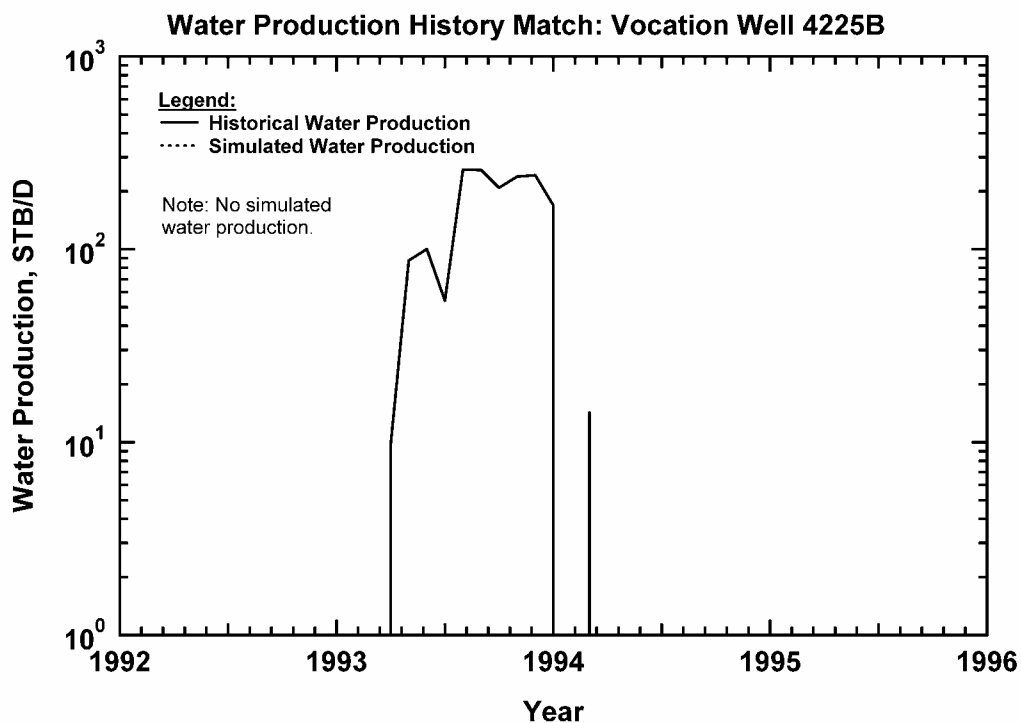


Fig. 227 — Water Production History Match, Vocation Well 4225B.

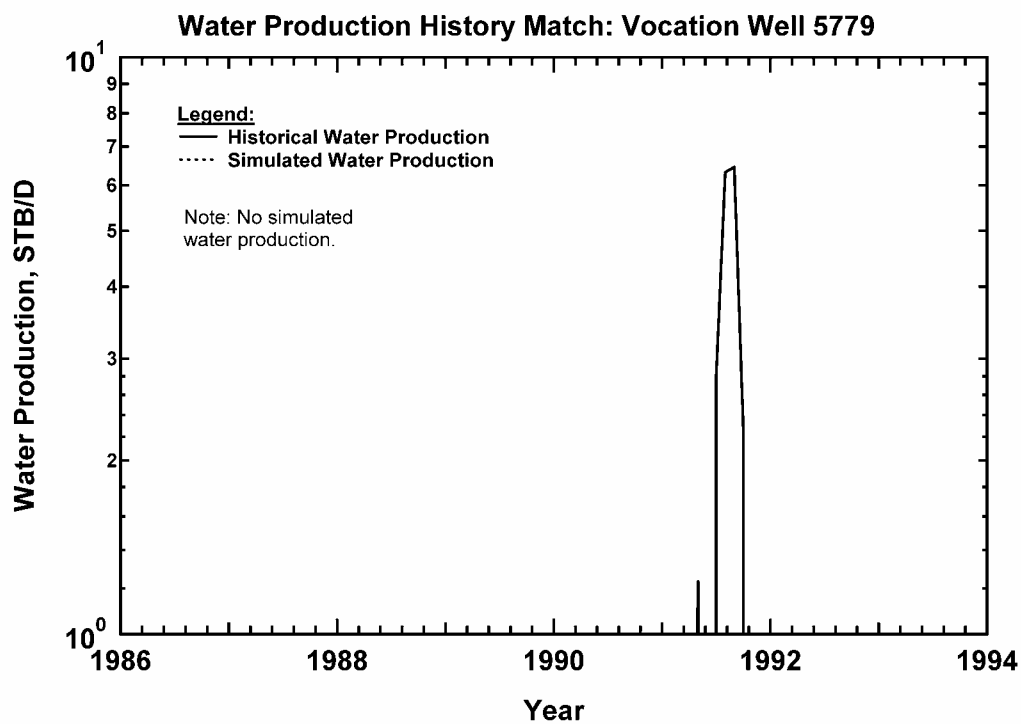


Fig. 228 — Water Production History Match, Vocation Well 5779.

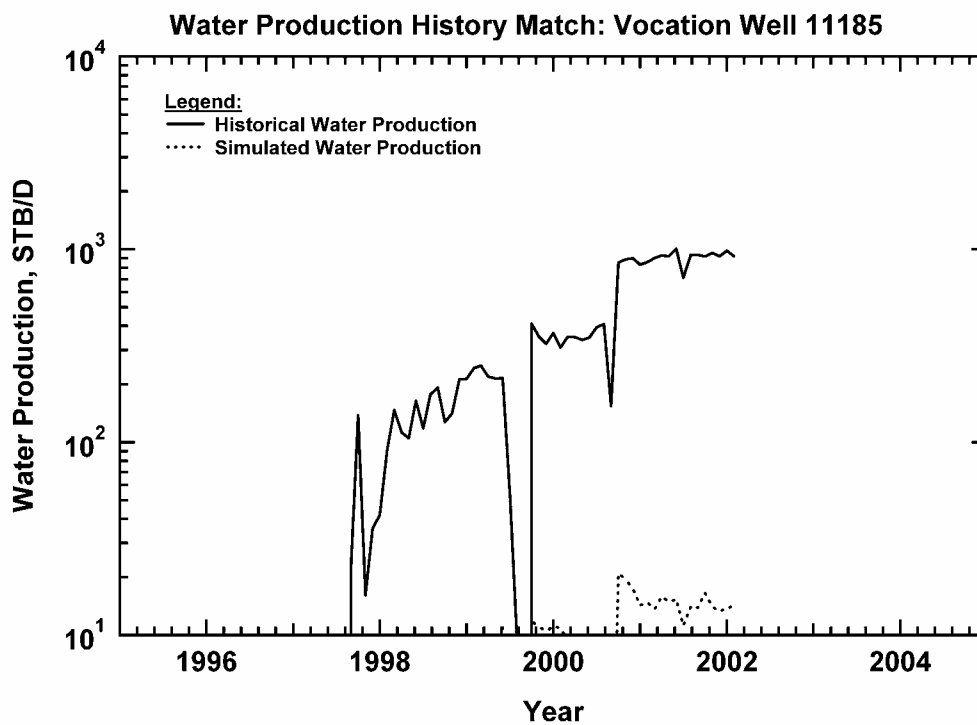


Fig. 229 — Water Production History Match, Vocation Well 11185



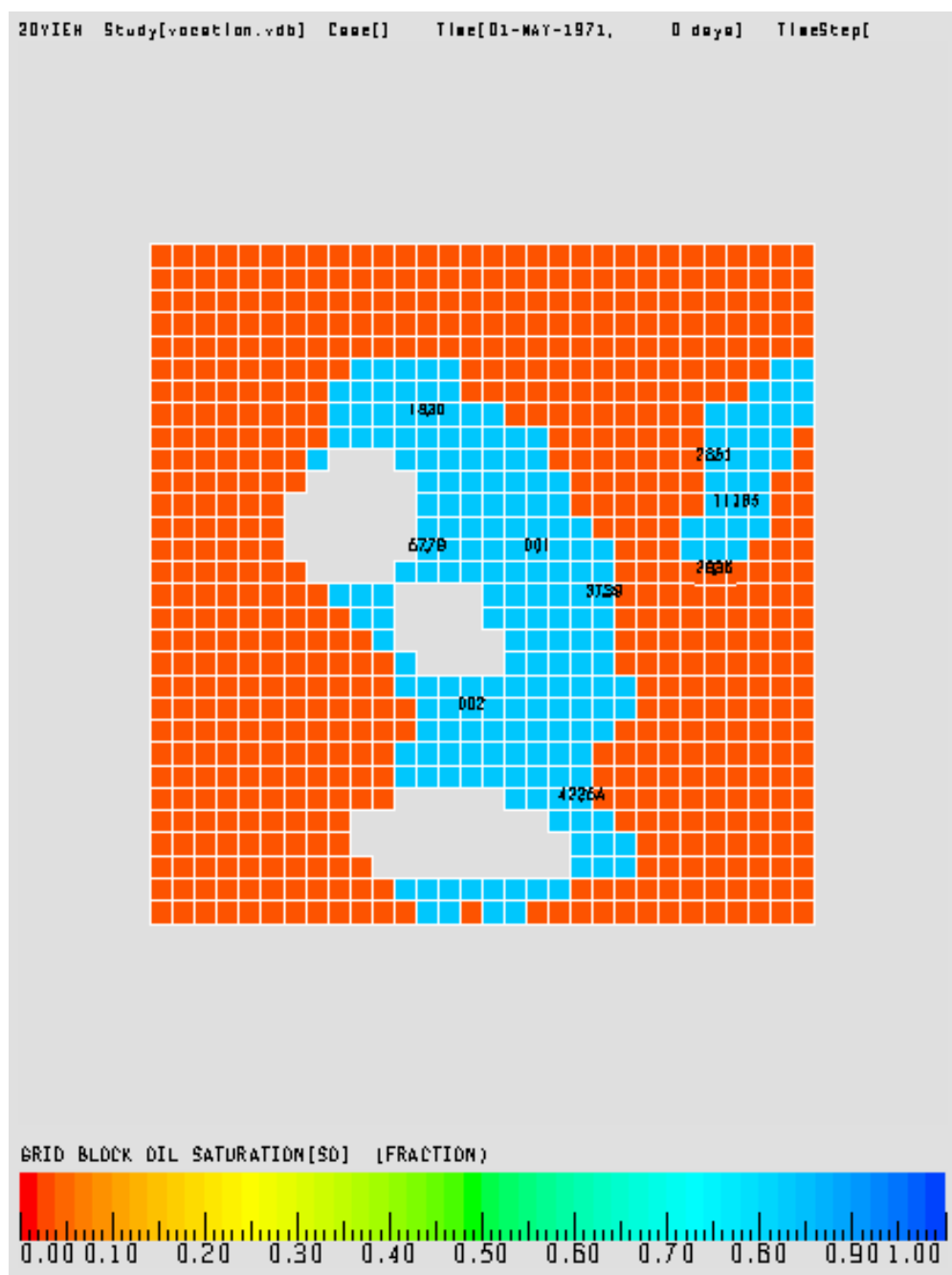


Fig. 230— Initial Oil Saturation (Cross Section), Vocation Field.

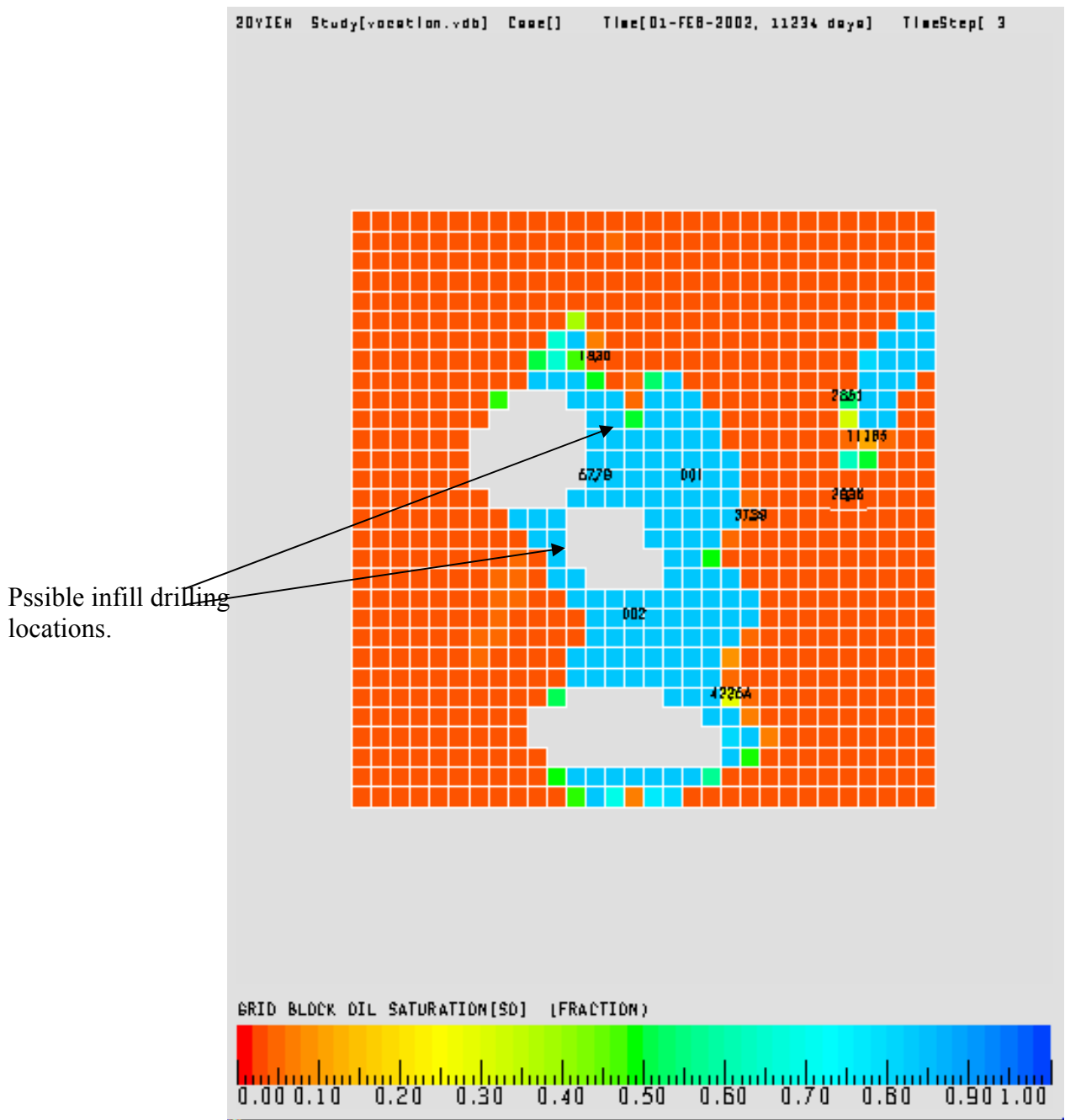


Fig. 231 – Final Oil Saturation (Cross Section), Vocation Field.

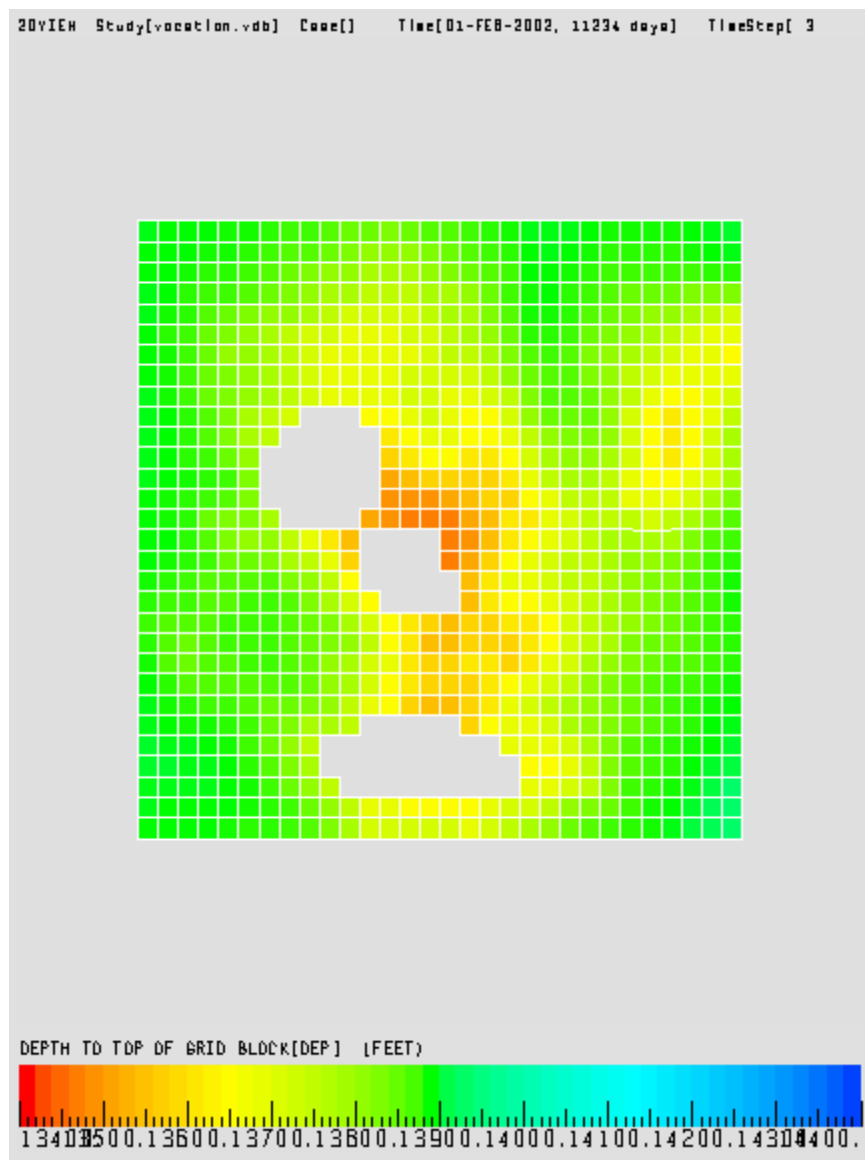


Fig. 232 — Depth to Reservoir Top, Vocation Field.

Table 27. Milestone Chart—Year 3.

Tasks	S	O	N	D	J	F	M	A	M	J	J	A
Task 7—Geologic-Engineering Model	x	x	x	x	x	x						
Task 8—Testing Geologic-Engineering Model							x	x	x	x	x	
Task 9—Applying Geologic-Engineering Model							x	x	x	x	x	
Task 10—Technology Workshop												x
Task 11—Final Report												x

xxxxx Work Planned

However, the incorporation of petrophysical and engineering data will improve our understanding of rock-fluid interactions, of subtle variations in reservoir architecture and heterogeneity, and of flow units, barriers to flow, and reservoir-scale flow patterns. As the integration of geoscience with engineering produces an improved reservoir simulation model to assess and enhance existing field recovery operations, the integration of engineering with geoscience yields an improved predictive geologic-engineering model. Coupling this geologic-engineering model(s) with seismic data, we can evaluate the potential of a prospective carbonate reservoir and structure for drilling. With the addition of well performance and production history data from existing wells, we can design a plan for optimum development of the prospect. From this work, we anticipate being able to create a single geologic-engineering model for reef and shoal reservoirs associated with basement paleohighs of varying degrees of relief though we realize that two models may be required—one for reef-shoal reservoirs associated with low-relief paleohighs and one for reef-shoal reservoirs associated with high-relief paleohighs.

**Task 8—Testing of Geologic-Engineering Model.**--This task focuses on the use of the geologic-engineering model(s) as a predictive methodology to evaluate the potential of a prospective reef-shoal reservoir associated with a basement paleohigh to be identified for study by Paramount. Seismic data from the prospective structure and reservoir will be integrated into the model(s). The model(s) will then be used in the interpretation of the seismic data to improve the detection, characterization and imaging of the reservoir and to improve the prediction of flow in the potential reef-shoal reservoir. The knowledge gained from studying the Appleton and Vocation reservoirs and structures will facilitate this seismic integration approach. As part of this process, seismic forward modeling will be performed to determine whether reef-shoal lithofacies are present on the crest, flanks, or both crest and flanks of this paleohigh. Seismic attributes will

be studied to determine whether reef-shoal reservoir porosity is expected on the crest, flank, or crest and flanks of this paleohigh. Based on the seismic forward modeling and seismic attribute studies, a decision will be made as to whether to drill and where on the paleohigh to drill this prospect. Although the drilling of this well and of any confirmation well will occur after the conclusion of the project, the geologic-engineering model will be used in determining the location for the confirmation well and in the design of the field development plan. This model(s) also will be utilized to predict fluid flow in this prospective reservoir based on the integrated geologic and engineering studies at Appleton and Vocation Fields. Landmark SeisWorks Family and KINGDOM Suite software, including 2d/3d PAK, will be used in the interpretation of the seismic data and attribute study. It is important that the geologic-engineering model(s) be compatible with the KINGDOM Suite software because this is the software that is commonly employed by independent operators in this region.

**Task 9—Application of Geologic-Engineering Model.--**This task will apply the geologic-engineering model(s) to the Appleton reservoir and the Vocation reservoir to evaluate the potential for new improved or enhanced oil recovery operations, such as a strategic infill drilling program and/or a waterflood or enhanced oil recovery project in these fields. The evaluation process will focus on the potential to improve field profitability, producibility and efficiency, and ultimately, to sustain the life of these reservoirs. The geologic-engineering model(s) will be applied with emphasis on reservoir management, and the recommendations resulting from these efforts will be compared to those from the reservoir simulation modeling. The benefits of each modeling approach (the geologic-engineering and the reservoir simulation) will be evaluated, and final recommendations to improve profitability, producibility and efficiency at Appleton and Vocation Fields will be made to the operators of these fields.

**Task 10—Technology Workshop.**--The project results will be transferred to producers in the Eastern Gulf Region through a technology transfer workshop to be held in Jackson, Mississippi. The workshop will focus on the presentation of our geologic-engineering model(s) and the application of the model(s) for the evaluation of prospective carbonate reservoirs.

## **RESULTS AND DISCUSSION**

The Project Management Team and Project Technical Team are working closely together on this project. This close coordination has resulted in a fully integrated research approach, and the project has benefited greatly from this approach.

### **Geoscientific Reservoir Characterization**

Geoscientific reservoir characterization is essentially completed. The architecture, porosity types and heterogeneity of the reef and shoal reservoirs at Appleton Field and Vocation Fields have been characterized using geological and geophysical data.

The architecture and heterogeneities of reservoirs that are a product of a shallow marine carbonate setting are very complex and a challenge technically to predict. Carbonate systems are greatly influenced by biological and chemical processes in addition to physical processes of deposition and compaction. Carbonate sedimentation rates are primarily a result of the productivity of marine organisms in subtidal environments. In particular, reef-forming organisms are a crucial component to the carbonate system because of their ability to modify the surrounding environments. Reef growth is dependent upon many environmental factors, but one crucial factor is sea-floor relief (paleotopography). In addition, the development of a reef structure contributes to depositional topography. Further, the susceptibility of carbonates to alteration by early to late diagenetic processes dramatically impacts reservoir heterogeneity. Reservoir characterization and the quantification of heterogeneity, therefore, becomes a major

task because of the physiochemical and biological origins of carbonates and because of the masking of the depositional rock fabric and reservoir architecture due to dissolution, dolomitization, and cementation. Further, the detection, imaging, and prediction of carbonate reservoir heterogeneity and producibility is difficult because of an incomplete understanding of the lithologic characteristics and fluid-rock dynamics that affect log response and geophysical attributes.

### ***Appleton Field***

Based on the description of cores (11) and thin sections (379), 14 lithofacies had been identified previously in the Smackover/Buckner at Appleton Field. Analysis of the vertical and lateral distributions of these lithofacies indicates that these lithofacies were deposited in one or more of eight depositional environments: 1) subtidal, 2) reef flank, 3) reef crest, 4) shoal flank, 5) shoal crest, 6) lagoon, 7) tidal flat, and 8) sabkha in a transition from a catch-up carbonate system to a keep-up carbonate system. These paleoenvironments have been assigned to four Smackover/Buckner genetic depositional systems for three-dimensional stratigraphic modeling. Each of these systems has been interpreted as being time-equivalent from that work, two principal reservoir facies, reef and shoal were identified at Appleton Field.

Based on the description of cores and thin sections, three subfacies have been recognized in the reef facies. These subfacies include thrombolitic layered, reticulate and dendroid. Each represents a different and distinct microbial growth form which has inherent properties that affect reservoir architecture, pore systems, and heterogeneity. The layered growth form is characterized by a reservoir architecture that is characterized by lateral continuity and high vertical heterogeneity. The reticulate form has a reservoir architecture that is characterized by high vertical and lateral continuity. The dendroid form has a reservoir architecture that is



characterized by high vertical and moderate lateral continuity and moderate heterogeneity. The pore systems in each of these reservoir fabrics consist of shelter and enlarged pore types. The enlargement of these primary pores is due to dissolution and dolomitization resulting in a vuggy appearing pore system. Three subfacies have been recognized in the shoal facies. These subfacies are the lagoon/subtidal, shoal flank, and shoal crest. The lagoon/subtidal subfacies has a mud-supported architecture and therefore is not considered a reservoir. The shoal flank has a grain-supported architecture but has considerable carbonate mud associated with it, and therefore, has low to moderate reservoir capacity. The shoal crest has a grain-supported architecture with minimal carbonate mud, and therefore, has the highest reservoir capacity of the shoal subfacies. The pore systems of the shoal flank and shoal crest reservoir facies consist of intergranular and enlarged pore types. The enlargement of the primary pores is due to dissolution and dolomitization. Heterogeneity in the shoal reservoir is high due to the rapid lateral and vertical changes in this depositional environment. Graphic logs were constructed for each of the cores. The core data and well log signatures are integrated and calibrated on these graphic logs.

Appleton Field was discovered in 1983 with the drilling of the D.W. McMillan 2-14 well (Permit #3854). The discovery well was drilled off the crest of a composite paleotopographic structure, based on 2-D seismic and well data. The well penetrated Paleozoic basement rock at a depth of 12,786 feet. The petroleum trap at Appleton was interpreted to be a simple anticline associated with a northwest-southeast trending basement paleohigh. After further drilling in the field, the Appleton structure was interpreted as an anticline consisting of two local paleohighs. The D.W. McMillan 2-15 well (Permit #6247) was drilled in 1991. The drilling of this well resulted in the structural interpretation being revised to consist of three local paleohighs. In 1995, 3-D seismic reflection data were obtained for the Appleton Field area. The interpretation

of these data indicated three local highs with the western paleohigh being separated into a western and a central feature.

Based on the structural maps that we have prepared for the Appleton Field, we have concluded that the Appleton structure is a low-relief, northwest-southeast trending ridge comprised of local paleohighs. This interpretation is based on the construction of structure maps on top of the basement, on top of the reef, and on top of the Smackover/Buckner from well log data and 3-D seismic data.

The Smackover reservoir at Appleton Field has been influenced by antecedent paleotopography. The Smackover thickness ranges from 177 feet in the McMillan 2-14 well (Permit #3854) to 228 feet in the McMillan Trust 11-1 well (Permit #3986) in the field. As observed from the cross sections based on well log data and on seismic data, the sabkha facies thins over the composite paleohigh, while the reservoir lithofacies are thicker on the paleohigh. Thickness maps of the sabkha facies, tidal flat facies, shoal complex, tidal flat/shoal complex, and reef complex facies illustrate the changes in these lithofacies in the Appleton Field.

### ***Vocation Field***

Smackover deposition in the Vocation Field area is the product of the interplay of carbonate deposition, paleotopography, and subsidence mainly of tectonic origin during a third order eustatic sea level rise. Based on core descriptions, five shallow-marine environments in the Smackover Formation were identified: microbial reef complex, shallow subtidal, shallow lagoon, shoal complex, and tidal flat/sabkha. The last environment includes the Buckner Anhydrite Member that in Vocation field is relatively thin with an average thickness of 20 to 30 feet. These subenvironments define an overall aggradational and finally progradational shallowing upward cycle developed in a restricted evaporate-carbonate setting.

The microbial reef complex facies is present in the lower part of the Smackover Formation. It is very heterogeneous and consists of bafflestone (thrombolitic reticulate), bindstone (thrombolitic layered) and oncoidal crusts, interbedded with dolomudstone/dolowackestone layers. Stylolitic laminae are common. Allochems are bioclasts mainly of algae and bivalve fragments, oncoids, peloidal clots, intraclasts, and ooids. The amount and types of pores are highly variable, including primary shelter, interparticle and intraparticle porosity and secondary solution enlarged/vuggy, moldic, and fracture pores. In some cases, anhydrite partially occludes vuggy pores and fractures. Significant development of microbial buildups are located on the northeastern side (leeward side) of the basement structure, while in the western side of the structure (windward side) grainy sediments were deposited, but their original texture is difficult to identify due to intense dolomitization.

The shallow subtidal facies is also present in the lower part of the Smackover succession but in off-structure locations. It is composed of dark brown skeletal dolowackestone with subtle plane parallel to wavy lamination. Some intervals display patchy textures indicative of microbial influence. Allochems are mainly peloids, and sporadic ooids and skeletal debris, such as echinoderm spines and bivalve fragments. Stylolites and horsetail lamination enriched in authigenic pyrite are very common. Scarce and small anhydrite nodules are also present.

The shallow lagoon facies represents deposits accumulated behind a reef and/or shoal barrier. It is composed of light brown dolowackestone to dolopackstone interbedded with darker dolomudstone and argillaceous beds. Microbial buildups of up to 10-feet thick and fine-grained grainstone are sporadically present. Allochems are scarce and consist mainly of isolated peloids, ooids, oncoids, and intraclasts. Localized wavy lamination showing effects of bioturbation is common in this facies.

Deposited in the upper parts of the Smackover Formation, the shoal complex facies comprises most of the producing intervals in the field. It consists of carbonate sand bars consisting of ooid/oncoidal dolograins/dolopackstone in thick, sometimes cross-stratified layers, interbedded with thinner dolopackstone/dolowackestone beds. Allochems are mainly ooids and oncoids though intraclasts and peloids are also common in the shoal flanks. Anhydrite in the form of nodules or as cement is an important constituent of this facies. Porosity is moderate to high and consists of primary interparticle and secondary moldic, intraparticle, and vuggy pores, and microfractures. Some intervals display low porosity (<5%) values due to cementation and compaction processes.

The shoal complex is the uppermost depositional facies of the Smackover Formation and consists of laminated dolomudstone to dolowackestone interbedded with thick anhydrite layers and microbial laminites (stromatolites). Stylolites and anhydrite nodules of varied sizes are very common. Allochems are peloids with less common ooids and bioclasts. Porosity is commonly low (< 6 %) due to the presence of dense anhydrite layers and the fine-grained texture of the carbonate sediments, although in some cases the extensive dolomitization of this facies has generated beds with high intercrystalline porosity. It consists of primary fenestral and secondary moldic and microfracture porosity. Sporadic beds with solution enlarged pores are also present.

Vocation Field was discovered in 1971 with the drilling of the B.C. Quimby 27-15 (Permit #1599) well. The discovery well was drilled near the crest of a paleotopographic structure based on 2-D seismic and well log data. The well penetrated Paleozoic basement rock at a depth of 14,209 feet.

The Vocation field structure has been interpreted as a high relief composite paleotopographic feature of the updip basement ridge play. It lies on the western flank of the

Conecuh Ridge in the southeastern margin of the Manila Sub-basin. Its position is updip of the subcrop limit of the Louann Salt and 10 miles northeast of the regional peripheral fault trend. The trap in Vocation field is combined (structural-stratigraphic), as the result of the onlap of reservoir facies against the basement paleohigh. The structure at Vocation field is a composite feature formed by Paleozoic granitic basement highs with irregular relief and steep slopes on the flanks. It consists of a main north-south trending basement feature with three local highs that remained subaerially exposed until the end of Smackover deposition. To the northeast, a smaller feature with lower elevations has been successfully tested by three wells. This smaller structure and the low area that separates it from the main feature were preferentially colonized by microbial reefs, probably due to the presence of gentler depositional slopes formed by crystalline igneous rocks. These surfaces provided the stable hardground necessary for the establishment and growth of the microbial reef. The Vocation structure is characterized by embayed margins and by high angle normal faulting that affected the Smackover Formation on the eastern and northern flanks. Seismic data interpretation shows greater thicknesses of the Smackover section on the downthrown blocks of the faults that cut the structure on the eastern flank indicating that these faults were active during Smackover deposition.

The depositional sequence of the Smackover Formation varies dramatically in thickness in the field from 0 ft (Well Permit 4786-B) in structurally elevated areas where the Smackover pinches out against crystalline basement rocks, to 440 ft off-structure (Well Permit 3029). On-structure, the Smackover section is the result of a shallowing-upward event in which four shallow marine subenvironments were identified as follows: microbial reef complex, consisting of bafflestone (reticulate thrombolites), bindstone (layered thrombolites) and oncoidal crusts, interbedded with skeletal and peloidal dolopackstone to dolowackestone layers; shallow lagoon,

consisting of dolomudstone and dolowackestone to dolopackstone layers, with some bioturbated levels and thin isolated microbial buildups that formed in a low energy environment behind the reef and shoal complex; shoal complex, consisting of irregular and discontinuous sand bars made up of ooid, oncoid and peloid dolograins and dolopackstone in thick, sometimes cross-stratified layers of variable thickness interbedded with thinner dolopackstone to dolowackestone levels and thin horizons rich in anhydrite nodules especially in the upper layers; and sabkha-tidal flat, consisting of laminated peloidal dolomudstone to peloidal dolowackestone interbedded with thick anhydrite layers and algal laminites (stromatolites). The Buckner Anhydrite Member, which is relatively thin in the area (0 to 40 ft), is included in this interval. In general, this facies is thicker close to the paleohigh crestal areas and progressively thinner toward the margins.

As in Appleton Field, the best potential reservoirs are associated with the microbial reef facies mainly in the levels with reticulate thrombolite texture, and with the grainstone-packstone shoal complex. The reservoir quality of these rocks is the result of the depositional fabric combined with the effects of diagenetic processes, such as dolomitization and dissolution that acted to increase the initial porosity and improved the connectivity of the pore network. Significant thicknesses of microbial boundstone have been found only in the northeastern side of the basement paleohigh but unfortunately below the oil/water contact. Instead, on the western flank, fine-crystalline, highly dolomitized limestone was deposited.

### **Rock-Fluid Interactions**

The study of rock-fluid interactions is near completion. Observation regarding the diagenetic processes influencing pore system development and heterogeneity in these reef and shoal reservoirs have been made.

### *Appleton Field*

Based on initial petrographic studies, reservoir-grade porosity in the Smackover at Appleton field occurs in microbial boundstone in the reef interval and in ooid, oncoidal, and peloidal grainstone and packstone in the upper Smackover. Porosity in the boundstone is a mixture of primary shelter porosity overprinted by secondary intercrystalline and vuggy porosity produced by dolomitization and dissolution that is pervasive throughout the field. Porosity in the grainstone and packstone is a mixture of primary interparticle and secondary grain moldic porosity overprinted by secondary dolomite intercrystalline porosity.

Based on core analysis data, there is a distinct difference in reservoir quality between the grainstone/packstone and boundstone reservoir intervals. Although the difference in reservoir quality between these lithofacies is principally the result of depositional fabric, diagenesis acts to enhance or impair the reservoir quality of these lithofacies. Porosity in the grainstone/packstone reservoir interval in the McMillan 2-14 well (Permit #3854) ranges from 9.7 to 21.5% and averages 14.8%. Permeability ranges from 1.1 to 618 md, having a mean of 63.5 md. Porosity in the reef boundstone reservoir interval in the McMillan Trust 12-14 well (Permit #4633-B) ranges from 11.9 to 25.0% and averages 18.1%. Permeability ranges from 14 to 1748 md, having a mean of 252 md.

The higher producibility for the reef lithofacies is attributed to the higher permeability of this lithofacies and to the nature of the pore system (pore-throat size distribution) rather than the amount of porosity. Pore-throat size distribution is one of the important factors determining permeability, because the smallest pore throats in cross-sectional areas are the bottlenecks that determine the rate at which fluids pass through a rock.

Although both the reef and shoal lithofacies accumulated in diverse environments to produce mesoscopic-scale heterogeneity, dolomitization and dissolution acted to reduce the microscopic-scale heterogeneity in these carbonate rocks. The grainstone/packstone accumulated in shoal environments and were later subjected to dolomitization and vadose dissolution. The resulting moldic pore system, which includes primary interparticulate and secondary grain moldic and dolomite intercrystalline porosities, is characterized by multisize pores that are poorly connected by narrow pore throats. Pore size is dependent on the size of the carbonate grain that was leached.

The boundstone accumulated in a reef environment and were later subjected to pervasive dolomitization and nonfabric-selective, burial dissolution. The intercrystalline pore system, which includes primary shelter and secondary dolomite intercrystalline and vuggy pores, is characterized by moderate-size pores having uniform pore throats. The size of the pores is dependent upon the original shelter pores, the dolomite crystal size, and the effects of late-stage dissolution. The reef reservoir and its shelter and intercrystalline pore system, therefore, has higher producibility potential compared to the shoal reservoir and its moldic pore system.

As confirmed from well-log analysis and well production history, hydrocarbon production in Appleton field has occurred primarily from the boundstone of the Smackover reef interval, with secondary contributions from the shoal grainstone and packstone of the upper Smackover. Total reservoir thickness in the producing wells ranges from 20 ft (6 m) in the McMillan Trust 11-1 well (Permit #3986) to 82 ft (25 m) in the McMillan Trust 12-4 well (Permit #4633-B). With the exception of the McMillan 2-14 well (permit #3854), where production has been primarily from grainstone and packstone of the upper Smackover, the majority of the productive reservoir occurs in boundstone.



The higher production from the reef interval is attributed to the better reservoir quality of the boundstone and to the better continuity and connectivity of these carbonates. Whereas, the grainstone/packstone interval is discontinuous, both vertically and laterally, the boundstone interval appears to possess excellent vertical and lateral continuity.

In addition, although the microbial reef reservoir interval is more productive than the shoal reservoir interval at Appleton Field, the dendroidal thrombolites have higher reservoir quality than the layered thrombolites. Dendroidal thrombolites have a reservoir architecture characterized by high lateral and vertical pore interconnectivity and permeability, while layered thrombolites have good lateral but poorer vertical pore interconnectivity and permeability. Both thrombolite architectures are characterized by pore systems comprised of shelter and enlarged pores.

### ***Vocation Field***

The sequence of diagenetic events in the Smackover at Vocation Field occurred in the eogenetic and mesogenetic stages. The eogenetic stage is the time interval between final deposition and the burial, below the influence of surface-derived fluids of marine, brine, or meteoric origin. The processes that occur within this stage are very active during relatively short periods of time. Generally, the sediments and rocks of the eogenetic zone are mineralogically unstable, or are in the process of stabilization, and therefore, porosity modification by dissolution, cementation, and dolomitization is quickly accomplished. The mesogenetic stage refers to the time interval in which sediments or rocks are buried below the influence of surficial diagenetic processes until final exhumation in association with unconformities. Progressively increased pressure and temperature and related rock-connate fluid interaction are the driving

mechanisms for burial diagenesis. In general, diagenetic processes that occur in the mesogenetic zone operate at very slow rates but over long spans of geologic time.

Micritization is one of the earliest eogenetic events since it largely occurs near the sediment / water interface. It is produced by repeated boring activity of microorganisms such as algae and fungi over the allochem surfaces and the subsequent infill of the borings with micrite generating rims around the grains. This is a very common process in Smackover deposits especially in the shoal facies at Vocation Field. Another early diagenetic event is the selective dissolution of aragonite allochems generating moldic pores. It is produced by the action of meteoric waters undersaturated with respect to calcium carbonate and affected mainly tidal and shoal deposits because of their deposition very close to the sea water surface and probably reflecting a relative sea-level fall. Isopachous rims of marine calcite cement (later dolomitized) coating allochemical constituents have been found mainly in shoal facies and microbial reef facies in Vocation Field. The vast majority of marine cementation occurs very near the sediment water interface where sea water actively moves into the sediments. Precipitation of this early cement preserved primary porosity from subsequent compaction. Mechanical compaction starts to affect carbonate sediments under early burial conditions destroying mainly primary intergranular pores. This process results in rotation and horizontal alignment of allochems and minor ductile grain deformation expressed by embayed contacts among the grains. Compaction was more intense where no early calcite cementation occurred. Dolomitization is one of the most significant diagenetic events that affects the Smackover Formation in the study area because it created new intercrystalline pores that improved the connectivity of the pore network. Dolomitization is ubiquitously present in the entire Smackover interval in Vocation Field. It is expressed by neomorphism of calcareous allochems, matrix and cements into dolomite. This process also

includes precipitation of dolomite cement. Gypsum and/or anhydrite precipitation also accompanied this process filling intergranular, vuggy and moldic pores, and as replacive nodules principally in the upper part of the Smackover Formation. Normally the size of the crystals is relative to the size of the grain being replaced. In some cases, penetrative dolomitization was able to obscure the primary texture preventing a reliable identification of the original rock. Rocks that experienced intense dolomitization display a sucrosic texture sometimes with high intercrystalline porosity.

Once carbonate sediment has been mechanically compacted, continued burial increases the chemical potential that eventually leads to the dissolution of the grains in a mesogenetic process known as pressure-solution. The result is the presence of abundant high amplitude stylolites, and anastomosing wispy seams and laminae of insoluble residue, mainly in the finer grained facies of the Smackover Formation. These features are impermeable barriers to fluid flow. Chemical compaction in the Smackover Formation is believed to be a significant source for later porosity occluding, subsurface cements. Fractures and microfractures are normally present in the Smackover Formation, especially in the microbial reef facies. Although time of formation is difficult to define, this event occurred after dolomitization and lithification since normally the fractures cut dolomitized particles. The partial infill with dolomitic, calcitic and late stage anhydritic cements may imply that they began to form shortly after burial. The causes of fracturing can be a combination of compaction and local tectonic activity. In the Smackover Formation, the dissolution predates oil migration, and therefore, it is possible that its origin may be related to the presence of aggressive pore fluids enriched in CO<sub>2</sub> and organic acids associated with early phases of oil maturation. This process is the result of the decarboxilation (loss of -COOOH group) of organic material during the oil maturation process. Various types of

cementing materials, including dolomitic, siliceous, calcitic, and anhydritic cements obliterated all types of porosity after burial. Ferroan dolomite cement is characterized by large crystals commonly with euhedral shapes and cloudy centers. This cement probably was precipitated immediately after the non-selective dissolution event since it normally fills vugs and cavities formed during this diagenetic episode. It often also fills moldic and intercrystalline pores. In some cases, the presence of saddle or baroque dolomite crystals with their characteristic undulose extinction indicates that dolomitization occurred under deep burial conditions. Saddle dolomite is commonly associated with hydrocarbons, and thus, implies late diagenetic formation by sulfate reduction processes. Siliceous cement is present in very small amounts in the form of isolated euhedral crystals. The source material for this cement is derived from pressure-solution processes affecting very fine authigenic quartz grains normally present in small amounts in Smackover deposits. Calcite cement is present normally as large sparitic crystals that embed crystals and allochems and fill the available pore space among them. Supersaturation in calcium carbonate of the formation fluids as the result of pressure-solution and late stage dissolution associated with hydrocarbon maturation may be responsible for the precipitation of the calcite cement. The time of formation may be close to the time of oil migration. This cementation process remains active during the precipitation of late stage anhydrite cement as evidenced by the common presence of the intergrowth of these two types of cements. Anhydrite is another important late stage cement. It is considered one of the last events as inferred from the characteristic coarse, slightly corroded crystals sometimes with a poikilotopic character and because the anhydrite normally fills spaces that were partially occluded by other cements. The source of material for this cement may be provided by former dissolution events of carbonate rocks rich in sulfates due to pressure-solution and organic acid activity. Authors have suggested

that this anhydrite is probably precipitated from ion-charged solutions migrating updip from the underlying Louann Salt.

Correlation between the depositional facies analysis of well cores and the petrophysical properties of these rocks leads to the conclusion that despite diagenesis, the depositional fabric defines the best reservoirs. In Vocation Field, the shoal complex and the microbial reef facies display the best porosity and permeability properties. Within the tidal flats and especially in the shallow lagoon environments, the deposition of isolated microbialite buildups and thin packstone-grainstone levels also have reservoir potential. Nonetheless, diagenesis can, in some cases, significantly affect and modify the distribution of reservoir grade rocks. Well Permit 2851 is an example of how penetrative dolomitization was able to generate reservoir grade intervals in tidal flat deposits that actually produced oil in this well. The opposite case is Well Permit 2966 where precipitation of dolomite and anhydrite cements obliterated porosity in the ooid shoal facies. Good correlation between porosity and permeability is the result of extensive dolomitization, late stage dissolution, and fracturing that combined to connect isolated moldic and vuggy pores to produce an effective pore system.

The shoal complex reservoirs are dolomitized ooid-oncoidal grainstone and packstone with primary intergranular porosity and secondary intercrystalline, moldic and vuggy pores. In this lithofacies, dolomitization improved connectivity among moldic pores and also generated new intercrystalline pores. Early marine cementation contributed in the preservation of primary porosity, while anhydrite and dolomite cementation are the main processes that occluded pores in the shoal facies. Total porosity is commonly between 4 and 15% with an average of 10% and permeability varies between 3 and 160 md with an average of 66 md. The thickness of the reservoir interval is normally between 20 and 40 feet, reaching 90 feet. The shoal facies is

widespread in the field, but probably the high-quality reservoir intervals are not connected along the entire length of the field due to pinch-outs and facies changes that are common in this depositional setting.

The potential reef reservoir intervals are characterized by reticulate and layered thrombolite fabrics commonly with primary shelter and intergranular porosity and secondary moldic, solution enlarged and fracture porosity. This potential reservoir is petrophysically heterogeneous due to the characteristic patchy texture of these deposits, and the presence of impermeable wackestone-mudstone levels and insoluble residual laminae. In this lithofacies, dolomitization, the nonselective dissolution episode, and fracturing substantially improved the amount of porosity and the connectivity of isolated shelter and vuggy pores. The normal thickness for the microbial reef intervals is between 100 and 150 feet, approximating a thickness of 200 feet (Well Permit #3739). Core and well-log analyses suggest that these thick sequences are limited spatially to the northeastern part of the structure. Porosity ranges between 8 and 20% with an average of 13%, while permeability is in the order of 30 and 410 md with an average of 175 md. Unfortunately, in Vocation Field significant accumulations of these facies are normally located below the oil-water contact.

The Smackover Formation at Vocation Field has undergone a long history of diagenetic events that document a paragenetic sequence similar to the ones described by other authors for nearby areas. Average values of porosity (10 % and 13 %, respectively) in Vocation Field for the shoal and microbial reef facies, which are commonly buried at depths greater than 14,000 feet, indicate that diagenesis has been critical for the preservation and generation of significant amounts of pore space. The most important diagenetic event for the preservation and improvement of the reservoir properties is dolomitization that not only generated new porosity

but improved the connectivity among the existing pore space. Dissolution (i.e. leaching of aragonite allochems and the deep non-fabric selective event) and fracturing were also important in the generation of secondary porosity. Diagenesis began soon after deposition and evolved through time due to progressively deeper burial conditions modifying the primary depositional texture of the rock. Despite all the diagenetic overprints, the depositional textures still define the best reservoirs.

### **Petrophysical and Engineering Property Characterization**

Petrophysical and engineering property characterization is essentially completed. Appleton and Vocation Fields have experienced a substantial decline in oil production since their initial discoveries.

#### ***Appleton Field***

Analysis of the core and log data indicate that the reservoirs at Appleton Field have a heterogeneous nature. Porosity and permeability data show a significant difference in reservoir quality between the shoal and reef reservoirs, with the reef facies having better reservoir quality compared to the shoal facies. There is poor correlation between the core and log porosity measurements for these facies. The oil in place calculated for Appleton Field using well performance analysis is an optimistic total. Flow capacity of the wells in the field shows a trend of improving reservoir quality in a north and easterly direction, and recoverable oil from each well is strongly correlated with its flow capacity. Structural factors do not appear to have a strong influence on oil recovery at Appleton Field.

#### ***Vocation Field***

Analysis of the core and log data indicate that the reservoirs at Vocation Field have a heterogeneous nature. Porosity and permeability show a significant difference in reservoir

quality between the shoal and reef reservoirs, with the reef reservoir having better reservoir quality compared to the shoal facies. There is reasonable correlation between the core and log porosity measurements for these facies. The correlation between core permeability and core porosity approximates a straight line representing a log linear model. This implies that the relationship between permeability and porosity at any point in the reservoir is more controlled by the location of the point structurally rather than in which lithofacies the point occurs. The primary production mechanisms in Vocation Field are believed to be depletion drive (fluid/rock/gas expansion) and water drive from an adjoining aquifer. The oil in place calculated for the field using well performance analysis is 33.8 million STB. It appears that oil recovery is not controlled by the flow capacity of a well, but rather is attributable to the proximity of a particular well's perforations to the oil-water contact.

### **3-D Geologic Modeling**

The 3-D geologic modeling of the structures and reservoirs at Appleton and Vocation Fields utilized the integrated database of geological, geophysical, and petrophysical information.

#### ***Appleton Field***

The 3-D geologic (structure and stratigraphic) model for Appleton Field included advanced carbonate reservoir characterization (structural, sequence and seismic stratigraphy, outcrop analog, depositional lithofacies, diagenesis and pore systems studies), three-dimensional geologic visualization modeling, seismic forward modeling, and porosity and permeability distribution analysis (seismic attribute and three-dimensional stratigraphic studies). The structure at Appleton Field is a low relief composite paleotopographic high. The well production differences in the field are related to the heterogeneous nature of the reservoir. The quality of the reef reservoir is greater than that of the shoal reservoir due to higher permeabilities and better



connected pore systems inherent to the depositional architecture and diagenetic fabric of the reef facies. Another significant factor controlling reservoir productivity is related to the variation in the size of individual reservoir compartments associated with the eastern and western paleohighs. The greater production from the eastern paleohigh is a reflection of the greater relief of the paleohigh, which places more reef reservoir above the oil – water contact. Production from the western paleohigh is limited by the lower relief of the structure, which places much of the reef reservoir below the oil – water contact. Thus, at Appleton Field, because the shoal and reef facies are continuous over this low relief composite paleohigh, reservoir producibility is principally controlled by reservoir quality, in combination, with structural relief.

### ***Vocation Field***

The 3-D geologic model for Vocation Field included advanced carbonate reservoir characterization (structural, sequence and seismic stratigraphy, outcrop analog, depositional lithofacies, diagenesis and pore systems studies), three-dimensional geologic visualization modeling, and porosity and permeability distribution analyses. The structure at Vocation Field is a high relief composite paleotopographic feature with multiple water levels. The well production differences in the field are related to the variable relief of the individual paleohighs and associated oil – water contact. The shoal and reef facies and resulting reservoir distribution is directly related to the individual paleohighs. The reef facies, which has higher reservoir quality than the shoal facies, is limited to the northern and eastern portions of the field. This distribution in reef facies is believed to be attributed to the microbial buildups occurring only on the leeward side of the Vocation composite feature. On the leeward side, the microbes could grow in a restricted environment not affected by ocean currents and circulation patterns. Another major factor controlling reservoir occurrence and producibility is related to the presence and variation

in the size of the individual reservoir compartments associated with the elevation of the individual paleohighs. If the paleohigh remained above sea level during Smackover deposition, no marine shoal or reef facies could be deposited. Thus, too high a relief precludes reservoir occurrence. However, greater production from certain paleohighs is a reflection of their greater relief, which places more of the shoal or reef facies above the oil – water contact. Thus, at Vocation Field because of the discontinuity of the shoal and reef facies due to the high relief of the composite paleotopographic high and because of the differential relief on the individual paleohighs, reservoir producibility is principally controlled by the degree of structural relief, in combination with reservoir quality.

### **3-D Reservoir Simulation**

The 3-D geologic models have served as the framework for the 3-D reservoir simulation models for Appleton and Vocation Fields.

#### ***Appleton Field***

The Appleton Field 3-D geologic model formed the foundation for reservoir simulation. The geologic model incorporated a much finer scale representation of the structure and petrophysical properties of the reservoir than could be accommodated for reservoir simulation. The simulation model was upscaled to contain 21,600 cells (30 x 30 x 24). The cells were approximately 330 ft. x 260 ft. x 20 ft.

The history matching study was conducted by withdrawing the amount of oil known to be produced from each well and observing the associated water and gas production. The field appears to be in hydraulic communication with an aquifer because of the volumes of water produced. The history match was achieved by placing the oil-water contact at a depth of -12,685 ft. and placing an aquifer under the field. Oil production matches very well, and water

production prior to 1990 is a reasonable match. There is difficulty explaining the high water production in the field after 1990. The history match and simulation model predict 11.8 million STB original oil in place. This prediction is significantly lower than the estimate resulting from well performance analysis. The simulation results indicate there is oil remaining to be recovered near the top of the structure.

### ***Vocation Field***

The Vocation Field 3-D geologic model formed the foundation for reservoir simulation. The geologic model incorporated a much finer scale representation of the structure and petrophysical properties of the reservoir than could be accommodated for reservoir simulation. The simulation model was upscaled to contain 30,600 cells (30 x 30 x 34). The cells were approximately 300 ft. x 300 ft. x 10 ft.

The history matching study was conducted by withdrawing the amount of oil known to be produced from each well and observing the associated water and gas production. The history match was achieved by placing the oil – water contact at a depth of -13,693 ft. and placing an aquifer under the western portion of the field. There may, however, be an aquifer under the entire field. The history match and simulation model predict 31.7 million STB original oil in place. This prediction agrees favorably with the estimate resulting from well performance analysis.

### **Data Integration**

All geological, geophysics, petrophysical and engineering data generated to date from this study have been entered and integrated into digital databases for Appleton and Vocation Fields.

## **CONCLUSIONS**

The University of Alabama in cooperation with Texas A&M University, McGill University, Longleaf Energy Group, Strago Petroleum Corporation, and Paramount Petroleum Company are

undertaking an integrated, interdisciplinary geoscientific and engineering research project. The project is designed to characterize and model reservoir architecture, pore systems and rock-fluid interactions at the pore to field scale in Upper Jurassic Smackover reef and carbonate shoal reservoirs associated with varying degrees of relief on pre-Mesozoic basement paleohighs in the northeastern Gulf of Mexico. The project effort includes the prediction of fluid flow in carbonate reservoirs through reservoir simulation modeling which utilizes geologic reservoir characterization and modeling and the prediction of carbonate reservoir architecture, heterogeneity and quality through seismic imaging.

The primary objective of the project is to increase the profitability, producibility and efficiency of recovery of oil from existing and undiscovered Upper Jurassic fields characterized by reef and carbonate shoals associated with pre-Mesozoic basement paleohighs.

The principal research effort for Year 2 of the project has been reservoir description and characterization. This effort has included four tasks: 1) geoscientific reservoir characterization, 2) the study of rock-fluid interactions, 3) petrophysical and engineering characterization and 4) data integration.

Geoscientific reservoir characterization is essentially completed. The architecture, porosity types and heterogeneity of the reef and shoal reservoirs at Appleton and Vocation Fields have been characterized using geological and geophysical data. All available whole cores have been described and thin sections from these cores have been studied. Depositional facies were determined from the core descriptions and well logs. The thin sections studied represent the depositional facies identified. The core data and well log signatures have been integrated and calibrated on graphic logs. The well log and seismic data have been tied through the generation of synthetic seismograms. The well log, core, and seismic data have been entered into a digital

database. Structural maps on top of the basement, reef, and Smackover/Buckner have been constructed. An isopach map of the Smackover interval has been prepared, and thickness maps of the Smackover facies have been prepared. Cross sections have been constructed to illustrate facies changes across these fields. Maps have been prepared using the 3-D seismic data that Longleaf and Strago contributed to the project to illustrate the structural configuration of the basement surface, the reef surface, and Buckner/Smackover surface. Seismic forward modeling and attribute-based characterization has been completed for Appleton Field. Petrographic analysis has been completed and a paragenetic sequence for the Smackover in these fields has been prepared.

The study of rock-fluid interactions is near completion. Thin sections (379) have been studied from 11 cores from Appleton Field to determine the impact of cementation, compaction, dolomitization, dissolution and neomorphism has had on the reef and shoal reservoirs in this field. Thin sections (237) have been studied from 11 cores from Vocation Field to determine the paragenetic sequence for the reservoir lithologies in this field. An additional 73 thin sections have been prepared for the shoal and reef lithofacies in Vocation Field to identify the diagenetic processes that played a significant role in the development of the pore systems in the reservoirs at Vocation Field. The petrographic analysis and pore system studies essentially have been completed. A paragenetic sequence for the Smackover carbonates at Appleton and Vocation Fields has been prepared. Pore systems studies continue.

Petrophysical and engineering property characterization is essentially completed. Petrophysical and engineering property data have been gathered and tabulated for Appleton and Vocation Fields. These data include oil, gas and water production, fluid property (PVT) analyses and porosity and permeability information. Porosity and permeability characteristics of

Smackover facies have been analyzed for each well using porosity histograms, permeability histograms and porosity versus depth plots. Log porosity versus core porosity and porosity versus permeability cross plots for wells in the fields have been prepared.

Well performance studies through type curve and decline curve analyses have been completed for the wells in Appleton and Vocation Fields, and the original oil in place and recoverable oil remaining for the fields has been calculated.

3-D geologic modeling of the structure and reservoirs at Appleton and Vocation Fields has been completed. The model represents an integration of geological, petrophysical and seismic data.

3-D reservoir simulations of the reservoirs at Appleton and Vocation Fields have been completed. The 3-D geologic model served as the framework for these simulations. The acquisition of additional pressure data would improve the simulation models.

Data integration is up to date, in that, geological, geophysical, petrophysical and engineering data collected to date for Appleton and Vocation Fields have been compiled into a fieldwide digital database for development of the geologic-engineering model for the reef and carbonate shoal reservoirs for each of these fields.

A technology workshop on reservoir characterization and modeling at Appleton and Vocation Fields was conducted to transfer the results of the project to the petroleum industry.

## **REFERENCES**

Ahr, W.M., and Hammel, B., 1999, Identification and mapping of flow units in carbonate reservoirs: an example from Happy Spraberry (Permian) field, Garza County, Texas USA: Energy Exploration and Exploitation, v. 17, p. 311-334.

- Baria, L.R., Stoudt, D.L., Harris, P.M., and Crevello, P.D., 1982, Upper Jurassic reefs of Smackover Formation, United States, Gulf Coast: American Association of Petroleum Geologists Bulletin, v. 66, p. 1449-1482.
- Benson, D.J., 1985, Diagenetic controls on reservoir development and quality, Smackover Formation of southwest Alabama: Gulf Coast Association of Geological Societies Transactions, v. 35, p. 317-326.
- Benson, D.J., 1988, Depositional history of the Smackover Formation in southwest Alabama: Gulf Coast Association of Geological Societies Transactions, v. 38, p. 197-205.
- Hart, B.S., and Balch, R.S., 2000, Approaches to defining reservoir physical properties from 3-D seismic attributes with limited well control: an example from the Jurassic Smackover Formation, Alabama: Geophysics, v. 65.
- Kerans, C., and Tinker, S.W., 1997, Sequence stratigraphy and characterization of carbonate reservoirs: SEPM Short Course No. 40, 130 p.
- Llinas, J.C., 2002, Diagenetic history of the upper Jurassic Smackover Formation and its effects on reservoir properties, Vocation Field, Manila sub-basin, eastern Gulf Coastal Plain: Gulf Coast Association of Geological Societies Transactions, v.52 (in press).
- Llinas, J.C., 2002, Carbonate sequence stratigraphy. Influence of paleotopography, eustasy and tectonic subsidence: upper Jurassic Smackover Formation, Vocation Field, Manila sub-basin (eastern Gulf Coastal Plain), Sequence Stratigraphic Models for Exploration and Production, Proceedings of the 22<sup>nd</sup> Annual Research Conference, Gulf Coast Section, SEPM Foundation (in press).
- Mancini, Ernest A., Badali, M., Puckett, T.M., Parcell, W.C., and Llinas, J.C., 2001, Mesozoic carbonate petroleum systems in the northeastern Gulf of Mexico, Petroleum Systems of

- Deep-Water Basins: Global and Gulf of Mexico Experience, Proceedings of the 21st Annual Research Conference, Gulf Coast Section, SEPM Foundation, p. 423-451.
- Mancini, E.A., and Benson, D.J., 1998, Upper Jurassic Smackover carbonate reservoir, Appleton Field, Escambia County, Alabama: 3-D seismic case history, 3-D Case Histories of the Gulf of Mexico, p. 1-14.
- Mancini, Ernest A., Benson, D.J., Hart, B.S., Balch, R.S., Parcell, W.C., and Panetta, B.J., 2000, Appleton field case study (eastern Gulf Coastal Plain): field development model for Upper Jurassic microbial reef reservoirs associated with paleotopographic basement structures: American Association of Petroleum Geologists Bulletin, v.84, p.1699-1717.
- Mancini, Ernest A., Benson, D. Joe, Hart, Bruce S., Chen, Hannah, Balch, Robert S., Parcell, William C., Yang, Wen-Tai, and Panetta, Brian J., 1999, Integrated geological, geophysical and computer modeling approach for predicting reef lithofacies and reservoirs: Upper Jurassic Smackover Formation, Appleton Field, Alabama, Advanced Reservoir Characterization for the Twenty-First Century, Proceedings of the 19th Annual Research Conference, Gulf Coast Section, SEPM Foundation, p. 235-247.
- Mancini, E.A., Mink, R.M., Tew, B.H., Kopaska-Merkel, D.C., and Mann, S.D., 1991, Upper Jurassic Smackover oil plays in Alabama, Mississippi and the Florida panhandle: Gulf Coast Association of Geological Societies Transactions, v. 41, p. 475-480.
- Mancini, Ernest A., and Panetta, B.J., 2002, Reservoir characterization and modeling of Upper Jurassic Smackover carbonate shoal complex reservoirs, Womack Hill oil field, Choctaw and Clarke Counties, Alabama: Gulf Coast Association of Geological Societies Transactions, v.52 (in press).



- Mancini, Ernest A., and Parcell, W.C., 2001, Outcrop analogs for reservoir characterization and modeling of Smackover microbial reefs in the northeastern Gulf of Mexico area: Gulf Coast Association of Geological Societies Transactions, v. 51, p. 207-228.
- Mancini, Ernest A., Puckett, T.M., and Parcell, W.C. (eds.), 2000, Carbonate Reservoir Characterization and Modeling for Enhanced Hydrocarbon Discovery and Recovery, AAPG/EAGE International Research Conference, Program and Abstracts Volume, 68 p.
- Mancini, E.A., Tew, B.H., and Mink, R.M., Jurassic sequence stratigraphy in the Mississippi Interior Salt Basin: Gulf Coast Association of Geological Societies Transactions, v. 40, p. 521-529.
- Marhaendrajana, T., and Blasingame, T.A., 1997, Rigorous and semi-rigorous approaches for the evaluation of average reservoir pressure from pressure transient tests: Paper 38725 presented at the 1997 Annual SPE Technical Conference and Exhibition, San Antonio, TX, October 6-8.